

**13th Symposium on
High-Performance Marine Vehicles**

HIPER'21

Tullamore, 13-15 September 2021

**13th Symposium on
High-Performance Marine Vehicles**

HIPER'21

Tullamore, 13-15 September 2021

Edited by Volker Bertram

13th Symposium on High-Performance Marine Vehicles, Tullamore, 13-15 September 2021, Hamburg, Technische Universität Hamburg, 2021

© Technische Universität Hamburg
Schriftenreihe Schiffbau
Schwarzenbergstraße 95c
D-21703 Hamburg
<http://www.tuhh.de/vss>



Sponsored by



tutech.de



www.numeca.de



wetech.fi



group-ib.com



www.hasytec.com

Index

Manfred Limbrunner <i>The Integration of Fuel Cells in the Maritime Sector for a Greener Future</i>	7
Volker Bertram <i>Fuel Options for Decarbonizing Shipping</i>	12
Volker Bertram <i>Visions and Sobering Reality in Maritime ICT</i>	21
Rodrigo Pérez Fernández <i>Internet of Ships - Just a Philosophical Approach?</i>	29
Volker Bertram <i>Robotic Hull Cleaning – State of the Art and Roadmap</i>	37
Tracy Plowman, Volker Bertram <i>Virtual Reality Applications in Maritime Training – A Survey</i>	45
Solène Guéré, Nicolas Gambini <i>Notilo Cloud AI Platform for Hull Condition Reporting</i>	62
Sophia Brans, Andre Rinne, Austin A. Kana <i>Applying a Needs Analysis to Promote Daughter Craft for Year-Round Access to Far-Offshore Wind Turbines</i>	71
Andrea Coraddu, Miltos Kalikatzarakis, Rinze Geertsma, Luca Oneto <i>Hybrid Modelling Approach of a Four-stroke Medium Speed Diesel Engine</i>	88
Sven Albert, Thomas Hildebrandt, Stefan Harries, Erik Bergmann, Massimo Kovacic <i>Hydrodynamic Optimization of a Small Electric Catamaran Ferry</i>	106
Jörg Albrecht <i>Optimization of the Aerodynamic Design of a Solar Houseboat Catamaran</i>	121
Matteo Barsotti <i>Road to Digitalization, Not so Simple</i>	127
Jan Kelling <i>EU Project CHEK – Ultrasonic Antifouling and other Measures to Meet the CII Challenge</i>	132
Giuseppe Carmosino, Francesca Balena, Silvia Piardi, Andrea Ratti <i>Cruise Ships and COVID-19 Emergency – How Smart Technologies Can Improve the Health Safety of Travel Onboard</i>	140
Alan Guégan, Quentin Rathier, Léa Lincker, Charles-Edouard Cady <i>Ship Design: Gameplay Matters!</i>	151
Steinar Låg, Vidar Vindøy, Kristian Ramsrud <i>A Standardized Sensor Naming Method to Support Digital Twins and Enabling New Data Driven Applications in the Maritime Industry</i>	161

Jonathan Evans, Nico Voorzee <i>Creating Sustainable Marine Structures Through the Adoption of Composites</i>	173
Sven Albert, Rodrigo Corrêa, Thomas Hildebrandt, Anton Du Toit, Samantha Krenski <i>Advanced CFD-based Design Approach for High-Performance Sailing Catamarans</i>	180
Emmet Ryan, Serkan Turkmen, Simon Benson <i>Challenges in the Application of Ultraviolet Irradiation for Biofouling Control</i>	192
Stefan Walheim, Thomas Schimmel, Matthias Barczewski, Lutz Speichermann-Jägel, Robert Droll, Susanna Dullenkopf-Beck, Johannes Oeffner, Jonathan Weisheit, Jean-Christophe Minor, Marina Beltri <i>Passive Air Lubrication: Demonstrating a Research Vessel Coated with a Hull of Air</i>	203
Chara Georgopoulou, Lefteris Koukouloupoulos, George Dimopoulos, Eirik Ovrum, Lampros Nikolopoulos, Kostas Bougiouris <i>Model-Based Assessment of a Fuel Cell Driven Very Large Crude Carrier Concept</i>	209
Mårten Storbacka <i>Power Distribution in Ultra-Efficient and Zero-Emission Ships</i>	218
List of authors	
Call for Papers for next HIPER	

The Integration of Fuel Cells in the Maritime Sector for a Greener Future

Manfred Limbrunner, Proton Motor Fuel Cell GmbH, Puchheim/Germany,
m.limbrunner@proton-motor.de

Abstract

This paper explains the different materials in fuel cells and their limitations. The paper also gives a comparison between graphite fuel cells and metallic bipolar plated fuel cells. It details the different opportunities for hydrogen storage and challenges with current fuel cell systems. An outlook on fuel cells and their development in regard to innovative technology and costs will offer a deeper insight into the green future of fuel cells.

1. Introduction

As more and more coastal areas and ports become subject to strict environmental regulations (such as SECA (Sulphur Emission Control Area) and ECA (Emission Control Area)), *IMO (2018,2020)*, it is important to push and advance the development of sustainable and environmentally friendly technologies in the maritime sector. In this development, fuels cells will play an increasingly important role as they work efficiently, quietly and without emissions (if fuelled by hydrogen and oxygen).

Between 2008 and 2014, the world's first fuel cell ship named "FCS Alsterwasser", <https://en.wikipedia.org/wiki/Zemships>, Fig.1, operated in Hamburg with a fuel cell system developed and designed by Proton Motor, Fig.2. Note that the operation was terminated due to insufficient demand for hydrogen as a fuel in 2014, leading to a closing down of the hydrogen fuelling station for economic reasons.

PEM (Polymer Electrolyte Membrane) fuel cells, e.g. *Barbir (2012)*, for the maritime electric propulsion systems and the multiple ways these can be integrated into the maritime sector offer a variety of opportunities for a greener and sustainable future.



Fig.2: Tourist boat "FCS Alsterwasser" in operation on Lake Alster in Hamburg

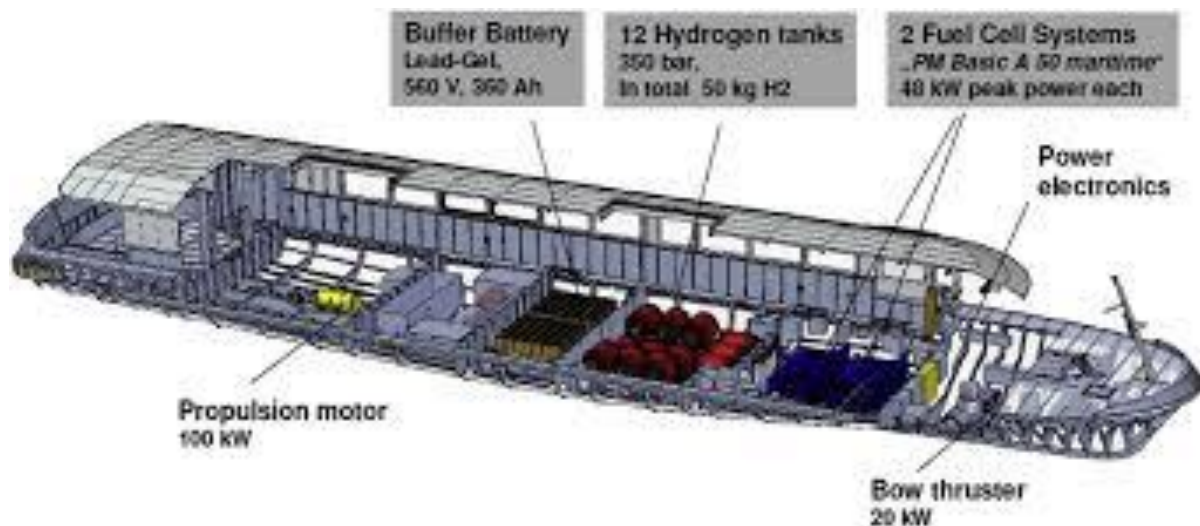


Fig.2: “FCS Alsterwasser” arrangement including Proton Moto fuel cells, source: [ZEMSHIPS](https://www.zemships.com/)

The fuel cells for the FCS "Alsterwasser" were specially developed for maritime applications. They are characterized above all by the fact that they are very powerful and also vibration resistant. The ship was equipped with two fuel cell systems, each with 48 kW of power, which drive the engine via the battery's intermediate storage with an output of up to 100 kW (approximately 130 HP). Previous maritime applications of fuel cell technology were limited to submarines and very low-powered vessels with an engine output of less than 5 kW. The ZEMSHIPS project demonstrated that larger and more powerful ships can also be powered by fuel cell systems.

2. Fuel cell working principle

A fuel cell is a device that converts the chemical energy bound in the molecular bonds of hydrogen and oxygen into electrical energy. In the PEM (Polymer Electrolyte Membrane)- technology, gaseous hydrogen (H_2) is used as a fuel and is reacted with oxygen (O_2) from the air to pure water. Other reaction products in the cell are electricity and heat.

In contrast to conventional internal combustion engines, coal-fired power plants and nuclear power plants, no toxic, radioactive or climate-damaging by-products are produced or emitted. If the hydrogen used comes from renewable sources, e.g. by electrolysis of water with electricity generated from wind or solar energy, this technology has zero carbon footprint. This makes the fuel cell an ideal component of a sustainable energy supply today and in the future.

Core components of a PEM fuel cell are the so-called bipolar plates (BPP), a gas diffusion layer (GDL) and the electrochemically active polymer electrolyte membrane with a thin catalyst layer (CCM = catalyst coated membrane), Fig.3.

The purpose of the bipolar plates is to guide the reaction gases (hydrogen and oxygen) uniformly over the entire active area to the catalyst layer via a specific channel structure (the flow field). A bipolar plate, as the name implies, consists of the two poles of a single fuel cell: the hydrogen-carrying anode plate (the negative (-) pole) and the cathode plate (the positive (+) pole) for supplying the reaction air. In between, a further cooling flow field for the removal of reaction heat can be integrated. Another purpose of the bipolar plate is the removal of the resulting reaction water in the chemical reaction.

The gas diffusion layer (GDL) between the bipolar plate and CCM is responsible distributing the reaction gases evenly from the channels of BPP on to the catalyst layer of CCM and the removal of product water from the catalyst into the channels of BPP.

The few microns thick polymer electrolyte membrane (PEM) has the task of separating the two gas spaces (H_2 and O_2). For this purpose, it is largely gas-tight and electrically insulating, but can very efficiently transport protons and water.

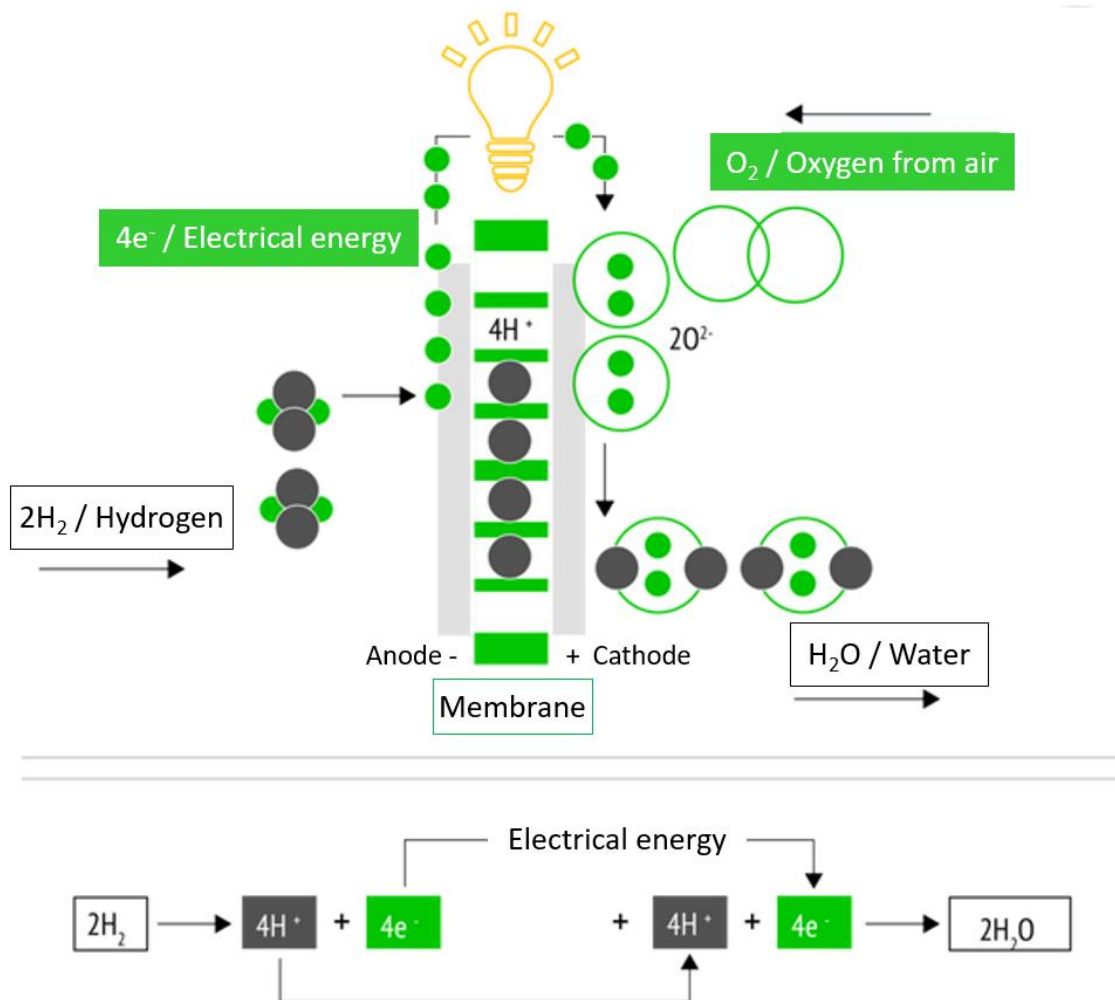
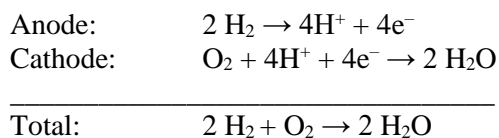


Fig.3. Working principle of PEM fuel cell

On both sides of the membrane is a thin layer of a catalyst that allows the reaction of oxygen and hydrogen at the low temperatures prevailing in the fuel cell. Small amounts of platinum metal ($\sim 5 \text{ mg/cm}^2$) are generally used as the catalyst material. The catalyst-coated polymer electrolyte membrane is thus the heart of a fuel cell, because it is here that the actual electrochemical reaction takes place, consisting of the two partial reactions:



On the anode side protons (H^+) and electrons (e^-) are separated. As the protons pass through the polymer electrolyte membrane to the cathode side, the electrons are forced through an external circuit. This creates an electrical potential and the electrons can perform (electrical) work along their path. On the cathode side, the protons along with the electrons react with the oxygen from the air to form pure water when the circuit is closed. As the reaction is exothermic, the heat of reaction can also be extracted from the cooling liquid.

In order to achieve greater performance and to be able to use the fuel for energy supply on meaningful

levels, several of these individual cells are interconnected to form a fuel cell stack. Here, each bipolar plate represents the cathode of one cell and the anode of the subsequent cell. This in turn represents the heart of a fuel cell system.

The active area of a cell determines the current of the fuel cell system by the number of simultaneous reactions and thus the number of flowing electrons. The corresponding voltage results from the number of interconnected individual cells.

In addition to the specific design of the individual components, Proton Motor know-how also includes the construction of a complete fuel cell system around the core component cell stacks. The stack is embedded in a module consisting of hydrogen, cooling and air management components as well as hardware and software and a sophisticated safety concept. Due to the modular structure of the Proton Motor fuel cell systems, simple integration into a higher-level system is possible. This allows us to address the diverse conditions in stationary, mobile or maritime use, resulting in a tailor-made concept for the respective application.

Advantages of fuel cell technology are:

- No harmful emissions
- High efficiency
- Use of waste heat possible
- Low noise
- No vibration
- Low wear of the components
- With off-grid or emergency power supply, the bridging time is limited only by hydrogen supply (tank capacity)
- Fast refueling possible (unlike batteries)

3. Latest developments for future ships

Following an order in December 2019, Proton Motors received a further order from Fincantieri to deliver a fuel cell system with 144 kW fuel cell power to be installed into Fincantieri's 25 m long demonstrator and testing vessel ZEUS (Zero Emission Ultimate Ship), Fig.4, which will be exclusively powered by Proton Motor's fuel cell system.



Fig.4: ZEUS, source: Fincantieri

References

BARBIR, F. (2012), *PEM Fuel Cells: Theory and Practice*, Academic Press

IMO (2018), *UN body adopts climate change strategy for shipping*, International Maritime Organisation, London, <http://www.imo.org/en/MediaCentre/PressBriefings/Pages/06GHGinitialstrategy.aspx>

IMO (2020), *Sulphur oxides (SO_x) - Regulation 14*, International Maritime Organisation, London, [http://www.imo.org/en/OurWork/Environment/PollutionPrevention/AirPollution/Pages/Sulphur-oxides-\(SOx\)-\T1\textendash-Regulation-14.aspx](http://www.imo.org/en/OurWork/Environment/PollutionPrevention/AirPollution/Pages/Sulphur-oxides-(SOx)-\T1\textendash-Regulation-14.aspx)

Fuel Options for Decarbonizing Shipping

Volker Bertram, DNV, Hamburg/Germany, volker.bertram@dnv.com

Abstract

This paper surveys key options for fuels to decarbonize shipping, including LNG, biofuels, synthetic fuels such as methanol and ammonia, as well as hydrogen. Key features, pros and cons, selected projects, and references give an introduction in layman's terms, intended as simple introduction to this rapidly evolving field.

1. Introduction

“Decarbonization” is not just a recent buzzword, it is on many political agendas, including (most notably for us) IMO’s agenda. The larger goals as such are clear, but what exactly do we have to achieve in the short and medium term and how do we collectively achieve this best is still very much subject to debate in scientific, business and political circles.

In essence, there are four enabling levers to decarbonize shipping:

1. Low/no-carbon fuels addressing the problem at the source – The problem is that these fuels generally will be significantly more expensive than Heavy Fuel Oil (HFO), the standard shipping fuel of pre-2020 times. Future no-carbon fuels may include nuclear fuels.
2. Economic frameworks (market-based measures), such as CO₂ compensation schemes or taxes/surcharges for CO₂ emissions respectively carbon-content of fuels. These will make traditional carbon-based fuels more expensive.
3. Wind-assisted ship propulsion (WASP) – The idea of using renewable energy sources directly for ship propulsion is not new, but has been enjoyed exponential growth in installations over the past few years after decades of being rather dormant. Business cases are difficult to establish due to the highly nonlinear nature of exploitable wind conditions.
4. Energy saving measures – The first two levers will make fuel more expensive. This is likely to motivate renewed scrutiny of energy-saving measures in design and operation. While there is little media focus on this lever, it is likely to be the dominant contributor to decarbonizing shipping in the short term (i.e. next 10-20 years), not least as many energy saving measures pay for themselves.

In the following, we will focus on the first lever, namely “new” fuels that are to be considered in the context of decarbonizing shipping.

2. Coming to terms with fuels

In general, any substance which in a chemical reaction with an oxidizer (typically oxygen from the surrounding air) releases heat is a fuel. Carbon is a fuel. It reacts with oxygen in complete reaction to CO₂ (carbon dioxide), releasing 53 kJ/g in the process. (Coal has roughly half this calorific value, as it contains not just carbon, but various contaminants like water, sand, sulphur, etc.) Hydrogen is also a fuel, reacting with oxygen to H₂O (water), releasing 143 kJ/g in the process, roughly 2.5 times more than carbon.

Hydrogen and carbon have the ability to form chains (hydrocarbons), methane CH₄, Ethane C₂H₆, etc. Higher percentage of hydrogen means generally better, more energy content, fuel. The longer the chain

in hydrocarbon fuels, the heavier the fuel, the more viscous the fuel, the lower the calorific value, and the higher are temperatures to get the fuels to turn liquid or to evaporate. In other words, at room temperature, short chains are gaseous, medium chains liquid and long chains solid. Each of the three states of matter has its implications for fuels:

- solid (keeping its shape) is the worst, as it cannot be pumped. (When ships used coal as fuel, much of the crew was needed to shovel the fuel to the engines.)
- liquid (dense, but adapting to shape) is the best, as it allows using odd spaces for tanks and relatively small volume for tanks.
- gas (fills shapes, but at low density) is pumpable, but at least for storage, we prefer to liquify these fuels to achieve higher density and, thus, enable smaller tanks.

Fuels can be fossil or renewable. Fossil fuels were formed millions of years ago and most fuels used in shipping have been fossil: coal, crude-oil derived products, and natural gas. Renewable fuels include wood (the oldest fuel used by mankind), refuse (the largest contributor to renewable energy is waste incineration), agricultural residues and specifically grown biofuels. Electricity could be in either category, depending on the way it is generated, using fossil fuels or renewables.

3. Fuel options

“The choice of energy converter and onboard fuel storage is one of the most critical decisions a ship-owner needs to take today”, *DNV (2020)*. Many stakeholders in the industry call urgently for clear instructions on what to do, which fuel and machinery to plan for. Unfortunately, the best we can offer are educated guesses, with transparent reasoning of factors influencing our predictions, and update our predictions and roadmaps as we move ahead. DNV does this in its Energy Transition Outlook - Maritime Forecast to 2050, with its 4th edition being the most recent update, *DNV (2020)*. In this report, we look at different socio-political scenarios and perform sensitivity analyses. While no clear recommendation for one single fuel can be given, the report in its latest edition is recommended for detailed studies.

With new developments there comes new jargon. See the Appendix for a quick introduction to what colours for (colourless) fuels mean, and a few other terms for the brave new world of fuels for decarbonizing shipping.

3.1. LNG

Liquefied natural gas (LNG) is natural gas (predominantly methane, CH₄) that at -163°C turns liquid, requiring only ~1/600th the volume of its gaseous state for storage. Still, compared to HFO, you need approximately twice the tank capacity (factor depends on choice of tank design) for LNG or accept half the range. LNG as a fuel technology is mature, benefitting from decades of experience with shipping LNG as cargo in LNG carriers and rules and regulations in place. We also have natural gas reserves for many decades, i.e. a comparatively abundant supply. Bunkering infrastructure is relatively (to other alternatively fuels) well established. Continued efforts for a global roll-out of LNG bunkering infrastructure are needed, but depend on political and economic signals which have been less encouraging recently.

Natural gas is a fossil fuel, contributing to the CO₂ footprint. IMO assigns a 12% lower emission factor (per ton of fuel) to LNG compared to HFO in the computation of EEDI, EEXI or EEOI. And considering the calorific value, we get frequently quoted ~25% lower CO₂ emission for LNG. However, this considers only the ship itself, or the “tank-to-propeller” carbon footprint. If we consider the overall carbon footprint from fossil fuel source to propeller (“well-to-propeller”), Fig.1, any significant advantage for

Greenhouse Gas (GHG) emission over traditional ship fuels is lost, Fig.2, especially if considering methane slip, as methane is 80 times worse for global warming than CO₂ (over a 20-year horizon).

LNG is an important bridging technology for the next one or two decades. *DNV (2020)* predicts a significant decline by 2050, possibly phasing out, of all fossil fuels, including fossil LNG. However, we may use methane as a fuel for longer, then in form of biogas or synthetic gas.

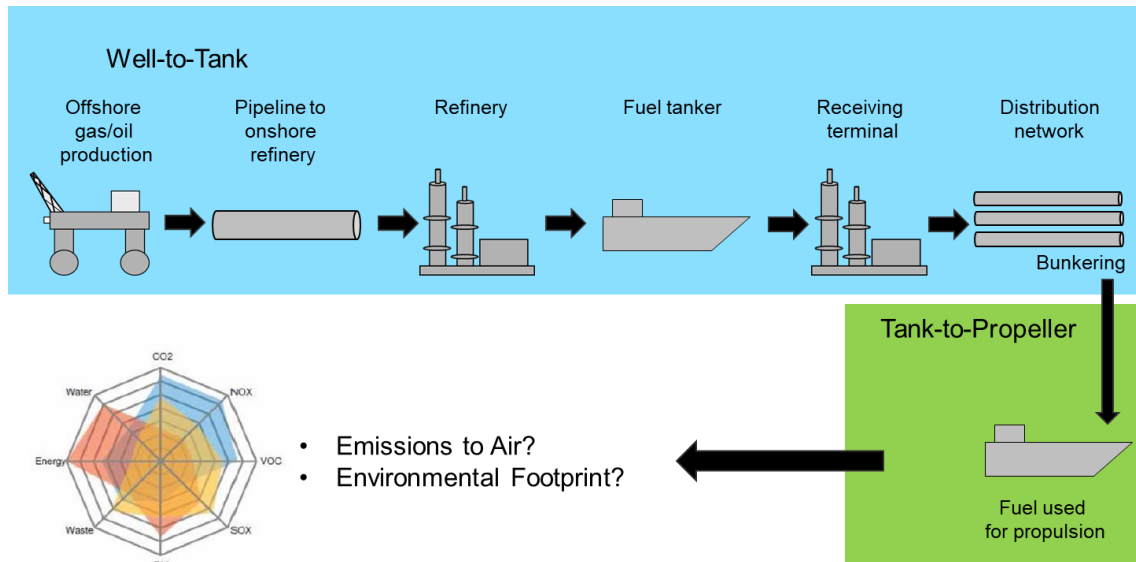


Fig.1: Carbon footprint of fuel with well-to-tank (blue) and tank-to-propeller (green) consideration

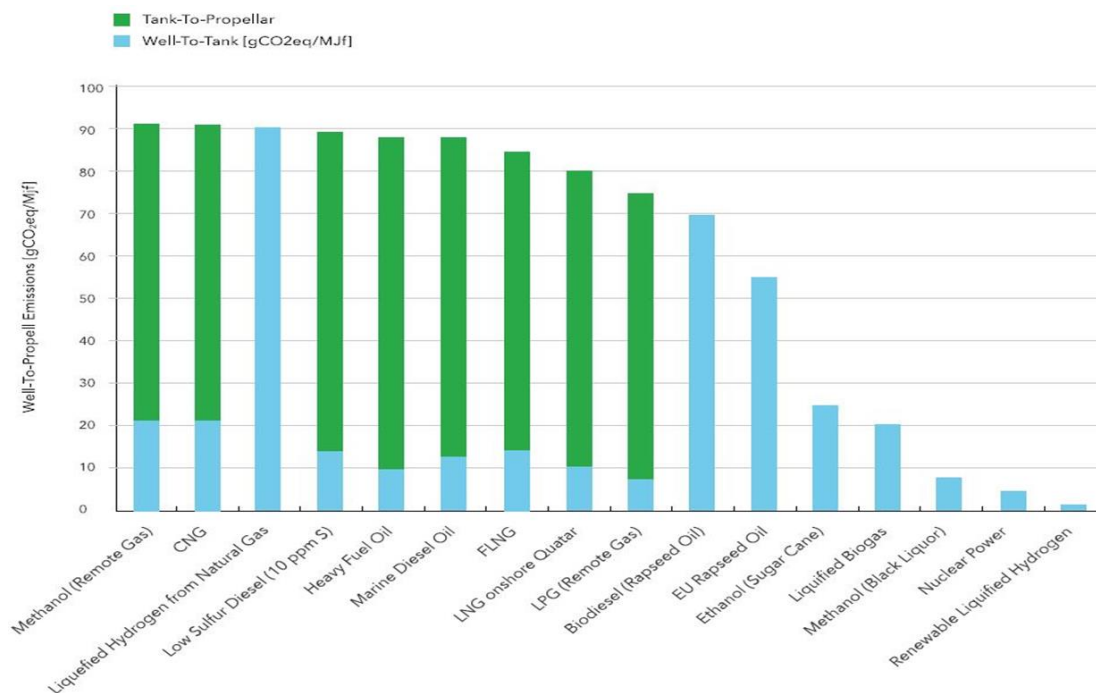


Fig.2: Associated carbon footprints for various fuels

3.2. Methanol

Methanol (a.k.a. methyl alcohol, CH₃OH) is a colourless, volatile and flammable hydrogen-rich liquid fuel. Methanol has been advocated as alternative fuel particularly in northern European countries, with

pilot projects in shipping since 2016, *Lundgren and Wachsmann (2014)*, *Andersson and Salazar (2015)*, *Ellis and Tanneberger (2015)*, *Iqbal (2017)*, *Bakhtov (2019)*.

Methanol is a clean fuel, with emissions similar to LNG. It is thus a low-carbon fuel, meeting all sulphur and nitrogen oxide emission regulations even in ECAs (Emission Control Areas). The technology for methanol as a fuel is mature. The machinery infrastructure is similar to traditional fuels, for (dual-fuel) diesel engines and piping, and fuel storage in integral atmospheric tanks is possible, Fig.3. The handling for the crew is thus easy; safety and health issues of Methanol can be addressed by operational guidelines and are not cause for major concerns.

However, methanol is not produced in large quantities worldwide and outside the North Sea and Baltic Sea area, the infrastructure to bunker methanol in ports is scarce and insufficient for many trade routes. Methanol is more expensive than traditional fuels and requires roughly twice the tank capacity for same range. Thus, current Methanol technology appears to be a bridging technology to a zero-carbon future, where carbon would be recycled or captured, i.e. using bio-methanol or so-called blue methanol.



Fig.3: Methanol is a low-carbon fuel option with mature technology for machinery, piping and tanks

3.3. Biofuels

Biofuels can be derived from edible crops, non-edible crops, or algae. Typical biofuels are bio-methanol, bioethanol, and biogas. The technology to produce biofuel is mature and biofuels are largely compatible with marine diesel engines. While biofuel production capacity is increasing worldwide, it generally makes more sense for an overall lower carbon footprint to use the biofuels close to where they are produced, i.e. for land-based transport if the biofuels are produced inland. There are also ethical questions for biofuels concerning use of agricultural land at the expense of food production, particularly in regions with populations suffering from malnutrition or even hunger.

For a detailed discussion of biofuels for shipping, see *Hsieh and Felby (2017)* who conclude that “larger scale introduction of biofuels requires involves a directed effort between engine manufacturers, biofuel suppliers, ship owners and infrastructure (port) operators.”

An interesting perspective are algae-based biofuels, *Alam et al. (2012)*, *De Nijs (2018)*. Algae can be cultivated in uncultivable areas and in offshore farming, avoiding competition with food production and biofuel production for land-based transport. However, algae-based biofuel production is still subject to research and development, needing at least another decade to become industry-mature.

3.4. Synthetic Fuels

Synthetic gaseous and synthetic liquid fuels are man-made fuels that are created using energy input. The lifecycle GHG emissions depend on the production pathway for both principal source materials as

well as the electricity used for the synthesis. Synthetic fuels containing carbon can at best be carbon neutral, meaning that captured carbon dioxide used in the fuel production is again emitted when the fuel is used. A variety of synthetic fuels is possible to be produced, e.g. synthetic methane, diesel, kerosine, methanol. The principle advantage for these is that existing infrastructure for fuel distribution and installation for fuel storage and use can be used without modifications. The manufacturing process for “blue” synthetic fuels (using renewable energy and carbon dioxide capturing) is still costly.

3.4.1. Ammonia

Ammonia (NH_3) is a prime contender for zero-carbon fuel in future shipping, *Eckle et al. (2019)*, *De Vries (2019)*, *Hansson et al. (2020)*. It is used as a building block in fertilizers, as feedstock for refining processes, and pharmaceutical products, making it a typical bulk cargo. Ammonia is rich in hydrogen, but easier to handle than liquid hydrogen in terms of production and distribution. With a boiling point of -33°C , moderate cryo-technology or pressure (8.6 bar at 20°C) suffice to liquefy ammonia for storage and transport. Typical LPG technology is suitable for handling of ammonia, i.e. the storage technology is mature and widely available.

Ammonia is widely available with large-scale production facilities worldwide (due to the high demand in fertilizers). Ammonia is synthesised using hydrogen and nitrogen. Most of the ammonia produced today is “brown” ammonia, using steam methane reforming involving CO_2 emission in the process. If the CO_2 is captured, “blue” ammonia can be produced (see appendix). When hydrogen is produced using electrolysis and renewable energy, “green” ammonia is the result.

Machinery for ammonia as a fuel is in prototype maturity, with both MAN and Wärtsilä testing dual-fuel diesel engines for ammonia, Fig.4, and 2 MW fuel cells are tested in the ShipFC project, <https://maritimecleantech.no/project/shipfc-green-ammonia-energy-system/>. Larger conceptual designs for ammonia-fuelled ships have been presented, Fig.5, *De Vries (2019)*.

Ammonia poses health and safety risks: Ammonia is corrosive to skin, eyes and lungs and flammable in air in 15-28% concentration. However, these risks are manageable. Humans have a low thresholds for detecting the pungent odour of ammonia in much lower than critical concentrations. Operational guidelines and procedures are well established as ammonia has been handled by crews for a long time as cargo. For ammonia as fuel, some additional safety measures will be needed, but this should not prevent, or even delay, the introduction of ammonia as a ship fuel.



Fig.4: Dual-fuel diesel for ammonia on test bed, source: Wärtsilä



Fig.5: Ammonia-fuelled conceptual ship design for a tanker, *De Vries (2019)*

3.4.2. Hydrogen

Hydrogen (H_2) is a zero-carbon fuel, that requires extremely temperatures (-253°C ; liquid hydrogen LH_2) or high pressure (350-700 bar; CH_2) for storage and transport. It can be used as fuel in combustion

engines (often in combination with diesel, as in a Belgian pilot project of CMB, *Hoecke et al. (2021)*, Fig.6) or fuel cells. In 2021, Global Energy Ventures (GEV) announced a project for a CH₂ tanker, Fig.7. Both CMB in Belgium and the German MariGreen R&D project, *NN (2018)*, have investigated hydrogen as fuel for inland water vessels.



Fig.6: Hydrogen-powered tug, source: CMB

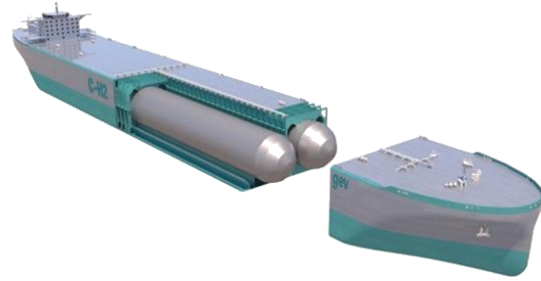


Fig.7: CH₂ ship project, Source: GEV

While ammonia is likely to be more widely adopted as shipping fuel, hydrogen will play a major role in future fuels as a building block in some likely contenders, such as e-methanol, e-ammonia, or blue ammonia, *DNV (2020)*.

3.5. Nuclear fuels

Nuclear ship propulsion is used today in large navy ships, submarines and ice breakers. Nuclear powered cargo ships are history, *Freire and De Andrade (2015)*. Rigorous safety standards, lack of trained personnel and negative public image have relegated nuclear power for cargo shipping to an obscure backseat in discussions for decades, mainly of academic interest, *Gravina et al. (2013)*. The urgent need to reduce the carbon footprint in relatively short time may lead to a renaissance in nuclear power production on land, but how realistic is nuclear energy for shipping? The question is at least worth debating for long-term options past 2050.

With a new generation of small and modular fission reactors being designed, start-up companies reconsider nuclear cargo ships and claim that such solutions may commercially be attractive. Potentially even fusion reactors could power ships in the long-term, with better safety, no radioactive waste and lower fuel cost.

For medium-term scenarios, nuclear power plays mainly an indirect role for shipping, in the production of (pink) e-fuels. Significant research and development would be needed for compact and lighter reactors, auxiliary machinery, design and operational safety regulations, and training for nuclear powered ship operation. The technology cannot and should not be ruled out, but will play no major role for the 2050 horizon.

4. Certain uncertainty

The Danish Nobel prize laureate Niels Bohr is credited with the aphorism: “It’s difficult to make predictions, especially about the future.” For future shipping fuels, this certainly applies. Only the uncertainty seems to be certain.

With all the disclaimers and pointing out the difficulties of predictions, DNV’s energy transition outlook, *DNV (2020)*, sees e-ammonia, blue ammonia, and bio-methanol among the top contenders for 2050, but this may change in future updates of the outlook. We refer to *DNV (2020)* for an in-depth discussion of the many uncertain factors influencing such predictions, such as raw material and

electricity prices, governmental interference (taxes and subsidies) and regulatory frameworks. Predictions for fuel prices vary widely, Fig.8, but obviously affect take-up by the industry significantly.

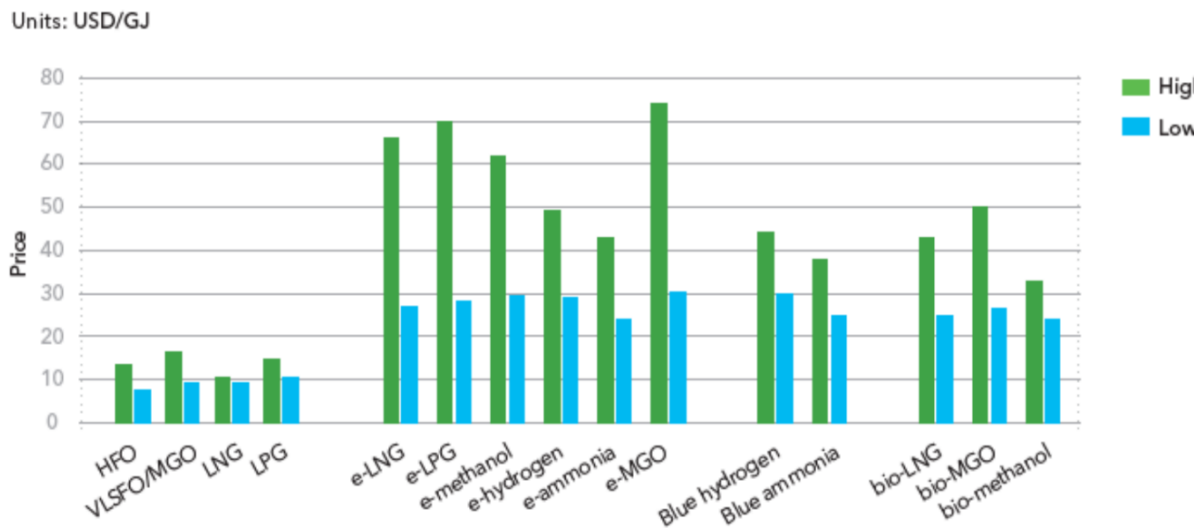


Fig.8: Predicted high and low prices for fuels by 2050, DNV (2020)

The uncertainty is a challenge for all stakeholders, but not a stranger to our industry. There are tried and proven strategies to manage uncertainty. Recipes for success in uncertainty are flexibility and (designing for) fast response. You can also prepare for the general direction and trends. For future shipping fuels, this means:

- We can be certain that future fuels will be more expensive than past fuels. Fuel efficiency will gain in importance, in design and in operation. If you charter your ships out, expect charterers to focus more on fuel efficiency and to monitor ship performance more closely.
- Most of the discussed future fuels will require more tank capacity for same range and same general design. Again, fuel efficiency improvement may mitigate to some extent, but most likely concessions on tank space or range will be unavoidable in future designs.
- Design for flexibility in the machinery system (main and auxiliary engines, piping, tanks) to ease transitions to future fuels, e.g. with dual-fuel diesel engines, high-temperature fuel cells accepting a wider range of fuels.
- Monitor the technical, regulatory and economic developments for decarbonization closely to avoid being caught offside by any changes.

Acknowledgement

I thank the HIPER community for countless little pieces of information on decarbonization technologies, and in particular my colleague Pierre C. Sames for valuable discussions in structuring my thoughts and writing this paper.

References

ALAM, F.; DATE, A.; RASJIDIN, R.; MOBIN, S.; MORIA, H.; BAQUI, A. (2012), *Biofuel from Algae - Is It a Viable Alternative?*, Proc. Eng. 49, pp.221-227, <https://www.sciencedirect.com/science/article/pii/S1877705812047881/pdf?md5=53b91c0341cdb376b890a08383f22603&pid=1-s2.0-S1877705812047881-main.pdf>

- ANDERSSON, K.; SALAZAR, C. (2015), *Methanol as a Marine Fuel Report*, Methanol Institute, <http://www.methanol.org/wp-content/uploads/2018/03/FCBI-Methanol-Marine-Fuel-Report-Final-English.pdf>
- BAKHTOV, A. (2019), *Alternative fuels for shipping in the Baltic Sea Region*, HELCOM Report, <https://www.helcom.fi/wp-content/uploads/2019/10/HELCOM-EnviSUM-Alternative-fuels-for-ship-ping.pdf>
- DE NIJS, S. (2018), *Reducing the emissions of greenhouse gases from ships by using biofuel made from microalgae*, Master thesis, Ghent University, https://libstore.ugent.be/fulltxt/RUG01/002/479/472/RUG01-002479472_2018_0001_AC.pdf
- DE VRIES, N. (2019), *Safe and effective application of ammonia as a marine fuel*, Master thesis, TU Delft, <https://repository.tudelft.nl/islandora/object/uuid%3Abe8cbe0a-28ec-4bd9-8ad0-648de04649b8>
- DNV (2020), *Maritime Forecast to 2050: Energy Transition Outlook 2020*, DNV, Høvik, <https://download.dnvgl.com/eto-2020-download>
- ECKLE, P.; LANGGUTH, A.; NAKHLE, C. (2019), *Towards Net Zero - Innovating for a Carbon-Free Future of Shipping in the North and Baltic Sea*, ETH Zürich, <https://www.towardsnetzero.com/>
- ELLIS, J.; TANNEBERGER, K. (2015), *Ethyl and Methyl Alcohol as Alternative Fuels in Shipping*, Report for EMSA, SSPA, Gothenburg, <http://www.emsa.europa.eu/publications/download/4142/2726/23.html>
- FREIRE, L.O.; DE ANDRADE, D.A. (2015), *Historic survey on nuclear merchant ships*, Nuclear Engineering & Design 293, pp.176-186, <http://repositorio.ipen.br/bitstream/handle/123456789/25368/21261.pdf>
- GRAVINA, J.; BLAKE, J.I.R.; SHENOI, A.; TURNOCK, S.; HIRDARIS, S. (2013), *Concepts for a modular nuclear powered containership*, 17th Int. Conf. Ships and Shipping Research, Naples, <https://eprints.soton.ac.uk/351357/1/CONCEPTS%2520FOR%2520A%2520MODULAR%2520NUCLEAR%2520POWERED%2520CONTAINERSHIP.pdf>
- HANSSON, J.; BRYNOLF, S.; FRIDELL, E.; LEHTVEER, M. (2020), *The Potential Role of Ammonia as Marine Fuel - Based on Energy Systems Modeling and Multi-Criteria Decision Analysis*, Sustainability 12, 3265, <https://www.mdpi.com/2071-1050/12/8/3265>
- HOECKE, L.v.; LAFFINEUR, L.; CAMPE, R.; PERREAULT, P.; VERBRUGGEN, S.W.; LE-NAERTS, S. (2021), *Challenges in the Use of Hydrogen for Maritime Applications*, Energy Environ. Sci. 14, pp.815-843, <https://pubs.rsc.org/en/content/articlepdf/2021/ee/d0ee01545h>
- HSIEH, C.C.; FELBY, C. (2017), *Biofuels for the Marine Shipping Sector*, IEA Bioenergy, <https://www.ieabioenergy.com/wp-content/uploads/2018/02/Marine-biofuel-report-final-Oct-2017.pdf>
- IQBAL, M.I. (2017), *Methanol as an Alternative Fuel for Shipping*, Bachelor thesis, HS Wismar, <https://repository.its.ac.id/45379/>
- LUNDGREN, A.; WACHSMANN, A. (2014), *The Potential of Methanol as a Competitive Marine Fuel*, Diploma thesis, Chalmers University of Technology, Gothenburg, <https://odr.chalmers.se/bitstream/20.500.12380/204087/1/204087.pdf>

NN (2018), *Perspectives for the Use of Hydrogen as Fuel in Inland Shipping – A Feasibility Study*, MariGreen Report, Mariko, Leer, https://marigreen.eu/wordpress_marigreen/wp-content/uploads/2018/11/Hydrogen-Feasibility-Study-MariGreen.pdf

Appendix: Decoding the colour code of fuels and other terminology

The decarbonizing discussion has its own jargon. As always, jargon is practical for concise communication when you understand it, and annoying when you don't understand it.

Biofuels are rather straightforward and virtually everybody understands the basic concept. Sometimes, they are dubbed as 'green' fuels, as 'green' has become synonymous with environmentally friendly.

E-fuels are synthetic fuel generated from water, air, CO₂, etc., which are chemically split and recombined to form fuels like methane ("e-LNG"), ammonia, hydrogen, etc., with electric energy as input to the process. Most of the future fuels under current discussion are synthetic fuels. Although the fuels are generally colourless in reality, they appear with a whole rainbow of colours in texts and on presentations, depending on the how they were generated. Let's look for example at hydrogen:

- "Brown hydrogen" is produced using 'dirty' coal through coal gasification (sometimes also called 'black')
- "Green hydrogen" is produced using renewable energy, such as from wind power
- "Pink hydrogen" is produced using nuclear energy
- "Yellow hydrogen" is produced from solar power (but may also be called 'green')
- "Grey hydrogen" is produced from natural gas, leaving carbon waste
- "Blue hydrogen" is like grey hydrogen, but with CCS (carbon [dioxide] capture & storage, where the CO₂ is captured and stored, e.g. pumping it in liquefied from deep below the ocean bed; see e.g. <https://northernlightscs.com>)
- "Turquoise hydrogen" is hydrogen from natural gas using methane pyrolysis (also known as low-carbon hydrogen)
- "Orange hydrogen" is a blend of blue, grey, or green hydrogen

Visions and Sobering Reality in Maritime ICT

Volker Bertram, DNV, Hamburg/Germany, volker.bertram@dnv.com

Abstract

This paper presents a critical review of key ICT technologies used in the maritime industries. The techniques are Virtual Reality, Digital Twin, Big Data, Artificial Intelligence and Unmanned Ships. Each of these terms is frequently used and came with grand visions. In this paper, we look behind the high and mighty terms and see the sober reality behind. Often it is a case of false labelling or relabelling of more mundane, down-to-earth ICT applications.

1. Introduction

We are living in a phase of ‘digital transformation’. There is wide consensus on that, but beyond that, things become muddy and hazy. When did this phase start? How long do we expect it to last? And what is digital transformation, as opposed to digitization and digitalization? I suspect digital transformation is ‘groovy’, as nobody has been able to explain to me what exactly ‘groovy’ means either.

Most of us survive on poorly understood buzzwords, some of us thrive on them. If feeling disadvantaged, you may resort to agile internet-based tools in the industry 4.0 eco-system like <https://www.makebullshit.com/>. More advanced tools probably exist where you can feed in some keywords and out comes an impressive buzzword phrase. But your management may have beaten you to it already.

But often, it is also a case of taking a great idea, and starting by necessity on a much smaller scale. As in: “In the future, we shall boil the ocean, but as a proof-of-concept implementation of limited functionality, I will make a coffee.” In other cases, marketing (including scientific self-marketing) has cleverly redefined goals to present success stories: “We define advanced calculus here as the ability to add two arbitrary positive one-digit numbers.” Or intelligence as the ability to memorize 5 items, as in person, woman, man, camera, TV.

In the following, let’s have a look at some of these new high and mighty terms and see how far reality lags behind the visions created when these buzzwords were originally coined.

2. Buzzwords or more?

2.1. Big Data

Enter the first buzzword: Big Data. Let’s have a look at the definition of Big Data: “Big data is a field that treats [...] data sets that are too large or complex to be dealt with by traditional data-processing application software.” But most of the time, “much data” is meant when “Big Data” is used. As an example, we may collect automatic performance monitoring data from ships, and use some statistical analysis on those. 50 ships in our fleet, recording every 15 s a data set, each record consisting of 10 real numbers (speed, power, draft, trim, etc.). This makes some 1,000,000,000 numbers, or 4 GB in single precision. That can be transported on a plain USB stick and can be processed with standard software. It may take a while to open in Excel on a standard laptop, but reading and processing the data would be standard fare for a computer scientist. So, by definition, it shouldn’t be called Big Data. You don’t need distributed computers, working on subsets of the data to handle them at all, exchanging intermediate data to converge to a common result. As you would, for example, if it really were Big Data. Very likely, there are no Big Data applications in naval architecture and very few in shipbuilding and shipping.

In most cases, we have data-based analyses to derive information for decisions, Fig.1. But that sounds so mundane that one can understand the temptation to resort to the mighty “Big Data” incantation. I plead guilty to have fallen into that trap myself, *Krapp and Bertram (2016)*. Processing Gigabytes or even Terabytes of data does not in itself justify using the term Big Data, as we can process such amounts with conventional software and hardware. It may still be smart to use hierarchical data processing, especially when processing data from ship-board sensors before transmitting processed, and much more aggregated data via expensive internet channels to shore-based offices, but that is another story.

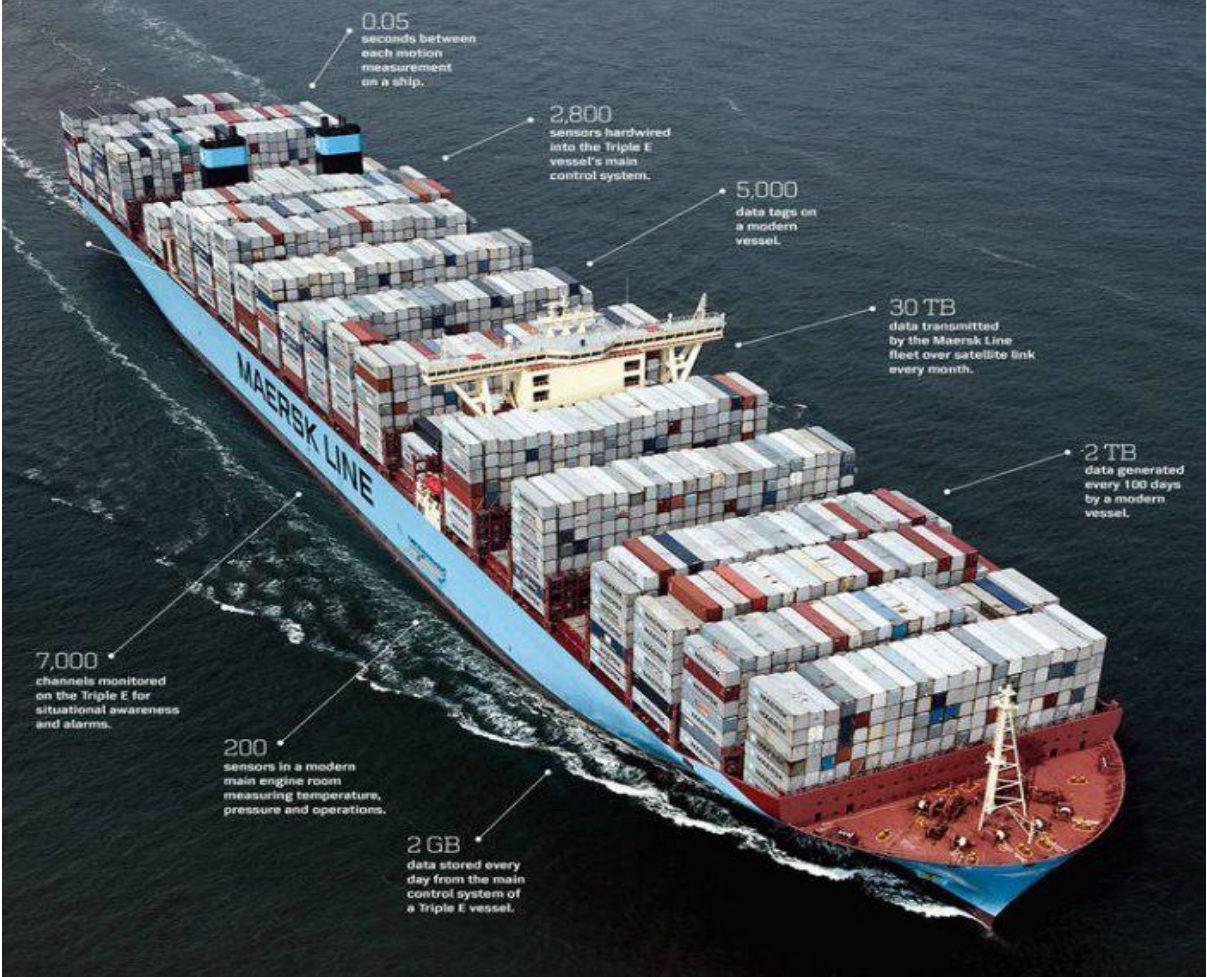


Fig.1: Processing Gigabytes or even Terabytes of data does not in itself mean “Big Data”

2.2. Artificial Intelligence

Another key buzzwords of our time is Artificial Intelligence, or A.I. as we really cool dudes call it. Alan Turing might be called the father of the concept of Artificial Intelligence, as he connected “computing” with “intelligence” in *Turing (1950)*. He proposed a machine (computer) that would converse so intelligently with humans that we wouldn’t be able to tell whether it is a machine or a human. So far, all attempts to pass this Turing Test have failed. But it was John McCarthy, who coined the expression “Artificial Intelligence” in 1955, and the term was widely adopted and favored over other contenders (machine intelligence, thinking machines, cybernetics, automata theory, complex information processing) after the 1956 [Dartmouth workshop](#). But even back then, A.I. experts couldn’t exactly define A.I.

Wikipedia defines A.I. as “intelligence demonstrated by machines, unlike the natural intelligence displayed by humans and animals”. The Oxford Dictionary defines A.I. as the development of computer systems able to “perform tasks normally requiring human intelligence”. So, is it like human

intelligence, or is it not? And what is human intelligence? Scientist still struggle with a clear definition of natural intelligence. But we have some common perceptions. Einstein was intelligent. And generally people who get Nobel prizes in physics must be very intelligent. So are top mathematicians, chess champions or world-class players of [Go](#), a 2500 year old board game sometimes called the Chinese chess.

But in 2016, the computer program [AlphaGo](#) beat some high-ranking professional Go players. The event made the world news, not least because AlphaGo had learned “by itself”, using artificial neural nets, a key technology of machine learning and thus A.I. In short, “self-taught A.I. computer beats best human”, and it (he?) had learned the game from scratch within 40 days. So, did we witness the coming out of a super-intelligence that would in due time mean the end of mankind, as many Hollywood movies have suggested? Not really. If AlphaGo were our child, we would start worrying. Five years later, AlphaGo still hasn’t shown any interest in learning anything else, say tic-tac-toe, or chess or Cluedo; it hasn’t shown any signs of common sense or come up with any smart ideas, or whatever we would associate with an intelligent child. On a human I.Q. test, A.I. software generally fares catastrophically badly, getting scores around 40, where below 70 is a sign of mental retardation. Ask “Which animal goes moo?” and AlphaGo will give it a pass.

We could try to argue that it is “alternative” intelligence. And indeed, if we re-define what we consider intelligent as an impressive feat performed and beyond what the human mind can do, A.I. fits the bill. But so does traditional computing. Adding up 1 million numbers without making a mistake, within seconds. If we look at the biggest part of A.I., namely machine learning and its applications (including voice and pattern recognition), it used to be called “numerical statistics”. That sounds immediately less groovy and less threatening than Artificial Intelligence, but you could put the A.I. sticker on any numerical statistics paper or application. Same thing, new label.

Numerical statistics is immensely powerful and, given enough and the right data, it can yield very powerful insight and enhance many applications in our field in the hands of intelligent engineers. Over the past two decades of COMPIT, I myself have presented many such possible applications, Fig.2, *Bertram (2000)*, *Mesbahi and Bertram (2000)*, *Bertram et al. (2016)*, *Bertram and Herradon (2016)*, but we should see A.I. as a sober engineering tool and not expect true intelligence as in Einstein’s out-of-the-box thinking from it. It is time to demystify A.I., *Bertram (2018)*.

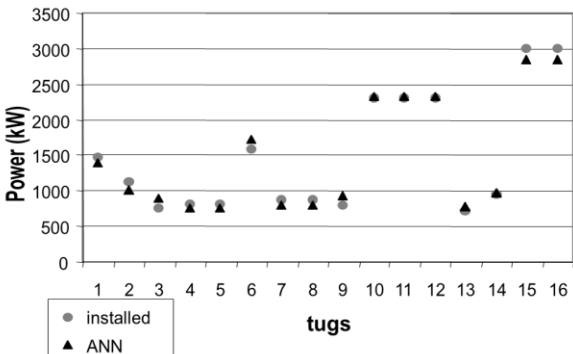


Fig.2: Artificial Intelligence is in most cases numerical statistics, immensely sensible like roomy underwear, but now with a sexier label

2.3. Unmanned ships

The vision of unmanned ships has been a recurrent theme at COMPIT for almost 20 years now, *Bertram (2003)*. But the whole theme really took off with an interview Oskar Levander (then Rolls-Royce) gave to the Financial Times in December 2013. The story went viral on the Internet and in print media, and invoked visions of large-scale unmanned shipping being imminent, Fig.3: “According to Rolls-Royce Marine, by 2030 autonomous ships will be a common sight on the oceans,” <https://www.raconteur.net/technology/autonomous-ships/>.



Fig.3: Vision of large-scale unmanned shipping by 2030, source: Rolls Royce



Fig.4: Likely reality, unmanned small ferries and tugs by 2030

Over time, not only ships got smarter, but also the maritime community. Most people now are more precise in their terminology, distinguishing between ‘unmanned’ (no crew on board, but under human command from a shore-based control centre) and ‘autonomous’ (controlled by software that acts independently, even if crew is on board; e.g. avoiding collisions if the crew does not act). While autonomous technology develops dynamically, the timelines and expectations for unmanned ships have sobered down significantly, e.g. *Bertram (2016)*, *Kooij and Hekkenberg (2019)*.

Unmanned ships need highly reliable systems on board, as there is no one on site to fix failures or perform maintenance. This is difficult to imagine with classical diesel propulsion with its many moving parts, even if cleaner fuels are used. In essence, the unmanned ship will be electrically powered. This makes the powering the limiting factor, rather than the information & communication technology. The key question is then: Can the ship take the kWh hurdle? How much power needs to be installed (mainly a matter of size and speed) and how far does the ship have to go before it can get recharged/refuelled. A containership with 50 MW power installed and a range of two weeks before refuelling would require excessive e-power and battery weight, Fig.4.

Even if we are much, much more modest, there remain significant hurdles to operating unmanned ships. The most advanced project today for unmanned cargo shipping is the [‘MV Yara Birkeland’](#). The ship has a capacity of 120 TEU and a service speed of 6 kn; i.e. the vessel is very small and very slow for a containership. The longest route it is intended to sail is 30 nm, thus very short. All this lowers the kWh hurdle to a tiny fraction of what a 10000 TEU containership, sailing at 17 kn between Hamburg and Singapore would need. Still, the vessel is at 25 million USD an estimated 3 times as expensive as a conventional ship of the same size would cost. Without massive subsidies from the Norwegian government, it would not have been built. The subsidies can be justified as research funding and the technical achievements still command respect, but the kWh hurdles and economic hurdles remain.

By 2030, we will see unmanned ships in civilian applications, but mainly for short-distance ferries, tugs, fire-fighting boats, maybe offshore supply vessels. We will also see autonomous ‘smart’ systems on board many ships, supporting nautical tasks and cargo supervision, for example. But it will probably take another 20-30 years before we see wider adoption of international (e.g. transpacific) unmanned cargo shipping, *Bertram (2016)*. Another case where the vision is far ahead of reality.

2.4. Digital Twin

Enter the ‘Digital Twin’, another recent buzzword. Wikipedia defines a Digital Twin as “a real-time digital replica of a physical device”. Siemens elaborates on this to give “a smart (dynamic), virtual representation (model) of the physical product, production process, or product’s utilization. It has the required accuracy and fidelity to predict actual, physical performance”, Fig.5. In simple terms, the vision was some IT model with the look and feel of the real deal. Not only would it look like its

physical twin (this would be mere Computer-Generated Imagery or Virtual Reality), but it would behave like its physical twin and evolve in time like it. The Digital Twin of a ship would lose strength in time as it rusts, slow down as the hull gets fouled, vibrate according to the propeller and engine excitation, etc.

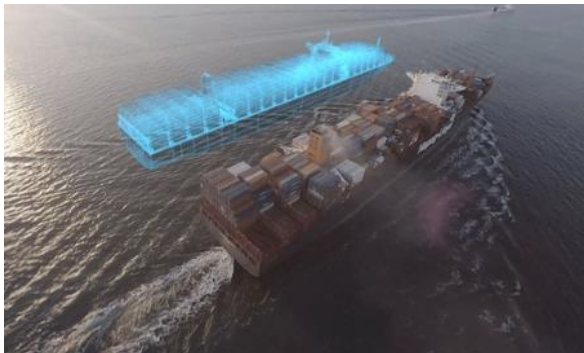


Fig.5: Digital Twin vision

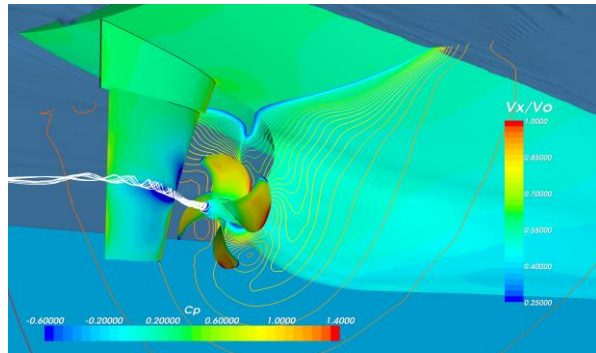


Fig.6: Typical hydrodynamic simulation model

Industry reality is much less ambitious. We now use the term “Digital Twin” where some years ago we would have used “simulation”, e.g. *Bertram (2004)*, *Peric and Bertram (2011)*, *Bertram and Peric (2013)*. Digital model (for simulation) would be much more appropriate as a term, *Cabos and Rostock (2018)*. The discrepancy between vision and reality is so large that one could speak of false labelling:

- Most often, ‘Digital Twins’ model geometrically only a small part of the real counterpart, e.g. only the underwater hull and propeller for hydrodynamic simulations, Fig.6.
- Most often, ‘Digital Twins’ simulate only one specific behaviour, e.g. calm-water propulsion, seakeeping in waves, static strength of steel structure, vibration of structure, etc. For each application, another model is needed due to different requirements of the numerical methods and different purposes of the simulations.
- Most often, ‘Digital Twins’ do not evolve in time. Instead, now we see expressions such as ‘design Digital Twin’ or ‘production Digital Twin’, indicating that this twin will expire once its real counterpart is delivered to the ship owner.

2.5. Virtual Reality

The term ‘Virtual Reality’ was coined by Jaron Lanier in the late 1980s. His vision for fully immersive Virtual Reality (VR) was a digital technology that allowed users to experience artificial environments as the real world, to the point where the difference between the virtual world and the real world could no longer be realised. You see, you hear, you smell, you taste, you feel. In short, the vision was akin to the Holodeck in *Star Trek*, the Holy Grail of the Virtual Reality community. You get kicked and your ribs break – and you hear the crack and you hurt, Fig.7.

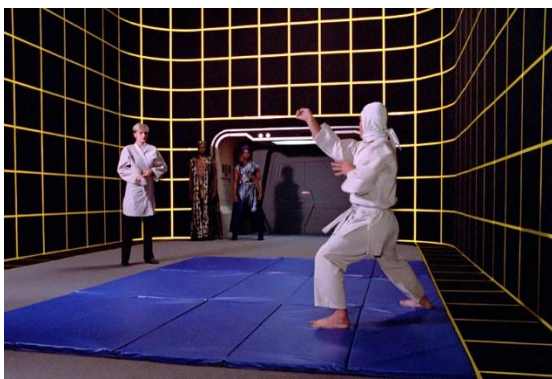


Fig.7: The Holy Grail of VR: The Holodeck; you get kicked, your ribs break



Fig.8: Current reality, (maybe) 3D viewing & walk-around with some high-res graphics

Beier (2000) described how this grand vision got reduced to something much more modest and tangible, namely a 3D computer model with walk-around capabilities: “The term Virtual Reality initially referred to [...] fully] immersive systems. With time, the meaning of VR broadened and, as of today, VR is also being used for semi-immersive systems, [...] even non-immersive systems, like monitor-based viewing of three-dimensional objects.”

The down-to-earth VR is useful for many applications in our industry, mainly in understanding and selling designs to training and marketing, Figs.9 and 10. Many papers in 20 years of COMPIT bear witness to that. But if we take a closer look at how much VR is really used in industry, beyond the smoke screen of marketing appearances and feasibility studies, the uptake of the technology, even in its much more mundane re-definition, is sobering for any VR aficionado, *Bertram and Plowman (2018)*. The vision is still far ahead of reality.



Fig.9: Training application of VR



Fig.10: Marketing application of VR, source: Lloyd’s Register

2.6. Other

But wait, there is more to come... Marketing is always ahead of the game and the engineers and programmers in the R&D departments. Just a few examples shall be given:

- 3D printing (additive manufacturing) came with grand visions. “The ONR (Office of Naval Research) of the US Navy published a report to explore the possibility of producing the whole ship using 3D printing,” in *Matsuo (2018)*. Possibly you could, but would it yield ship structures of same strength at lower prices than current welding technology? The maritime applications so far are for structures with low strength requirements, such as boats, Fig.11, where fibre-reinforced plastics and wood are also options.



Fig.11: 3D printed boat

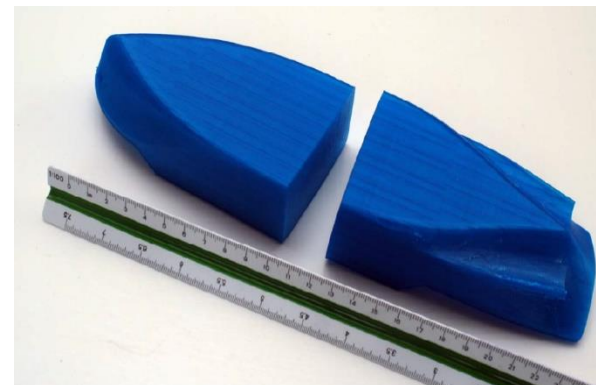


Fig.12: 3D printed demo model, Source: SARC

The best arguments for 3D printing in the maritime industry are for spare parts of limited lifetime, where a broken part in some machinery can be 3D printed on board as a quick repair

to continue operation. As a marketing gadget or as scaled-down model for discussion with customers, 3D printing may come in handy, Fig.12, *Koelman (2013)*. Afficionados of a technology focus on what is feasible, not what makes economic sense. And even the 3D printing aficionados admit “that the vision of 3D printing an entire ship is (still) somewhat into the future,” *NN (2017)*.

- Enter Industry 4.0. “Industry 4.0 refers to the transformation of industry through the intelligent networking of machines and processes with the help of information and communication technology (ICT). The term is used interchangeably with the 'fourth industrial revolution' in industry,” <https://www.i-scoop.eu/industry-4-0/>. Which sounds good, except that at least in the maritime industry the factories (shipyards) are mostly too small to recover the required investment into further robotization and the unfortunate policies of closed data formats creates interfacing barriers, *Danese and Vannas (2020)*. Fast internet connections of ‘things’ are fairly useless, unless the ‘things’ can communicate in a common language to exchange information. We have promising ideas, but they will take time to enter the industry and take hold in daily practice. The vision is once again far ahead...
- Enter PLM. “In industry, product lifecycle management (PLM) is the process of managing the entire lifecycle of a product from inception, through engineering design and manufacture, to service and disposal of manufactured products,” [Wikipedia](#). Of course, this can be synchronised in an agile solution, etc. But apart from the mandatory inventory of hazardous materials (IHM), the reality is that a ship has at least two lives in terms of product data models: It grows from inception (= concept design) to manufacture (= shipyard assembly) and then dies, with a minimum of information passed on to the customer (= ship owner), often in the form of paper. During service (=operation), we may see occasional creation of new island solutions for product models, but these most often also die when the ship is passed on to a charterer or sold to the next owner. But if we redefine ‘disposal’ as meaning ‘delivery’ by the shipyard, we have some nice PLM solutions on the market.

I am sure that the list could be continued with many more examples of where we have boastful claims and visions far ahead of industry reality.

3. Conclusions

The glass is half full or the glass is half empty. All technologies discussed have progressed in the past 20 years, and often we have also progressed towards a realistic understanding of what is (at present) meant by a certain buzzword, what it can do, and what its limitations are. Realistically, we should also be resigned to the use of more new buzzwords for concepts that have been around for a long time, and to marketing departments promising us far more than production can actually deliver. Let’s be grateful for the occasional contribution to this conference that takes a sceptical point of view and is not fooled by the misuse of widely accepted buzzwords.

References

BEIER, K.P. (2000), *Web-based virtual reality in design and manufacturing*, 1st COMPIT Conf., Potsdam, pp.45-55, http://data.hiper-conf.info/compit2000_potsdam.pdf

BERTRAM, V. (2000), *Expert systems in ship design and ship operation*, 1st COMPIT Conf., Potsdam, pp.63-71, http://data.hiper-conf.info/compit2000_potsdam.pdf

BERTRAM, V. (2003), *Cyber-ships – Science fiction and reality*, 2nd COMPIT Conf., Hamburg, pp.336-349, http://data.hiper-conf.info/compit2003_hamburg.pdf

BERTRAM, V. (2004), *Towards intelligent simulation-based design*, 3rd COMPIT Conf., Sigüenza, pp.5-16, http://data.hiper-conf.info/compit2004_siguenza.pdf

- BERTRAM, V. (2016), *Unmanned & Autonomous Shipping – A Technology Review*, 10th HIPER Conf., Cortona, pp.10-24, http://data.hiper-conf.info/Hiper2016_Cortona.pdf
- BERTRAM, V. (2018), *Demystify Artificial Intelligence for maritime applications*, 17th COMPIT Conf., Pavone, pp.22-35, http://data.hiper-conf.info/compit2018_pavone.pdf
- BERTRAM, V.; HERRADON, E. (2016), *Predicting added resistance in wind and waves employing Artificial Neural Nets*, 1st Hull Performance & Insight Conf. (HullPIC), Pavone, pp.14-22, <http://data.hullpic.info/HullPIC2016.pdf>
- BERTRAM, V.; PERIC, M. (2013), *Advanced Simulations for Offshore Industry Applications*, 12th COMPIT Conf., Cortona, pp.7-20, http://data.hiper-conf.info/compit2013_cortona.pdf
- BERTRAM, V.; PLOWMAN, T. (2018), *Virtual Reality for Maritime Training – A Survey*, 17th COMPIT Conf., Pavone, pp.7-21, http://data.hiper-conf.info/compit2018_pavone.pdf
- BERTRAM, V.; SÖDING, H.; MESBAHI, E. (2007), *PDSTRIP fin and sails treatment – Physics and expert knowledge*, 6th COMPIT Conf., Cortona, pp.5-18, http://data.hiper-conf.info/compit2007_cortona.pdf
- CABOS, C.; ROSTOCK, C. (2018), *Digital Model or Digital Twin?*, 17th COMPIT Conf., Pavone, pp.403-411, http://data.hiper-conf.info/compit2018_pavone.pdf
- DANESE, N.; VANNAS, A. (2020), *Intelligent Industrial Internet of Things & Services (IIoT&S): An Innovative, Plug & Play, High-ROI Approach for The Extended Enterprise*, 12th HIPER Conf., Cortona, pp.359-375, http://data.hiper-conf.info/Hiper2020_Cortona.pdf
- KOELMAN, H. (2013), *A Mid-Term Outlook on Computer Aided Ship Design*, 12th COMPIT Conf., Cortona, pp.110-119, http://data.hiper-conf.info/compit2013_cortona.pdf
- KOOIJ, C.; HEKKENBERG, R. (2019), *Towards Unmanned Cargo-Ships: The Effects of Automating Navigational Tasks on Crewing Levels*, 18th COMPIT Conf., Tullamore, pp.104-117, http://data.hiper-conf.info/compit2019_tullamore.pdf
- KRAPP, A.; BERTRAM, V. (2015), *Hull performance monitoring – Combining Big Data and simulation*, 14th COMPIT Conf., Ulrichshusen, pp.57-63, http://data.hiper-conf.info/compit2015_ulrichshusen.pdf
- MATSUO, K. (2018), *Technology Mega Trends That Will Change Shipbuilding*, 17th COMPIT Conf., Pavone, pp.153-162, http://data.hiper-conf.info/compit2018_pavone.pdf
- MESBAHI, E.; BERTRAM, V. (2000), *Empirical design formulae using artificial neural nets*, 1st COMPIT, Potsdam, pp.292-301, http://data.hiper-conf.info/compit2000_potsdam.pdf
- NN (2017), *The Opportunity Space of 3D Print in the Maritime Industry*, Green Ship of the Future, Copenhagen, <https://greenship.org/wp-content/uploads/2017/01/The-maritime-opportunity-space-of-3D-print.pdf>
- PERIC, M.; BERTRAM, V. (2011), *Trends in industry applications of CFD for maritime flows*, 10th COMPIT Conf., Berlin, pp.8-18, http://data.hiper-conf.info/compit2011_berlin.pdf
- TURING, A.M. (1950), *Computing Machinery and Intelligence*, Mind 49, pp.433-460, <https://academic.oup.com/mind/article/LIX/236/433/986238>

Internet of Ships - Just a Philosophical Approach?

Rodrigo Pérez Fernández, SENER, Madrid/Spain, rodrigo.fernandez@sener.es

Abstract

The aim of this paper is to explain how to implement a technological revolution in the design and production phases in order to build efficient, safe and sustainable vessels. In a decentralized sector, like naval, where often the engineering and production are in different locations and where critical decisions cannot wait, the Internet of Ships (IoS) or connection through the network of critical components in the design / shipbuilding, starts to glimpse as something that the sector cannot obviate. The idea is to monitor all those parts in which early detection of events allows us to make the right decisions. In this sense, the available sensors during the early stages of construction of the ship, allow us to identify if the construction of the boat is completely according to the design we have created with CAD. If we can reduce materials or use another material, if we must change anything according with naval architecture calculations... The continuous monitoring integrated with a naval design CAD will reduce costs and avoid mistakes and make decisions in real time from the shipyard, design offices or from remote locations. Shipbuilding process, generates a lot of information and data, which a priori makes it seem impossible to have all this data in real time, but the new processors, simpler and smaller, with a good connection to the Internet, make it possible. The growth of the IoS is linked to the increase of Information and the management of big data, with the property that somehow IoS identifies Information and direction and order to a specific purpose, while the concept of big data is more generic. The possibilities are countless, but the beginning is the same. It must begin in the initial design. It is necessary to consider what is needed to correctly fulfill the mission of the atomic elements. These requirements must be configurable in the initial design from where it will be extended to relations between each of them with other entities. CAD is one of the first steps, because it is where begins to collect systematically the concept of each component. That is why it is necessary to provide CAD tools to carry out the design for IoS.

1. Introduction to the future of the shipbuilding CAD systems

There are several fields where CAD systems could improve in the near future. However, here the focus is on functionalities that are being improved right now. E.g. in hull forms fairing, the global shape modelling or the advance continuity and capping could transform complex surfaces with excellent results, less interaction, high accuracy, and full control. These techniques shorten dramatically the design time, from days to minutes while obtaining excellent results, *Pérez and Penas (2015)*.

Another area of improvement concerns one of the most time-consuming tasks in outfitting design, the routing of pipes, HVAC ducts and cable trays. Automatic routing options minimize this time, but without reducing the robustness of the design. Automatic routing provides simple solutions, with optimization of material, and several algorithms exist. But the matter is not only to consider existing elements for future routings; it is also necessary to assign priorities, and eventually handle automatic modifications of existing elements as a consequence of new ones. The complexity of the problem explains that there is not yet fully satisfactory solution for the automatic routing in practice. Current solutions provided by CAD systems solve partial problems, offering already significant support.

Another area where the CAD companies are active is Virtual Reality. The objective is to create a user-friendly environment in order to review, audit, obtain metrics such as the progress of a project, etc. This type of review process of the model does not need to use tools for designing, just a simplified tool allowing easy access (viewer). In Fig.1, a 3D visualization model is reviewed in a software, where the authorized designers/engineers could have all the project information. These navigators allow access for reading 3D information in order to load the component tree of any customer project to obtain information about any item. Other basic tools available in these programs have different modes, allowing navigation commands to take action such as measuring distances or angles, creating sections

to access internal components, etc. The interface with the program is via a mouse, but Virtual Reality opens windows of opportunities, with globes, glasses or helmets.

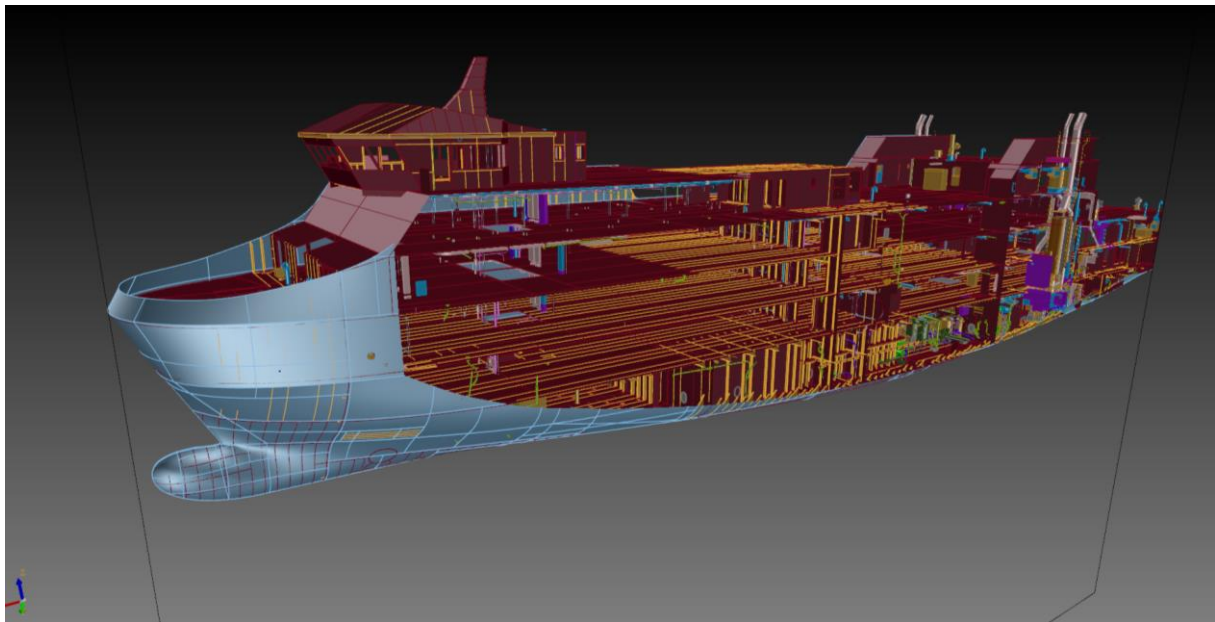


Fig.1: 3D representation of a ferry in a complete CAD tool

Advanced browsers allow incorporating human models in order to study ergonomic aspects, creating highlights and textures for advanced renders, movements of components to perform simulations, etc. Browsers can connect to the database of a project in order to access information in real time. Sometimes there is a need to take information from an on-line database and if there is an Ethernet network through the shipyard, it is possible to implement a shared computer with a viewer that allows connecting to a project. If there is not an accessible database, viewers should be able to read files with the project information required for 3D modelling of the product and component data with optimal performance. So far it was prevalent to implement viewers on laptops, because laptops are usually equipped with processor and graphics cards that allow navigating through the entire project. In recent years there has been a breakthrough in mobile devices like tablets or smartphones. This hardware progressively incorporates new processors that enable enhanced graphics. On the software side, operating systems have been developed specially adapted for such devices (such as Android or IOS) allowing interfacing naturally by touch gestures.

The widespread use of these devices nowadays has precipitated its use by software companies. Software developers have taken their time preparing oriented solutions and among those that allow us to have project plans or 3D models on tablets or others electronic displays. In modern projects, there is the need, for technicians, to carry these devices to work better, with a quickly access the 3D model of the project, with all parts information and construction drawings needed. A wi-fi connection would allow connecting to an information server to be updating the information needed, mainly in files, as for example: 3D models, classification, or production drawings, between others. Another advantage of mobile devices is that the user interface might interact with the project model or parts using gestures just as everybody does every day with smartphones. One implementation line of navigator's evolution would incorporate augmented reality technology. It would be helpful for production technicians to scroll through the project and pointing the camera of their mobile device to a particular component to obtain information from it and have the actual image of the same 3D design model displayed. This is possible through the use of markers that help the device to position itself within the project and also for the use of QR codes.

CAD systems must handle the information necessary for creating a collision-free design and for generating all production and assembly information, but not only this. The 3D model information is, at

the same time, necessary for other activities and other departments involved in the construction of the ship, as planning, purchasing, subcontracting, accounting, etc. It is common that several design agents collaborate in the same project; so, it is necessary that 3D model information should be shared between them to serve as reference. The paradigm of this problem appears when two or more design agents collaborate in the same project, using different CAD tools. In this case, the CAD systems must provide data exchange between them, leading to different degrees of integration, like visualization, spatial integration and cross manufacturing, depending on the characteristics and size of 3D model information transferred. At least, it should be geometry and key attributes. A worldwide format for data transfer has not yet been found. Despite recognized international standards, in most cases we see dedicated formats or particular adaptations from standard ones. Transfer of 3D model information could produce loss of performance due to different geometrical approaches to represent elements in both CAD systems. In this case, special solutions must be adopted in order to minimize this impact.

Another recent milestone is the integration between different CAD systems and Product Lifecycle Management (PLM) tools, e.g. the FORAN Product Lifecycle Management (FPLM) tool with a neutral architecture. In this case, all the information generated in the CAD may be transferred to a PLM and may be subject to all processes: control, configuration and releases lifecycle and process management. FPLM consists of a series of tools and features that enable bidirectional integration between different modules of the CAD and PLM tools. The solution is based on standards such as XML, Web Services and Common Object Request Broker Architecture (CORBA). Fig.2 shows an example of tool integration. The colors highlight parts or elements that are or are not to be transferred to PLM.

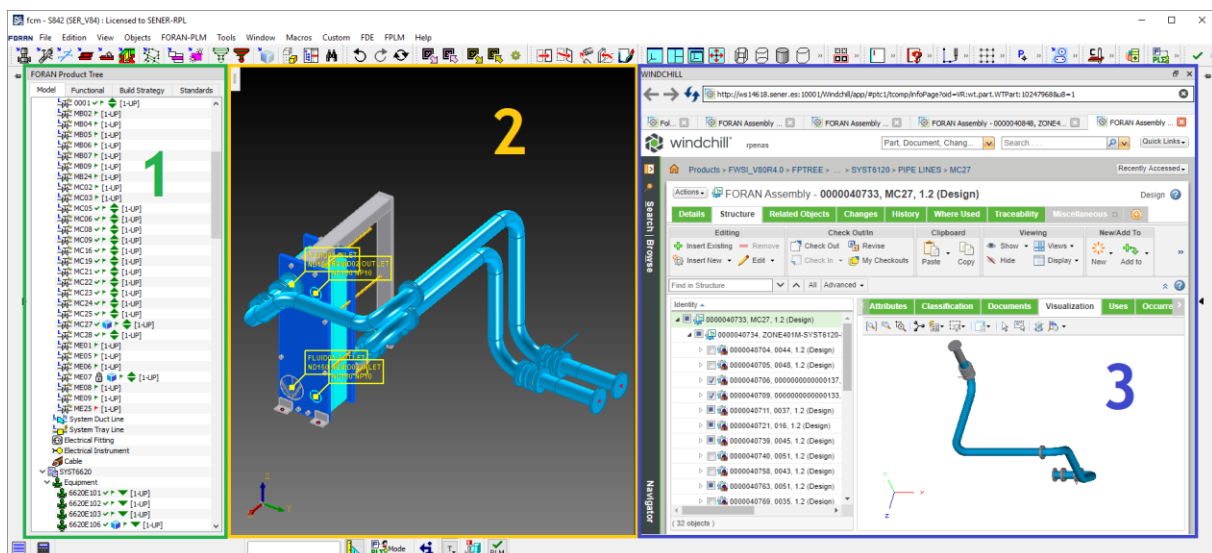


Fig. 2: Example of integration between a CAD system and a Project Lifecycle Management tool

There are many advantages of using CAD in shipbuilding: ease of design, speed of construction, use and reuse of information, etc. It is expected that in the future CAD tools will advance further and allow greater information management and virtual access through smart devices. In general, CAD systems provide tangible benefits while the process is optimized, reducing design time and production, and therefore costs.

2. What is IoT and how to be applied on the software world?

IoT is the abbreviation of Internet of Things which is known as technology and process of connecting objects to internet. The objective is to make objects exchange data with internet and among each other, *Benayas and Pérez (2018)*.

The concept IoT was born in the research center Auto ID in MIT around 1999 in research for realizing the object identification using radio frequency (RFID) which is the main idea of Kevin Ashton. The

idea of the research was to identify all the objects and all the people in some way permitting some of the objects could exchange data with others through internet. The object identification was the prerequisite of IoT.

Humans interact with objects in a more or less direct way. But if the objects are allowed to interact among each other, it would be possible that the objects themselves can exchange data for their own needs. This would create a network of Smart Objects that they can interact independently in the context of its mission. This network is known as IoT. The “Intelligence” property of objects or devices does not need to be complex and exhaustive. For example, a refrigerator would require a way of measurement of the elements which can get information of the refrigerant and request recharge when it is lower than required. These examples clearly show what is intelligence of the devices.

To make connectivity it is required to meet certain requirements among which exclusive identification is one of the requirements. But more importantly, it is necessary to determine whether the object is connected to the global network. The object will be related to its mission, but also be related to the needs of the object such that the object can fulfill its mission.

The connectivity of objects requires several technical properties: hardware, the connection method and software. Hardware are physical devices that are “intelligent” and software are intelligent programs for the object and connection method is way with which objects can communicate through physical devices or virtual devices (for instance radio frequency, wireless etc.). Obviously, this is a very simply description of connection, but it is enough for illustrating the components involving in this concept.

The following four aspects can identify whether a product is connected to the IoT:

- Be able to monitor the use and function of the product or object.
- Be able to be operated remotely or designed appropriately for their use.
- Be able to be diagnosed predictively, repaired or improve its performance.
- Combination of the above.

There is enormous potential growth. In this area and it can induce extraordinary potential economic growth. Report from the McKinsey Global Institute titled “disruptive Technologies: Advances that will transform Life, Business, and the Global Economy”, *McKinsey (2013)* concludes that the economic impact of IoT in 2015 has a potential annual growth of 2.7-6.2 billion dollars. Furthermore, it predicts that 80%-100% of the market of manufacturing will use IoT applications with an economic impact of 0.9-2.3 billion dollars, *McKinsey (2015)*.

All economic sectors will be affected by this revolution. It will be the software world without any doubt, and it will be also the case for the shipbuilding. The ship itself and all its elements will join the connection. What can be done is an extraordinary field.

The meaning of objects in IoT should not only be limited to physical objects. The concept can be extended to those programs called “virtual objects” and do not have a physical element in the world no objects exist. Accordingly, we can know what the programs for IoT should be. In particular, how should the programs be oriented in the world of IoT.

We can find several origins of the IoT programs. When a program suddenly stops working and indicates that there is a problem and that if we want to transmit the diagnostic information to the supplier. That is an emergent IoT, although in this case requires user’s acceptance. In other levels this acceptance is configurable, and it will be automatic.

These concepts can be applied not only to objects and devices but also to their own CAD programs.

3. A new concept - The internet of ships

According to Juniper Research's latest report, the number of IoT devices in 2021 will reach the eye-opening 46 billion. For comparison, this is a 200% increase compared to 2016. Many more will arrive, very fast and it seems that 2021 will be the year in which we will see the definitive takeoff of 5G. This revolution that began a few years ago has aroused enormous interest in all industries and in some of them already works with apparent normality.

Nowadays it is possible to order directly from our refrigerator as soon as it detects that we need our regular products or smart lamps that light up alone when needed lighting.

The world goes on steadily toward what will be undoubtedly one of the most important revolutions in the history of humanity.

We could define the IoT as consolidation through the network of networks a network that staying a multitude of objects or devices, that means, to connect all things of this world to a network, we are talking about vehicles, appliances, mechanical devices, or simply objects such as shoes, furniture, luggage, measuring devices, biosensors, or anything that we can imagine.

At its core, IoT is simple: it's about connecting devices over the internet, letting them talk to us, applications, and each other. But IoT is more than smart homes and connected appliances, however. It scales up to include smart cities – think of connected traffic signals that monitor utility use, or smart bins that signal when they need to be emptied – and industry, with connected sensors for everything from tracking parts to monitoring crops.

In this context the question is if the naval sector is ready for this revolution. Is it possible that this traditional and conservative sector moves into this technology?

There is already evidence that the shipbuilding industry is no stranger to these developments and is already connected to the Internet some components of ships, Fig.3.

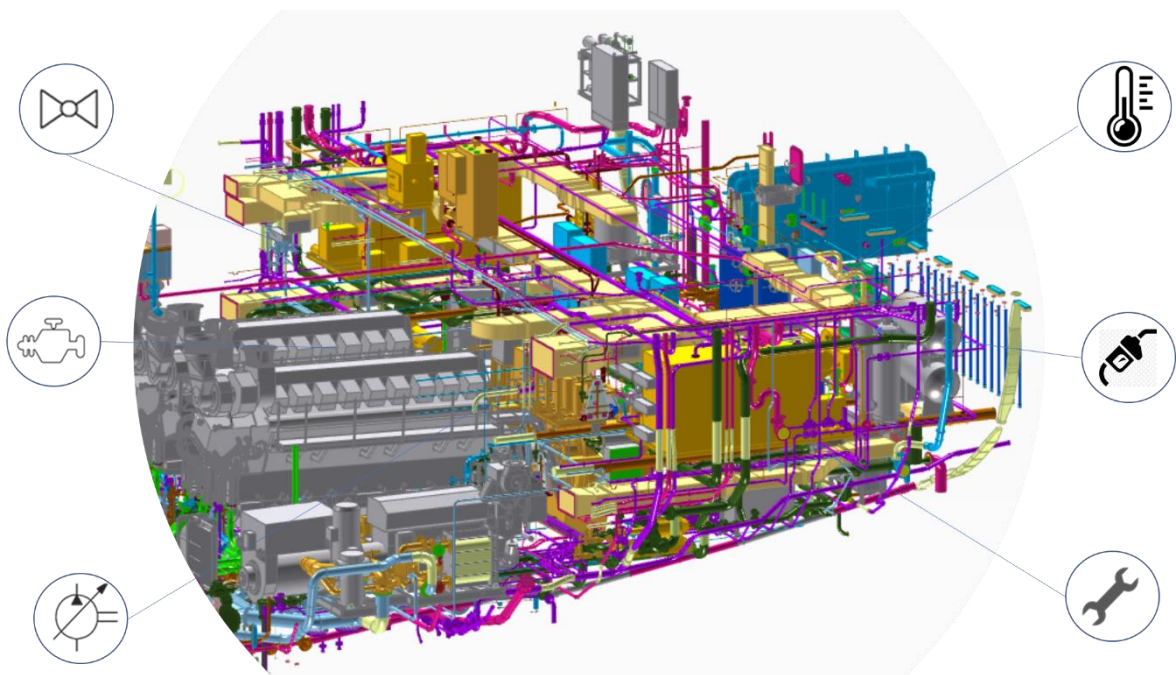


Fig.3: 3D model with access to the different components of the ship connected to IoT

As there are smart homes, there are new smart ships that will be equipped with a network of sensors that capture a range of voyage information, including:

- Location
- Weather
- Ocean current
- Status of on-board equipment and cargo

Ship owners can monitor the vessel's status in real time and apply analytics to current and historical data to make decisions that enable them to run more efficiently, saving time and fuel.

Sensors and IT technologies are facilitating the introduction of new applications at sea, like energy distribution, water control and treatment, equipment monitoring in real time...

The aim is to take this technological revolution also acting in the design and production phases in order to build efficient, safe and sustainable vessels.

In a decentralized sector, like naval, where often the engineering and production are in different locations and where critical decisions cannot wait, the Internet of Ships (IoS) or connection through the network of critical components in the design / shipbuilding, starts to glimpse as something that the sector cannot obviate.

The idea is to monitor all those parts in which early detection of events allows us to make the right decisions.

In this sense, the available sensors during the early stages of construction of the ship, allow us to identify if the construction of the boat is completely according to the design we have created with CAD. If we can reduce materials or use another material, if we must change anything according with naval architecture calculations...

The continuous monitoring integrated with a marine design CAD system will reduce costs and avoid mistakes and make decisions in real time from the shipyard, design offices or from remote locations.

Nowadays CAD solutions can be used in a pocket tools, making it the indispensable ally in this new technological revolution, Fig.4.

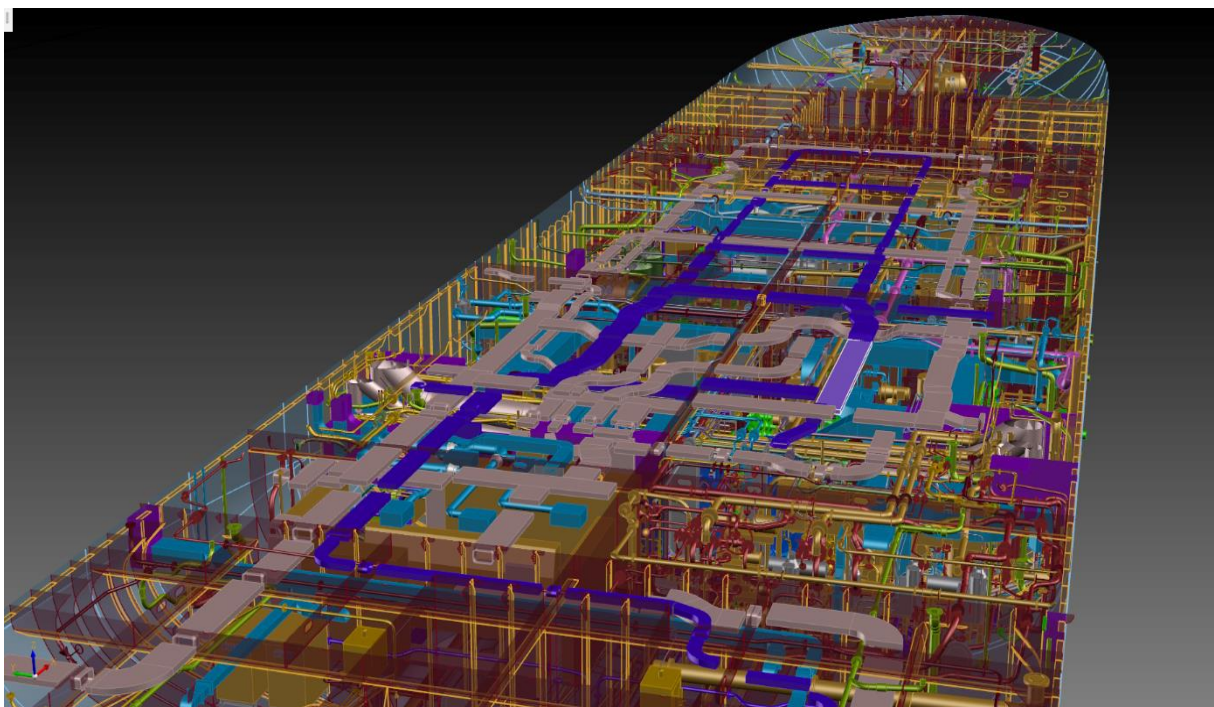


Fig.4: 3D model on a virtual portable solution like tablets or smartphones

Shipbuilding process generates a lot of information and data, which a priori makes it seem impossible to have all this data in real time, but the new processors, simpler and smaller, with a good connection to the Internet, make it possible.

The data management is, however, only one side of the coin of the IoS. Energy efficiency is a fundamental aspect also in new devices that connect to the network.

But IoS not only covers the stages of design or production of the boat. Once the sensors are in the components whose information want to monitor, we will be able to obtain information throughout the life of the ship.

IoS is presented as a solution capable of detecting when a component on a boat is close to fail and must be replace, when we take the boat to repair when we have to paint again, when corrosion has reached a certain limit ... and all this from our pocket tool and early enough to avoid late or unforeseen performances.

IoS reaches this sector to ensure profitable production, or safe, efficient and sustainable process for all types of fishing vessels, tugboats, tankers, charges, ferries, dredgers and oceanographic ...

4. The IoS in a cad shipbuilding environment

How this revolution could affect the shipbuilding world? Could we consider the concept IoS, *Muñoz and Pérez (2017)*?

The ship projects are developed with CAD platforms, but every day we are looking for integrated development of the product involving all its Life Cycle. CAD system integrated with PLM and from the PLM we can conceive all the design but also control the production and include the use of the vessel.

The PLM can contain information of all systems of the vessel and also all its components. If the components are designed for the IoS it will have technology that allows to share their situation, diagnosis, functionality with the PLM system which distributes the initial design.

The PLM system can use this information for knowing whether they are working properly or if we can improve its performance. It is also possible to identify whether it is necessary to make maintenance of the object or if it is necessary to replace it because its life ends or because it's working wrongly. It will be possible to determine and evaluate its performance comparing to other similar components or comparing to it different operating periods. It will also be possible to know how their performance affects the functioning of the whole product, i.e., the vessel. Furthermore, if the connection of the objects is realized with its PLM, *Pérez and Penas (2015)*, it would be possible to record their history status, make change tracking, and know what its function or its performance is after realizing programmed maintenance.

In case of a vessel, this connectivity will be extended to the commercial mission to act autonomously in operation conditions. A commercial vessel can transmit its navigation situation, load situation, the things to be discharged or to be recharged.

All these means a huge amount of information to be managed and analyzed. New programs have to be developed to obtain the best use of such information so that the design can be improved from real function information of the design and it can be self-maintained with the connection with this huge cloud information to create method that the objects can achieve certain "intelligence".

The growth of the IoS is linked to the increase of Information and the management of big data, with the property that somehow IoS identifies Information and direction and order to a specific purpose, while the concept of big data is more generic.

The possibilities are countless, but the beginning is the same. It must begin in the initial design. It is necessary to consider what is needed to correctly fulfill the mission of the atomic elements. These requirements must be configurable in the initial design from where it will be extended to relations between each of them with other entities. CAD is one of the first steps, because it is where begins to collect systematically the concept of each component. That is why it is necessary to provide CAD tools to carry out the design for IoS.

References

BENAYAS, A.; PÉREZ, R. (2018), *RFID tagging for a connected shipyard*, The Innovation in Shipbuilding - A supplement to The Naval Architect, pp.22-23

McKINSEY (2013), *Disruptive Technologies: Advances that will Transform Life, Business, and the Global Economy*, McKinsey Global Institute, May

McKINSEY (2015), *The Internet of Things: Mapping the Value Beyond the Hype*, McKinsey Global Institute, June

MUÑOZ, J.A.; PÉREZ, R. (2017), *The Internet of Ships: a new design for Smart Ship*, The Naval Architect, January, pp.26-30

PÉREZ, R.; PENAS, R. (2015), *Integration between shipbuilding CAD Systems and a generic PLM tool in naval projects*, Computer Science and Applications 2/5, pp.181-191

Robotic Hull Cleaning – State of the Art and Roadmap

Volker Bertram, DNV, Hamburg/Germany, volker.bertram@dnv.com

Abstract

This paper describes the development of robotic hull cleaning from academic research in the 1980s to current industry standard, including likely further paths of developments towards mass-produced, standardized robotic designs with more advanced capabilities.

1. Introduction

In the quest for future, more sustainable hull management strategies, some of the most promising contenders involve frequent ‘pro-active cleaning’ or ‘grooming’ to remove the biofouling at an early stage, e.g. *Oftedahl and Enström (2020)*, *Hunsucker et al. (2018)*, *Swain et al. (2020)*. “Frequent” may mean every two weeks, to give an idea. Such frequent cleaning would remove biofilms before advanced calcareous fouling can develop, addressing issues of aquatic invasive species and energy efficiency at the same time. In order to be widely available and affordable, such proactive cleaning would have to be largely robotic.

The required technologies have been coming together, recently maturing to commercial applications. Perhaps the appearance of a dedicated Wikipedia site on in-water cleaning can be seen as a sign of the generally larger interest in the theme: https://en.wikipedia.org/wiki/In-water_surface_cleaning. We may be at the dawn of a new era of mechanical cleaning (by robots), *Bertram (2020)*.

2. Diversity and fragmentation in a young industry

In-water cleaning robots come in a large variety of designs/concepts and are usually one-of-a-kind productions. This fragmented approach with its lack of standardization is typical for young industries. (Most of the developments started within the last decade). *Noordstrand (2020)* discusses the typical issues of young industries afflicting currently the in-water robotic cleaning market.

The current state of the industry with its design diversity has various reasons:

- The appropriate cleaning approach depends on the paint coating used on the hull, e.g. soft dissolving self-polishing copolymer paints, mechanically sensitive foul release coatings, or hard varnishes.
- The in-water cleaning industry is highly fragmented and relatively small in total volume. The market leader for robotic in-water cleaning, [HullWiper](#), is at best a small-to-medium enterprise with less than 50 employees.
- Cleaning companies develop their own designs and build or have them built in near-by workshops, in a “do-it-yourself” style typical for young industries. (Think of how the first automobiles or PCs were designed and built in private garages.)
- There are no standards yet for design or production of such robots.

With time, we should see some consolidation of market and robot designs as we did for other industries (automotive, airplanes, PCs, ...).

Eventually, we may see dedicated in-water robot cleaning robot manufacturers supplying the service providers with mass produced or at least mini-series produced robots, possibly with modular design approaches to allow the necessary flexibility while maintaining low-cost production. We will also see robot design move from “do-it-yourself” assembly design moving to more professional approaches, using computer-aided design including hydrodynamic optimization, as indicated by *Lee et al. (2012)*.

3. Past, present and prospects

3.1. Past – The academic research era

Research into hull cleaning robots started probably in the 1990s. *Bertram (2000)* mentions some research projects. The robots of the time were bulky do-it-yourself assemblies of academic research laboratories, Fig.1. Several EU projects advanced robotic inspection and cleaning technology, e.g. the AURORA project, Fig.2, *Armada et al. (2004)*. However, while these efforts prepared the ground for today’s state-of-the-art, they remained research focussed and did not directly translate into industrial applications.



Fig.1: Cleaning robot of Hiroshima University, *Bertram (2000)*

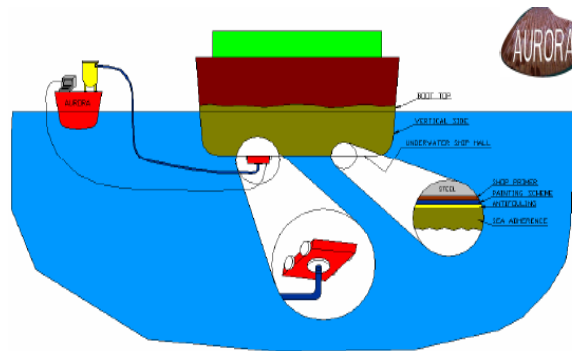


Fig.2: AURORA cleaning robot, *Armada et al. (2004)*

3.2. Present – The start-up and adapt era

My overview benefitted from previous surveys which are highly recommended for more in-depth information, namely *Souto et al. (2015)*, *Albitar et al. (2016)*, *Curran et al. (2016)*, *Song and Cui (2020)*. Table I lists current in-water cleaning robotic solutions. Within 5 years, for a third of the robotic solutions listed in *Curran et al. (2016)*, there were no longer supported websites or more recent publications, suggesting that these would-be contenders had left the market. There are fewer new entries than drop-outs. This is partly due to Table I listing only commercial solutions, partly due to the still volatile market where start-ups disappear or are absorbed in merger & acquisitions.

Table I: Overview of commercial in-water robotic cleaning solutions

Robot	Country	Adhesion system	Cleaning system
COLLECTOR	Norway	Magnetic	Waterjet
Daewon robot	Korea	Thrusters	Brush
Fleet Cleaner	NL	Magnetic	Waterjet
Hullbot	Australia	Thrusters	Brush
Hull BUG	USA	Magnetic/Vacuum	Brush/Waterjet
Hull Cleaner	USA	Magnetic	Brush/Ultrasonic
HullSkater	Norway	Magnetic	Brush
Hull Surface Treatment	Australia	Magnetic	Thermal shock
HullWiper	UAE	Vacuum	Waterjet
KeelCrab	Italy	Vacuum	Brush
Vertidrive M-series	NL	Magnetic	Waterjet
Magnetic Hull Crawler	France	Magnetic	Waterjet
Magnetic crawler	USA	Magnetic	Ultrasonic
Rovingbat	France	Vacuum	Brush/Waterjet
ITCH	Norway	Ship flow field	Brush

There are many ways to categorize in-water cleaning robots, including:

- Cleaning technology (brushes, high-pressure or cavitational waterjets, laser, ...)
- Adhesion technology (magnetic, vacuum (negative pressure), thrusters, ...)
- Level of autonomy (diver controlled, remotely controlled, more or less autonomous)
- Region/country (USA, Europe, Japan, ...)
- Market (pleasure boats, commercial ships, navies, ...)
- ...

Most systems on the market favour magnetic adhesion by now, making them unsuitable for aluminium, reinforced plastics and wooden hulls commonly found in the pleasure craft industry. Vacuum (= negative pressure) adhesion is also popular, while use of thrust force, e.g. *Ishii et al. (2014)*, *Souto et al. (2015)*, or adhesive elastomer materials in research applications is rather exotic, *Song and Cui (2020)*. Adhesion by flow forces of the moving ship is only applicable for largely flat sides, not the ship ends and the ship bottom, *Freyer and Eide (2020)*.

Rotary brushes and waterjets are commonly used, with waterjets taking a more prominent role in the most recent developments. This shouldn't come as a surprise, as the concept of gentler and more frequent cleaning in itself has been accepted by a wider public only in recent years. Ultrasonic technology and laser cleaning technology have been proposed by various researchers, but do not play a significant role in industry practice, *Song and Cui (2020)*. (Note that ultrasonic antifouling protection in stationary installations for niche areas and internal pipes gains in popularity, e.g. *Kelling (2020)*, but use of the technology in underwater robots is rare.) *Akinfiyev et al. (2007)*, *Morrissey and Woods (2015)*, *Song and Cui (2020)* give more in-depth discussions of cleaning technologies.

3.2.1. Key players for commercial applications

Several companies have defined the state of the art through pioneering developments and presentations at professional events like HullPIC and PortPIC:

- HullWiper, www.hullwiper.co, is the market leader in terms of size (employees and probably turnover) and ports served (**10 ports** in late 2020, with 3 more planned for 2021). The HullWiper robot, Fig.3, *Doran (2019,2020)*, “collects marine fouling removed from hulls, rather than polluting local port water and risking the spread of harmful invasive species. Captured residues are pumped into a filter unit and then deposited into dedicated drums onshore, which are collected by a [locally approved] environmental waste disposal company. [... The robot] sprays adjustable high-pressure seawater jets directly onto a ship's hull at a very high velocity to dislodge waste materials, without using scrubbing, harsh chemicals or abrasive materials required for traditional methods. [...] The use of high-pressure jets for cleaning ensures that HullWiper does not damage the ship's [...] antifouling coatings.” The robot is relatively large (3.3 m (L) x 1.7 m (W) x 0.85 m (H)) and heavy (1275 kg).

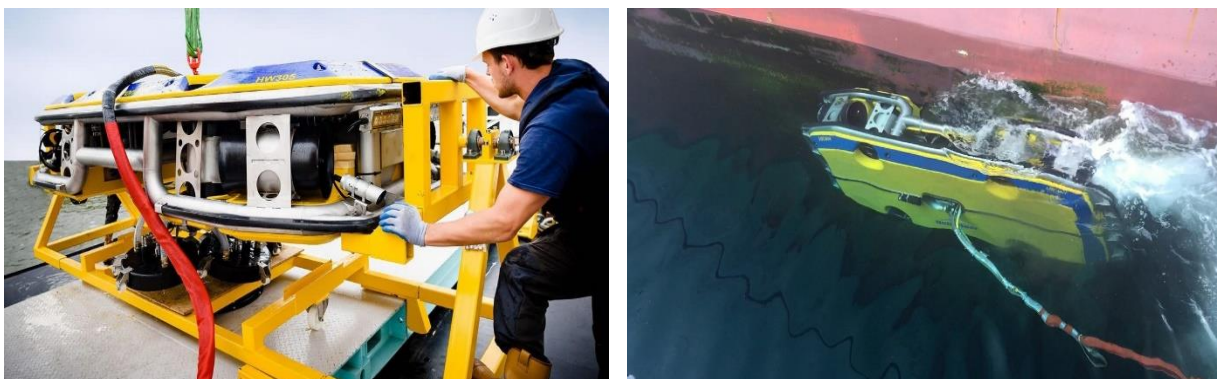


Fig.3: HullWiper robot, www.hullwiper.co

- Fleet Cleaner, www.fleetcleaner.com, has developed its robotic cleaning solution since 2011, with first field trials in 2016, *Noordstrand (2018)*. In subsequent years, the service was extended to all Dutch ports and eventually also to Belgian ports, *Cornelis et al. (2020)*. The self-developed [robot](#) uses magnetic attachment and cleans with high-pressure waterjets. The design is relatively compact (2.0 m (L) x 1.8 m (W) x 0.6 m (H)). Cleaning a ship takes typically 10 h with the latest technology. Like the HullWiper robot, the Fleet Cleaner robot is collecting the removed debris for proper disposal.



Fig.4: Fleet Cleaner robot, www.fleetcleaner.com

- ECOsubsea, www.ecosubsea.com, started in 2008 in Norway, but has its main operational base in Southampton. Its robot ‘Collector’, Fig.5, uses magnetic adhesion, waterjet cleaning and collects the debris, giving “more than 97.5%” as collection rate. The ‘Collector’ has similar size as the HullWiper (3.0 m (L) x 2.0 m (W) x 0.7 m (H)), but is considerably lighter (715 kg). Cleaning a ship takes typically 5 h. The collected debris is properly disposed and serves to generate biogas. The service is offered in 19 ports according to the company’s website, Fig.6, mainly covering North Sea and Baltic ports.



Fig.5: ‘Collector’ robot

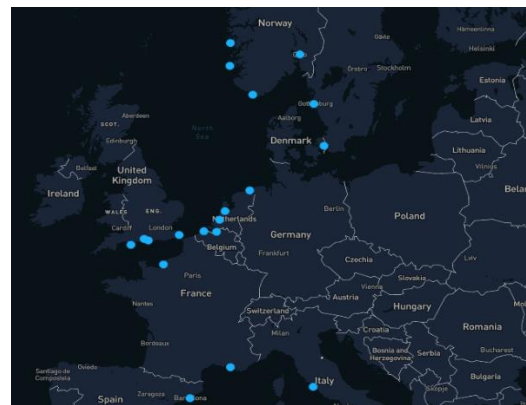


Fig.6: Ports served by ECOsubsea

- SeaRobotics, www.searobotics.com, developed the ‘Hull BUG’ (BUG = bioinspired underwater grooming) funded by the Office of Naval Research in the USA, Fig.7, *Schütz (2012)*. The robot uses vacuum suction for adhesion and brushes to remove biofilm. It is designed for autonomous operation, like a robotic lawnmower or pool cleaner. Onboard sensors allow it to steer around obstacles, and a fluorometer lets it detect biofilm to be removed. The robot is relatively small (1.5 m (L) x 0.75 m (W) x 0.75 cm (H)) and light (55 kg). This makes it easier to cope with curved parts of the ship. SeaRobotics has continued the development with the SR-HullBUG, Fig.8, which is larger (1.5 m (L) x 1.1 m (W) x 0.75 cm (H)) and heavier (370 kg). It has changeable grooming or cleaning tools, listing cavitation waterjet tools explicit-

ly. As the SR-HullBUG addresses cleaning at the biofilm stage, before macrofouling can develop, there is no need to collect the removed fouling.



Fig.7: Hull BUG

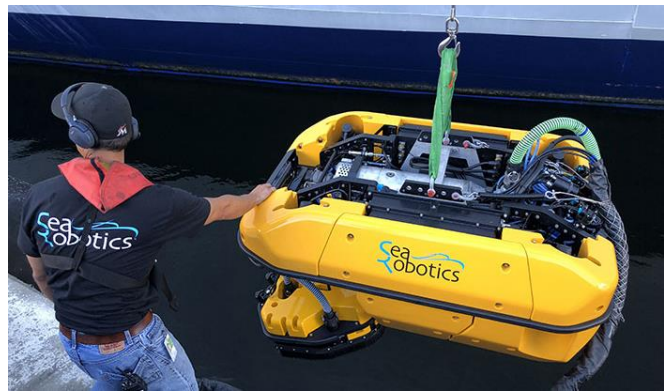


Fig.8: SR-HullBUG

- Jotun, <https://jointherevhullution.com>, launched its HSS (Hull Skating Solutions) in 2020, Fig.9, which was developed in partnership with Kongsberg, Semcon, Telenor, DNV GL and Wallenius Wilhelmsen. The Hull Skater robot uses magnetic adhesion and soft brush cleaning. As it is only intended to remove biofilm, there is no need to collect debris. The Hull Skater robot, https://octagavs.com/JotunHSS_mobile/, travels on-board with the ship, and is launched and retrieved by the crew. The inspection and cleaning missions are remotely controlled by Jotun. During inspection, the robot identifies areas of advanced fouling, which are not cleaned by the robot and are subject to later cleaning by other means allowing collection of removed advanced fouling to prevent spread of aquatic invasive species. The Hull Skater is relatively small (1.6 m (L) x 1.0 m (W) x ~0.5 m (H)) and light-weight (200 kg), <https://semcon.com/uk/jotunhullskater/>. Cleaning a (150 m) ship takes typically 4-5 h.

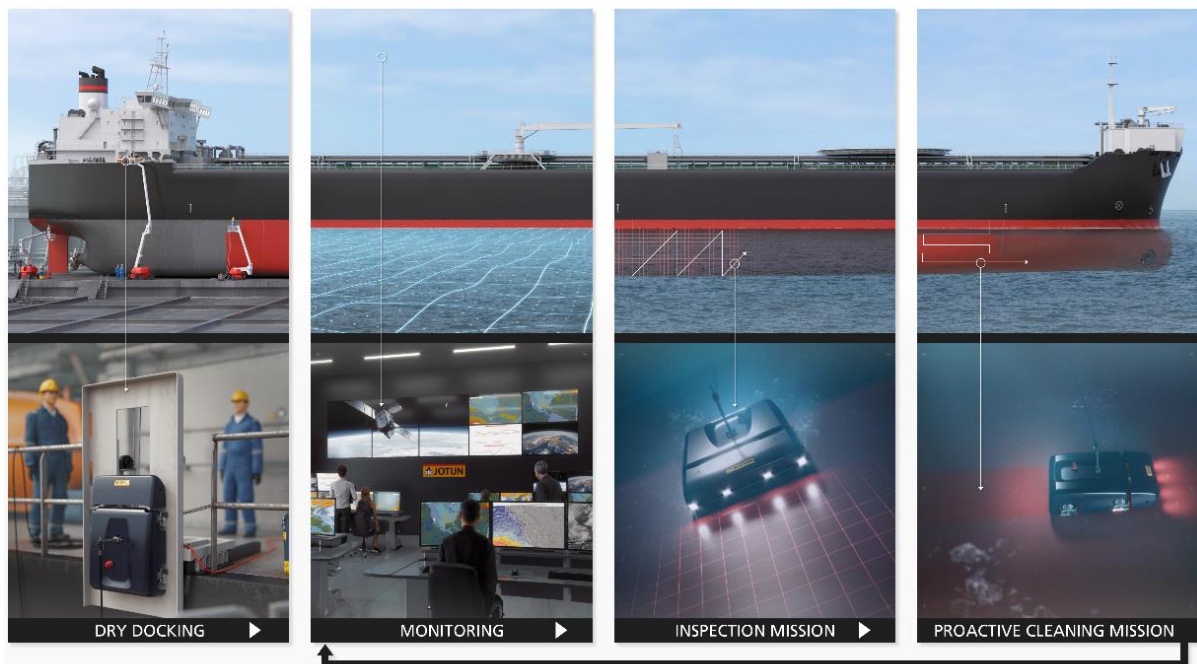


Fig.9: Hull Skating Solutions with (from left to right) robot launched by crew; performance monitoring and remote control of robot by Jotun experts; inspection mode to identify no-go areas with fouling beyond biofilm; and subsequent cleaning of biofilm

3.2.2. Flanking measures

Besides the technical and economic development of in-water cleaning robots, there are additional measures needed to develop the ‘eco-system’ of in-water, in-port cleaning:

- Guidelines are needed for various aspects, such as accreditation for in-port cleaning, matching of cleaning method and coating, collection and disposal of removed fouling, documentation of cleaning results, etc. E.g. *Oftedahl and Enström (2020)*, *Sørensen (2020)*, the NACE TG 581 on NACE’s Standard Practice ‘Inspecting and Reporting Biofouling and Antifouling System Condition during an Underwater Survey’, and several proposals for the due update of IMO’s ‘Guidelines for the Control and Management of Ships’ Biofouling to Minimize the Transfer of Invasive Aquatic Species’ are such useful contributions benefitting the industry at large.
- Ports need to adapt policies to the changing coating and cleaning technologies, requiring adequate proof of environmentally acceptable procedures, but also allowing in-port cleaning if required documentation can be given by service providers. E.g. Belgian ports, *Cornelis et al. (2020)*, set a good example in this respect. Policies should be aligned at least within regions, to avoid the “wild west” unaligned and unregulated practice rightfully lamented by *Noordstrand (2020)*.

3.3. Prospects

“Prediction is very difficult, especially about the future”, as Nobel laureate Niels Bohr so wisely said. Still, we can look at recent research and development and make speculate on what may come:

- Team capability in cleaning robots – Cooperative robotics is one of the major research areas within the robotics community. The basic idea is to have two or more robots working as a team on a task. In the maritime field, there have been some applications of such cooperative robotics, e.g. for mapping of seabed, establishing towline connections, or search/patrolling tasks, e.g. *Odetti et al. (2016)*, *Lewis (2017)*. For hull cleaning, cooperative robotics would allow parallelization of work and thus much shorter cleaning times. One could also imagine smaller robots focussing on areas of high curvature, while a larger robot is used for large flat areas. The technology of robot location, ship surface mapping, and communication between robots (and possibly a central surface control centre) is available, we need “just” to get the robotics community and the hull cleaning industry connected. It seems a perfect opportunity for an EU project.
- System solutions – Mismatching coating solution, cleaning technology and procedures has led repeatedly to problems and finger-pointing between the various stakeholders. While we hear repeatedly the mantra that cleaning and coating should be matched properly, a multitude of products/services coming from a multitude of changing suppliers seems like a recipe for failures to happen. We need system solutions, at least in the form of clear instructions for cleaning coming from the coating suppliers and procedures that ensure that these instructions were received and understood by the cleaning providers. Information loss between stakeholders is best avoided by integrated solutions. Jotun’s [Hull Skating Solutions](#), *Oftedahl and Enström (2020)*, are a role model that hopefully will inspire larger parts of the industry to follow. Here, coating, robotic cleaning, performance monitoring (to trigger the cleaning and monitor the effect on performance) and contractual warranties come under one umbrella.
- Port services or on-board equipment – Most robotic cleaning solutions assume a dedicated service provider, providing the robot and the cleaning service in certain (and, so far, few) ports. Exceptions from this rule have appeared in 2020 with Jotun’s hull skating solutions and Shipshave’s ITCH (In Transit Cleaning of Hulls) semi-autonomous robot. Both are launched and retrieved by the ship’s crew, travel with the ship and are thus independent of available

port infrastructure. On-board cleaning robots overcome issues with scarce port services. In-port services have the advantage that equipment is utilized over many ships, with the associated economies of scale. In the long term, say over a decade or two, these economies of scale may favour in-port service providers, echoing a similar development away from multi-purpose ships (with their under-utilized on-board cargo handling equipment) towards container-ships (relying on port-side services), but this requires wider deployment of port-side robotic cleaning solutions which I am confident we will see, but which will take time. In the meantime, we may see more rapid growth of on-board solutions.

4. Conclusion

Robotic in-water cleaning technology has come a long way from early research attempts to the current state of the art. We are currently in a steep part of the learning curve and the development of this still young industry. Technology, regulatory frameworks and procedural guidelines, as well as markets, are developing dynamically. Teething problems and occasional set-backs (or learning moments) are to be expected, but the future looks rather bright for this particular segment of the maritime world.

References

AKINFIEV, T.; JANUSHEVSKIS, A.; LAVENDELIS, E. (2007), *A brief survey of ship hull cleaning devices*, Transport and Eng. Mech. 24, pp.133-146, <https://ortus.rtu.lv/science/en/publications/3661/fulltext.pdf>

ALBITAR, H.; DANDAN, K.; ANANIEV, A.; KALAYKOV, I. (2016), *Underwater Robotics: Surface Cleaning Technics, Adhesion and Locomotion Systems*, Int. J. Advanced Robotic Systems 13, <https://journals.sagepub.com/doi/pdf/10.5772/62060>

ARMADA, M.; GONZÁLEZ DE SANTOS, P.; PRIETO, M.; GARCÍA, E.; AKINFIEV, T.; FERNÁNDEZ, R.; MONTES, H.; NABULSI, S.; PEDRAZA, L.; PONTICELLI, R.; SARRIÁ, J.; ESTREMER, J. (2004), *State of the art in climbing and walking robots*, 3rd COMPIT Conf., Sigüenza, pp.315-321, http://data.hiper-conf.info/compit2004_sigüenza.pdf

BERTRAM (2020), *Biofouling Management at the Dawn of a Mechanical Era*, 1st PortPIC Conf., Hamburg, pp.87-92, http://data.hullpic.info/PortPIC2020_Hamburg.pdf

CORNELIS, J.; VAN ESPEN, L.; POLFLIET, K. (2020), *Underwater Cleaning in the Flemish Ports*, 1st PortPIC Conf., Hamburg, pp.8-13, http://data.hullpic.info/PortPIC2020_Hamburg.pdf

CURRAN, A.P.; O'CONNOR, B.W.; LOWE, C.M.; KING, E.F. (2016), *Analyzing the Current Market of Hull Cleaning Robots*, Worcester Polytechnic Institute, <https://digitalcommons.wpi.edu/iqp-all/2693>

DORAN, S. (2019), *A short history of hull cleaning and where do we go now*, 4th HullPIC Conf., Gubbio, pp.97-102, http://data.hullpic.info/HullPIC2019_gubbio.pdf

DORAN, S. (2019), *A short history of hull cleaning and what is next*, 1st PortPIC Conf., Hamburg, pp.4-7, http://data.hullpic.info/PortPIC2020_Hamburg.pdf

FREYER, R.; EIDE, E. (2020), *In-Transit Cleaning of Hulls*, 5th HullPIC Conf., Hamburg, pp.120-125, http://data.hullpic.info/HullPIC2020_Hamburg.pdf

HUNSUCKER, K.; BRAGA, C.; ERGODAN, C.; GARDNER, H.; HEARIN, J.; RALSTON, E.; SWAIN, G.; TRIBOU, M.; WASSICK, A. (2018), *The Advantages of Proactive in Water Hull Grooming from a Biologists Perspective*, 3rd HullPIC Conf., Redworth, pp.210-222, http://data.hullpic.info/hullpic2018_redworth.pdf

ISHII, K.; NASSIRAEI, A.A.F.; SONODA, T. (2014), *Design concept of an underwater robot for ship hull cleaning*, 13th COMPIT Conf., Redworth, pp.540-545, http://data.hiper-conf.info/compit2014_redworth.pdf

KELLING, J. (2020), *Ultrasound - The Future Way to Match IMO's Biofouling Guideline*, 1st PortPIC Conf., Hamburg, pp.83-86, http://data.hullpic.info/PortPIC2020_Hamburg.pdf

LEE, M.H.; PARK, Y.P.; PARK, H.G.; PARK, W.C.; HONG, S.P.; LEE, K.S.; CHUN, H.H. (2012), *Hydrodynamic design of an underwater hull cleaning robot and its evaluation*, Inter. J. Naval Archit. Ocean Eng. 4, pp.335-352, <https://www.sciencedirect.com/science/article/pii/S2092678216303533>

LEWIS, C. (2017), *Marine Bees: Robotic Ocean Exploration Inspired by Nature*, 11th HIPER Conf., Zevenwacht, pp.224-229, http://data.hiper-conf.info/Hiper2017_Zevenwacht.pdf

MORRISEY, D.; WOODS, C. (2015), *In-Water Cleaning Technologies*, Ministry for Primary Industries, New Zealand, https://www.researchgate.net/profile/Chris_Woods/publication/276920200_In-water_cleaning_technologies_Review_of_information/links/569300c608aee91f69a7300f/In-water-cleaning-technologies-Review-of-information.pdf

NOORDSTRAND, A. (2018), *Experience with robotic underwater hull cleaning in Dutch ports*, 3rd HullPIC Conf., Redworth, pp.4-9, http://data.hullpic.info/hullpic2018_redworth.pdf

NOORDSTRAND, A. (2020), *Roadmap from the Wild West to the Promised Land of Ship Cleaning*, 1st PortPIC Conf., Hamburg, pp.38-41, http://data.hullpic.info/PortPIC2020_Hamburg.pdf

ODETTI, A.; BIBULI, M.; BRUZZONE, G.; CACCIA, M.; RANIERI, A.; ZEREIK, E. (2016), *Cooperative robotics – Technology for future underwater cleaning*, 1st HullPIC Conf., Pavone, pp.163-177, <http://data.hullpic.info/HullPIC2016.pdf>

OFTEDAHL, G.A.; ENSTRÖM, A. (2020), *Proactive Cleaning and the Jotun Hull Skating Solution*, 1st PortPIC Conf., Hamburg, pp.66-78, http://data.hullpic.info/PortPIC2020_Hamburg.pdf

SCHÜTZ, A. (2012), *Hull cleaning robot for large ships*, Maxon Motor, https://www.maxongroup.com/medias/sys_master/8808089911326.pdf

SØRENSEN, A.F. (2020), *Industry Standard for In-water Cleaning with Capture*, 1st PortPIC Conf., Hamburg, pp.79-82, http://data.hullpic.info/PortPIC2020_Hamburg.pdf

SONG, C.; CUI, W. (2020), *Review of underwater ship hull cleaning technologies*, J. Marine Science and Application, <https://link.springer.com/content/pdf/10.1007/s11804-020-00157-z.pdf>

SOUTO, D.; FAINA, A.; LOPEZ-PENA, F.; DURO, R.J. (2015), *Morphologically intelligent underactuated robot for underwater hull cleaning*, 8th IEEE Int. Conf. Intelligent Data Acquisition and Advanced Computing Systems: Technology and Applications, Warsaw, pp.879-886, https://www.researchgate.net/profile/Fernando_Lopez_Pena2/publication/304990148_Morphologically_intelligent_underactuated_robot_for_underwater_hull_cleaning/links/578254cf08ae5f367d3b5a37/Morphologically-intelligent-underactuated-robot-for-underwater-hull-cleaning.pdf

SWAIN, G.; TRIBOU, M.; GARDNER, H.; HUNSUCKER, K. (2020), *In-Water Grooming of Fouling Control Coatings: From Research to Reality*, 1st PortPIC Conf., Hamburg, pp.29-37, http://data.hullpic.info/PortPIC2020_Hamburg.pdf

Virtual Reality for Maritime Training – A Survey

Tracy Plowman, DNV, Hamburg/Germany, tracy.plowman@dnv.com

Volker Bertram, DNV, Hamburg/Germany, volker.bertram@dnv.com

Abstract

This paper reviews literature on using Virtual Reality (VR) technology for maritime training purposes. Most applications are 3D in modelling, but not 3D in viewing. The field of published VR applications for maritime training is still small enough to be reviewed in such a paper, with few applications in commercial shipping with the notable exception of the well-established nautical simulators. The high costs for VR based training limit applications. Business cases usually appear when large assets or human health/life is at risk in real-world training.

1. “Virtual Reality” – Reality

The term 'Virtual reality' (VR) was initially coined by the artist Jaron Lanier who envisioned the user fully immersed in an artificial world completely generated by a computer. Despite significant progress in the last 20 years, we are far from this vision. While Virtual Reality has progressed from vision to industry reality, it has fallen short of expectations, compare e.g. *Rosenblum's (2000)* vision for Virtual Reality in 2020 with current state of the art and industry adaptation. The state of the art in VR applications can be summarized as follows:

1. Navigation in 3D space with look-around, walk-around, and fly-through capabilities in virtual environments. Control devices allow manipulation, operation, and control of virtual worlds. This is the minimum capability to qualify for a “Virtual reality” denotation. VR models thus always require an underlying 3D CAD model of the “world” modelled, typically enhanced by surface structure, mapped images, etc.
2. Stereoscopic viewing enhances the perception of depth and sense of space. This is a nice-to-have gadget for most training applications. Experience shows that trainees may encounter discomfort, sometimes resembling motion sickness, after 5-20 minutes of immersion in stereoscopic worlds, which has not been observed in “poor-man’s” VR on screens with trainees perceiving the normal training room environment.
3. The virtual world is presented in full scale and relates properly to human size. While important for many training applications, this aspect might be omitted on purpose in some applications (having an overview from a giant perspective or shrinking to go e.g. inside blood vessels in medical training).
4. The convincing illusion of being fully immersed in an artificial world can be enhanced by auditory, tactile and other non-visual technologies. Sound effects are common in video games; data gloves are used in some applications but interfere with the immersive feeling, *Rosenblum (2000)*.
5. Networked applications allow shared virtual environments: users at different locations (anywhere in the world) can meet in the same virtual world, see each other, communicate, and interact. Shared virtual environments appear in some cases, *Nordby et al. (2016)*, but there seems to be more the “thrill of the new” than convincing applications in an industry work context. The more people participate in shared virtual environments, the more difficult speech communication becomes. The “cocktail party effect” is amplified by the limited frequency bandwidth in electronic voice transmission.

Virtual Reality applications often use “immersive” as a marketing distinction. Stereoscopic vision using e.g. Oculus Rift glasses is then hailed as more immersive than plain PC screens (without stereoscopic vision). However, the degree of immersion depends largely on the willingness of the viewer to accept the immersion (same as with any movie).

Increased reality (level of detail, stereoscopic view, lighting effects) and model size come at a price. Pragmatic applications have just the necessary level of detail. The main cost factor is the creation of a tailored Virtual World. Many 3D models can be found for free on the internet, but specific models and elements require (sometimes prohibitively expensive) work to create. Model reuse from other applications, e.g. finite-element or CFD models, is not straightforward, Fig.1, *Lindenau and Bertram (2003)*.

Creating a VR model for a given ship is likely to take man-months. In most maritime cases, the business case does not exist (personal communication with David Thomson (AVEVA); Denis Morais (SSI): “Virtual Reality (VR) technology is still around a decade away from providing consumers with a good VR experience”, Mark Zuckerberg (CEO Facebook)).

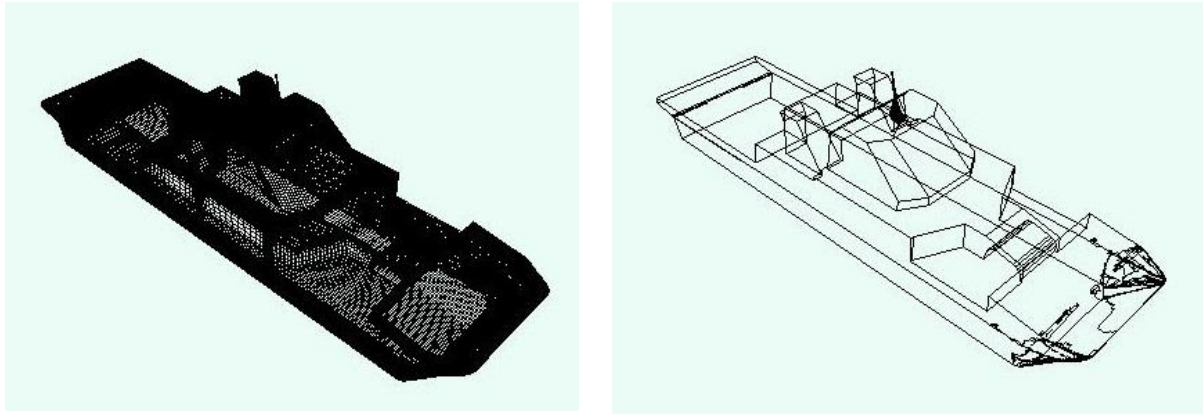


Fig.1: Original CFD model (left) and post-processed VR model with much fewer edges (left)

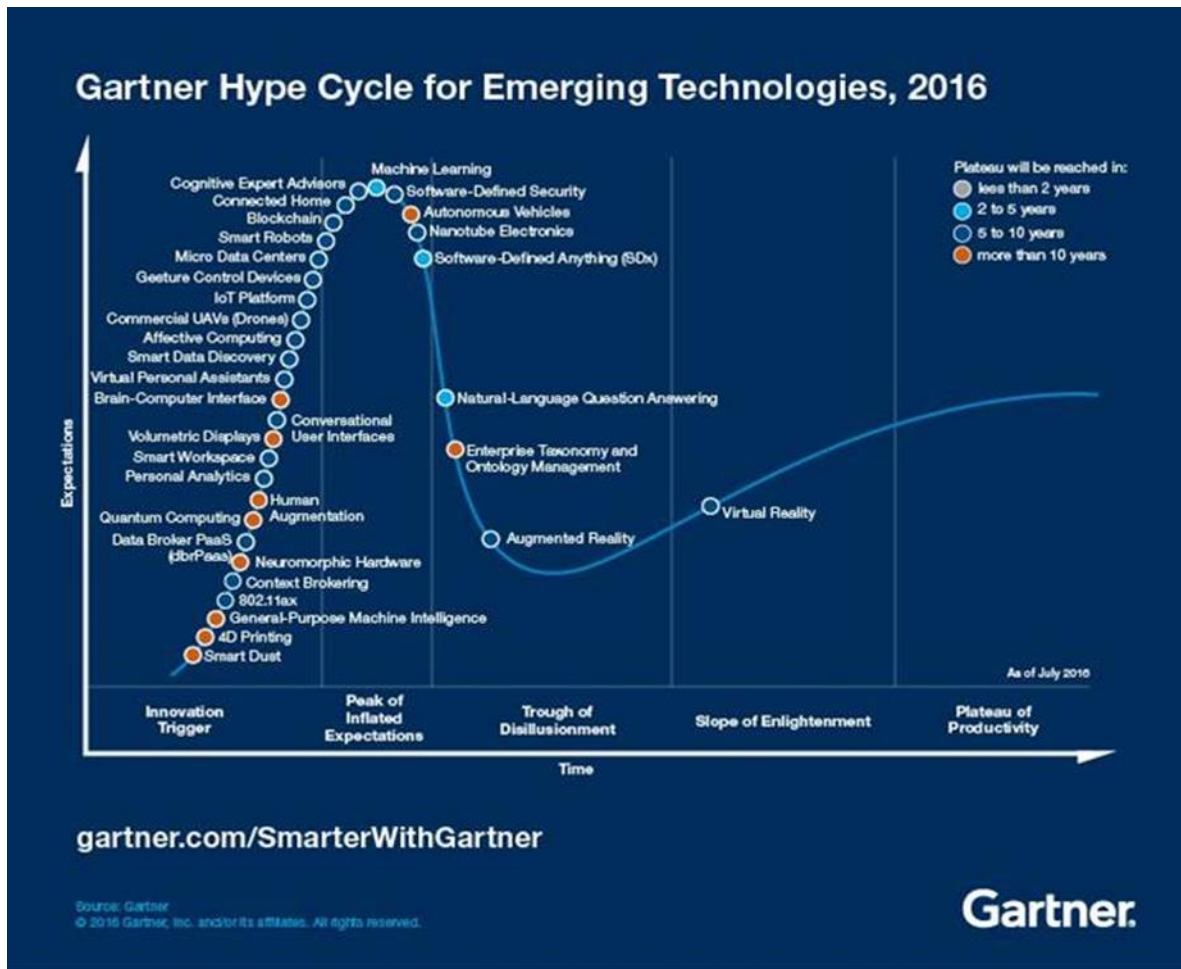


Fig.2: Gartner hype cycle for emerging technologies

Still, there is reason for moderate optimism. With more and more maritime 3D models, we have more starting points to create VR models for a multitude of applications, *Seppälä (2021)*. This has been reducing the cost for VR model creation - and will continue to do so. In the specific case of DNV, such models come typically from 3D ship modelers such as POSEIDON and NAUTICUS.

Fig.2 illustrates the mildly optimistic view on VR in the manic-depressive technology cycle, where hype is followed by disillusion, taken from Denis Morais' (SSI) blog waveform <http://blogs.ssi-corporate.com/waveform/2017/technology/industry-will-drive-enhancements-in-vr/>.

2. Virtual Reality in maritime training

2.1. Nautical Simulators

Classical nautical simulators are akin to Virtual Reality, and purely VR-based nautical training has been proposed and implemented, *Magee (1997)*, *Lvov and Popova (2020)*, *Van der Ende et al. (2020)*. Here a view of the world outside a nautical bridge is projected with other ships and waterways. The simulators generate increasingly realistic visual effects of environment (night/day, fog/rain/etc., waves) and mimic the maneuvering physics of own ship and encountered ships. Simulators range from small desktop to large full-mission solutions.

A typical solution is Simflex4 of FORCE Technology, <https://forcetechnology.com/en/maritime-industry/cargo-vessels/simulation-studies-for-maritime-operations>. The brochure mentions visual effects in 3D, but all images shown reflect standard practice of 2D displays and are far less photorealistic than state-of-the-art video games, compare Fig.3 and Fig.4. A very realistic portrait of the outside world is apparently not required to meet the training needs. FORCE Technology mentions four vital ingredients for their simulation-based training:

1. models of ships and shipping areas (= 3D worlds and maneuvering models for each ship),
2. the simulator (the display and interaction option),
3. experienced instructors (!),
4. pedagogical training methods and insights (!).

Developing such simulators is an interdisciplinary task. A video game playing a captain is much simpler than having a simulation-based training facility.

A simulator facility charges ~4000 € per day (8 h) in the simulator. Setting up a specific ship and specific environment and training crews may then cost 70000 – 110000 €. More recent entries focus more on visual effects, e.g. <https://unigine.com/en/industries/simulation/maritime>, <http://osc.no/#solutions>.



Fig.3: Nautical simulator (FORCE Technology)

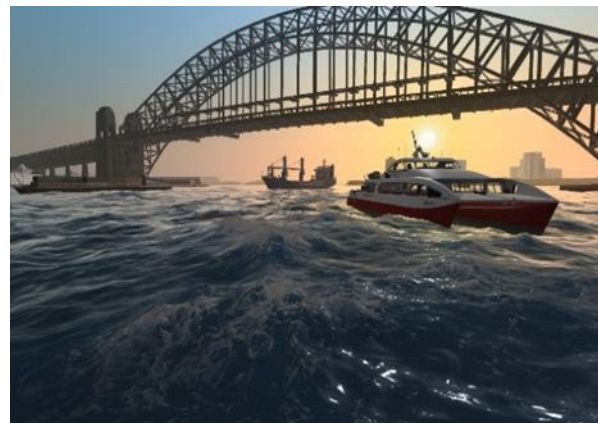


Fig.4: Video game shipsim.com

2.2. Navy/military simulators

Navies employ simulators to train military staff for combat situations. The Italian provider IBR Sistemi offers such a solution employing Virtual Reality technology, the “Joint Tactical Theatre Simulator”, <http://www.naval-technology.com/contractors/simulators/ibr-sistemi/>. “The scenario can be displayed on unlimited multiple screens/360[°] projections or through special stereoscopic displays and head mounted displays (HMD).” The photorealistic visuals rival state-of-the-art video games, Fig.5. The solution is rather sophisticated, with many ships, equipment systems, geographical areas, etc. in the database.

The Bremen-based software provider Szenaris (www.szenaris.com) has developed VR based training and e-learning solutions for underwater vehicle operations, Fig.6, and submarine operation, Fig.7, *Katzky (2014)*. The latter was for one specific submarine (U 212) and served to familiarize new crews with the submarine in a risk-free training environment. The involved effort seems too high to create a business case outside the specific naval applications.



Fig.5: High degree of photorealism in IBR Sistemi simulator



Fig.6: PC-based VR training for underwater vehicle handling



Fig.7: VR model of U212 (control room)

2.3. Ship survey simulator

DNV has developed SuSi (Survey Simulator), a Virtual Reality based training solution for ship inspections, *Wardell (2010), Kubiak (2011), Bertram et al. (2020)*, see also the Appendix. SuSi provides realistic and cost-efficient 3D training software for survey inspections, using Virtual Reality technology and detailed models of ships and offshore structures, Figs.8a and 8b.



Fig.8a: Level of detail in SuSi (Virtual Reality based survey simulator)

The virtual inspection gets trainees exposed to deficiencies that would take years for a surveyor to experience in real life. An inspection run can be recorded and discussed in a debriefing with an experienced supervisor/trainer, pointing out oversights and errors by the trainee. If trainees navigate themselves in the virtual worlds, we observed occasional problems with some trainees struggling with navigation or task, while others went ahead and started to get sidetracked. Alternatively, courses can be run with solely the trainer in command ensuring a common vision on a projected screen. This form of teaching, while not immersive at all, has been very well received.

The experience so far is based on blended learning, where classical classroom training alternates with SuSi-based elements. The classroom training focuses e.g. on regulations, inspection techniques or frequently found deficiencies on ships, before a virtual ship inspection starts.

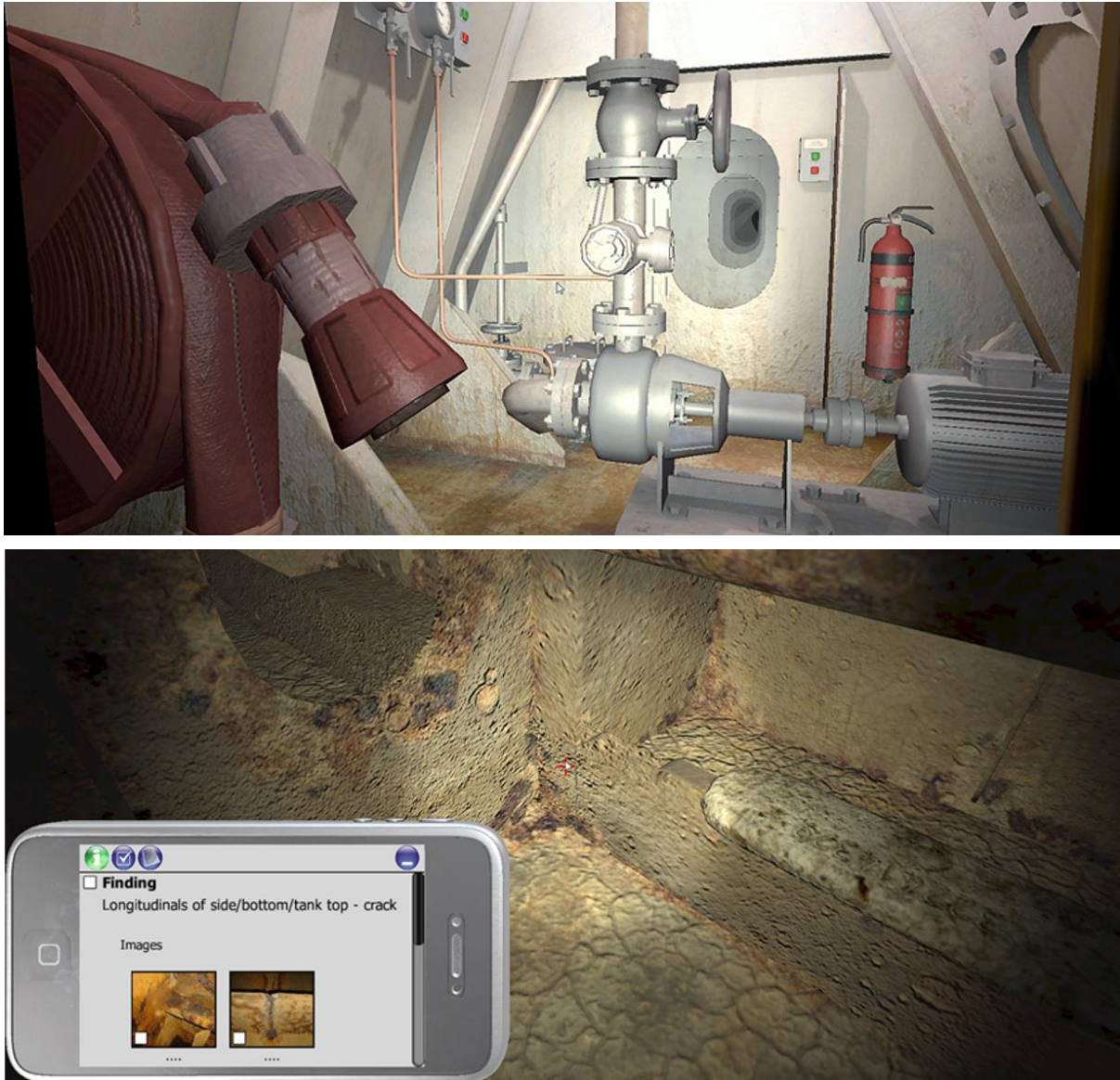


Fig.8b: Level of detail in SuSi (Virtual Reality based survey simulator)

In addition to the blended teaching form, SuSi combines Virtual Reality scenarios with a knowledge base of thousands of photos of actual surveyor findings linked to the deficiencies incorporated in the VR model. Trainees can then use a virtual smartphone to retrieve photos of associated real-world defects with attached text information adding to the training effect, Fig.9.

The initial vision was that SuSi would revolutionize the way we conduct (surveyor) training, *Wardell (2010)*. Eight years later it still seems to be a great training solution ahead of state of the art in maritime training, but adoption has been slower than originally envisioned. The combination of hardware requirements, surveyor competence, trainer competence, course content competence and SuSi operating competence makes global roll-out difficult, for the same reasons that potential new entries offering comparable solutions face significant hurdles. The combination of software, sophisticated scenarios, pedagogical solution and trainer competence would require significant effort to copy.

Korean Register of Shipping (KRS) has developed its own VR-based ship survey simulator to train ship surveyors on classification rules and inspection procedures, *Kil et al. (2018)*. The 3D stereoscopic images are combined with physics engines to recreate scenarios such as drops or collisions. The player has elementary functions such as ladder climbing, photographing and hand lighting.



Fig.9: VR finding and corresponding real-world finding

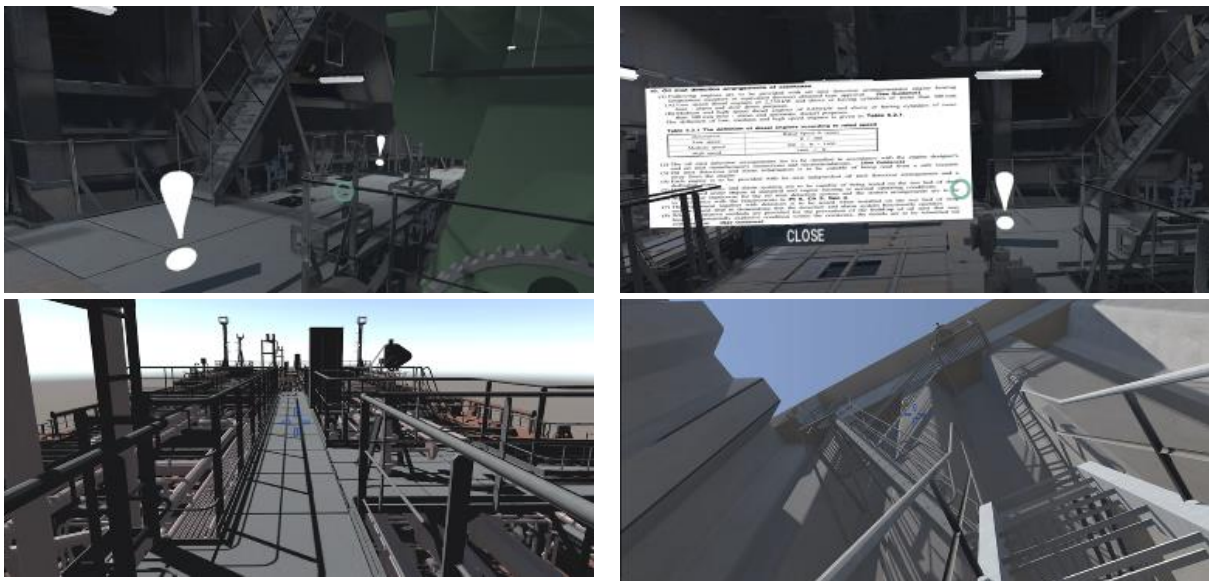


Fig.10: KRS ship survey simulator

2.4. Ship familiarization

The NRL (National Research Laboratory) has developed InterShip, a VR tool to familiarize personnel with the layout of a ship, Fig.11, *Wauchope et al. (2003)*, *Wauchope and Bertram (2004)*. InterShip combines VR techniques with a knowledge-based route planner (shows how to get from one compartment to another) and speech control (user can e.g. open door by command; user can query system for information, e.g. invoking route planner.) Using the head-mounted display and a hand-held joystick, users could walk through portions of a ship and ask questions about compartment names, numbers and locations. (“What compartment is this?”, “Which deck is the communications center on?”)

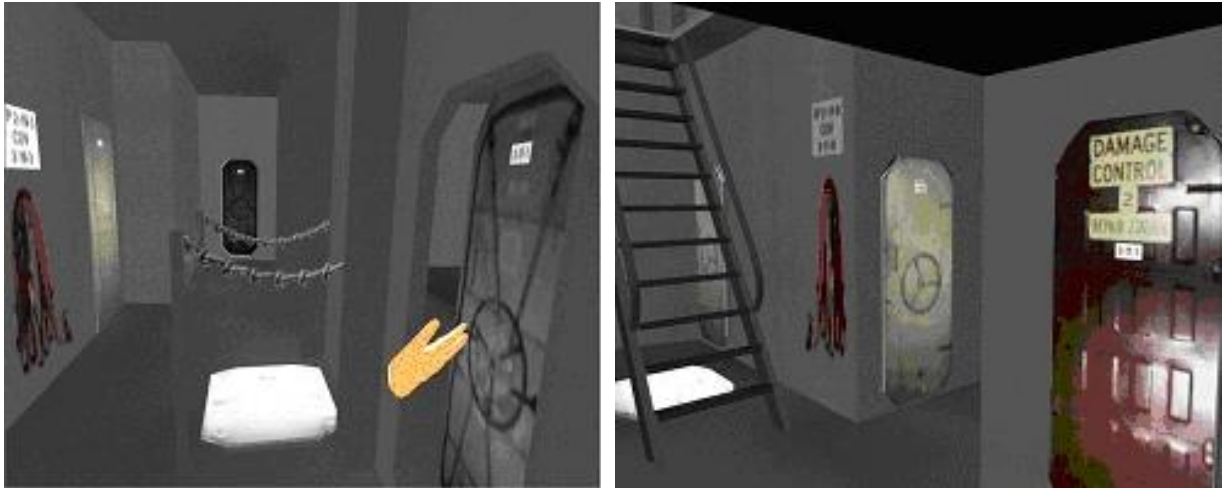


Fig.11: VR tool InterShip to explore a ship with glove avatar opening door

Newell and Luck (2017) describe a 3D walkthrough training system for the Queen Elizabeth Class (QEC) aircraft carriers for the Royal Navy, Fig.12. BMT used its in-house VR training solution ENGAGE as a platform. For this new class of warships, support personnel must be safe to work onboard, requiring training. A needs analysis determined that such training would be best delivered employing a 3D walkthrough with interactive functionality based on a game-based simulation engine (augmenting classroom training). This approach provides a through-life solution, is electronically distributable and has wider possible applications. Technical information behind equipment or systems within the model can be reviewed in the virtual environment. Despite the high-quality graphics, the system is pedagogy driven and not technology driven: “[The] training system is designed around the needs of the trainee and the desired outcome, rather than just developing the highest fidelity system for the sake of it,” *Newell and Luck (2017)*. Consequently, only the QEC bridge was developed for 3D viewing with HTC Vive VR hardware, for use at public-relations and outreach events.

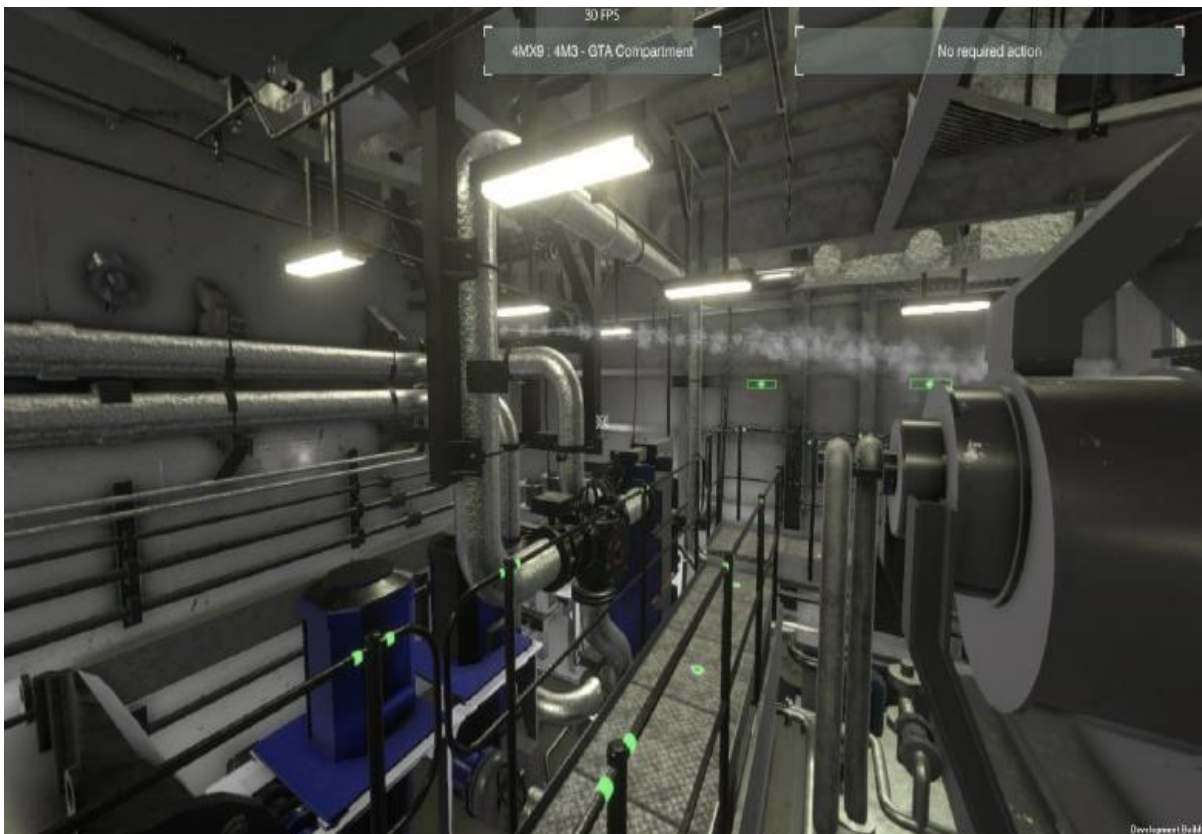


Fig.12: BMT’s training solution ENGAGE for aircraft carrier familiarization, *Newell and Luck (2017)*

Besides ship familiarization, further possible applications are mentioned: safety training including emergency response, escape routes, and maintenance options such as on-board transport routes for the removal/replacement of large equipment.

2.5. Marine fire-fighting

The National Research Laboratory (NRL) of the USA has investigated employing virtual reality to improve the performance of firefighters, Fig.13, *Tate et al. (1997)*. Using a mixture of physically based modeling and fractal techniques, the fire changed color and transparency levels to simulate the appearance of real flames.

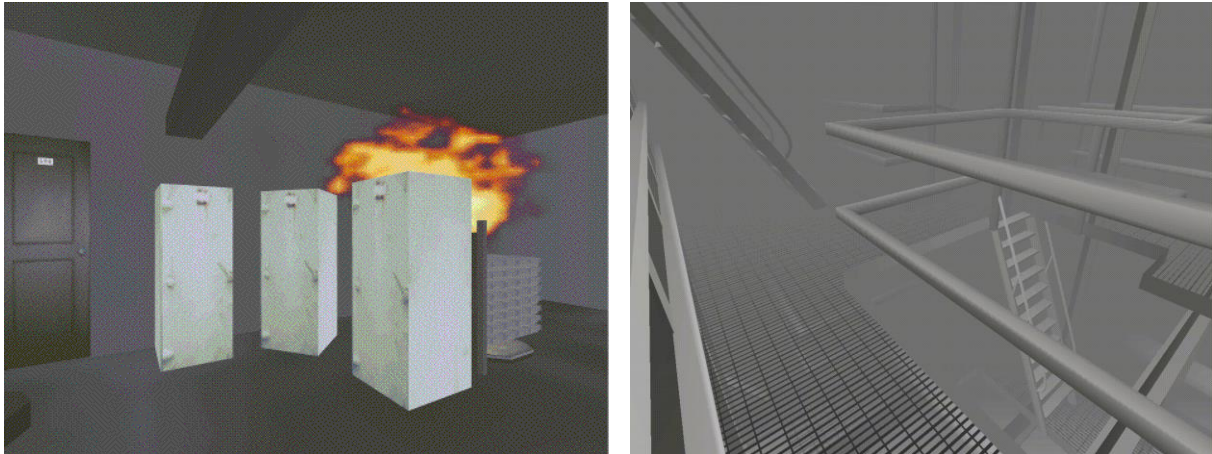


Fig.13: VR fire-fighting training environment of NRL

The density of simulated smoke varied with distance to the simulated fire and could be changed by operator control. There was a measurable improvement in the performance of firefighters that used VR training over firefighters without such training. VR trained firefighters made fewer wrong turns and reached the fire faster than untrained firefighters.

The Dutch company VSTEP (www.vstepsimulation.com) offers VR based training for emergency response, e.g. fire-fighting, both for land-based applications and for ships (three different ships were modelled). The training is designed to be part of STCW, https://en.wikipedia.org/wiki/STCW_Convention, requirements with blended learning combining classroom elements and supervised simulations.

2.6. Maritime safety training

Venter and Juricic (2014) describe a VR-based training using elements of video gaming to familiarize the crew of an offshore oil & gas platform with the platform and safety procedures, Fig.14. Fig.15 gives an idea of the effort involved in creating the 3D world for an oil platform with sufficient level of detail. Here a CAD vendor (Intergraph, supplying the 3D world for the platform) and a gaming specialist (Samahnzi) cooperated to create a tailored training solution. “Players” (=trainees) embraced this solution, but most likely the project received subsidies to match development costs and price expectations of the customer.

MacKinnon et al. (2016) report that such VR-based training results in faster evacuation of platforms (as measured in mock-ups with groups that were just instructed and groups that could explore the platform in VR). As in the application of *Venter and Juricic (2014)*, the improved training result is probably due to stronger involvement and interest in the offered information. As VR technology has been largely driven by the gaming industry, we can often tap into the gaming features and experience to improve training solutions.



Fig.14: Gamification of training – Scenario to train correct behavior in emergency situations, *Venter and Juricic (2014)*

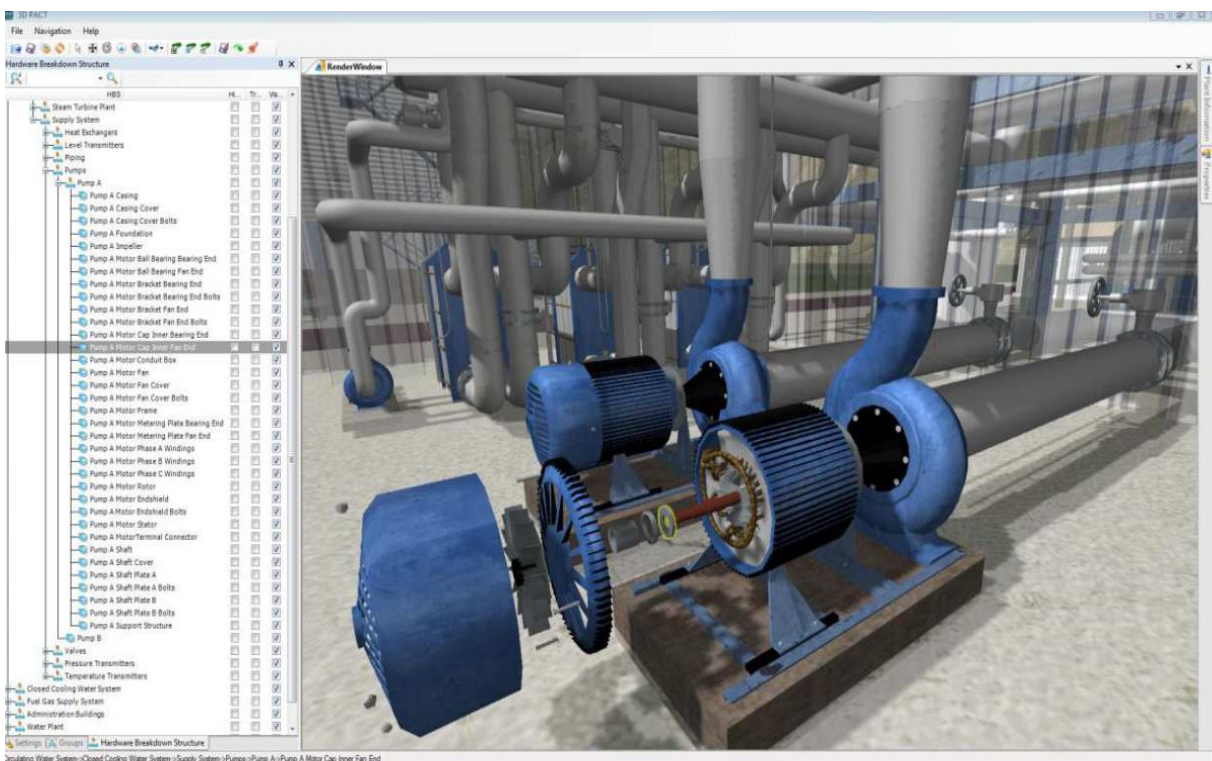


Fig.15: Small part of the 3d model to create the training environment in *Venter and Juricic (2014)*

The Institute of Technical Education (ITE) in Singapore uses advanced Virtual Reality and Augmented Reality for maritime and offshore training. EON Reality and ITE partnered to create several such applications to increase the engagement of today's digital learners. For example, trainees can work virtually on an oil rig, Fig.16(left). Trainees can familiarize themselves with the complex structure and various equipment used, but also perform important safety operations in various weather condi-

tions. The hardware park at ITE seems to be impressive, as they offer group training using holograms and CAVE-like environments with data gloves, motion tracking, etc. Apparently, ITE also uses the VR environment to create interactive learning sequences, Fig.16(right). The focus is on safety related (high-risk) training for crews on board ships and offshore platforms.



Fig.16: ITE training offers involving Virtual Reality

Lloyd’s Register announced plans for VR based training on safety issues for the oil & gas market in 2017. No further conference or journal paper is available yet. Demo versions on fairs show relatively simple scenarios, but with stereoscopic viewing via head-mounted devices.

Kil et al. (2018,2019) present a multi-user VR-based crew training application for on-board emergency situations required by the International Safety Management (ISM) Code, Fig.17.



Fig.17: Emergency response training for crew following ISM, *Kil et al. (2018)*

Markopoulos et al. (2020) present ShipSEVR (Ship Safety Education with Virtual Reality), Fig.18, a VR-based training application for ship engine rooms, with involvement of Wärtsilä. We expect similar training applications to evolve for key machinery on board, where the major maritime equipment suppliers support training using available 3D models of equipment. In addition, Digital Twin information of equipment (engine characteristics etc.) and digital manuals may be added to enhance the training impact.



Fig.18: ShipSEVR screenshots, *Markopoulos et al. (2020)*

2.7. Assorted other applications

The University of Sao Paulo in Brazil has developed a virtual model basin for offshore technology applications, *Gaspar et al. (2009)*. Besides high-performance computing for CFD (computational fluid dynamics), there is also a “4D visualization” hall, Fig.19. Here an instructor guides the audience (wearing 3D glasses) through a 3D world changing in time (the fourth Dimension), while the platform moves simulating the motions of a ship. It is unclear how extensively the facility is used.

The EU-project SLIM-VRT (Self-Learning Integrated Methodology - Virtual Reality Tool), *Lambrou et al. (2006)*, describes rather vaguely how VR might be embedded in maritime training, but apparently did not result in any concrete tool, despite 3 years and 2.2 M€ funding. There may be a general lesson in this, namely that significant resources are needed to develop workable and sustainable VR solutions and 3 years and 2.2 M€ may not be enough in many cases.



Fig.19: “4D visualization” hall

Nordby et al. (2016) [involving my ex-DNV colleague Etienne Gernez] report a rather advanced application of “mixed reality” to design ship bridges. The system enables real-time scanning of human avatars for use in VR supported design processes. The system uses off-the-shelf 3D sensors to generate high-density 3D meshes and high-resolution textures of human beings in real-time, Figs.20 and 21. Designers can insert real time avatars in virtual scenes using a game engine. One motivation of the research is enabling human-to-human communication in a virtual environment – in essence, such a vision could be used to have a teacher appearing virtually on stage anywhere. The system reaches its limits when the real person turns and the avatar appears with zig-zag lines where the body scanning is lost. In addition, issues with sound must be expected if multiple speakers are involved.



Fig.20: 3D scanner and view of VR view with avatar on bridge

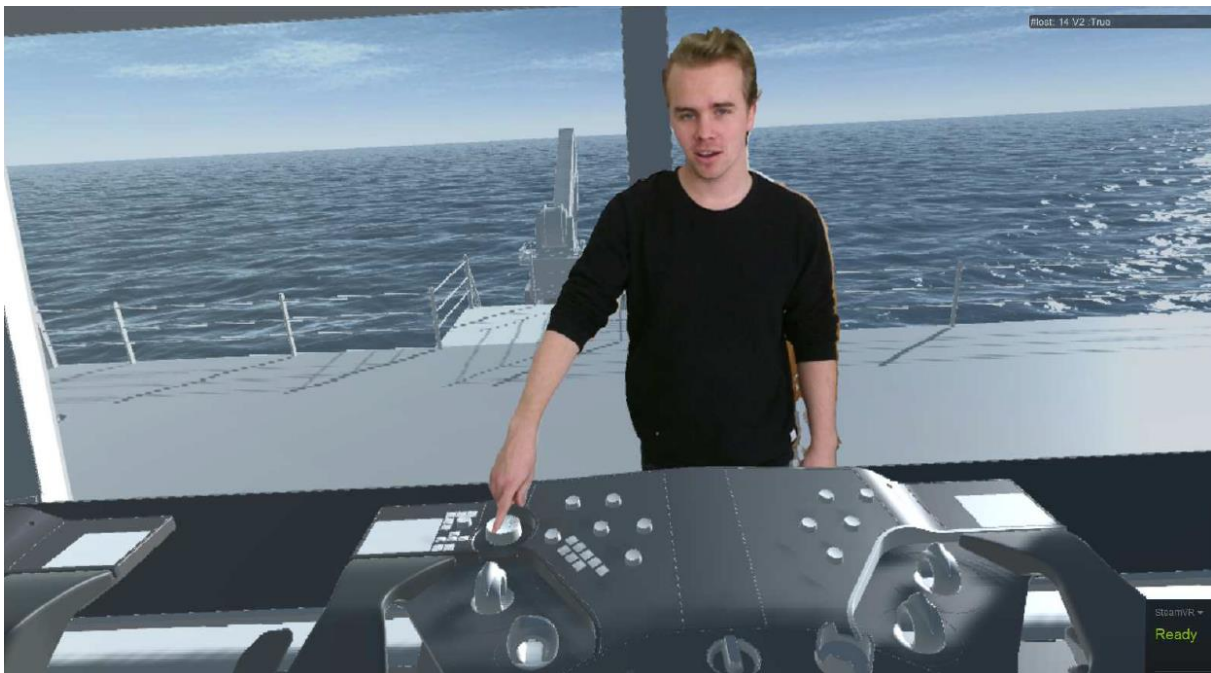


Fig.21: Virtual Kjetil Nordby avatar appearing on a virtual nautical bridge

MacGregor opened a VR based training center in Arendal/Norway, Fig.22. Using stereoscopic vision, trainees operate cargo-handling equipment. The intention is to reduce the likelihood of causing injury to personnel or damage to equipment because operators have already tried and tested it in the virtual world. The training room uses an authentic operating chair for offshore crane simulations and a displayed virtual world, like nautical bridge simulators.



Fig.22: MacGregor cargo handling simulator (source: MacGregor)

Ocean Technologies (www.oceantg.com), the largest maritime training provider with legacies in Vid-eotel, Seagull, Tero, Coex Marlin and MTX, has assorted digital training courses in its portfolio. The website uses the lure of VR, in promising training based on “learning games, micro learning and VR to engage the new generation of seafarers”. However, in the webinars we followed, there were only some simple 3D models with minimum interaction shown, essentially to add some interactivity to otherwise conventional online learning courses.

3. Take-home lessons

VR based training is well received by a majority of participants, but not all; for mature specialists, the thrill of computer-generated imagery fades quickly, and a clear pedagogical value needs to be seen to convince, *Van der Ende et al. (2020), Chae et al. (2021)*.

Creating 3D models as a starting point for Virtual Reality applications is costly and beyond the capabilities of a training department. Instead, training scenarios are usually opportunistic and employ existing (in-house or downloadable) 3D models.

The high costs for VR based training limit applications. Business cases can usually be made only when large assets or human health/life is at risk in real-world training.

Stereoscopic vision and high-res photorealism are nice to have, but for most training purposes not vital. The more trainees immerse in a virtual world, the more they leave the real world. Trainees may then no longer be aware of trainers or fellow trainees with detrimental effects for pedagogy. Full immersion may also create health and safety problems.

VR “cinemas” with special rooms mean that trainees must come to a specific location, reducing the potential customer group and making convincing business cases difficult.

References

BERTRAM, V.; PLOWMAN, T.; FEINER, P. (2020), *Survey Simulator – A Virtual Reality Training Tool for Ship Surveys*, 19th Conf. Computer and IT Applications in the Maritime Industries (COMPIT), Pontignano, pp.7-15, http://data.hiper-conf.info/compit2020_pontignano.pdf

CHAE, C.J.; KIM, D.; LEE H.T. (2021), *A Study on the Analysis of the Effects of Passenger Ship Abandonment Training Using VR*, Applied Sciences 11/13, <https://www.mdpi.com/2076-3417/11/13/5919/htm>

GASPAR, H.M.; TANIGUCHI, D.; RUOCCO, P.; NISHIMOTO, K. (2009), *A real-time 3d post-processor for a numerical model-basin simulator*, 8th Conf. Computer and IT Applications in the Maritime Industries (COMPIT), Budapest, pp.512-524, http://data.hiper-conf.info/compit2009_budapest.pdf

KATZKY, U. (2014), *Virtual reality simulation training for underwater operations*, 13th Conf. Computer and IT Applications in the Maritime Industries (COMPIT), Redworth, pp.504-511, http://data.hiper-conf.info/compit2014_redworth.pdf

KIL, W.S.; SON, M.J.; LEE, J.Y. (2018), *Development of multi-purpose VR simulator for a ship from 3D CAD model*, 17th Conf. Computer and IT Applications in the Maritime Industries (COMPIT), Pavone, pp.250-258, http://data.hiper-conf.info/compit2018_pavone.pdf

KIL, W.S.; BYUN, S.H.; LEE, J.Y.; SON, M.J. (2019), *Development of Real-Time Emergency Response Training Simulator for Collective Ship Crews Based on Virtual and Mixed Reality*, 18th Conf. Computer and IT Applications in the Maritime Industries (COMPIT), Tullamore, pp.180-190, http://data.hiper-conf.info/compit2019_tullamore.pdf

KUBIAK, M. (2011), *Virtual training – a way to improve operational performance*, Bulk Carrier Update 3, DNV, Høvik, pp.28-31

LAMBROU, M.A.; POLYDOROPOULOU, A.; NIKITAKOS, N.; LITINAS, N. (2006), *Personalized, virtual maritime self-learning in the SLIM-VRT environment*, 5th European Conf. on e-Learning, Winchester

LINDENAU, O.; BERTRAM, V. (2003), *The making of a VRML model for an SES with streamlines and pressure distribution*, 2nd Conf. Computer and IT Applications in the Maritime Industries (COMPIT), Hamburg, pp.5-14, http://data.hiper-conf.info/compit2003_hamburg.pdf

LVOV, M.S.; POPOVA, H.V. (2020), *Simulation technologies of virtual reality usage in the training of future ship navigators*, 2nd Int. Workshop on Augmented Reality in Education, Krvyvi Rih, <http://ceur-ws.org/Vol-2547/paper04.pdf>

MacKINNON, S.N.; BRADBURY-SQUIRES, D.; BUTTON, D. (2016), *Virtual reality based training improves mustering performance*, 15th Conf. Computer and IT Applications in the Maritime Industries (COMPIT), Lecce, pp.75-83, http://data.hiper-conf.info/compit2016_lecce.pdf

MAGEE, L.E. (1997), *Virtual Reality Simulator (VRS) for Training Ship Handling Skills*, Virtual Reality, Training's Future?, Defense Research Series 6, Springer, pp.19-29

MARKOPOULOS, E.; LUIMULA, M.; PORRAMO, P.; PISIRICI, T.; KIRJONEN, A. (2020), *Virtual Reality (VR) Safety Education for Ship Engine Training on Maintenance and Safety (ShipSEVR)*, AHFE 2020 Virtual Conf. on Creativity, Innovation and Entrepreneurship, and Human Factors in Communication of Design, https://www.researchgate.net/publication/342680306_Virtual_Reality_VR_Safety_Education_for_Ship_Engine_Training_on_Maintenance_and_Safety_ShipSEVR

NEWELL, J.; LUCK, S. (2017), *Testing the boundaries of virtual reality within ship support*, Engine as a Weapon Int. Symp. VII (EAAW VII), Bristol

NORDBY, K.; BØRRESEN, S.; GERNEZ, E. (2016), *Efficient Use of Virtual and Mixed Reality in Conceptual Design of Maritime Work Places*, 15th Conf. Computer and IT Applications in the Maritime Industries (COMPIT), Lecce, pp.392-400, http://data.hiper-conf.info/compit2016_lecce.pdf

ROSENBLUM, L. (2000), *Virtual and Augmented Reality 2020*, IEEE Computer Graphics and Applications 20/1, pp.38-39, www.nrl.navy.mil/itd/imda/sites/www.nrl.navy.mil.itd.imda/files/pdfs/2000_CGA_VRAR2020.pdf

SEPPÄLÄ, L. (2021), *3D Model – Technology Island in Ship Design or a Central Piece for Ship-building Project Data?*, 20th Conf. Computer and IT Applications in the Maritime Industries (COMPIT), Mülheim, pp.228-234

TATE, D.L.; SIBERT, L.; KING, T. (1997), *Virtual environments for shipboard firefighting training*, Virtual Reality Annual Int. Symp., Albuquerque, https://www.nrl.navy.mil/itd/imda/sites/www.nrl.navy.mil.itd.imda/files/pdfs/cp_VRAIS97.pdf

VENTER, A.; JURICIC, I. (2014), *Virtual Reality for crew education in on-board operational and emergency conditions*, 13th Conf. Computer and IT Applications in the Maritime Industries (COMPIT), Redworth, pp.437-446, http://data.hiper-conf.info/compit2014_redworth.pdf

WARDELL, A. (2010), *DNV's survey simulator: A ship in every classroom*, Bulk Carrier Update 2, DNV, pp.14-16

WAUCHOPE, K.; EVERETT, S.; TATE, D.; MANEY, T. (2003), *Speech-interactive virtual environments for ship familiarization*, 2nd Conf. Computer and IT Applications in the Maritime Industries (COMPIT), Hamburg, pp.70-83, http://data.hiper-conf.info/compit2003_hamburg.pdf

WAUCHOPE, K., BERTRAM, V. (2004), *Ship familiarization in virtual reality using speech interaction*, Schiff+Hafen 56/6, pp.53-56

VAN DER ENDE, H.; VAN ASSELT, M.; KOELMAN, H. (2020), *The Effectiveness of Virtual Reality in Maritime Education*, 19th Conf. Computer and IT Applications in the Maritime Industries (COMPIT), Pontignano, pp.254-262, http://data.hiper-conf.info/compit2020_pontignano.pdf

Appendix – Features of DNV’s Survey Simulator (SuSi)

We refer to *Bertram et al. (2020)* for a more extensive description of SuSi.

The Survey Simulator offers elements of four maritime vessels: Bulk Carrier, Tanker, Containership, Mobile Offshore Unit. Each vessel has several disconnected survey areas, such as cargo hold, deck, double bottom, etc. The vessels and their areas were modelled after real ships or structures, with high-level of detail.

Thousands of deficiencies were placed in the inspection areas, both safety-related and of technical nature. These deficiencies are based on DNV’s global inspection experience.

The Survey Simulator offers four training modes:

1. Ship knowledge mode - Covers maritime naming convention, parts naming and certificate requirements
2. Areas of attention mode - Highlights areas where hull structural deficiencies are likely to occur
3. Survey requirements mode - Visualization of class and statutory survey requirements (based on DNV GL rules)
4. Findings mode - Display of built in deficiencies and descriptions

A strong feature of the Survey Simulator is interactivity. Several virtual tools are available:



PDA (Personal Digital Assistant) – enables access to essential information about naming, survey requirements and findings during virtual inspection. Gives access to attached documentation, photos, drawings, manuals and reporting templates.



Flashlight – necessary in dark areas as with real on-board surveys



Camera – essential in preparing documentation of deficiencies during virtual inspection



Spray – handy tool to mark-up deficiencies



Telescopic boom (cherry picker) – useful when checking upper part of ship’s structure



Raft – common way of inspecting upper parts of internal structures of tankers when tanks are filled with water.

Notilo Cloud AI Platform for Hull Condition Reporting

Solène Guéré, Nicolas Gambini, Notilo Plus, Marseille/France, solene@notiloplus.com

Abstract

With new regulations to improve ship efficiency and reduce species invasion, the number of underwater hull inspections is expected to increase greatly. But how can we scale them effectively, from in-water inspection to report generation? Notilo Plus has designed a suite of technologies that will enable fast and replicable inspections as well as automatic, consistent report generation. Using AI algorithms for image recognition, it classifies hull images according to their degree of fouling, coating conditions, and generates insights that are compliant with the best standards of the industry. Firstly, designed for the Seasam ROV with localization capability of every image on the General Arrangement plan of the hull, it is now available for all service providers, regardless of their inspection method. Any underwater, diving or ROV video can now be turned into actionable recommendations on Notilo Cloud platform. It opens the door for better hull management, optimized cleaning patterns and predictive models for shipowners and ship managers at a fleet scale, thus facilitating compliance with the strictest regulations. Seasam and Notilo Cloud are now used by shipowners and service providers around the globe, and are selected by DNV on Veracity platform.

1. Introduction

For a ship, hull fouling is responsible of a significantly increased fuel consumption, *Hakim et al. (2017)*, and therefore, unnecessary GreenHouse Gases (GHG) emissions. Furthermore, globalization requires transcontinental transportation. Therefore, ships are passing by very different ecosystems, which develops on their hulls an unnatural fouling mixing up living species from incompatible environments. This last phenomenon jeopardizes wildlife in the areas around the cargo ports. Biofouling is therefore a main issue to tackle to reach sustainable maritime transportation, *Davidson et al. (2016)*. In the context of globalization where maritime transportation represents almost 3% of GreenHouse Gases emissions, *IMO (2021)*, in addition of a increasing awareness of ecosystem endangerment, many initiatives have been deployed to tackle these issues and tends toward Green shipping.

2. New standards and regulations

2.1. BIMCO and local regulations

The launching of the new Baltic and International Maritime Council (BIMCO) standards, coming into effect by 2023, intends to make biofouling detection and cleaning mandatory. This knowledge is already required for some countries (especially in Oceania) such as New Zealand whose Ministry of Primary Industries has edited “Guidelines For Diving Service Providers”. These guidelines share the same purpose as BIMCO standards, and consequently, we will focus on these standards on the following as they are intended to become the global norm.

BIMCO is the largest international shipping association representing shipowners and is accredited as a Non-Governmental Organisation by the United Nations. To promote greener standards across the shipping industry, and limit the potential damage of hull-related invasive species, the council has created an in-water cleaning industry standard documentation, *BIMCO (2021)*.

This documentation states the need to perform regular inspections of the hulls, also considering aggravating factors which require an increase in inspections frequency (temperature, salinity, distance from the shore, depth, ...). In addition, even if the purpose is before everything the cleaning, inspections will always be required. Indeed, despite a cleaning is already scheduled, the documentation indicates that a pre-cleaning inspection is always mandatory in order to identify the areas of the hull where the effort needs to be concentrated.

This report also requires that “during the inspection of the underwater area (hull and niche areas) of the ship, the following shall be ascertained:

- Types of biofoulings.
- Percentage of biofouling coverage for each type.
- Height of biofouling for hard calcareous types.
- Condition of the AntiFouling Systems (AFS) on the hull and reference areas.”

These key pieces of information are at the center of latest Notilo Plus developments for our Shipping solution as we will explain it in the following.

2.2. EEXI/CII

The International Maritime Organization (IMO) of the United Nations adopted amendments on MARPOL on June 2021 in order to enforce by 2023 a new regulation centered around two calculations for each ship: Efficiency EXisting ship Index (EEXI) and Carbon Intensity Indicator (CII) in order to cut off GHG shipping emissions.

The EEXI indicator is based on ships specifications, and is estimated from the documentation emitted by the ship manufacturer.

The CII perfectly completes the EEXI as it is an operational carbon emissions indicator. This one will consist of a mark from A to E, with a legal target on the A to C range. It will be based on real emissions measured during the operations performed by the ship. Conforming to the regulation will consequently require an accurate, regular and efficient maintenance of the hull. At the scale of a fleet, it will be a real challenge to rise up for ship owners, and turn-key quick and efficient ship inspections solutions represent a significant asset to prepare for this new regulation, and go beyond the future standards thanks to good practices made easy to implement.

3. Notilo Plus Solution, combining reliable hardware with powerful software

3.1. State of the art

Nowadays, all these inspections are performed by diving teams or Remotely Operated Vehicles. In the first case, it requires a specific organization because of regulatory requirements to ensure a safe diving team in any port. As a consequence, the inspections take more time and human resources, for a result which is not optimized as it consists of generally poor-quality photographs and videos of the hull that are used to interpret a general status. This solution is rather expensive, sometimes complicated to schedule, and requires a long time before the report is ready because all the data collected needs to be processed by experts, but image localization is complicated to pinpoint in post-processing.

The other option, the inspection by a ROV, is quite easier on the supply part (if we consider an easy-to-pilot mini ROV) but faces the same issues on the time it takes to perform the inspection and then to edit the report. Times of 3 h of preparation, 6 h of inspection, and 10 h of post-processing have been reported in personal communication with industry players. In addition, not all the ROVs have a good stabilization system as well as a high definition to ensure enough image quality and hull visibility, so the possibility of post-processing and accurate guidelines is not necessarily satisfying.

Thus, the state-of-the-art is not satisfying at all to answer the growing needs by the main actors of Shipping. The process is tedious, unoptimized and gives poor information about the hull which will hardly encourage the inspections that are perceived today as a painful obligation. Reports are, in the best case, impossible to merge together to extract useful information such as monitoring of change over time, crossing data with other sources, etc. In the worst case, the reports can be inaccurate and partial due to inadequate survey or difficult post-processing.

With the current context in shipping and the pressure to shift towards Green Shipping for the main actors of the sector, inspections will need to scale. The industry could use a more extensive, more reliable and more informative solution.

3.2. Seasam solution: A hardware suite

Notilo Plus was historically specialized in drone conception with first automation features with an autonomous diver tracking system. Building on our ability to develop autonomous inspections scenarios, we started with developing a hardware solution to perform hull inspections easily.

The aim was to provide them with an easy-to-use solution, bringing to the surface reliable and high-quality data: localized images, steady frames, consistent distance to the hull.

To do so, our Seasam solution, Fig.1, is composed of a Seasam drone, a Seasam Navigator, a ground station, a WiFi reel and a touchscreen tablet with our application - Seasam control. It can be used as a Remotely Operated Vehicle after a very short training as the remote control makes it intuitive to pilot. Equipped with a high-definition camera and possibly with powerful lights and extra-sensors (such as acoustic camera), it is the perfect tool to perform inspections on the hull with higher quality data than a diving team, without the danger and for a lower cost . (Pay-as-you-inspect plans are available from 1000 € per inspection.)

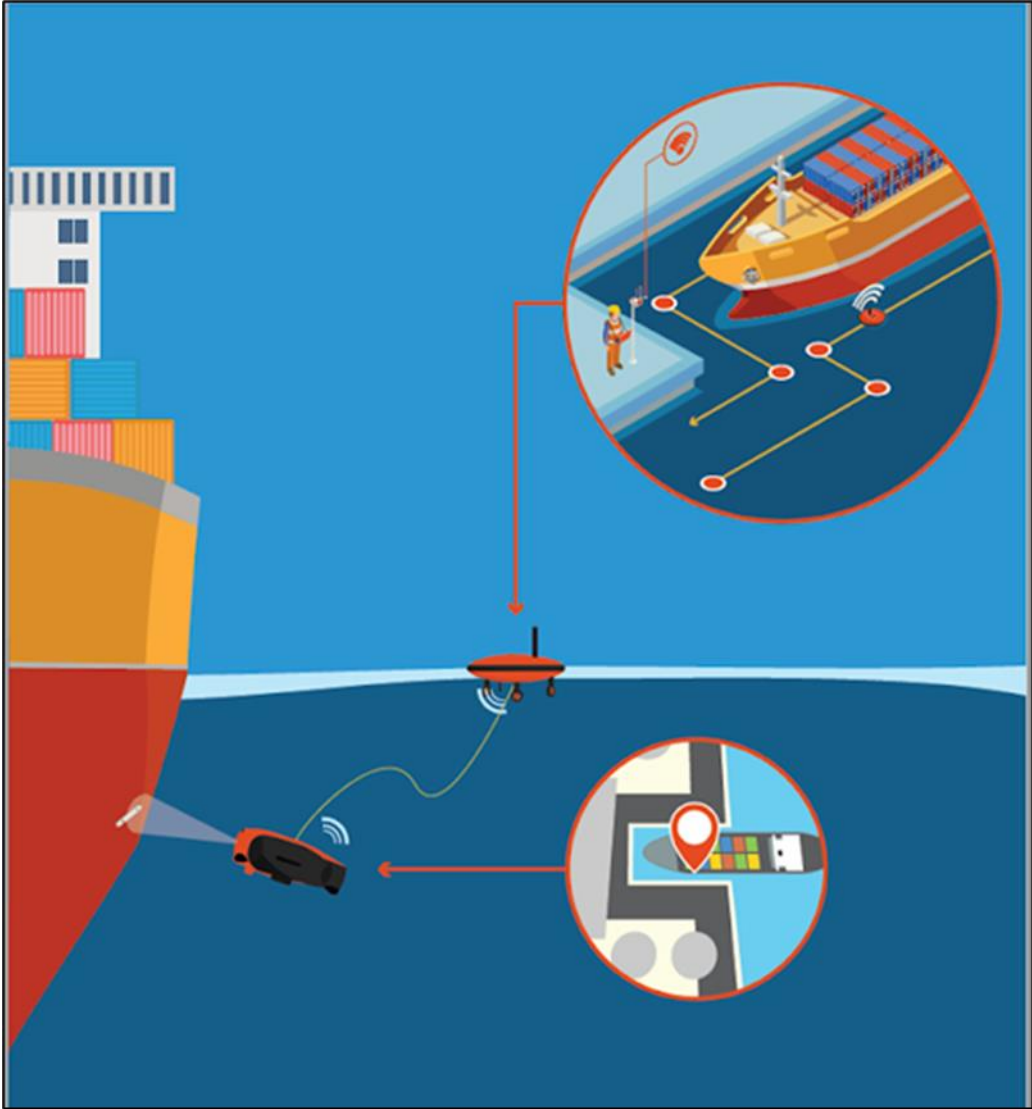


Fig.1: Seasam solution

In addition, using the ground station and Seasam Navigator —equipped with a GPS – allows live autonomous location of the Seasam drone in relation to the hull thanks to an acoustic system. It means that during the inspection, the precise location (accuracy: few meters) of the Seasam drone is recorded and linked to the data acquired on the hull, Fig.2. The correlation of these pieces of data enables a full exploitation that will be described later. Further developments allow us to propose a fully autonomous inspection, based on live location and hull-servoing to ensure the inspection is always optimized.



Fig.2: A suite of hardware, from mini-ROV with localization declaration to autonomous inspection



Fig.3: Inspection with localized images placed on the general arrangement plan of a vessel

With these several options, Seasam is a suite of Hardware that can adapt to the level of simplicity necessary during the inspection, and to the level of precision that is required for the reports.

3.3. Notilo Cloud: The platform to exploit the whole extent of the collected data

Notilo Cloud is the perfect prolongation of the Seasam suite. Designed to valorise the data collected, the videos recorded with the position are easily uploaded to the platform in order to be analysed. Indeed, we built four classifiers trained with a 25000 images dataset enabling us to determine a fouling score for each image, to evaluate the status of the coating, to identify the niche areas and to categorize the images according to their visibility.

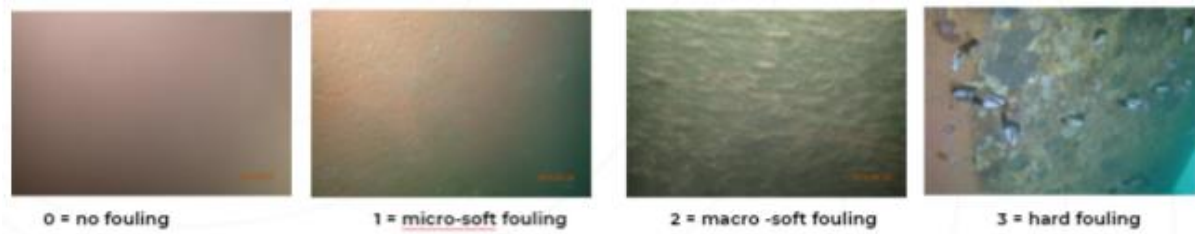


Fig.4: Example of classification for the fouling algorithm

These classifiers are Convolutional Neural Networks for which we used transfer learning: it means that they are pre-trained for classification tasks, and we added a few layers called the “Head” at the exit to adapt it to our specific problems. The whole network has then been trained again with our datasets in order to adjust the weights and to gain in accuracy. This design allows an accuracy of 90% for coating status, Fig.5 (left), 90% for visibility evaluation, Fig.5 (right) and 97% for niche areas identification, Fig.6.

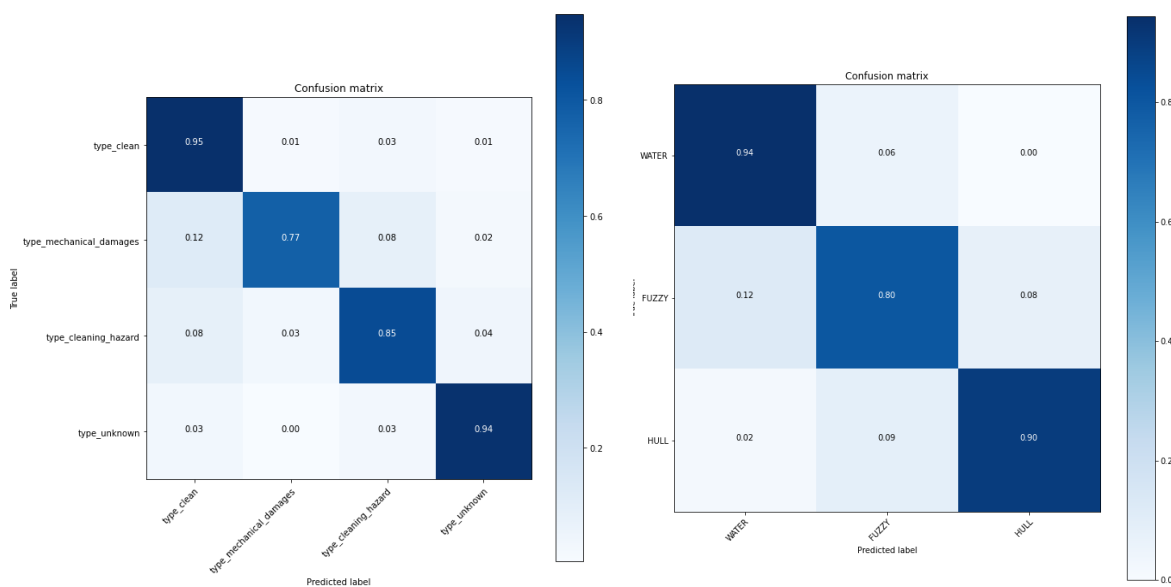


Fig.5: Neural net accuracy for coating status (left) and visibility evaluation (right)

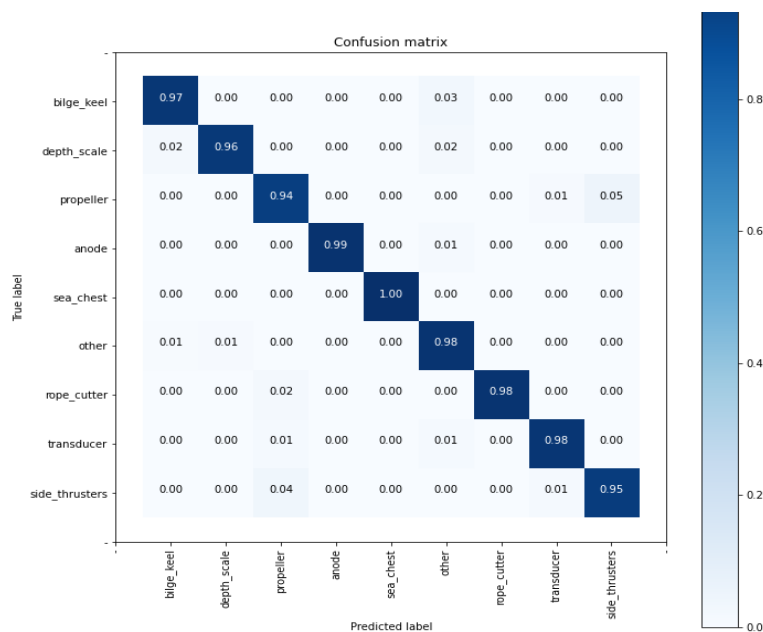


Fig.6: Neural net accuracy for niche area identification

Concerning fouling, the accuracy is limited to 83% but the mistakes are concentrated on neighbouring scores, Fig.7. After further review, we detected that 56% of these mistakes were due to human scoring in the first place as the experts we integrated in our initial qualification process showed a lack of consensus on the concerned frames.

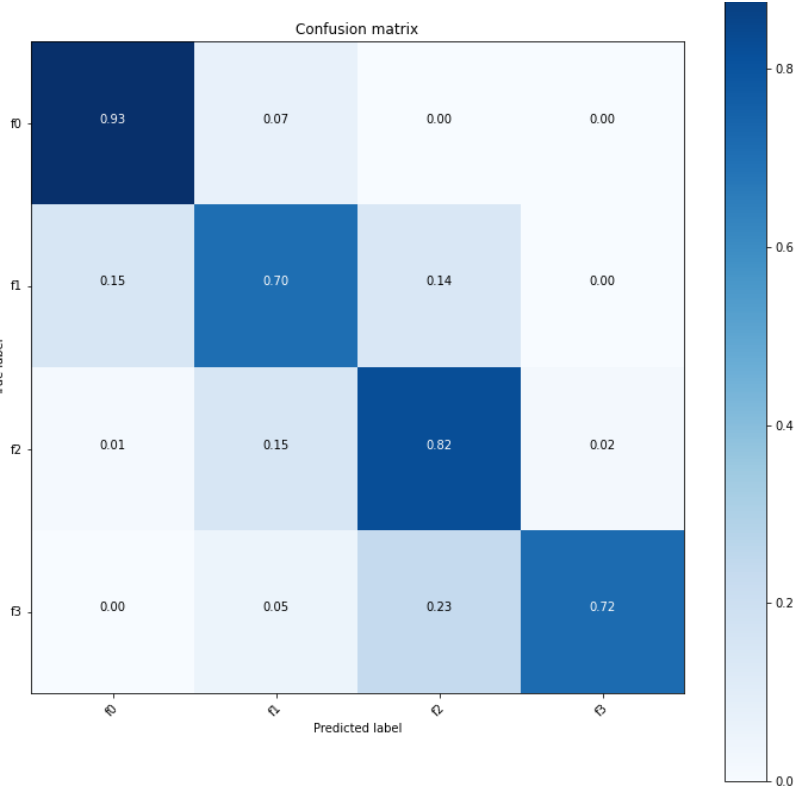


Fig.7: Mistakes concentrate on neighbouring scores

At the end of inspections, the users upload their videos on Notilo Cloud. In the software are several actions available:

- store all previous dives
- create a report
- share with relevant partners or customers.

The report generation consists in itself in several tasks and four different algorithms:

- Extract relevant frames from all inspection videos, with a visibility algorithm. Only images actually showing the hull will be selected. After the frame extraction, a preprocessing algorithm adapts the format of the data to make it compatible with the other classifiers.
- Render more precisely if the frame consists in a niche area, and in that case, which niche area
- Evaluate for each frame the level of fouling from 0 to 3
- Determine if any coating defect is present: painting defect or mechanical damage
- Link each frame to the corresponding location on the hull out of the raw dive data

All these actions lead to the creation of a report, with 30 hull sections that have color and information on the status of each area, Fig.8.

This automatic evaluation enables us to better understand the status of the hull after inspection, to identify the areas to prioritize during the next cleaning operation and to save much time because there is no requirement for an expert analysis of the video as the results of our algorithms have already been validated by experts. This first step permits the automatic edition of an inspection report in less than

30 minutes - compared to 10 hours for traditional reports - which is far quicker, more cost-effective, and more efficient than traditional inspection.

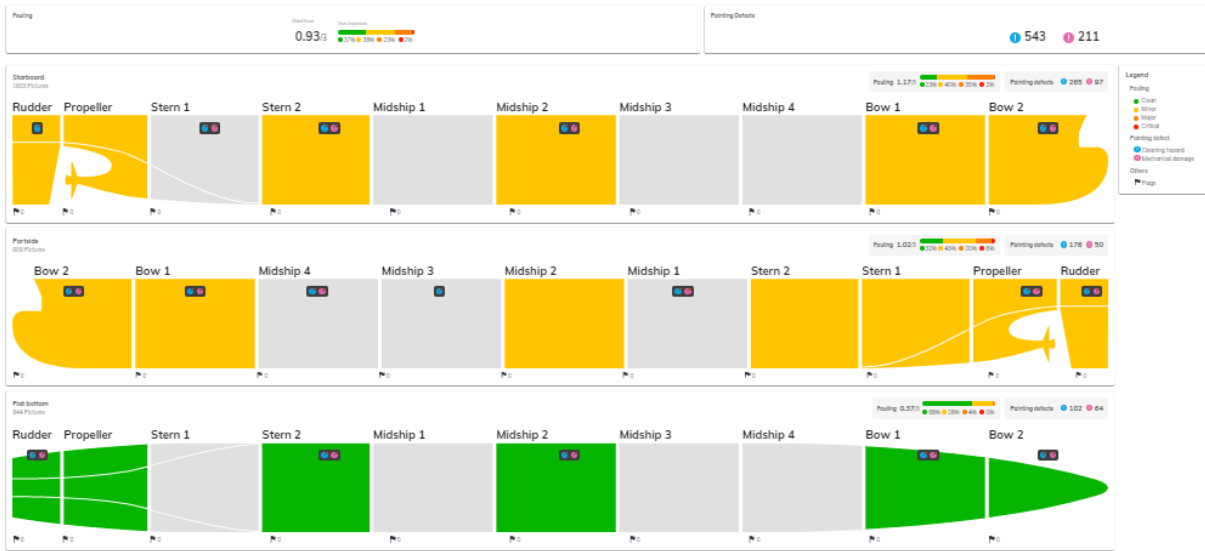


Fig.8: Example of report with various hull section inspected and degree of fouling/ number of coating defects

3.4. Notilo Cloud for any ROV source: opening data for all

Furthermore, in order to democratize the predictive maintenance of hulls and the understanding of underwater assets, Notilo Plus has opened a stand-alone version of Notilo Cloud for any ROV, Fig.9. It opens the use of our algorithms and autonomous report tool to anyone who performs underwater inspections with any underwater camera (GoPro, ROV, ...). The main difference resides in the need to declare directly on the platform the location of the different images. Classification and filtering of all images is possible to have a closer look to all relevant frames of the video.

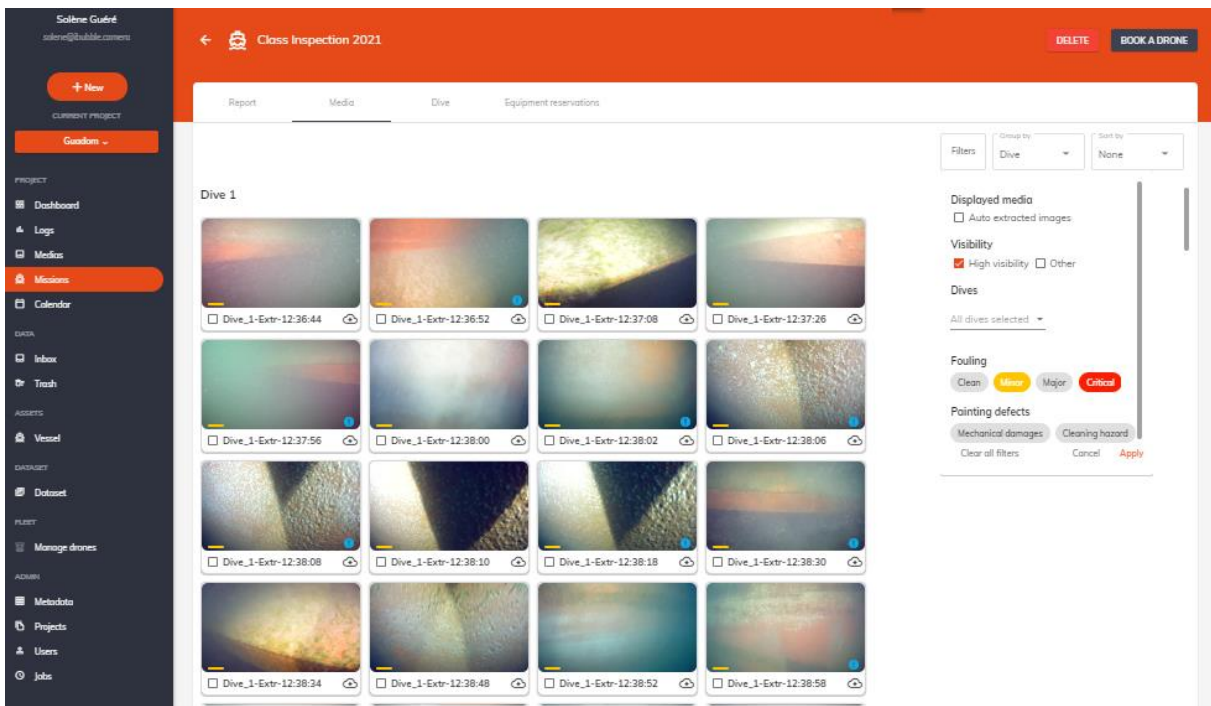


Fig.9: Notilo Cloud

4. Discussion

Currently, our solution appears as a great help for CII as it helps to understand the origin of any problem on the actual carbon consumption of the ships. Indeed, by indicating an overall fouling status of the hull to the Ship Owners, Notilo Cloud helps them to optimize their cleaning operations in order to keep the carbon (and GHG in general) emissions of their ships under control.

Our fouling algorithm is not yet fully compliant with BIMCO standards or other regulations for invasive species control. BIMCO standards differentiate many types of fouling and various types of coverage, Table I.

Table I: Fouling types according to BIMCO

Soft biofouling		Hard calcareous biofouling
Micro	Macro	Macro
Slime	Soft corals	Barnacles
	Sponges	Mussels
	Hydroids	Tube worms
	Anemones	Bryozoa
	Algae	Oysters
	Tunicates	

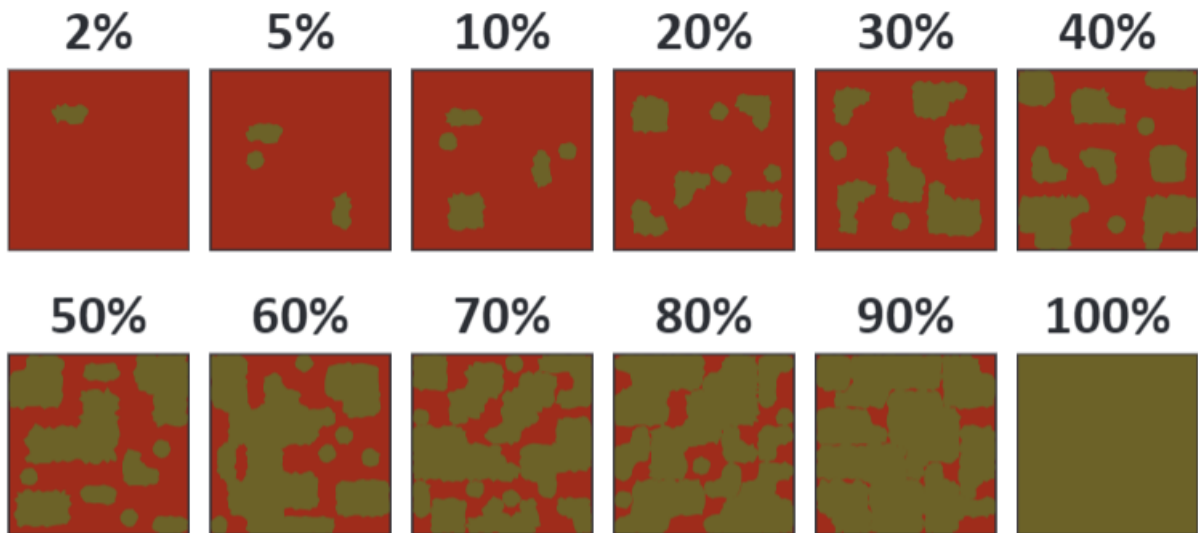


Fig.10: Coverage

We have found it difficult to find experts able to converge in their classification of images between various types of macro soft fouling and macro hard fouling. The experts had often diverging opinions on classification.

We found that, for now the type classification (hard or soft, micro or macro) was sufficient, from an operational point of view, to plan maintenance and cleaning action. We recommend that these official classifications should not be overly precise, to account for the actual capabilities of experts to differentiate between fouling types. Alternatively, a new and more complete dataset labeled by experts should allow us to tackle this challenge.

The coverage of fouling in BIMCO standards is a way of classifying images from a human eye perspective: i.e. looking at a frame, how scattered the fouling zones are, Fig.10. From an A.I. perspective, and with the possibility of extensive classification of each and every image from a video inspection, it becomes more relevant to use broader information, such as the actual severity of fouling depending on the frames.

We propose that international standards for underwater inspections use more precise, AI driven framework for underwater hull inspections.

5. Conclusion

Notilo Cloud has been designed to fit with emerging regulations. It has already been identified by many majors in the sector as a high-end tool to exploit the full extent of all the data that can be collected during inspections. Moreover, combined with the Seasam solution, it offers a turn-key solution for underwater hull inspection. Seasam solution is making possible quick, optimized, easy to set up inspections, at lower cost than traditional inspection solutions. All these features make Notilo Plus’ ecosystem a key set of tools to tend toward Green Shipping through predictive maintenance. In other words, to make a step towards a sustainable activity while making savings.

As a versatile tool, that can be used anywhere in the world, from any data source, Notilo Cloud makes possible intensive hull monitoring and management, bringing together all data sources and creating predictive models for hull efficiency.

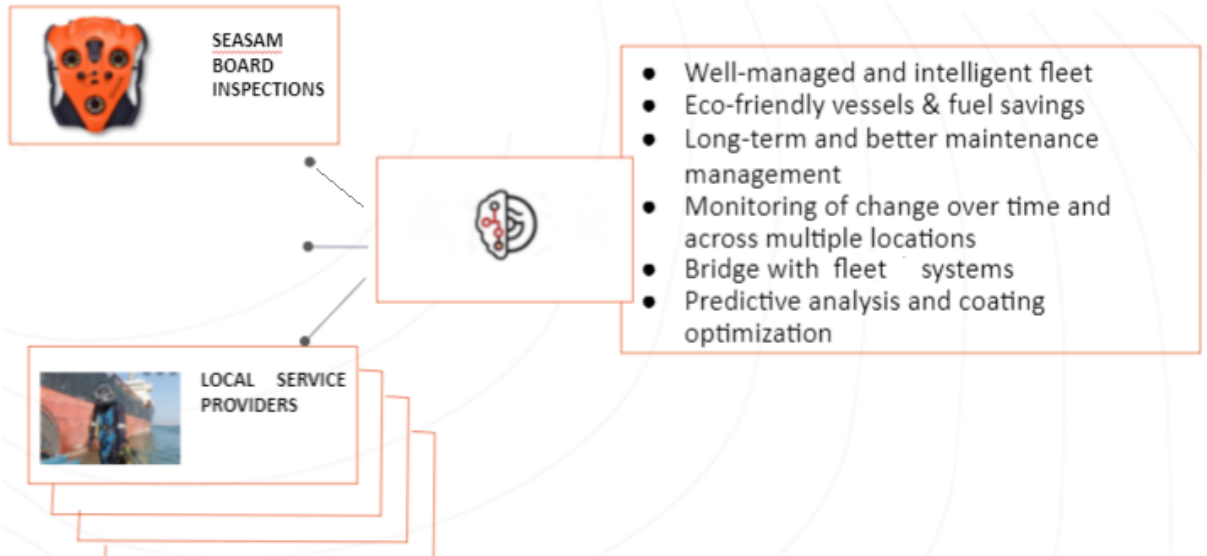


Fig.11: A vision for integrated hull management

The scoring of 83% to 97% accuracy of our algorithm will continue to improve as the number of inspections increase, and we foresee a future where inspectors will never have to spend more than 1 hour to produce a full hull inspection report, with a greater accuracy than any previous method. This opens the door to efficiently scaling hull inspections, and better protecting our planet and our oceans.

References

BIMCO (2021), *Industry standard on in-water cleaning with capture*, BIMCO, Copenhagen

DAVIDSON, I.; SCIANNI, C.; HEWITT, C.; EVERETT, R.; HOLM, E.; TAMBURRI, M.; RUIZ, G. (2016), *Mini-review: Assessing the drivers of ship biofouling management – aligning industry and biosecurity goals*, Biofouling 32/4, pp.411-428

HAKIM M.L.; UTAMA, I.K.A.P.; NUGROHO, B., YUSIM, A.K.; BAITHAL, M.S.; SUASTIKA, I.K. (2017), *Review of correlation between marine fouling and fuel consumption on a ship*, 17th Conf. on Marine Technology (SENTA), Surabaya

IMO (2021), *Fourth IMO GHG Study*, Int. Maritime Org., London

Applying a Needs Analysis to Promote Daughter Craft for Year-Round Access to Far-Offshore Wind Turbines

Sophia Brans, Siemens Gamesa, The Hague/The Netherlands, sophia.brans@siemensgamesa.com

Andre Rinne, Siemens Gamesa, Hamburg/Germany, andre.rinne@siemensgamesa.com

Austin A. Kana, TU Delft, Delft/The Netherlands, a.a.kana@tudelft.nl

Abstract

Service Operation Vessels (SOVs) are purpose-built maintenance vessels that provide high accessibility to far-offshore wind turbines, but they lack multitasking capabilities. Its daughter craft (DC) is a valuable asset for unplanned maintenance in the summer when it can operate safely, but it is often not deployable during rough weather conditions. The main research question is: What are the deficiencies of current DCs, and how can these access vessels be modified to operate year-round at far-offshore wind farms? The results show that the current DC's deficiencies lie in its current operational requirements. Also, performance in oblique waves is currently riskiest since that is when there are higher vertical accelerations or a combination of vertical and lateral accelerations. Furthermore, wave steepness has significantly more effect on accelerations than wave height. Lastly, future DC designs should be focussed on stable seakeeping performance during transfers rather than high-speed transit. An analysis into the seakeeping performance of four prototypes showed that it is feasible to increase the transfer requirement from $H_s \leq 1.5$ m to $2.0 \text{ m} \leq H_s \leq 2.5$ m. The catamaran type DCs have a high potential to realise year-round accessibility to far-offshore wind farms due to their resulting performance in oblique wave conditions.

1. Introduction

With the known negative effects linked to the use of fossil fuels, it is becoming increasingly important to switch to cleaner energy. Among many alternatives, wind farms are one of the most environmentally feasible solutions to reduce greenhouse gasses when the entire lifecycle is assessed, *Guezuraga et al. (2012)*. *Walsh (2019)* reports that offshore wind farms in Europe are moving farther from shore. This is because operators want to attain stronger and more stable wind resources, and due to depleting locations near the shore.

However, this trend makes it more challenging and expensive for wind farm operators to provide service. The harsher weather conditions require offshore wind turbines to be maintained more frequently than those situated onshore. Also, both the weather and the distance complicate the process of accessing wind turbines. *Shafiee (2015a)* describes that the availability of offshore wind farms is in the range of 60% to 70%, while for onshore wind farms, it is typically between 95% to 99%.

1.1. Problem definition

The main adverse effect of the remoteness of far-offshore wind farms is the increased transit times from ports, which decreases the time available for maintenance tasks and causes fatigue in technicians. A common solution is to work from an offshore-based hub, such as a Service Operation Vessel (SOV). SOVs are used primarily for calendar based (preventive) maintenance. This minimises the need for unforeseen (corrective) maintenance but does not eliminate it. When an unforeseen event occurs, an SOV is often occupied and cannot reach the defective turbine fast enough. So, the problem is that SOVs are not flexible enough to carry out corrective maintenance next to preventive maintenance, and that does not benefit wind farm availability.

Other access vessels can assist in the event of unforeseen events by transporting technicians from the SOV or the shore. But with farms moving farther from shore, each solution becomes impractical for reasons such as limited weather window, longer transit times and cargo capacity, making them less suitable to access defective far-offshore turbines. In short, the accessing capabilities of smaller vessels

are insufficient for far-offshore wind farms. If both problems persist, O&M operators will not be able to repair a (sudden) turbine malfunction in time, leading to turbine downtime and high revenue losses.

1.1 Goal

The overall goal of this study is to improve accessibility to (defective) far-offshore wind turbines. Based on the stated problems, (i) SOVs require new or improved subsystems to increase their multitasking capability and (ii) its daughter craft (DC) shows the most potential to do so. Hence, this study aims to confirm that DCs are the system-of-interest based on their capabilities and deficiencies and determine what is required to resolve them. This is done by applying a Needs analysis, which is part of the Systems Engineering approach by *Kossiakoff et al. (2011)*, and consists of four steps: Operations Analysis, Functional Analysis, Feasibility Definition, and Needs Validation. These steps start from section 4.

2. Scope of stakeholders

This study considered the stakeholders identified by *Ahsan et al. (2018)*, who have a high interest in and high power to influence the far-offshore activities: wind farm owners/investors, the turbine supplier, the vessel supplier, and the O&M operator's technicians. Either of the two first stakeholders can also take on the additional role of O&M operator, whose primary interests are preserving turbine availability, minimising costs and ensuring turbine accessibility. However, the two remaining stakeholders can have conflicting interests with the O&M operator. First, the vessel supplier may require engineering and design costs that the O&M operator is unwilling to pay. Second, it is paramount that the technicians can work in a safe environment. Their safety imposes lower and upper limits to vessel performance and, thus, accessibility. The TU Delft is an external stakeholder with high interest in such a project since they wish to encourage and contribute to the energy transition but has low influence because they are not involved in how business is done.

3. State-of-the-art access vessels

Accessibility is defined as the fraction of time when safe access to wind turbines is achieved, *Shafiee (2015b)*. To understand where the need for a new system comes from, it is first necessary to be familiar with current access methods in offshore O&M.

SOVs are best suited for calendar-based maintenance due to their large weather window; access is possible up to $H_s \leq 3.0$ m. Their ability to accommodate 25-40 technicians onsite for extended periods makes them more efficient due to reduced transit time. They are primarily used for preventive maintenance but will be used for corrective maintenance if necessary.

Some SOVs are fitted with a DC. These are ship-based vessels used to send technicians to wind turbines for corrective/preventive maintenance or to prepare the wind turbine before the SOV arrives. However, these vessels are currently only operable in the summer due to their smaller weather window. Existing DCs have been designed to transfer at $H_s \leq 1.5$ m since that is predominantly observed in their current operational area, i.e. at wind farms situated closer to shore.

Crew Transfer Vessels (CTV) are similar to DCs but are much larger and port-based vessels. These are used to cover the entire range of maintenance strategies. However, they are more suitable for offshore wind farms located not far from the shore to limit transit times and avoid motion sickness. In literature, they are occasionally mistaken for a DC. This study adheres to the following distinction: a CTV is an independent vessel that always heads back to port at the end of the day while a DC is dependent on its mothership, which launches, recovers, and stores it.

A Service Accommodation and Transfer Vessel (SATV) combines the capabilities of CTVs and SOVs. They can also remain offshore for (less) extended periods, which reduces transit times and can cover the entire range of maintenance strategies because they are meant for smaller wind farms.

Lastly, helicopters are the only non-seaborne access vessel at an O&M operator's disposal. They are not limited by metocean phenomena but are mainly used for urgent corrective maintenance.

4. Operations analysis

This section defines the deficiencies in current systems and operational objectives of the new system.

4.1. Operational area

This study is limited to offshore wind farms located in the North Sea because most are currently located there. The focus lies on the wind farms where offshore-based hubs (i.e. SOVs) are considered useful, but accessibility has become an issue because they are either occupied or not fast enough to take care of unplanned events. So, their operational area represents the operational area of the DCs. Two criteria were used to select the wind farms.

The first criterion is the distance from shore. This plays a significant role when selecting a vessel because they must have sufficient range to reach and operate at these wind farms. *Phillips et al. (2013)* estimated that the most cost-effective distance to implement offshore-based hubs, i.e. SOVs, is 35 nm (65 km) from the port.

The second criterion is the number of wind turbines. An SOV can visit approximately six scheduled turbines per day. With a yearly weather window of 90% an SOV can then be scheduled to service nearly 2000 turbines per year. *Krause and Stead (2017)* estimated that offshore wind turbines need to be visited 15 times per year for both scheduled service and troubleshooting. In that case, wind farms with at least 120 turbines are expected to properly occupy an SOV, which is this study's benchmark.

There are three wind farms in the North Sea that meet these two criteria: Hornsea One, Gemini and East Anglia Three. For conciseness, this paper will solely focus on the weather data from Hornsea One.

4.2. Operating conditions

Whether a turbine is accessible depends on the access vessel's ability to navigate the ongoing weather conditions. Specifically, wind speed, significant wave height and wave steepness predominantly affect vessel seakeeping, *MaTSU (2001)*. It should be noted that the performance of a majority of vessels is characterised by significant wave height. However, since these phenomena all interact and influence each other, it is doubtful whether a vessel's operability can be determined using a single parameter, *MaTSU (2001)*. Because of the interaction, experience shows that vessels still occasionally fail during conditions they were designed to handle. Here, wind speed was acknowledged but will not be considered a design criterion due to its minimal and indirect influence on the vessel and crew.

4.2.1. Significant wave height

Significant wave height (H_s) is defined as the mean height of the highest one-third of waves and is a popular design criterion to determine a vessel's operational limit, *MaTSU (2001)*. Fig.1 shows the cumulative occurrence of significant wave heights measured over 21 years at Hornsea One. This wind farm observed $H_s \leq 2.5$ m for 90% of the time annually. Furthermore, the occurrences differ throughout the seasons: 90% of waves in the summer are $H_s \leq 2.0$ m, while this increases to $H_s \leq 3.0$ m in the winter. Overall, this graph gives an initial impression of how often a range of significant wave heights is likely to occur. It is ultimately used to determine the theoretical weather window.

4.2.2. Wave steepness

While H_s is a more popular parameter to determine a vessel's operational limit, *MaTSU (2001)* considers wave steepness to be a better indicator because it determines the force upon a fixed or floating structure, how it will behave and when waves are likely to break. Like H_s , wave steepness is linked to

its location. Table I is a wave scatter diagram of the waves measured at Hornsea One. It indicates how many waves correspond to a specific combination of H_s and peak period (T_p). Where there is no data implies that waves will break due to steepness.

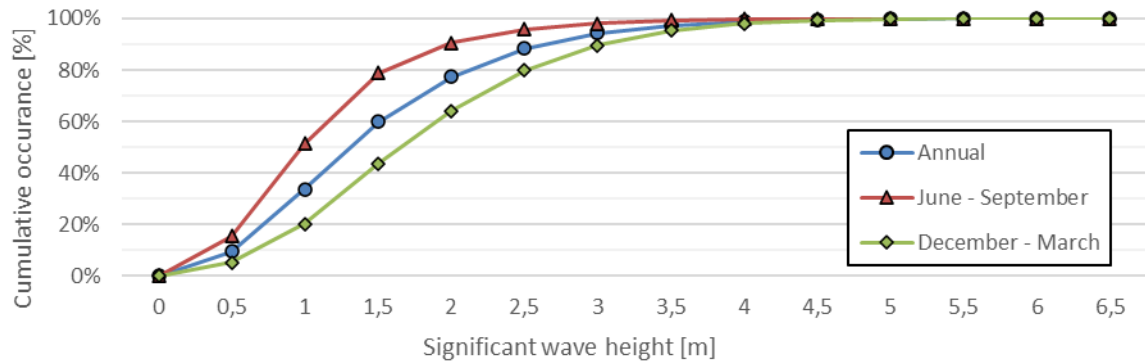


Fig.1: Measured wave data at Hornsea One (adapted from *Stavenuiter (2009)*)

Wave steepness (S) is defined as the ratio between H_s and wavelength (λ). However, wavelengths were not included in the used weather database. According to *Antão and Soares (2016)*, the wavelength can be calculated from the dispersion relation given in Eq.(1).

$$\lambda = \frac{gT^2}{2\pi} \tanh \frac{2\pi d}{\lambda} \quad (1)$$

Where, g is the gravity acceleration, T is the wave period, and d is the water depth. Deepwater assumptions are applied since the ratio between wave heights and water depth is relatively large, which means that $\frac{2\pi d}{\lambda} \gg 1$, *Gerritsma (n.d.)*. Inserting the simplified Eq.(1) into the definition for wave steepness gives Eq.(2). Applying Eq.(2) to the values in Table I shows that the majority of waves have $S = 0.03$ and that waves will mostly break when $S > 0.05$.

$$S = \frac{H_s}{\lambda} = \frac{2\pi H_s}{gT^2} \quad (2)$$

Table I: Scatter diagram of sea states at Hornsea One (adapted from *Jiao et al. (2018)*)

Hornsea 1		Significant wave height (H_s)										Sum	
		0.5	1.0	1.5	2.0	2.5	3.0	3.5	4.0	4.5	5.0		
Peak period (T_p)	2.5	86	1										87
	3.0	718	10										728
	3.5	2885	203										3088
	4.0	5677	3910	9									9596
	4.5	3624	9684	569									13877
	5.0	3345	9069	6245	84	1							18744
	5.5	2852	4963	9668	2379	33							19895
	6.0	2149	3690	5111	7415	1115	13						19493
	6.5	1867	3368	3847	4671	4040	422	1					18216
	7.0	1466	2871	3038	2923	2596	1847	91					14832
	7.5	934	2114	2235	2120	2136	1526	860	104				12029
	8.0	954	2307	1749	1792	2157	1610	702	315	69	2		11657
	8.5	894	2223	1531	1025	921	1408	619	151	66	36		8874
	9.0	501	982	882	601	471	654	732	236	44	17		5120
Sum	27952	45395	34884	23010	13470	7480	3005	806	179	55		156236	

No data here because waves break due to steepness

Steepness value

	0.01
	0.02
	0.03
	0.04
	0.05
	≥ 0.06

4.2.3. Prominent wave directions

The wind turbines of the reference farms have the boat loading oriented such that vessels encounter head waves the most. This is because head waves are generally considered to induce the lowest responses. This is also beneficial because the chance of large roll motions is then minimised. Besides head waves, there are other wave directions that are then encountered most frequently. For Hornsea One, there are mainly head, beam and following waves.

4.3. Deficiencies

The SOV's large weather window makes them ideal for upholding scheduled maintenance. However, its primary deficiency is its capacity to provide maintenance for unforeseen events due to its low response time. The SOV often cannot travel to a turbine far away because they are restricted by safety regulations that state that the operator must reach a turbine within an hour when an emergency occurs, and technicians need rescuing or medical treatment. SOVs can be equipped with DCs to increase their multitasking capability for unforeseen events. But DCs have a much smaller weather window. With offshore wind farms moving farther from the shore, the rougher weather conditions and sea states will continue to restrict operators from utilising DCs because they lack performance, especially during the winter season. CTVs have better access performance than DCs and are faster than SOVs. However, since they operate from the port, the vast distances make them ill-suited for far-offshore applications. SATVs are unsuitable because their functions are similar to that of an SOV, making them obsolete if an SOV already operates there. The main deficiency of helicopters is that it is not able to transport many technicians (usually 3-6) and cargo (usually less than 100 kg), *Hu et al. (2019)*, especially large components which the seagoing vessels are better capable of transporting.

4.4. The daughter craft is the system-of-interest

Solutions should be sought in increasing the SOV's multitasking capability. This could be achieved by improving one of the SOV's existing subsystems, and the system-of-interest is the DC because:

- DCs are already useful in the summer when weather conditions are calmer.
- DCs have a relatively cheap day rate compared to SOVs (around €500, which is included in the SOV's charter rate of roughly €25.000 per day), so they are more accessible for a redesign.
- DCs are included in the charter rate; it is more convenient and efficient to use the already paid vessels instead of hiring another access vessel.
- Altering a CTV to fit on and work from an SOV technically classifies it as a daughter craft.
- Even at lower speeds, the DC will reach the turbine faster than a CTV at top speed.

Since DCs are SOV-based, their overarching objective is to increase the multitasking capability of the SOV assigned to far-offshore wind farms. These far-offshore locations are characterised by wave conditions that are expected to induce extreme responses from existing DCs. So, the DC's operational objectives are deficiency driven. Based on the weather data from Hornsea One and the DC's deficiencies, the main operational objective is "Allow access in $2.0 \text{ m} \leq H_s \leq 2.5 \text{ m}$ ". This applies to both the transit and transfer phase, but it is mainly an enhanced objective with respect to the original transfer requirement since existing DCs are already required to transit in $H_s \leq 2.5 \text{ m}$ with 25 knots.

Also, different phenomena are present during high-speed transits and zero-speed transfers. This makes it hard to optimise a system towards both access phases. However, it was determined that 25 knots should no longer be required as a design speed. Instead, it should become the desired top speed because the (SOV-based) DCs are always closer to their destination than port-based access vessels.

5. Functional analysis

The second step of the Needs Analysis establishes whether there is a feasible and technical approach to design a system that could meet the operational objective. The DC's enhanced objective is essentially

about improving seakeeping. *Beukelman (1986)* states that a ship's behaviour in a seaway primarily depends on its speed, main dimensions, and proportions. The second point of interest is the underwater hull form parameters and the weight distribution, especially for fast semi-planing ships. A majority of these points can be traced back to the hull, making that the DC's component-of-interest.

5.1. Seakeeping analysis method

The analysis method is shown in Fig.2 and is similar to the approach by *Tan (1995)*. The sea spectra were defined using weather data, described in section 4.2, and three existing DCs were replicated digitally. The resulting seakeeping performance (for heave, roll and pitch) at the bow transfer point was obtained by applying Strip Theory through the software MAXSURF Motions. Evaluating the results and the original operational requirements leads to a design assessment and operator guidance. Note that the DCs were compared to each other based on ship performance priorities and not operational criteria. The operator guidance segment does not include operability plots but rather demonstrates which DC works best, given the set of responses to certain conditions. Also, since this step analyses existing DCs, the design assessment feedback will be applied in section 6; where a reflection on the original DC will lead to new DC designs.

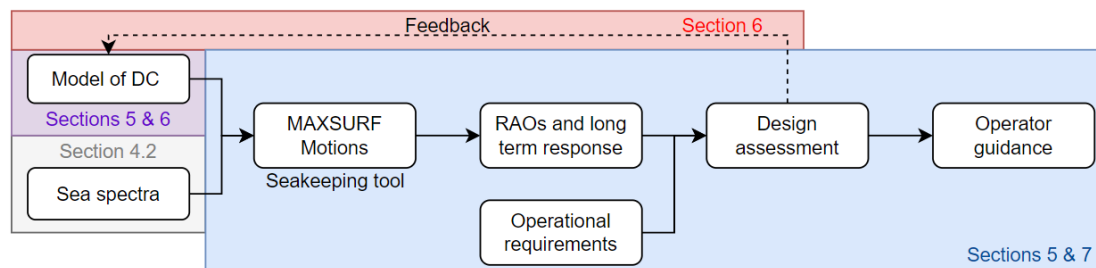


Fig.2: Seakeeping performance analysis method (Adapted from *Tan (1995)*)

5.1.1. Applicability of Strip Theory

Strip Theory is a linear, frequency domain approach to study seakeeping. In essence, it converts the three-dimensional underwater hull into two-dimensional sections or strips, each of which has associated local hydrodynamic properties (added mass, damping and stiffness), which contribute to the coefficients for the complete hull, *Lloyd (1998)*. In this case, it is expected to overestimate the resulting motions because it neglects the effects of three-dimensional flow, viscosity and nonlinearities, *Tezdogan et al. (2014)*. Nevertheless, as argued by *Keuning and Pinkster (1995)*, the linear approach may be justified for the sake of comparison.

This is not the only way to study seakeeping, but the main advantage is that this method requires significantly less computation time to produce seakeeping predictions compared to 3D methods. It is especially useful for including seakeeping in the early design analysis of alternatives and calculating mission operability, *Smith and Silva (2017)*. Note that the reference DCs are not in an early design stage, but the method is deemed valid for this study since it uses mock-ups that will be compared.

5.1.2. Daughter craft models

Mock-ups of a small, medium and large existing DCs were created with lengths of 10, 13 and 16 m, respectively. These three were chosen to gain an insight into the capabilities of a range of DCs currently available. These models were inspected visually and deemed to have a good resemblance to the confidential line plans. Still, the results may deviate slightly from the actual motions of these vessels since these mock-ups were not optimised through iterations. This is acceptable as these models serve to study (hard chine) monohull behaviour in high waves. An example of one of the mock-ups is shown in Fig.3.

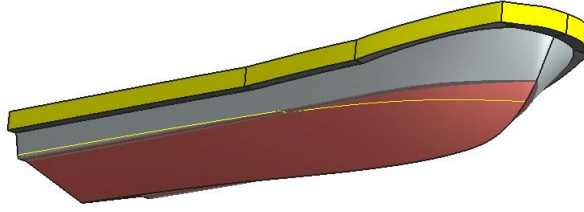


Fig.3: Mock-up of medium DC

5.1.3. Input parameters

The radii of gyration were specified for roll, pitch and yaw. These are often estimated as a percentage of the beam and length. The default settings in MAXSURF Motions correspond to widely accepted values, namely $0.35B$, $0.25L$ and $0.25L$, *Journée and Massie (2001)*, respectively. These values were left unchanged since the real values were unknown.

The vertical centre of gravity depends on, among others, the location of the installed machinery, equipment, fuel and number of passengers. Based on existing data, the vertical centre of gravity averaged around 1.4 metres for all DCs.

Motion damping occurs because the oscillating hull radiates energy away from the ship in the form of waves, *Lloyd (1998)*. For most motions, Strip Theory makes a decent estimation of the damping factors based on (potential) wave damping while neglecting the minimal viscous effects, *Journée and Massie (2001)*. However, viscous effects dominate the roll motion, while wave making is only a small portion of the total roll damping coefficient, *Journée and Massie (2001)*. So, the total roll damping coefficient (ν) must be specified to include viscous effects. The DCs were assumed to have a total roll damping coefficient within the range of 0.15 and 0.20.

Possible wave angles (μ) were grouped into five headings: following, stern-quartering, beam, bow-quartering, and head waves; $\mu = 0^\circ$, $\mu = 45^\circ$, $\mu = 90^\circ$, $\mu = 135^\circ$ and $\mu = 180^\circ$, respectively. The groups are still expected to give a complete impression of the resulting motions.

The JONSWAP spectrum was used to specify the wave spectra needed to simulate the various (irregular) sea states of the North Sea. Seven wave spectra were set up, which are based on current requirements and the weather conditions found at the reference farms, see Table II. The labels were established using the spectra characteristics.

The first spectrum (denoted by 10-3) resembles common and calm weather conditions; when it is generally safe to use DCs. In addition, there are three pairs of spectra, each with a specific significant wave height: (i) $H_s = 1.5$ m; the current transfer requirement for DCs, (ii) $H_s = 2.0$ m; the objective's lower boundary, and (iii) $H_s = 2.5$ m; the objective's upper boundary. Of the pairs, the first spectrum represents the steepest condition, and the second represents the most common for that wave height.

Table II: Simulated wave spectra

Spectrum label	10-3	15-6	15-3	20-5	20-3	25-5	25-3
Significant wave height [m]	1.0	1.5	1.5	2.0	2.0	2.5	2.5
Peak wave period [s]	4.5	4	5.5	5	6.5	5.5	7
Steepness [-]	0.03	0.06	0.03	0.05	0.03	0.05	0.03

5.2. Seakeeping assessment

This section discusses the resulting motions and accelerations that can be expected from the reference DCs. This is presented as Response Amplitude Operators (RAOs) and long-term responses to (wind) waves. For conciseness, only the medium DC's graphs are shown here since it is referred to in later sections, but all results will be discussed. The green-shaded histogram represents the common frequencies observed at the reference wind farms. For an in-depth explanation, see *Brans (2021)*.

5.2.1. Resulting Response Amplitude Operators

RAOs are transfer functions that show how the vessels are likely to respond to waves at sea. Each motion has its own graph due to different mass, damping and stiffness coefficients, *Bentley Systems (2014)*. They are also independent of the significant wave height, *de Jong (2011)*, because the heave RAOs were made non-dimensional against wave height, and the roll and pitch RAOs against wave slope. Here, the encounter frequency is the same as the wave frequency due to zero-speed. Fig.4 shows the results.

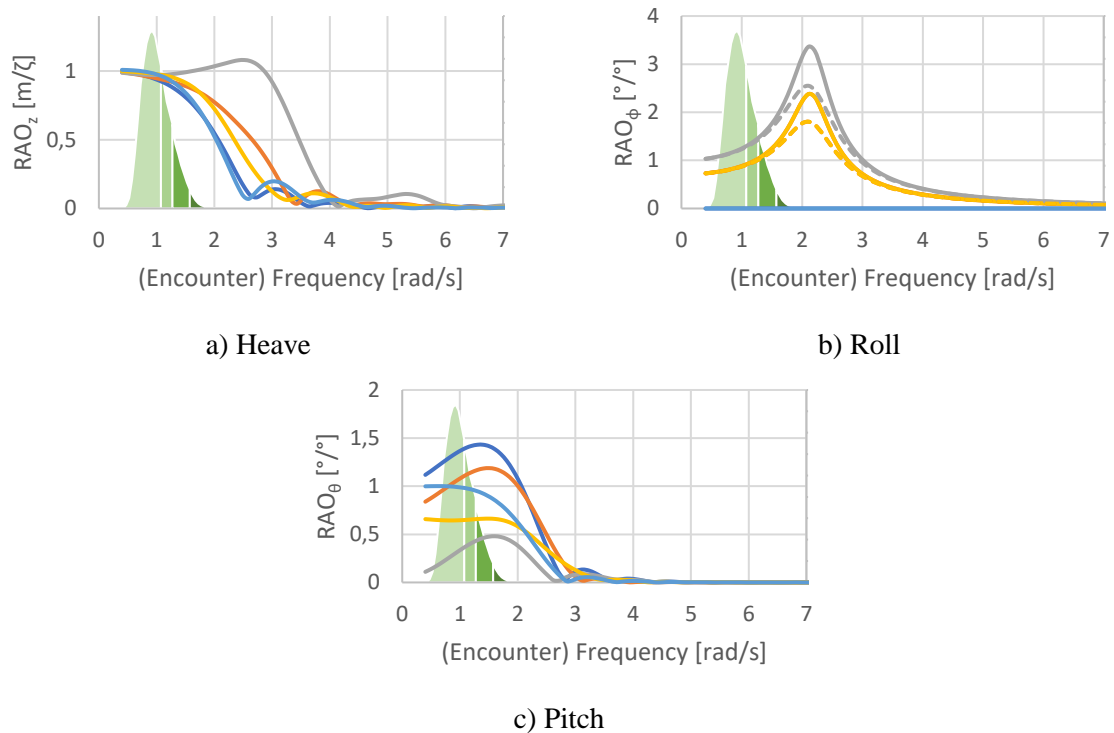


Fig.10: RAOs of medium DC

For heave, the DCs have good performance. There is a small peak resonance in beam waves, but all of the DCs' natural frequencies are situated outside the common frequencies range. So, the chance that DCs will experience heave resonance in beam waves during transfers is insignificant. In the event that there are beam waves travelling with $\omega \approx 2.5$ rad/s, the large DC will experience the highest responses.

For roll, the response amplitudes of each DC are similar to one another; i.e. their maximum responses are more or less equal. This is logical since all three DCs were given the same roll damping coefficients. Most importantly, the graphs show how $v = 0.20$ leads to lower responses, which would be beneficial during transfers. Also, the natural roll frequency of the small DC is approximately $\omega_n = 1.7$ rad/s. This is within the range of the common frequencies, but the chance that these waves will occur is meagre. With $\omega_n = 2.1$ rad/s and $\omega_n = 2.4$ rad/s, the medium and large DC, respectively, have less chance to experience resonance. Note that the response induced by stern-quartering waves is similar to the bow-quartering waves due to zero-speed.

For pitch, following waves will induce the largest pitch rotations. This is because the flatter stern is less suited to pierce waves compared to the bow. Also, all resonance peaks are located quite within the range of expected encounter frequencies. But those of the medium and large DCs are closer to the frequently observed wave frequencies. So, although the small DC has the highest amplitude, the natural frequencies of the medium and large DC make them more unfavourable.

5.2.2. Long-term responses to waves

The graphs in this section are comprised of the responses to the wave spectra given in Table II. Together, the results show how the DCs respond to wave conditions that are observed throughout the year. Each set of results corresponds to $v = 0.15$ since the results for $v = 0.20$ were similar. The polar graphs display the absolute motions and accelerations at the bow for all wave directions and spectra. Here, only the graphs for the medium DC are shown.

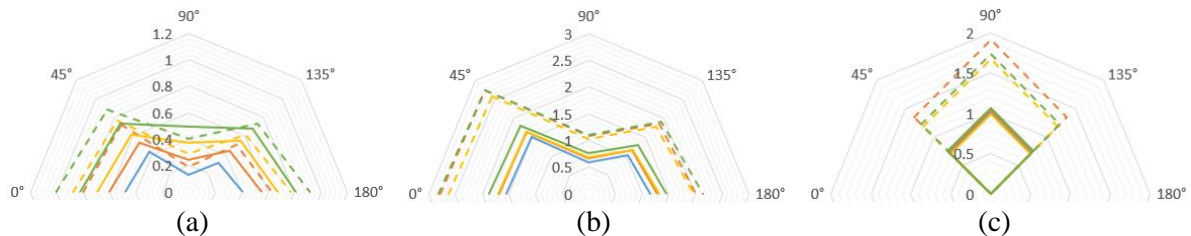


Fig.5: RMS absolute responses of medium DC; (a) Vert. motion, (b) Vert. accel., (c) Lat. accel.

The vertical motions at the bow, Fig.5a, show how much the bow moves. It includes all (three) motions and depends on the wave spectrum and incoming angle. The highest motions are induced by head and following waves. Also, higher wave heights increase the motion, while wave steepness increases the motion further. There is little difference between the three DCs. Fig.5b shows that the highest vertical accelerations at the bow are caused by following and stern-quartering waves. Also, steeper waves will increase the accelerations, while a varying wave height seems to have relatively less effect. In addition, the results for the “highest” steepness give an impression for the maximum observable accelerations. This is because steeper waves do not exist due to wave breaking. Thus, accelerations are not expected to exceed this limit either. When the motions are compared between DCs, they are reduced for the medium and large DC. But the medium DC achieves the lowest accelerations in beam waves. Fig.5c shows the lateral accelerations at the bow of the medium DC. The large DC has comparable lateral accelerations in all wave directions, but the small DC has the lowest accelerations overall. Again, steeper waves increase the accelerations, while a varying wave height has relatively less effect.

5.3. Main observations

5.3.1. Performance at zero speed

Following, stern-quartering and beam waves induce the largest accelerations. In contrast to the studies on vessels with a forward speed, the RAOs and long-term responses show that head waves seem to cause the least or relatively fewer excitations when all (three) motions are considered. Thus, it is smart to position the wind turbine’s boat landing to ensure these vessels encounter head waves the most. But as discussed in section 0, waves from other directions are not significantly less likely to occur.

5.3.2. Effect of wave parameters

The wave steepness seems to increase the DC’s responses more than higher wave heights. This makes sense looking at the rotational RAOs from section 05.2.1. These are made non-dimensional against wave slope, which is a function of wave frequency, directly related to the wave period. So, the higher the slope, the higher the response of the DC. This is also logical considering that an infinitely long wave with any wave height will give minor pressure changes and low accelerations. Therefore, the combination of wave period, i.e. wave steepness, and wave height, should be considered, rather than wave height alone, when deciding whether it is safe to deploy DCs.

5.3.3. Motions to be improved

Based on the RAOs of these reference DCs, the roll motion shall be prioritised for improvement since it is the riskiest motion when there are oblique waves. Looking at the long-term responses, then there

are sometimes low vertical accelerations, but lateral accelerations are high. After that, pitch is prioritised due to its performance in waves from the aft. Heave will be investigated last. So, modifications will be made based on the prioritised motions. For example, if a modification to improve heave will undermine the roll response, it will not be implemented.

6. Feasibility definition

In the third step, a system's feasibility is defined by how compatible it is with its interfaces which can impose constraints. The interfaces included here are the SOV and the technicians. Technically, the wind turbine is also an important interface. Although it is a highly relevant interface during transfers, it is not considered here because it has more to do with fender type and material, which are excluded from this study.

6.1. Size and weight constraints

The DC must be stored on the SOV. Although minimal changes are considered allowed, the general arrangement of any SOV imposes limits to size and weight and will be heavily included to guide the prototype's design.

The ESVAGT FARADAY was selected as the reference SOV to determine size constraints because the SOV's superstructure does not surround its current DC. Fig.6 is a sketch of the surrounding area and includes notable systems. In short, there is no room for a DC to expand in length because the fast rescue craft cannot be placed elsewhere. There will be room in the width if the deck-crane and DC's davit are moved towards to centreline. Deducting the space needed for the DC's davit leaves roughly 7.5 m available in the width.

When the DC is being launched or recovered, the SOV's davit lifts the DC by its hook. This means two things for the DC: (i) it must have the structural integrity to be lifted by its hook, and (ii) its total weight must be within the current davit's lifting capacity of 14 t, <https://www.redrock.no/portfolio/a-frame-davit-rda/>.

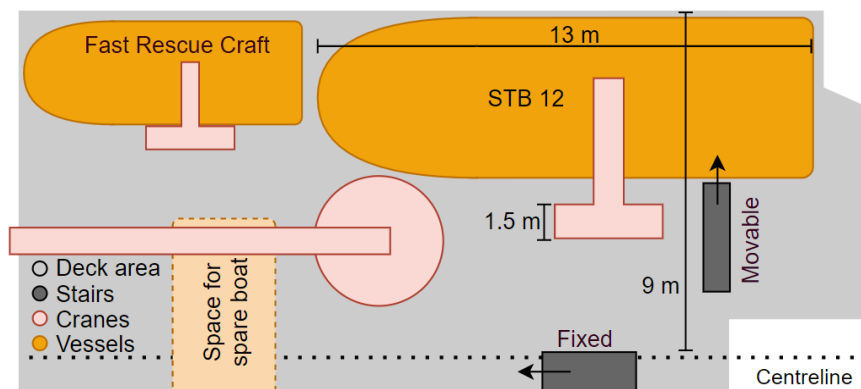


Fig.6: Sketch of available deck space on ESVAGT FARADAY

6.2. Habitability constraint

An operable DC will be able to reach the turbine and stay there, but a habitable vessel will have limited excitations to allow the technicians to transfer safely to the wind turbine. If a vessel is mainly operable, the motions are within an acceptable range for the vessel itself, but a wrongly timed move could cause injury to the technicians. So, because human comfort and safety have a crucial role in a DC's operability, habitability will define the limits as to how a vessel should respond to waves.

Phillips et al. (2015) state that there is little experience and consensus for the limits of vessel motion for transfers but point out that the vertical and horizontal acceleration limits should at least be lower

than the values for transit. Specifically, they suggest that the thresholds at the wheelhouse should be 0.5 m/s² for vertical acceleration, 0.4 m/s² for horizontal acceleration and predominantly zero at the transfer point. It is uncertain how feasible these values are in practice, especially for the relatively small DC that cannot guarantee a low frequency of slip in high waves. Therefore, this study does not consider the proposed thresholds as a constraint but as a goal.

6.3. Physical characteristics of prototypes

Many solutions have emerged from extensive research in the field to improve seakeeping performance. To summarise, seakeeping can be improved by:

- (i) modifying the hull dimensions and proportions, *Tan (1995), Keuning and Pinkster (1995,1997), Özüim et al. (2011)*,
- (ii) applying a more suitable hull type or bow shape, *Belga et al. (2018), Jupp et al. (2014), Keuning and Gelling (2007), Keuning et al. (2001)*,
- (iii) adding stabilisation devices, *Tan (1995), Yang et al. (2019), Irkal et al. (2019), Liang et al. (2017)*.

However, this study excludes stabilisation devices because analysing their influence requires other and higher fidelity methods. Furthermore, these can be added later in the design process.

Ultimately, two different hull types were selected to be tested, namely a monohull and a catamaran. Furthermore, two versions of those two hull types were generated to understand the effects of changing certain parameters, especially since most of the modifications are based on results obtained for (much) larger vessels. These prototypes were made based on the priority to improve roll motions, as stated in section 5.3.3. The new DCs and their characteristics are summarised in Table III. Note that no attempt was made to seek optimum designs in this step because the aim was establishing the feasibility to meet the set of operational objectives, *Kossiakoff et al. (2011)*. Furthermore, all new DC models were fitted with an Axe bow to reduce heave and pitch motions. So, the difference between Monohull 1 and the parent hull, for example, is not only due to the decreased metacentric height (GM). Still, the following analysis will isolate the effects of all the modifications.






7. Needs Validation

The resulting performance is evaluated against measures of effectiveness (MOE). The transfer thresholds (given in section 6.2) were deemed too idealistic to be feasible, especially for far-offshore wind farms that frequently observe rough weather conditions. So, the new DCs are evaluated against the parent hull, whose performance (shown in section 5.2) represents the MOE. The results were obtained using the same method described in section 5.1.

7.1. Response Amplitude Operators

Table III: Physical characteristics of DC models

	Parent hull (Medium DC)	Monohull 1 (M1)	Monohull 2 (M2)	Catamaran 1 (C1)	Catamaran 2 (C2)
Main differences	NA.	Smaller GM	Larger beam	New hull type	Small clearance
Bow shape	Sharp bow	Axe bow	Axe bow	Axe bow	Axe bow
Waterline length	12.39 m	13 m	13 m	13 m	13 m
Waterline beam	3.68 m	3.67 m	4.27 m	7.10 m	4.70 m
Demihull width	NA.	NA.	NA.	1.60 m	1.60 m
Draught	0.85 m	1.22 m	1.22 m	1.41 m	1.41 m
GM	1.92 m	0.80 m	1.90 m	11.83 m	3.38 m
LCB	5.58 m	5.49 m	5.69 m	6.248 m	6.248 m

Weight	13.49 t	12.60 t	15.43 t	20.36 t	20.36 t
Symbol in graphs					

The effectiveness of the DCs was analysed by normalising the area under their RAOs with respect to that of the parent hull, Figs.7 to 9. This gives a better indication of how the RAOs change in certain wave conditions. Note that an effectiveness level under 1.0 indicates a better performance than the parent hull because the RAO area is lower. Although all five waves directions were studied, only the results for beam waves are shown here for conciseness. All results can be found in *Brans (2021)*.

7.1.1. Heave

Compared to the parent hull, the monohulls' natural frequencies (i.e. resonance peaks) in beams waves moved closer to the peak of common wave frequencies. This shift is presumably due to the Axe bow since the response from M1 and M2 are similar. So, the Axe bow seemed to have changed the secondary parameters such that natural frequency is lowered. Still, according to Fig.7, which shows the level of effectiveness, their absolute responses are generally similar to that of the parent hull; only at higher frequencies is there a notable improvement compared to the parent hull.

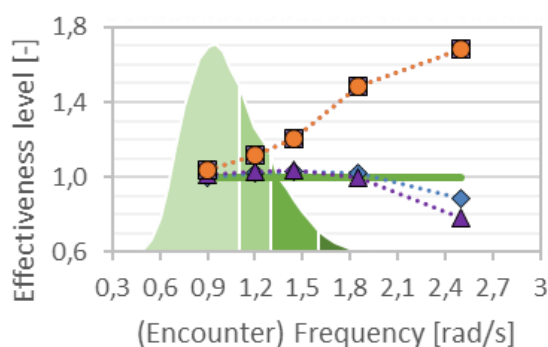


Fig.7: Effectiveness of heave in beam waves

Also, the new monohulls perform poorer than the parent hull in waves from the aft. The catamarans show a much larger resonance peak at their natural frequency in beam waves. Although it is positioned outside the range of expected encounter frequencies, Fig.7 shows how the heave response to beam waves is always higher than the parent hull and the new monohulls. The same goes for the other wave directions. In short, all DCs match for the first range of frequencies. As the frequencies rise, the catamarans show the poorest performance while the monohulls are mostly comparable to the parent hull.

7.1.2. Roll

The roll damping coefficient of the catamarans was calculated to be $\nu = 0.20$. So, the effectiveness was evaluated for this value. The monohulls have the same resonance amplitude as the parent hull. However, M1 has a lower natural frequency than the parent hull and M2. So, it is presumed that the shift is due to a lower GM and not the Axe bow. Moreover, it is fairly in the range of wave frequencies expected to occur often, which is a considerable disadvantage. Fig.8 confirms this: M1 matches the rest of the DCs in the first frequency range but is the worst at other common frequencies. So, M1 would be ill-suited to use at Hornsea One, where beam waves frequently occur. The roll response from M2 is similar to the parent hull. Besides a slightly decreased amplitude after the resonance peak, the roll RAOs are unaffected by a wider beam. The resonance amplitude from both catamarans is significantly lower than the parent hull: C1 and C2 reduced the amplitude by roughly 50% and 18%, respectively. Moreover, C1's natural frequency shifted farther from the frequency spectrum's peak, while C2 shifted closer to it. So, C1 is most effective in reducing the roll motions in all (oblique) wave directions, especially in beam waves.

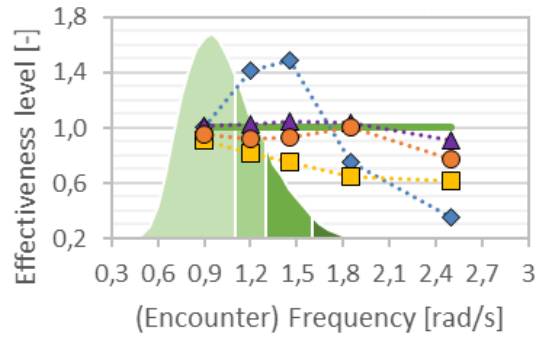


Fig.8: Effectiveness of roll in beam waves

7.1.3. Pitch

The pitch response from both monohulls is nearly identical to that of the parent hull. Fig.9 confirms this for the common frequencies and most wave directions. This was anticipated since modifying the Axe bow and shifting the LCB are known to have little effect on pitch. The LCB of M1 even moved backwards, but the (negative) effect is not large. Also, it seems that the positive LCB shift of M2 was not large enough for there to be a notable reduction.

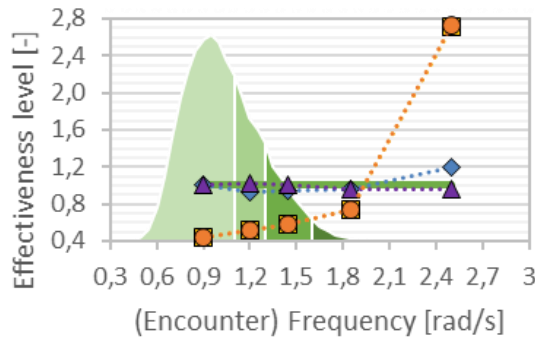


Fig.9: Effectiveness of pitch in beam waves

The natural frequencies of the catamarans shifted farther from the frequency spectrum's peak. According to *Gutsch et al. (2020)*, this is what lowers vessel motions. So, although the absolute pitch response in stern-quartering waves is higher than the monohulls, the natural frequency shifted to a more favourable position. Furthermore, the resonance amplitude in following waves was reduced as well. It seems that the catamarans' LCB was moved forward enough for it to (positively) affect pitch. Fig.9 shows that catamarans performed best in beam waves, except in the high (but uncommon) frequencies. They also performed best in following and stern-quartering waves. Only in waves from the front did they perform slightly worse than the monohulls for all frequencies. Considering that head waves occur the most due to the boat landing's orientation, catamarans would then not immediately be the vessel of choice.

7.2. Long-term response

Fig.10 shows the prototypes' effectiveness in terms of vertical motions and accelerations and lateral accelerations. Table III defines the colour codes. For conciseness, it only contains results from three wave conditions.

7.2.1. Vertical motions and accelerations

The monohulls have nearly identical responses to the various wave spectra. Just like the parent hull, the highest response is induced by head and following waves. The catamarans show larger motions for all wave directions. This alone does not indicate that the catamarans are less safe, but the accelerations are higher as well. However, their accelerations in longitudinal waves are very similar to the monohulls.

The difference found here corresponds to the results found by the RAOs; the catamarans also had a higher response to quartering and beam waves compared to the monohulls.

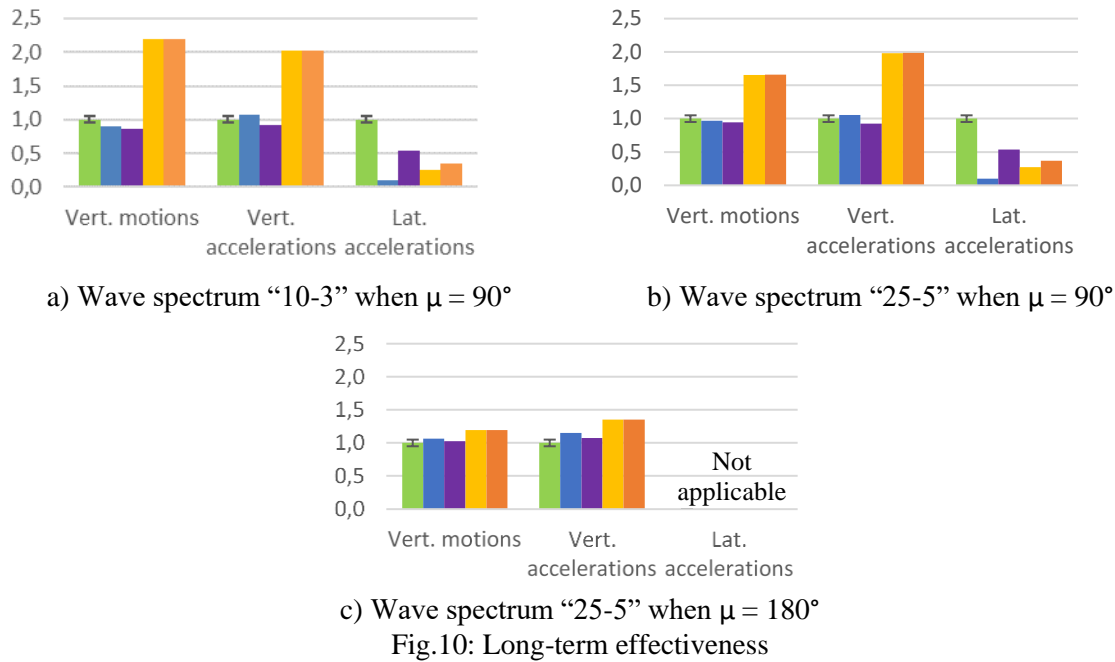


Fig.10: Long-term effectiveness

7.2.2. Lateral accelerations

In this case, the parent hull has the largest accelerations. The lowered GM of M1 significantly reduces the lateral accelerations to near-zero levels, and at first glance, this is the ideal response. This reduction was expected because a smaller GM leads to a smaller righting arm, which slows down the roll period. However, an analysis into static stability showed that the GM of M1 is so low that it will already tend to capsize at a heeling angle of 15° - 20° . So, M1 is deemed unpractical and will not be promoted for far-offshore use. M2 has the same GM as the parent hull and a wider beam. The accelerations were cut in half, but a wider beam was not as “effective” as a lowered GM. This corresponds with the conclusions by *Gutsch et al. (2020)*. Both catamarans also have significantly reduced accelerations. Those of the quartering waves are even reduced with a greater scale. C1 has the lowest accelerations among the two, so the larger clearance is more effective in lowering the lateral accelerations; the same conclusion was drawn for the RAOs.

7.3. Overview of best-performing daughter craft

This section summarises the results in Table IV by presenting which model performed the best for various seakeeping parameters. Specifically, three points were considered to determine which DC (type) is most useful at the reference farms: the most prominent wave directions (section 0), the notion that the response should be as low as possible (to meet the ideal seakeeping criteria for transfers given in section 6.2) and the estimation of their intact stability (excluded in this paper).

In short, the monohulls are suitable if only head waves are considered. Once other wave angles are included in the analysis, catamarans start to outperform the monohulls. The new monohulls also had poorer transverse stability than the parent hull. Still, there are occasions when the catamarans are slightly inferior, i.e. heave and vertical responses. However, these DCs were simulated to be floating freely. The heave results could perhaps improve when the interaction with the boat landing is included in the analysis.

Table IV: DCs best suited for combinations of seakeeping and wave direction

	Head	Beam	Stern-qtr.	Following
Heave RAO	Monohulls	Monohulls	Parent hull	Parent hull
Roll RAO	Not applicable	C1	Catamarans	Not applicable
Pitch RAO	Parent hull and monohulls	Catamarans	Catamarans	Catamarans
Vertical bow response	Parent hull	Monohulls	Monohulls	Monohulls
Lateral bow response	Not applicable	Catamarans	Catamarans (matched threshold in common steepness)	Not applicable

8. Conclusions

The seakeeping performance of existing DCs was analysed to determine where the deficiencies lie and what could be done to resolve them. The first notable deficiency of current DCs stems from their operational requirement to transfer in $H_s \leq 1.5$ m. As a result, DCs will have a low accessibility rate in areas frequented by higher significant wave heights, which undermine their value for far-offshore applications. The second deficiency is that they are required to achieve a high speed of 25 knots in transit when the emphasis should be laid on safe transfer conditions. This is due to their closer proximity to the wind farm than port-based O&M access vessels. For existing DCs already under a charter-contract, it is recommended to refit them with motions stabilisation devices to improve their seakeeping performance at zero-speed. For future DCs meant to operate far offshore, this paper recommends requiring them to be able to access wind turbines in $2.0 \text{ m} \leq H_s \leq 2.5 \text{ m}$ to realise year-round access while considering the effects of wave steepness. Various combinations of solutions were analysed to establish the access requirement's feasibility while focusing on the transfer phase. No prototype had improved responses in all conditions. But overall, the prototypes outperformed the parent hull for a majority of conditions. Moreover, the catamaran DC have a high potential to realise year-round accessibility to far-offshore wind farms due to their performance in oblique waves. Lastly, it is believed that accessibility can be improved further if the wind turbine facilitates the daughter craft during transfers. But this solution is more suited for wind farms still in the development phase.

Acknowledgements

This work was performed as part of the MSc thesis for the lead author, *Brans (2021)*. The thesis was performed in Marine Technology at Delft University of Technology and the authors would like to acknowledge both Delft University of Technology and Siemens Gamesa for their support of this research.

References

- AHSAN, D.; PEDERSEN, S. (2018), *The influence of stakeholder groups in operation and maintenance services of offshore wind farms: Lesson from Denmark*, Renewable Energy 125, pp.819-828
- ANTÃO, E.M.; SOARES, C.G. (2016), *Approximation of the joint probability density of wave steepness and height with a bivariate gamma distribution*, Ocean Eng. 126, pp.402-410
- BELGA, F.; VENTURA, M.; GUEDES SOARES, C. (2018), *Seakeeping optimization of a catamaran to operate as fast crew supplier at the alentejo basin*, 4th Int. Conf. Maritime Technology and Engineering, pp.587-599

- BENTLEY SYSTEMS (2014), *Maxsurf Motions User Manual v20*, Bentley Systems
- BEUKELMAN, W. (1986), *Prediction of Operability of Fast Semi-Planing Vessels in a Seaway*, Issue 700
- BRANS, S. (2021), *Applying a Needs Analysis to promote Daughter Craft for year-round access to far-offshore wind turbines*, Delft University of Technology, Available at: <https://repository.tudelft.nl/islandora/object/uuid%3Ac1de0299-b8f5-42a8-9a0e-71549756f57d?collection=education>
- DE JONG, P. (2011), *Seakeeping Behaviour of High Speed Ships: An Experimental and Numerical Study*, Delft University of Technology
- GERRITSMA, J. (n.d.), *Hydromechanica 4 – Golden*, TU Delft
- GUEZURAGA, B.; ZAUNER, R.; PÖLZ, W. (2012), *Life cycle assessment of two different 2 MW class wind turbines*, *Renewable Energy*, 37(1), pp.37-44
- GUTSCH, M.; STEEN, S.; SPRENGER, F. (2020), *Operability robustness index as seakeeping performance criterion for offshore vessels*, *Ocean Eng.* 217, 107931
- HU, B.; STUMPF, P.; VAN DER DEIJL, W. (2019), *Offshore Wind Access 2019*, TNO Publ.
- IRKAL, M.A.R.; NALLAYARASU, S.; BHATTACHARYYA, S.K. (2019), *Numerical prediction of roll damping of ships with and without bilge keel*, *Ocean Eng.* 179, pp.226-245
- JIAO, J.; CHEN, C.; SUN, S.; ADENYA, C.A.; REN, H. (2018), *Reproduction of ocean waves for large-scale model seakeeping measurement: The case of coastal waves in Puerto Rico & Virgin Islands and Gulf of Maine*, *Ocean Eng.* 153, pp.71-87
- JOURNEE, J.M. ; MASSIE, W.W. (2001), *Offshore Hydromechanics*, Delft University of Technology
- JUPP, M.; SIME, R.; DUDSON, E. (2014), *XSS - A next generation windfarm support vessel*, RINA Conf. Design and Operation of Wind Farm Support Vessels, London, pp.43-51
- KEUNING, J.A.; GELLING, J.L. (2007), *The influence of the bow shape on the operability of a fast ship in a seaway*, 2nd Int. Conf. Marine Research and Transportation
- KEUNING, J.A.; PINKSTER, J. (1997), *Further design and seakeeping investigations into “Enlarged Ship Concept”*, 4th Int. Conf. Fast Sea Transportation FAST’97, 1090-P
- KEUNING, J.A.; PINKSTER, J. (1995), *Optimisation of the seakeeping behaviour of a fast monohull*, 3rd Int. Conf. Fast Sea Transportation
- KEUNING, J.A.; TOXOPEUS, S.; PINKSTER, J. (2001), *The Effect of Bowshape on the Seakeeping Performance of a Fast Monohull*, 6th Int. Conf. Fast Sea Transportation
- KOSSIAKOFF, A.; SWEET, W.N.; SEYMOUR, S.J.; BIEMER, S.M. (2011), *Systems Engineering: Principles and Practice*, John Wiley & Sons
- KRAUSE, G.; STEAD, S.M. (2017), *Governance and offshore aquaculture in multi-resource use settings*, *Aquaculture Perspective of Multi-Use Sites in the Open Ocean: The Untapped Potential for Marine Resources in the Anthropocene*
- LIANG, L.; ZHAO, P.; ZHANG, S.; YUAN, J.; WEN, Y. (2017), *Simulation and analysis of Magnus rotating roll stabilizer at low speed*, *Ocean Eng.* 142, pp.491-500

- LLOYD, A.R.J.M. (1998), *Seakeeping: Ship behaviour in rough weather*, self-publ.
- MaTSU (2001), *Marine Offshore Rescue Advisory Group: Good practice in offshore rescue*
- ÖZÜM, S.; ŞENER, B.; YILMAZ, H. (2011), *A parametric study on seakeeping assessment of fast ships in conceptual design stage*, *Ocean Eng.* 38(13), pp.1439-1447
- PHILLIPS, J.; FITCH-ROY, O.; REYNOLDS, P.; GARDNER, P. (2013), *A guide to UK offshore wind operations and maintenance*, Scottish Enterprise and The Crown Estate, September
- PHILLIPS, S.; SHIN, I.B.; ARMSTRONG, C. (2015), *Crew transfer vessel performance evaluation*, *Design and Operation of Wind Farm Support Vessels*, pp.29-33
- SHAFIEE, M. (2015a), *A fuzzy analytic network process model to mitigate the risks associated with offshore wind farms*, *Expert Systems with Applications*42(4), pp.2143-2152
- SHAFIEE, M. (2015b), *Maintenance logistics organization for offshore wind energy: Current progress and future perspectives*, *Renewable Energy* 77(1), pp.182-193
- SMITH, T.C.; SILVA, K.M. (2017), *Linear seakeeping high sea state applicability*, *Int. Ship Stability Workshop*, pp.111-116
- STAVENUITER, W. (2009), *The missing Link in the Offshore Wind Industry: Offshore Wind Support Ship*, Delft University of Technology
- TAN, S.G. (1995), *Seakeeping Considerations in Ship Design and Operations*, Regional Maritime Conf.
- TEZDOGAN, T.; INCECIK, A.; TURAN, O. (2014), *Operability assessment of high speed passenger ships based on human comfort criteria*, *Ocean Eng.* 89, pp.32-52
- WALSH, C. (2019), *Offshore wind in Europe*, *Refocus* 3(2)
- YANG, W.; TIAN, W.; WEI, K.; PENG, Z.; & HUANG, Z. (2019), *Research on a cost-effective measure dedicated to stabilizing offshore wind farm crew transfer vessels*, *Renewable Energy* 133, pp.275-283

Hybrid Modelling Approach of a Four-stroke Medium Speed Diesel Engine

Andrea Coraddu, University of Strathclyde, Glasgow/UK, andrea.coraddu@strath.ac.uk
Miltos Kalikatzarakis, University of Strathclyde, Glasgow/UK, miltos.kalikatzarakis@strath.ac.uk
Rinze Geertsma, Delft University of Technology, Delft/The Netherlands, R.D.Geertsma@tudelft.nl
Luca Oneto, Università Degli Studi di Genova, Genova/Italy, luca.oneto@unige.it

Abstract

Diesel engines will remain a fundamental component of propulsion systems due to their maturity, reliability, and power density. Building Digital Twins of the propulsion system is one feasible solution to pursue the optimal propulsion system operation, estimating system states and efficiency. This work will investigate a modelling approach that combines high accuracy while satisfying real-time prediction capabilities by coupling a physics-based model with a data-driven modelling approach. We will demonstrate that the proposed hybridisation framework can provide state-of-the-art prediction capabilities in real-time, utilising operational data from a turbocharged, four-stroke medium-speed diesel engine.

1. Introduction

In recent years the maritime industry is confronted by several challenges, including volatile bunker prices, *García-Martos et al. (2013)* that affect cargo transportation costs and the shipowners' competitiveness and viability of their operations, and strict regulations to limit emissions and their environmental impact to reduce CO₂ emissions from shipping by 40-50%, *European Commission (2013a)*. As a result of this combination, the issue of energy efficiency and environmental sustainability of maritime operations is currently prioritised in the maritime industry, with shipowners and operators adopting measures to lower fuel consumption and associated emissions, and researchers studying innovative technologies and methods that can increase the environmental efficiency and cost-effectiveness of ship operations.

Propulsion system design is facing the challenge of continuously rising complexity to satisfy these demands. However, energy efficiency should not only be a design issue but also be preserved in operation. In pursuing the optimal propulsion system operation, estimating system states and efficiency is of great importance. In this respect, building a Digital Twin (DT) of the propulsion system that coexists during operation, providing predictions and offering insight into the operation, is one feasible solution. A critical requirement for the DT is the need for a modelling approach that can precisely reflect the characteristics intrinsic to the propulsion plant and precisely predict the state of its physical counterpart under all operating conditions in real-time, as reported in *Bondarenko and Fukuda (2020)*. Main engines are the main factors of energy loss and emission production on-board and will remain an unavoidable part of propulsion systems due to their maturity, reliability, and power density, *Baldi et al. (2014, 2015)*. Diesel engine (DE) modelling has evolved over the years, and various types of models can be found in the literature, with varying degrees of computational complexity and prediction quality. Most widely employed are Mean Value Engine Models (MVEMs), *Guan et al. (2014)*, *Grimmelius et al. (2010)*; *Geertsma et al. (2017)*, which provide adequate accuracy in the prediction of most engine parameters while being computationally cheap, and zero-dimensional (0D) models that operate on per crank basis, allowing the calculation of parameters of the gas within the engine cylinders as reported in *Sapra et al. (2020)*, *Catania et al. (2011)*, *Asad et al. (2014)*.

Suppose the requirements for a modelling approach include real-time prediction of the main engine performance parameters with a high degree of accuracy. In that case, neither MVEM nor 0D models are applicable due to moderate prediction capabilities (MVEMs) and computational time requirements (0D models). More sophisticated approaches, with respect to MVEMs and 0D, are one-dimensional (1D) and three-dimensional (3D) models that operate on a per-crank basis, *Merker et al. (2005)*. These approaches are more computationally demanding compared to MVEMs. However, they can predict the

detailed gas processes inside the cylinders with higher accuracy, *Mohammadkhani et al. (2019)*. Several attempts to combine MVEM and 0D, 1D, or 3D models have been proposed, enhancing the predictive abilities of MVEMs with lower computational requirements than their 0D, 1D, or 3D counterparts, as suggested by *Livanos et al. (2007)* and *Ding et al. (2010)*. For instance, *Baldi et al. (2015)* combined MVEM and 0D models to investigate the propulsion behaviour of a Handymax-size product carrier under constant and variable engine speed operations. PMs can adequately capture most process parameters of a DE under a broad range of operating conditions. However, there is a clear trade-off between accuracy and computational requirements. The most accurate 3D models cannot run in real-time, whereas MVEMs lack accuracy, especially during transient operations.

DDMs have been successfully applied in a variety of maritime applications, provided that the necessary quality and quantity of historical data is available, as reported in *Coraddu et al. (2017,2019a,2019b, 2020,2021a,2021b)* and *Cipollini et al. (2018a, 2018b)*. For instance, *Nikzadfar and Shamekhi (2014)* developed an Artificial Neural Network (ANN) to study the relative contribution of several operating parameters to the performance of a DE. The ability of ANNs to predict performance parameters of a DE was also demonstrated in *Özener et al. (2013)* to predict a variety of performance parameters and emissions. A hydrogen dual-engine for automotive applications was the case study of *Syed et al. (2017)*: ANNs proved to be highly efficient to predict specific fuel consumption and a variety of emissions.

HMs are a pretty recent modelling approach, especially in the maritime field, and just very few works showed the advantages of a hybrid approach regarding pure PMs and DDMs, as reported in *Coraddu et al. (2018, 2021a)* and *Miglianti et al. (2019, 2020)*. For instance, *Coraddu et al. (2017)* show that it is possible to predict fuel consumption with HMs effectively. Moreover, *Coraddu et al. (2018, 2021a)* attempted to model the engine exhaust gas temperature with HMs under steady-state and transient conditions. *Mishra and Subbarao (2021)* compared the performance of a PM, a DDM, and an HM to predict dynamic combustion control parameters of a Reactivity Controlled Compression Ignition engine across five engine loads. The parameters included the start of combustion, the 50% mass fraction burnt crank angle, and combustion peak pressure. The authors compared the model predictions with measured data from experiments, concluding that the prediction capability of the HM was far superior to the DDM and PM across all parameters. *Bidarvatan et al. (2014)* developed an HM to predict several performance parameters of Homogeneous Charge Compression Ignition (HCCI) engines. Namely, the 50% mass fraction burnt crank angle, the indicated mean effective pressure, exhaust temperature, and concentration of CO, total unburned hydrocarbons and NO_x. The proposed HM combined a PM and 3 ANNs, designed to minimise computational time requirements. The authors compared the predictions of the proposed HM with experimental data at 309 steady-state and transient conditions for two HCCI engines concluding that the HM offered approximately 80% better accuracy compared to the PM, or 60% compared to the DDM.

The amount of literature available on the HMs is limited, as this is a relatively new research field. Moreover, focusing on the marine DE applications, a consistent and clear description of a modelling framework for marine DEs able to hybridise PMs and DDMs is not yet readily available.

This work will investigate a modelling approach that combines high accuracy whilst satisfying real-time prediction capabilities by coupling a physics-based, low-computational MVEM with a Data-Driven model. We will demonstrate that combining these two approaches in a hybrid modelling framework can provide state-of-the-art prediction capabilities in real-time, utilising several months of operational data from a turbocharged, four-stroke medium-speed DE. With this in mind, first, a 0D DE model, already available in *Kalikatzarakis et al. (2021)*, is briefly described. Subsequently, different DDMs will be developed, tested, and compared. These models will leverage the information encapsulated in historical data to produce accurate predictions on a set of performance parameters of the DE. Finally, we will present the hybridisation framework where HM will be proposed, leveraging on both the DDM and the PM previously developed. The authors will showcase the performance in terms of accuracy, reliability, and computational requirements of the HM, demonstrating the superiority of the proposed hybridisation framework on a comprehensive dataset containing operational data from a marine DE for a time of approximately three years.

2. Physical Models

In this section, we report an overview of the DE modelling approach for the sake of completeness. A more detailed explanation and the validation results are available in *Kalikatzarakis et al. (2021)*. The vessel's DEs have been modelled utilising a modular approach. Inputs include the geometric data of the engine, the intake and exhaust valves profiles, the compressor and turbine performance maps, the waste gate geometric and control details, the constants of engine sub-models (combustion, heat transfer and friction), the engine operating point (load/speed), and the ambient conditions. Initial conditions are required for the temperature, pressure and composition of the working medium contained in the engine cylinders, pipes, and receivers. The engine scavenging air and exhaust gas receivers are modelled as flow receiver elements (control volumes), whereas flow elements represent the compressor, air cooler, cylinders, and turbine. The engine boundaries are modelled using fixed fluid elements of constant pressure and temperature, and shaft elements are utilised to compute the rotational speed of the turbocharger and crankshaft. The governor of the engine is responsible for adjusting the fuel rack position and incorporates the appropriate fuel rack limiters. Finally, air and exhaust gas properties are dependent on temperature, fuel-air equivalence ratio and composition. For the calculation of the exhaust gas composition, oxygen, nitrogen, carbon dioxide and steam were considered. All flow elements are modelled using the open thermodynamic system concept of *Watson and Janota (1982)* and *Heywood (1988)*, and use as inputs the pressure (p), temperature (T), and the properties of the working medium contained in the adjacent elements. Subsequently, mass (\dot{m}) and energy flow rates entering and exiting each element are computed by applying the mass and energy conservation laws. These flow rates are further provided as inputs in the adjacent flow receiver elements, whereas torque outputs are utilised as inputs in the shaft elements. The latter, through the angular momentum conservation, compute the rotational speeds of the turbocharger (ω_{tc}) and propulsion plant shafts. The compressor is modelled using its steady-state performance map, estimated utilising the method proposed by *Casey and Robinson (2013)*, whereas the turbine is modelled using its swallowing capacity and efficiency map. Moreover, the pressures losses occurring in the air cooler and air filter are dependent on the air mass flow rate, as is the air cooler effectiveness. No heat transfer is considered in the model of the scavenging air receiver, whereas the transferred heat to the ambient from the gas in the exhaust gas receiver is calculated from the overall heat transfer coefficient, using a Nusselt-Reynolds number correlation for gas flowing in the pipes according to *Rohsenow and Hartnett (1988)*. Moreover, pressure losses in the exhaust gas receiver are dependent on the exhaust gas mass flow rate. The in-cylinder process is described by a two-zone zero-dimensional model as in *Merker et al. (2005)*. This type of model operates on per crank-angle basis, using the mass and energy conservation equations, along with the gas state equation, which are solved in their differential form, so that the parameters of the gas within the engine cylinders and manifolds, such as pressure, temperature and gas composition can be calculated. Combustion is modelled through a two-zone model, considering a zone containing the combustion products and an unburned mixture zone according to *Merker et al. (2005)*. The Woschni heat transfer model, originating from *Woschni (1967)*, and employed extensively in various studies, is utilised to compute the in-cylinder gas to wall heat transfer coefficient, *Merker et al. (2005)*. According to the Vibe model, the heat release rate is simulated, as described in *Merker et al. (2005)*. The combustion products are evaluated utilising the method of *Rakopoulos et al. (1994)*, due to its minimal computational time requirements and reasonable agreement with experiments: for the burning zone, given its volume, temperature, mass of fuel burnt and mass of air entrained, the concentration of each gas composition species discussed in *Kalikatzarakis et al. (2021)*, can be evaluated by solving an 11×11 non-linear system obtained from 7 non-linear equilibrium equations and 4 linear atom balance equations. Thermal NO has been evaluated according to the extended Zeldovich mechanism, for which the reaction rates were selected according to *Hanson and Salimian (1984)*.

3. Hybrid Models

This section will introduce our hybridisation framework, starting from a formal description of the DDMs.

3.1. Data-Driven Models

To develop a fast yet accurate dynamic model of a four-stroke marine DE, a general modelisation framework is here defined, characterised by an input space $\mathcal{X} \subseteq \mathbb{R}^d$, an output space $\mathcal{Y} \subseteq \mathbb{R}^b$ and an unknown relation $\mu: \mathcal{X} \rightarrow \mathcal{Y}$ to be learned, *Shalev-Shwartz and Ben-David (2014), Hamilton (2020)*. In this work, \mathcal{X} is composed by the measurements available from the engine monitoring system (see Section 4), while the output space \mathcal{Y} refers to the target features accounting for the engine fuel consumption \dot{m}_f , turbocharger rotational speed N_{tc} , turbine outlet temperature $T_{t,out}$ and exhaust manifold temperature T_{er} . We define the model $h: \mathcal{X} \rightarrow \mathcal{Y}$ as an artificial simplification of μ . The model h , as described in Section 1, can be obtained with different kinds of techniques, for example, requiring some physical knowledge of the problem, as in PMs (see Section 2), or the acquisition of large amounts of data, as in DDMs or using both information (see Section 3). Between the DDMs, it is possible to identify two families of approaches, *Shalev-Shwartz and Ben-David (2014)*. The first one, comprising traditional Machine Learning (ML) methods, needs an initial phase where the features must be defined a-priori from the data via feature engineering or implicit or explicit feature mapping, *Shawe-Taylor and Cristianini (2004)*. The second family, which includes Deep Learning (DL) methods, automatically learns both the features and models from the data, *Goodfellow et al. (2016)*. For small cardinality datasets and outside particular applications (e.g., computer vision and natural language processing), DL does not perform well since they require a large amount of data to be reliable and to outperform traditional ML models, *Wainberg et al. (2016)*. In the ML, the above-mentioned can be easily mapped in a typical regression problem, *Vapnik (1998)*. In fact, ML techniques aim at estimating the unknown relationship μ between input and output through a learning algorithm $\mathcal{A}_{\mathcal{H}}$ which exploits some historical data to learn h and where \mathcal{H} is a set of hyperparameters that characterises the generalisation performance of \mathcal{A} , *Oneto (2020)*. The historical data consists of a series of n examples of the input/output relation μ and are defined as $\mathcal{D}_n = \{(\mathbf{x}_1, \mathbf{y}_1), \dots, (\mathbf{x}_n, \mathbf{y}_n)\}$ where $\mathbf{x} \in \mathcal{X}$ and $\mathbf{y} \in \mathcal{Y}$.

This paper will leverage ML models from the Kernel Methods family called Kernel Regularised Least Squares (KRLS), *Vovk (2013)*. The idea behind KRLS can be summarised as follows. During the training phase, the quality of the learned function $h(\mathbf{x})$ is measured according to a loss function $\ell(h(\mathbf{x}), \mathbf{y})$, as reported in *Rosasco et al. (2004)*, with the empirical error

$$\hat{L}_n(h) = \frac{1}{n} \sum_{i=1}^n \ell(h(\mathbf{x}_i), \mathbf{y}_i). \quad (1)$$

A simple criterion for selecting the final model during the training phase could then consist of simply choosing the approximating function that minimises the empirical error $\hat{L}_n(h)$. This approach is known as Empirical Risk Minimisation (ERM), *Vapnik (1998)*. However, ERM is usually avoided in ML as it leads to severe overfitting of the model on the training dataset. As a matter of fact, in this case, the training process could choose a model complicated enough to perfectly describe all training samples (including the noise, which afflicts them). In other words, ERM implies memorisation of data rather than learning from them. A more effective approach is to minimise a cost function where the trade-off between accuracy on the training data and a measure of the complexity of the selected model is achieved, *Tikhonov and Arsenin (1979)*, implementing the Occam's razor principle

$$h^*: \min_h \hat{L}_n(h) + \lambda C(h). \quad (2)$$

The best-approximating function h^* is chosen as the one that is complicated enough to learn from data without overfitting them, where $C(\cdot)$ is a complexity measure: depending on the exploited ML approach, different measures are realised. $\lambda \in [0, \infty)$ is a hyperparameter, that must be set a-priori and is not obtained as an output of the optimisation procedure: it regulates the trade-off between the overfitting tendency, related to the minimisation of the empirical error, and the underfitting tendency, related to the minimisation of $C(\cdot)$. The optimal value for λ is problem-dependent, and tuning this hyperparameter is a non-trivial task, as will be discussed later in this section. In KRLS, models are defined as

$$h(\mathbf{x}) = \mathbf{w}^T \boldsymbol{\varphi}(\mathbf{x}), \quad (3)$$

where $\boldsymbol{\varphi}$ is an a-priori defined Feature Mapping (FM) as reported in *Shalev-Shwartz and Ben-David (2014)*, allowing to keep the structure of $h(\mathbf{x})$ linear.

The complexity of the models in KRLS is measured as

$$C(h) = \|\mathbf{w}\|^2, \quad (4)$$

i.e., the Euclidean norm of the set of weights describing the regressor, which is a standard complexity measure in ML, *Vovk (2013)*. Regarding the loss function, the square loss is typically adopted because of its convexity, smoothness, and statistical properties, as shown in *Rosasco et al. (2004)*

$$\hat{L}_n(h) = \frac{1}{n} \sum_{i=1}^n \ell(h(\mathbf{x}_i), y_i) = \frac{1}{n} \sum_{i=1}^n [h(\mathbf{x}_i) - y_i]^2 \quad (5)$$

Consequently, problem (2) can be reformulated as

$$\mathbf{w}^*: \min_{\mathbf{w}} \sum_{i=1}^n [\mathbf{w}^T \boldsymbol{\varphi}(\mathbf{x}_i) - y_i]^2 + \lambda \|\mathbf{w}\|^2. \quad (6)$$

By exploiting the Representer Theorem, *Schölkopf et al. (2001)*, the solution h^* of the problem (6) can be expressed as a linear combination of the samples projected in the space defined by $\boldsymbol{\varphi}$

$$h^*(\mathbf{x}) = \sum_{i=1}^n \iota_i \boldsymbol{\varphi}(\mathbf{x}_i)^T \boldsymbol{\varphi}(\mathbf{x}). \quad (7)$$

It is worth underlining that, according to the kernel trick, it is possible to reformulate $h^*(\mathbf{x})$ without explicit knowledge of $\boldsymbol{\varphi}$, and consequently avoiding the curse of dimensionality of computing $\boldsymbol{\varphi}$, by using a proper kernel function $K(\mathbf{x}_i, \mathbf{x}) = \boldsymbol{\varphi}(\mathbf{x}_i)^T \boldsymbol{\varphi}(\mathbf{x})$

$$h^*(\mathbf{x}) = \sum_{i=1}^n \iota_i K(\mathbf{x}_i, \mathbf{x}). \quad (8)$$

Several kernel functions can be retrieved in literature, such as those reported in *Schölkopf (2001)* and *Cristianini and Shawe-Taylor (2000)*, each with a particular property that can be exploited the problem under exam. Usually, the Gaussian kernel is chosen

$$K(\mathbf{x}_i, \mathbf{x}) = e^{-\gamma \|\mathbf{x}_i - \mathbf{x}\|^2}, \quad (9)$$

because of the theoretical reasons described in *Keerthi and Lin (2003)* and *Oneto et al. (2015)*, and because of its effectiveness as reported in *Fernández-Delgado et al. (2014)* and *Wainberg et al. (2016)*. γ is another hyperparameter that regulates the solution's nonlinearity that must be tuned, as explained later. The Gaussian kernel can implicitly create an infinite dimensional $\boldsymbol{\varphi}$ and thanks to this, the KRLS can learn any possible function, *Keerthi and Lin (2003)*. The KRLS problem of Eq. (6) can be reformulated by exploiting kernels as

$$\boldsymbol{\iota}^*: \min_{\boldsymbol{\iota}} \|\mathbf{Q}\boldsymbol{\iota} - \mathbf{y}\|^2 + \lambda \boldsymbol{\iota}^T \mathbf{Q} \boldsymbol{\iota}, \quad (10)$$

where $\mathbf{y} = [y_1, \dots, y_n]^T$, $\boldsymbol{\iota} = [\iota_1, \dots, \iota_n]^T$, the matrix \mathbf{Q} such that $Q_{i,j} = K(\mathbf{x}_j, \mathbf{x}_i)$, and the identity matrix $\mathbf{I} \in \mathbb{R}^{n \times n}$. By setting the gradient equal to zero w.r.t. $\boldsymbol{\iota}$ it is possible to state that

$$(\mathbf{Q} + \lambda \mathbf{I}) \boldsymbol{\iota}^* = \mathbf{y}, \quad (11)$$

which is a linear system for which effective solvers have been developed over the years, allowing it to cope with even very large sets of training data, *Young (2003)*.

3.2. Model Selection and Error Estimation

The problems that still must be faced are how to tune the hyperparameters (λ and γ) and estimate the performance of the final model. Model Selection (MS) and Error Estimation (EE) deal precisely with these problems, *Oneto (2020)*. Researchers and practitioners commonly use resampling techniques since they work well in most situations, and therefore we will exploit them in this work. Other alternatives exist based on the Statistical Learning Theory, but they tend to underperform resampling techniques in practice, as demonstrated by *Oneto (2020)*. Resampling techniques are based on a simple

idea: the original dataset \mathcal{D}_n is resampled once or many (n_r) times, with or without replacement, to build three independent datasets called learning, validation and test sets, respectively \mathcal{L}_l^r , \mathcal{V}_v^r , and \mathcal{T}_t^r , with $r \in \{1, \dots, n_r\}$ such that

$$\mathcal{L}_l^r \cap \mathcal{V}_v^r = \emptyset, \mathcal{L}_l^r \cap \mathcal{T}_t^r = \emptyset, \mathcal{V}_v^r \cap \mathcal{T}_t^r = \emptyset, \mathcal{L}_l^r \cup \mathcal{V}_v^r \cup \mathcal{T}_t^r = \mathcal{D}_n. \quad (12)$$

Subsequently, to select the best hyperparameters' combination $\mathcal{H} = \{\lambda, \gamma\}$ considering a set of possible ones $\mathcal{h} = \{\mathcal{H}_1, \mathcal{H}_2, \dots\}$ for the algorithm $\mathcal{A}_{\mathcal{H}}$ or, in other words, to perform the MS phase, the following procedure must be applied:

$$\mathcal{H}^*: \arg \min_{\mathcal{H} \in \mathcal{h}} \sum_{r=1}^{n_r} M(\mathcal{A}_{\mathcal{H}}(\mathcal{L}_l^r), \mathcal{V}_v^r), \quad (13)$$

where $h = \mathcal{A}_{\mathcal{H}}(\mathcal{L}_l^r)$ is a model built with the algorithm \mathcal{A} with its set of hyperparameters \mathcal{H} and with the data \mathcal{L}_l^r , and where $M(h, \mathcal{V}_v^r)$ is a desired metric. Since the data in \mathcal{L}_l^r is independent of the data in \mathcal{V}_v^r , \mathcal{H}^* should be the set of hyperparameters that allows achieving a small error on a data set that is independent of the training set. Then, to evaluate the performance of the optimal model, which is $h_{\mathcal{A}}^* = \mathcal{A}_{\mathcal{H}^*}(\mathcal{D}_n)$ or, in other words, to perform the EE phase, the following procedure must be applied:

$$M(h_{\mathcal{A}}^*) = \frac{1}{n_r} \sum_{r=1}^{n_r} M(\mathcal{A}_{\mathcal{H}^*}(\mathcal{L}_l^r \cup \mathcal{V}_v^r), \mathcal{T}_t^r) \quad (14)$$

Since the data in $\mathcal{L}_l^r \cap \mathcal{V}_v^r$ are independent from the ones in \mathcal{T}_t^r , $M(h_{\mathcal{A}}^*)$ is an unbiased estimator of the true performance, measured with the metric M , of the final model, *Oneto (2020)*. In this work, we will rely on Complete k-fold cross validation, which means setting

$$n_r \leq \binom{n}{k} \binom{n-k}{k}, l = (k-2) \frac{n}{k}, v = t = \frac{n}{k}, \quad (14)$$

and resampling without replacement. Note that, in our application, we have a further constraint in terms of dependence in time between the samples. For this reason, when resampling the data from \mathcal{D}_n we keep data of different periods in \mathcal{L}_l^r , \mathcal{V}_v^r , and \mathcal{T}_t^r As reported in *Hamilton (2020)*. For what concerns the applied metric M , we will rely on the Mean Absolute Error (MAE), the Mean Absolute Percentage of Error (MAPE), and the Pearson Product-Moment Correlation Coefficient PPMCC according to *Willmott and Matsuura (2005)*. Since in regression, it is pretty hard to synthesise the quality of a predictor in a single metric, we will also rely on visualisation techniques like the scatter plot and histograms, *Shao et al. (2017)*.

3.2. Hybrid Models

In this section, we depict a framework able to consider both the physical knowledge about the problem encapsulated in the PMs of Section 2 and the information hidden in the available data as the DDMs of Section 3.1. For this purpose, we will start from a simple observation: an HM, based on the previous observation, should learn from the data without being too different or too far away from the PM. From the Data Science and ML point of view, this requirement can be straightforwardly mapped to a typical ML Multi Task Learning (MTL) problem, *Baxter (2000)*, *Caruana (1997)*, *Evgeniou and Pontil (2004)*, *Bakker and Heskes (2003)*, *Argyriou et al. (2008)*. MTL aims at simultaneously learning two concepts, in this case the PM and the available data, through a learning algorithm $\mathcal{A}_{\mathcal{H}}$ which exploits the data in \mathcal{D}_n to learn a function h which is both close to the observation, the data \mathcal{D}_n and the PM, namely its forecasts. Consequently, in this case, a slightly different scenario is presented where the dataset is composed of a triple of points $\mathcal{D}_n = \{(\mathbf{x}_1, \mathbf{y}_1, \mathbf{p}_1), \dots, (\mathbf{x}_n, \mathbf{y}_n, \mathbf{p}_n)\}$ where \mathbf{p}_i is the output of the PM in the point \mathbf{x}_i with $i \in \{1, \dots, N\}$. The target is to learn a function able to approximate both μ , namely the relation between the input $\mathbf{x} \in \mathcal{X}$ and the output $\mathbf{y} \in \mathcal{Y}$, and the PM, namely, the relation between the input and the output of the PM. Two tasks must be learned, and for this purpose, there are two main approaches: the first approach is called Shared Task Learning (STL) and the second Independent Task Learning (ITL). While the latter independently learn a different model for each task, the former aims to learn a model that is common between all tasks. A well-known weakness of these methods is that they tend to generalise poorly on one of the two tasks, *Baxter (2000)*. In this work, we show that an appealing

approach to overcome such limitations is provided by MTL as suggested by *Baxter (2000)* and *Argyriou et al. (2008)*. This methodology leverages the information between the tasks to learn more accurate models. To apply the MTL approach to this case, it is possible to modify the KRLS problem of Eq. (6) to simultaneously learn a shared model and a task specific model which should be close to the shared model. In this way, we obtain a model which can simultaneously learn the two tasks. The model we are interested in is the shared model, while the task specific models are just used as a tool. A shared model is defined as $h(\mathbf{x}) = \mathbf{w}^T \boldsymbol{\varphi}(\mathbf{x})$, and two task specific models as

$$h_i(\mathbf{x}) = \mathbf{w}_i^T \boldsymbol{\varphi}(\mathbf{x}), \quad i \in \{y, p\}. \quad (15)$$

Then, it is possible to state the MTL version of Eq. (6), as follows

$$\begin{aligned} \mathbf{w}^*, \mathbf{w}_y^*, \mathbf{w}_p^*: \min_{\mathbf{w}, \mathbf{w}_y, \mathbf{w}_p} & \sum_{i=1}^n [\mathbf{w}^T \boldsymbol{\varphi}(\mathbf{x}) - y_i]^2 + [\mathbf{w}^T \boldsymbol{\varphi}(\mathbf{x}) - p_i]^2 \\ & + \sum_{i=1}^n [\mathbf{w}_y^T \boldsymbol{\varphi}(\mathbf{x}) - y_i]^2 + [\mathbf{w}_p^T \boldsymbol{\varphi}(\mathbf{x}) - p_i]^2 \\ & + \lambda \|\mathbf{w}\|^2 + \kappa (\|\mathbf{w} - \mathbf{w}_y\|^2 + \|\mathbf{w} - \mathbf{w}_p\|^2) \end{aligned} \quad (16)$$

where λ is the usual regularisation of KRLS and $\kappa \in [0, \infty)$, instead, is another hyperparameter that forces the shared model to be close to the task specific models. Basically, the MTL problem of Eq. (16) is a concatenation of three learning problems solved with KRLS plus a term that tries to keep a relation between all the three different problems. By exploiting the kernel trick as in KRLS, it is possible to reformulate the problem (16), as follows

$$\mathbf{t}^*: \min_{\mathbf{t}} \left\| \begin{bmatrix} Q & Q & 0 & 0 \\ Q & Q & 0 & 0 \\ 0 & 0 & Q & 0 \\ 0 & 0 & 0 & Q \end{bmatrix} \mathbf{t} - \begin{bmatrix} \mathbf{y} \\ \mathbf{p} \\ \mathbf{y} \\ \mathbf{p} \end{bmatrix} \right\|^2 + \mathbf{t}^T \begin{bmatrix} (\lambda + 2\kappa)Q & (\lambda + 2\kappa)Q & -\kappa Q & -\kappa Q \\ (\lambda + 2\kappa)Q & (\lambda + 2\kappa)Q & -\kappa Q & -\kappa Q \\ -\kappa Q & -\kappa Q & \kappa Q & 0 \\ -\kappa Q & -\kappa Q & 0 & \kappa Q \end{bmatrix} \mathbf{t} \quad (17)$$

where $\mathbf{p} = [p_1, \dots, p_n]^T$.

The solution of this problem is again equivalent to solving a linear system

$$\begin{bmatrix} Q + (\lambda + 2\kappa)I & Q + (\lambda + 2\kappa)I & -\kappa I & -\kappa I \\ Q + (\lambda + 2\kappa)I & Q + (\lambda + 2\kappa)I & -\kappa I & -\kappa I \\ -\kappa I & -\kappa I & Q + \kappa I & 0 \\ -\kappa I & -\kappa I & 0 & Q + \kappa I \end{bmatrix} \mathbf{t}^* = \begin{bmatrix} \mathbf{y} \\ \mathbf{p} \\ \mathbf{y} \\ \mathbf{p} \end{bmatrix} \quad (18)$$

The function that the authors are interested in, the shared one, can be expressed as follows

$$h(\mathbf{x}) = \mathbf{w}^T \boldsymbol{\varphi}(\mathbf{x}) = \sum_{i=1}^n (\iota_i + \iota_{i+n}) K(\mathbf{x}_i, \mathbf{x}). \quad (19)$$

4. Data Description

Data from a naval vessel equipped with a MAN B&W V28-33D medium speed four-stroke DE, Table I, has been exploited in this work.

Table I: Main characteristics of the MAN 12 V28-33D engine

Feature	Value	Unit	Feature	Value	Unit
Cylinders	V12, 16, 20	[-]	Brake power at 60% MCR	3240	[kW]
Bore diameter	280	[mm]	Brake power at 80% MCR	4320	[kW]
Stroke length	330	[mm]	Brake power at MCR	5400	[kW]
Number of cylinders	12	[-]	Mean Effective Pressure	26.9	[bar]
Revolutions per cycle	2	[-]	Mean Piston Speed	11	[m/s]
Engine speed at MCR	1000	[rpm]	Specific Fuel consumption	191	[g/kWh]

The DE is installed on board one of the Holland Class Oceangoing Patrol Vessels. The propulsion system of the vessel consists of two shafts with Controllable Pitch Propellers (CPP), a gearbox, and one DE per shaft. The vessel is equipped with a data logging system used both for on board monitoring and control and for land-based performance analysis. The dataset utilised consists of two different data sources, Table II: standard measurements (steady-state) performed during Shop Trials (ST) that were used to calibrate the PM model (see Section 2), *Kalikatzarakis et al. (2021)*, and operational data originating from the vessel's data logging system, used by the ship operator for performance monitoring purposes, which has been exploited to evaluate the performance of the PM model in dynamic conditions (see Section 2), and training, validate, and test the DDMs and HMs (see Sections 3.1 and 3).

Table II: Table captions above table

Variable Name	Symbol	Unit
Timestamp	t	[hh:mm:ss]
Governor Position	G_p	[-]
Engine Rotational Speed	n_e	[rpm]
Engine Torque	M_e	[kNm]
Charge Air Temperature at Scavenging Receiver	T_{sc}	[°C]
Charge Air Temperature at Compressor Inlet	$T_{c,in}$	[°C]
Charge Air Temperature at Compressor Outlet	$T_{c,out}$	[°C]
Exhaust Gas Temperature at Turbine Outlet	$T_{t,out}$	[°C]
Main Bearing Temperature	$T_{b,1}$	[°C]
Main Bearing Temperature	$T_{b,2}$	[°C]
Main Bearing Temperature	$T_{b,3}$	[°C]
Main Bearing Temperature	$T_{b,4}$	[°C]
Main Bearing Temperature	$T_{b,5}$	[°C]
Main Bearing Temperature	$T_{b,6}$	[°C]
Main Bearing Temperature	$T_{b,7}$	[°C]
Lube Oil Compartment No. 1 Temperature	$T_{l,1}$	[°C]
Lube Oil Compartment No. 2 Temperature	$T_{l,2}$	[°C]
Lube Oil Compartment No. 3 Temperature	$T_{l,3}$	[°C]
Lube Oil Compartment No. 4 Lube Oil	$T_{l,4}$	[°C]
Lube Oil Compartment No. 5 Lube Oil	$T_{l,5}$	[°C]
Lube Oil Engine Inlet Temperature	$T_{le,in}$	[°C]
Lube Oil Engine Outlet Temperature	$T_{le,out}$	[°C]
High-Temperature Sea Cooling Water - Inlet	$T_{ht,in}$	[°C]
High-Temperature Sea Cooling Water - Outlet	$T_{ht,out}$	[°C]
Low-Temperature Sea Cooling Water - Inlet	$T_{lt,in}$	[°C]
Low-Temperature Sea Cooling Water - Outlet	$T_{lt,out}$	[°C]
Fuel Oil Supply Temperature	T_f	[°C]
Charge Air Temperature at Compressor Outlet – Bank A	$T_{c,out}^A$	[°C]
Charge Air Temperature at Compressor Outlet – Bank B	$T_{c,out}^B$	[°C]
Charge Air Temperature at Compressor Inlet – Bank A	$T_{c,in}^A$	[°C]
Charge Air Temperature at Compressor Inlet – Bank B	$T_{c,in}^B$	[°C]
Charge Air Engine Inlet Pressure	$p_{ca,in}$	[Pa]
Charge Air Engine Inlet Temperature	$T_{ca,in}$	[°C]
Fuel Consumption	\dot{m}_f	[kg/h]
TC rotational speed	N_{tc}	[rpm]
Turbine Outlet Temperature	$T_{t,out}$	[°C]
Exhaust Receiver Temperature	T_{er}	[°C]

5. Experimental Results

In this section, we test the models developed in Sections 2 and Sections 3 on the data described in Section 4, comparing the performance of PMs, DDMs, and HMs in dynamic operational conditions. First, we report the hyperparameters ranges for the DDM and HM.

For the DDM, the set of hyperparameters tuned during the MS phase are $\mathcal{H} = \{\lambda, \gamma\}$ chosen in $\mathcal{K} = \{10^{-4.0}, 10^{-3.8}, \dots, 10^{+4.0}\} \times \{10^{-4.0}, 10^{-3.8}, \dots, 10^{+4.0}\}$. For the HM, the set of hyperparameters tuned during the MS phase are $\mathcal{H} = \{\lambda, \gamma, \kappa\}$ chosen in $\mathcal{K} = \{10^{-4.0}, 10^{-3.8}, \dots, 10^{+4.0}\} \times \{10^{-4.0}, 10^{-3.8}, \dots, 10^{+4.0}\} \times \{10^{-4.0}, 10^{-3.8}, \dots, 10^{+4.0}\}$.

All the tests have been repeated 30 times, and the average results are reported together with their t-student 95% confidence interval to ensure the statistical validity of the results. Table III reports the performance (MAE, MAPE, and PPMCC) of the different models (PM, DDM, and HM) for the different targets using to predict.

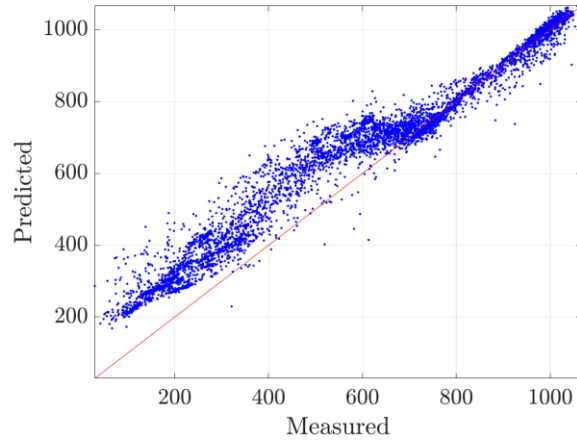
Table III: Table captions above table

Model	MAE [°C]	MAPE [%]	PPMCC	MAE [°C]	MAPE [%]	PPMCC
Fuel Consumption \dot{m}_f [kg/h]			Turbine Outlet Temperature $T_{t,out}$ [°C]			
PM	76.62 ± 4.37	26.93 ± 1.54	0.98 ± 0.01	9.66 ± 0.57	2.53 ± 0.13	0.92 ± 0.01
DDM	24.11 ± 1.39	6.30 ± 0.38	0.99 ± 0.01	3.80 ± 0.20	0.97 ± 0.05	0.99 ± 0.01
HM	18.64 ± 0.98	4.89 ± 0.17	1.00 ± 0.01	3.18 ± 0.22	0.81 ± 0.05	0.99 ± 0.01
TC Rotational speed N_{tc} [rpm]			Exhaust Manifold Temperature T_{er} (°C)			
PM	2090 ± 78.43	15.39 ± 0.75	0.97 ± 0.01	19.92 ± 1.06	4.81 ± 0.15	0.96 ± 0.01
DDM	302.6 ± 21.42	2.18 ± 0.15	1.00 ± 0.01	5.02 ± 0.19	1.13 ± 0.04	0.99 ± 0.01
HM	214.44 ± 9.54	1.53 ± 0.08	1.00 ± 0.01	3.94 ± 0.24	0.88 ± 0.05	0.99 ± 0.01

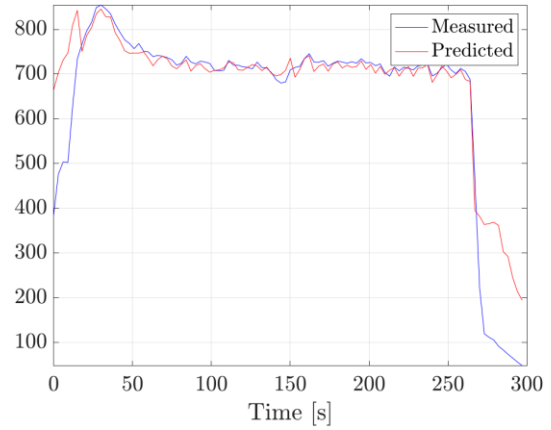
A substantial decrease in the errors can be observed from Table III across all the targets. Considering \dot{m}_f , we can observe a MAPE decrease from 26.93% (PM) to 6.30% (DDM), to 4.89% (HM). The same general trend can be reported for N_{tc} , $T_{t,out}$, and T_{er} .

Figs.2-5 report the scatter plot and examples of the trend in time for the different targets using PM, DDMs, and HMs. Compared to the PM, the proposed DDMs are more accurate in predicting the four targets. In addition, it is possible to observe that DDMs are capable of fully capturing the transient behaviour of the fuel consumption, Fig.2d, the turbocharger rotational speed mechanical transient, Fig.3d, and the thermodynamic transients of both the turbine outlet gases, Fig.4d, and exhaust manifold, Fig.5d. Also, Figs.2-5 show that the DDMs are characterised by both lower bias and lower variance compared to the PM.

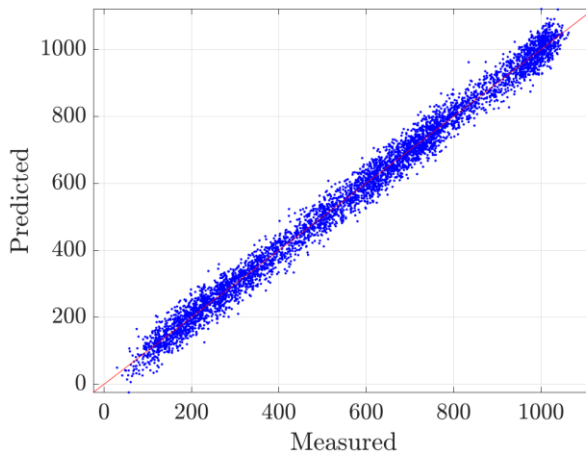
Although DDMs are computationally demanding in the training phase, they are characterised by lower computational complexity in the feed-forward phase as they just require matrix manipulation methods. The combination of both accurate and fast predictions makes DDMs an ideal candidate for real-time performance and condition estimation. However, the necessary data to reach this level of performance is rather high, as reported in *Cipollini et al. (2018a, 2018b)*, making this type of model applicable only after extensive measurement campaigns have been undertaken. In addition, another disadvantage of DDMs is the lack of interpretability as it is not supported by any physical interpretation. To overcome those limitations, we proposed the use of HMs. These allow the exploitation of both the mechanistic knowledge of the underlying physical principles from the PM and any available measurements taken during the operation of the vessel. An advantage of the HMs is their ability to exploit the coarse but physically supported predictions of the PM. Therefore, HMs have much smaller requirements regarding the use of actual measurements for the learning phase. While they will still require a measurement campaign to be deployed, they can be reliably used already after a few months worth of measurements, in contrast with pure DDMs that would require at least half a year of available data.



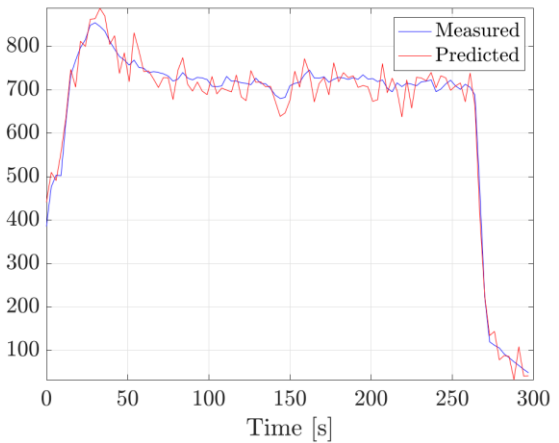
(a) Scatter Plot - PM



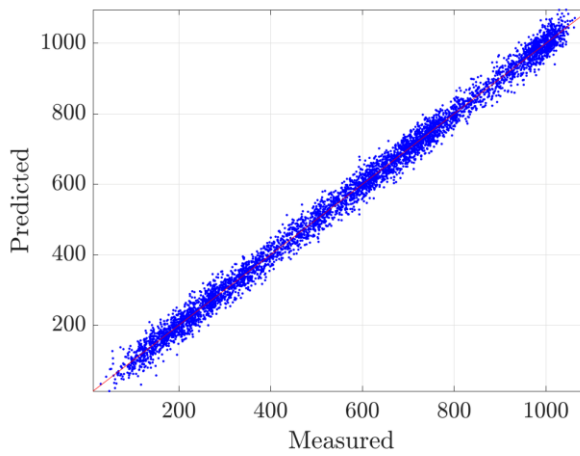
(b) Trend in time - PM



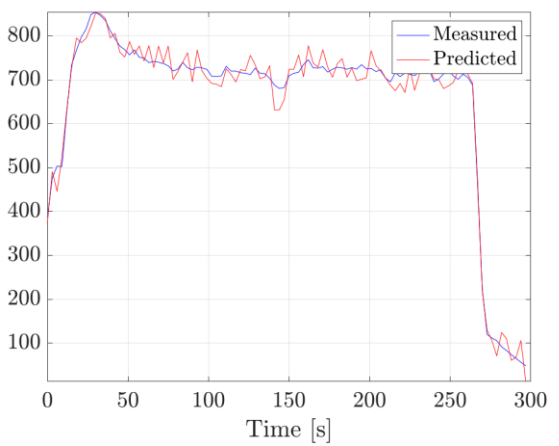
(c) Scatter Plot - DDM



(d) Trend in time - DDM



(e) Scatter Plot - HM



(f) Trend in time - HM

Fig.2: Scatter plot and trend in time for the \dot{m}_f (kg/h) output feature - PMs, DDMs, and HMs.

The novelty introduced by the HMs led to more accurate predictions of the four targets compared to the rest of the models (PM and DDMs), as can be seen from Table III.

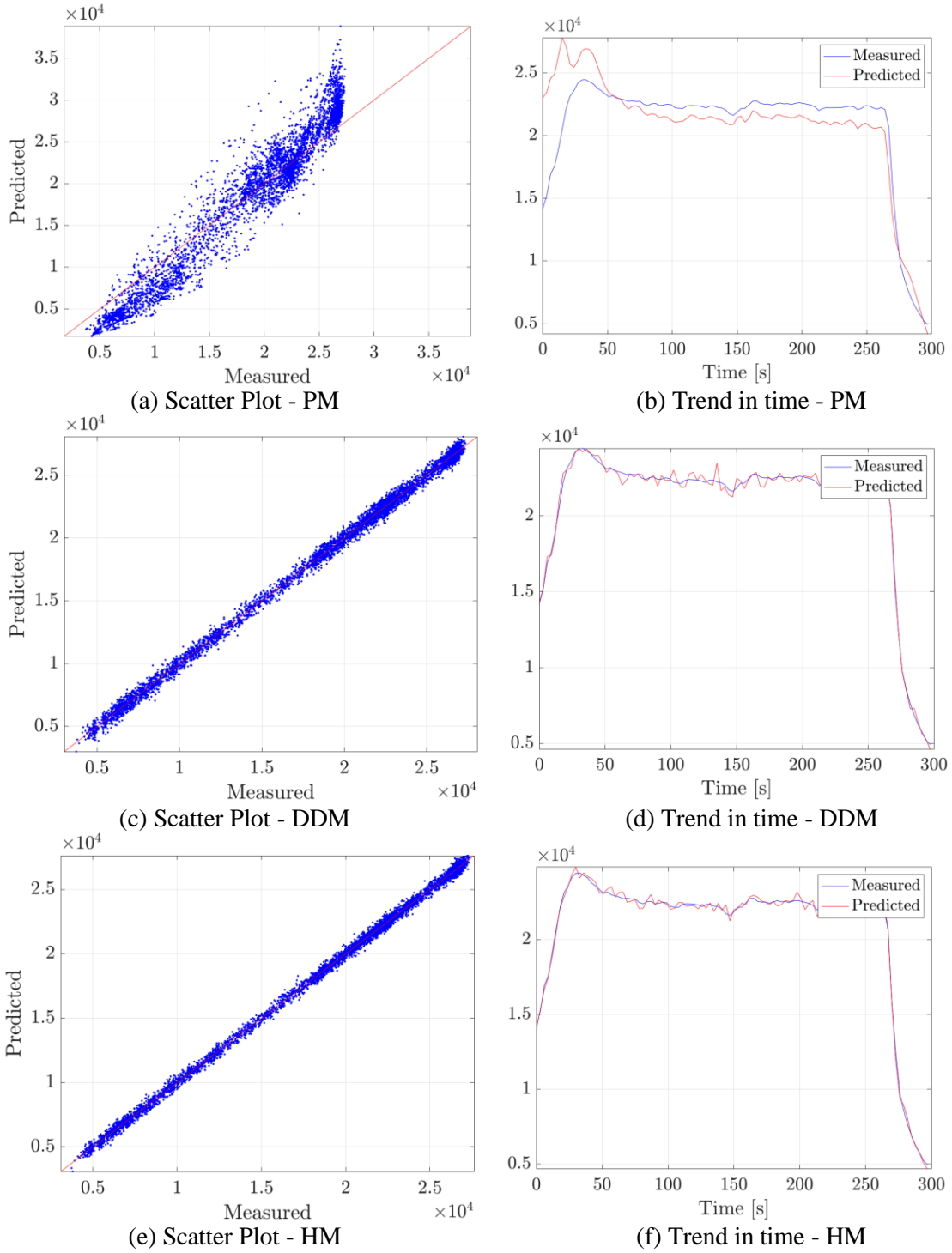
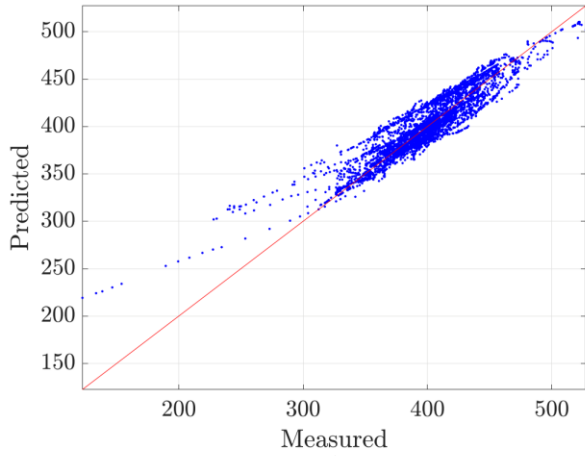
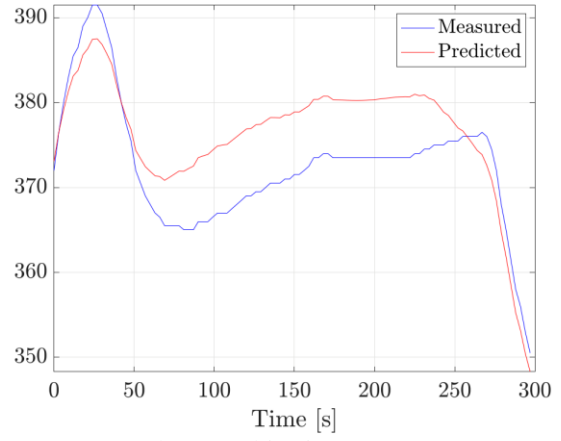


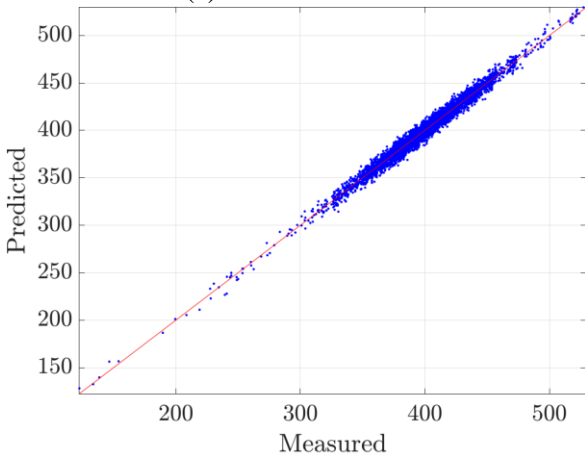
Fig.3: Scatter plot and trend in time for the N_{tc} (rpm) output feature - PMs, DDMs, and HMs.



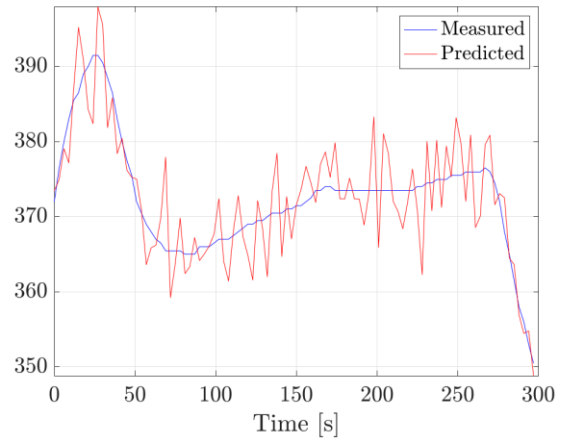
(a) Scatter Plot - PM



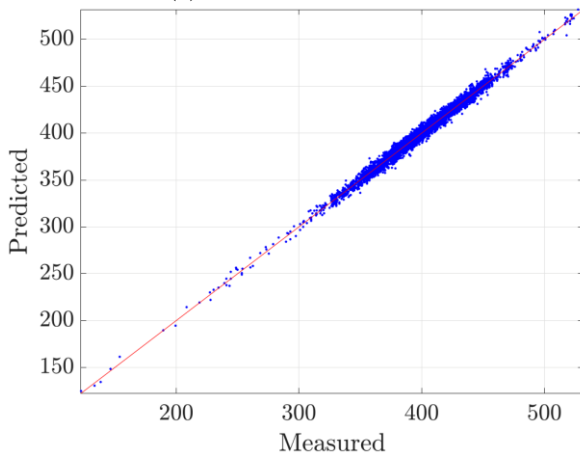
(b) Trend in time - PM



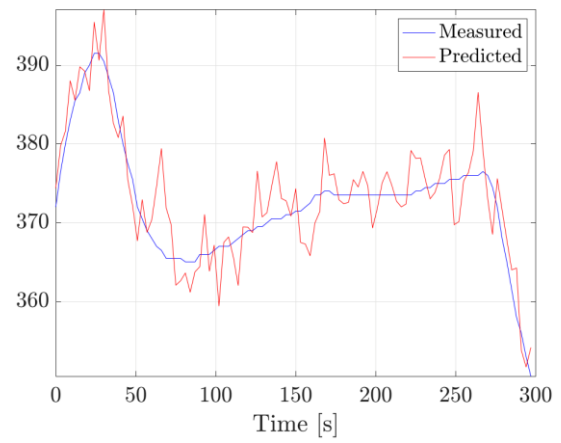
(c) Scatter Plot - DDM



(d) Trend in time - DDM



(e) Scatter Plot - HM



(f) Trend in time - HM

Fig.4: Scatter plot and trend in time for the $T_{t,out}$ ($^{\circ}\text{C}$) output feature - PMs, DDMs, and HMs.

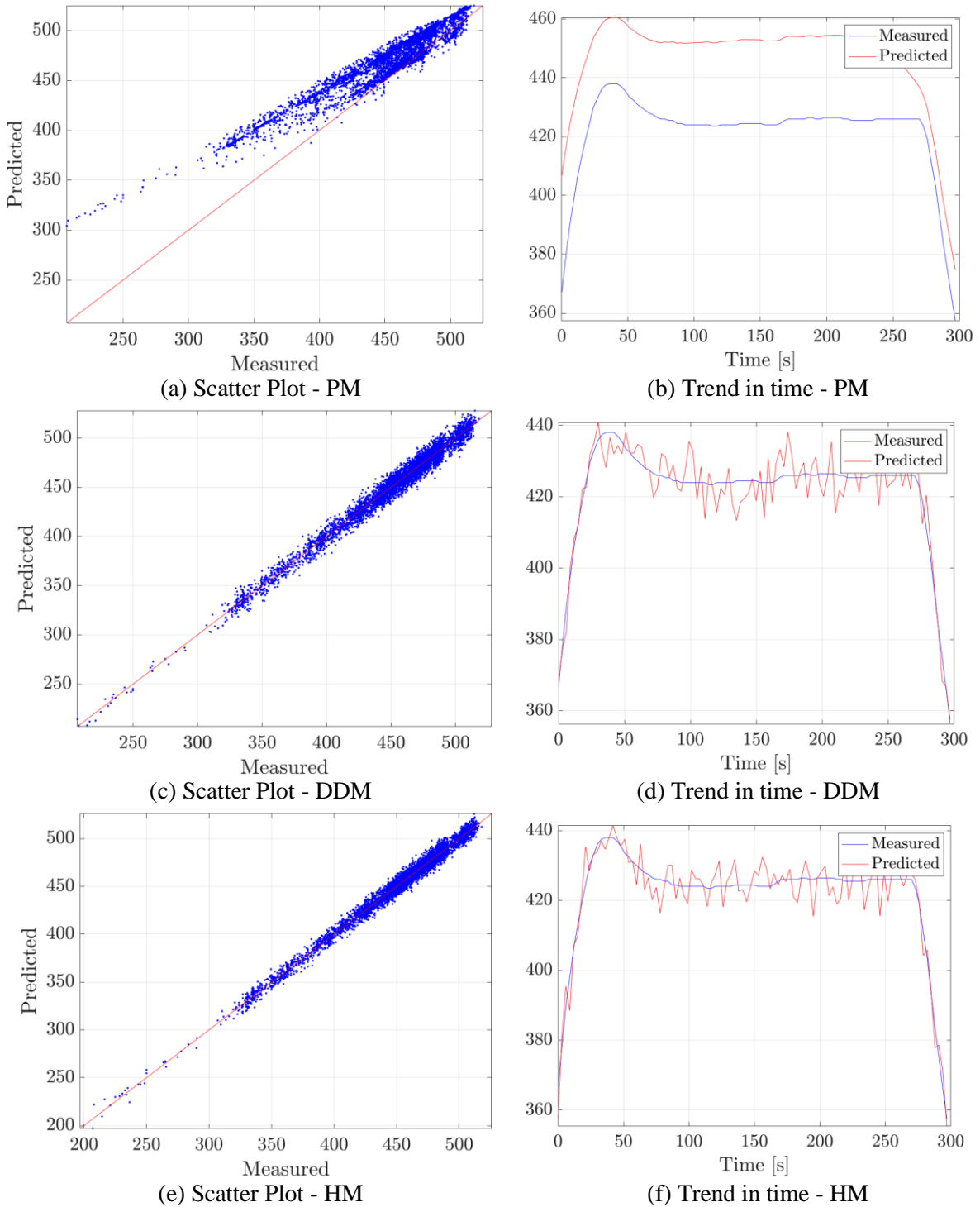


Fig.5: Scatter plot and trend in time for the T_{er} ($^{\circ}\text{C}$) output feature - PMs, DDMs, and HMs.

6. Conclusions

In this work, the authors focused their attention on demonstrating a novel modelling framework for the hybridisation of physical and data driven models. The proposed framework can deliver accurate, reliable, and computationally inexpensive models suitable for real-time performance assessment and condition monitoring applications. State-of-the-art data-driven methods have been presented, able to exploit the information provided by on-board measurements from one Holland Class Oceangoing Patrol Vessel, provided by the Royal Netherlands Navy and Damen Schelde Naval Shipbuilding. First, a 0D physical model of a medium speed two-stroke diesel

engine (MAN 12 V28-33D) was described. Data-driven models have been discussed and proposed in Section 3.1 to predict the engine's behaviour, with a focus on four different targets: fuel consumption, turbocharger rotational speed, turbine outlet temperature, and exhaust receiver temperature. The models proved to be very accurate, with the enhanced capability of exploiting time-series information from the past, achieving relative errors below 1% on the validation data for the turbine outlet temperature and exhaust receiver temperature. However, due to their nature, these data-driven models are hard to interpret. To overcome the limitations of both the physical and the data-driven models, we proposed a hybrid approach that can consider past information, capable of improving accuracy, easily interpreted, and have low computational time requirements. The hybridisation of physical and data driven models proved to be highly accurate, achieving even lower errors when compared to the simple data-driven approach. These hybrid models can potentially also be used to improve the accuracy of predictions for operation in other conditions than the measured ones, as purely data-driven models cannot be used for extrapolation, but the physical model contribution will improve hybrid model performance during extrapolation.

References

ARGYRIOU, A.; EVGENIOU, T.; PONTIL, M. (2008), *Convex multi-task feature learning*, Machine Learning 73, pp.243-272

ASAD, U.; TJONG, J.; ZHENG, M. (2014), *Exhaust gas recirculation-zero dimensional modelling and characterisation for transient diesel combustion control*, Energy Conversion and Management 86, pp.309-324

BAKKER, B.; HESKES, T. (2003), *Task clustering and gating for Bayesian multitask learning*, J. Machine Learning Research 4, pp.83-99

BALDI, F.; JOHNSON, H.; GABRIELI, C.; ANDERSSON, K. (2014), *Energy and exergy analysis of ship energy systems-the case study of a chemical tanker*, Int. Conf. on Efficiency, Cost, Optimisation, Simulation and Environmental Impact of Energy Systems

BALDI, F.; THEOTOKATOS, G.; ANDERSSON, K. (2015), *Development of a combined mean value-zero-dimensional model and application for a large marine four-stroke diesel engine simulation*. Applied Energy 154, pp.402-415

BAXTER, J. (2000), *A model of inductive bias learning*, J. Artificial Intelligence Research 12, pp.149-198

BIDARVATAN, M.; THAKKAR, V.; SHAHBAKHTI, M.; BAHRI, B.; AZIZ, A. (2014), *Grey-box modeling of HCCI engines*, Applied Thermal Engineering 70, pp.397-409

BONDARENKO, O.; FUKUDA, T. (2020), *Development of a diesel engine's digital twin for predicting propulsion system dynamics*, Energy 196, 117126

CARUANA, R. (1997), *Multitask learning*, Machine Learning 28, pp.41-75.

CASEY, M.; ROBINSON, C. (2013), *A method to estimate the performance map of a centrifugal compressor stage*, J. Turbomachinery 135

CATANIA, A.; FINESSO, R.; SPESSA, E. (2011), *Predictive zero-dimensional combustion model for di diesel engine feed-forward control*, Energy Conversion and Management 52, pp.3159-3175

CIPOLLINI, F.; ONETO, L.; CORADDU, A.; MURPHY, A.; ANGUITA, D. (2018a), *Condition-based maintenance of naval propulsion systems: Data analysis with minimal feedback*, Reliability Engineering & System Safety 177, pp.12-23

CIPOLLINI, F.; ONETO, L.; CORADDU, A.; MURPHY, A.; ANGUITA, D. (2018b), *Condition-based maintenance of naval propulsion systems with supervised data analysis*, Ocean Eng. 149, pp.268–278

EUROPEAN COMMISSION (2013a), *Integrating maritime transport in the EU's green house gas reduction policies: Communication from the commission to the European parliament, the council, the European economic and social committee and the committee of the regions*, Tech. rep. European Union

IMO (2011), *Amendments to the annex of the protocol of 1997 to amend the international convention for the prevention of pollution from ships, 1973, as modified by the protocol of 1978 relating thereto*, Resolution MEPC. 203 (62)

CORADDU, A.; KALIKATZARAKIS, M.; ONETO, L.; MEIJN, G.J.; GODJEVAC, M.; GEERTSMAD, R.D. (2018), *Ship diesel engine performance modelling with combined physical and machine learning approach*, Int. Naval Engineering Conf.

CORADDU, A.; LIM, S.; ONETO, L.; PAZOUKI, K.; NORMAN, R.; MURPHY, A. (2019a), *A novelty detection approach to diagnosing hull and propeller fouling*, Ocean Eng. 176, pp.65–73

CORADDU, A.; ONETO, L.; BALDI, F.; ANGUITA, D. (2017), *Vessels fuel consumption forecast and trim optimisation: a data analytics perspective*, Ocean Eng. 130, pp.351–370

CORADDU, A.; ONETO, L.; BALDI, F.; CIPOLLINI, F.; ATLAR, M.; SAVIO, S. (2019b), *Data-driven ship digital twin for estimating the speed loss caused by the marine fouling*, Ocean Eng. 186, 106063

CORADDU, A.; ONETO, L.; CIPOLLINI, F.; KALIKATZARAKIS, M.; MEIJN, G. J.; GEERTSMA, R. (2021a), *Physical, data-driven and hybrid approaches to model engine exhaust gas temperatures in operational conditions*, Ships and Offshore Structures, pp.1–22

CORADDU, A.; ONETO, L.; ILARDI, D.; STOUMPOS, S.; THEOTOKATOS, G. (2021b), *Marine dual fuel engines monitoring in the wild through weakly supervised data analytics*, Engineering Applications of Artificial Intelligence 100, 104179

CORADDU, A.; ONETO, L.; DE MAYA, B.; KURT, R. (2020), *Determining the most influential human factors in maritime accidents: A data-driven approach*, Ocean Eng. 211, 107588

CRISTIANINI, N.; SHAWE-TAYLOR, J. (2000), *An introduction to support vector machines and other kernel-based learning methods*, Cambridge University Press

DING, Y.; STAPERSMA, D.; KNOLL, H.; GRIMMELIUS, H.; NETHERLAND, T. (2010). *Characterising heat release in a diesel engine: A comparison between seiliger process and vibe model*, CIMAC International Council on Combustion engines, pp.1–13

EVGENIOU, T.; PONTIL, M. (2004), *Regularised multi-task learning*, Int. Conf. on Knowledge Discovery and Data Mining

FERNÁNDEZ-DELGADO, M.; CERNADAS, E.; BARRO, S.; AMORIM, D. (2014), *Do we need hundreds of classifiers to solve real world classification problems?*, J. Machine Learning Research 15, pp.3133–3181

- GARCÍA-MARTOS, C.; RODRÍGUEZ, J.; SÁNCHEZ, M. J. (2013), *Modelling and forecasting fossil fuels, CO₂ and electricity prices and their volatilities*, Applied Energy 101, pp.363–375
- GEERTSMA, R.; NEGENBORN, R.; VISSER, K.; LOONSTIJN, M.; HOPMAN, J. (2017), *Pitch control for ships with diesel mechanical and hybrid propulsion: Modelling, validation and performance quantification*, Applied Energy 206, pp.1609–1631
- GOODFELLOW, I.; BENGIO, Y.; COURVILLE, A. (2016), *Deep Learning*, MIT Press
- GRIMMELIUS, H.; BOONEN, E.; NICOLAI, H.; STAPERSMA, D. (2010), *The integration of mean value first principle diesel engine models in dynamic waste heat and cooling load analysis*, CIMAC Congress, Bergen, Vol 31, p.51
- GUAN, C.; THEOTOKATOS, G.; ZHOU, P.; CHEN, H. (2014), *Computational investigation of a large containership propulsion engine operation at slow steaming conditions*, Applied Energy 130, pp.370–383
- HAMILTON, J.D. (2020), *Time series analysis*, Princeton University Press
- HANSON, R.K.; SALIMIAN, S. (1984), *Survey of rate constants in the N/H/O system*, Combustion Chemistry, pp.361–421
- HEYWOOD, J.B. (1988), *Internal combustion engines fundamentals*, McGraw-Hill
- KALIKATZARAKIS, M.; CORADDU, A.; THEOTOKATOS, G.; ONETO, L. (2021), *Development of a zero-dimensional model and application on a medium-speed marine four-stroke diesel engine*, Int. Conf. on Modelling and Optimisation of Ship Energy Systems
- KEERTHI, S.S.; LIN, C.J. (2003), *Asymptotic behaviors of support vector machines with gaussian kernel*, Neural computation 15, pp.1667–1689
- LIVANOS, G.; PAPALAMBROU, G.; KYRTATOS, N.; CHRISTOU, A. (2007), *Electronic engine control for ice operation of tankers*, 25th CIMAC World Congress on Combustion Engine Technology, Vienna, pp.21–24
- MERKER, G.P.; SCHWARZ, C.; STIESCH, G.; OTTO, F. (2005), *Simulating Combustion: Simulation of combustion and pollutant formation for engine development*, Springer Science & Business Media
- MIGLIANTI, F.; CIPOLLINI, F.; ONETO, L.; TANI, G.; VIVIANI, M. (2019), *Model scale cavitation noise spectra prediction: Combining physical knowledge with data science*, Ocean Eng. 178, pp.185–203
- MIGLIANTI, L.; CIPOLLINI, F.; ONETO, L.; TANI, G.; GAGGERO, S.; CORADDU, A.; VIVIANI, M. (2020), *Predicting the cavitating marine propeller noise at design stage: A deep learning based approach*, Ocean Eng. 209, 107481
- MISHRA, C.; SUBBARAO, P. (2021), *A Comparative Study of Physics Based Grey Box and Neural Network Trained Black Box Dynamic Models in an RCCI Engine Control Parameter Prediction*, Technical Report SAE Technical Paper
- MOHAMMADKHANI, F.; YARI, M.; RANJBAR, F. (2019), *A zero-dimensional model for simulation of a Diesel engine and exergoeconomic analysis of waste heat recovery from its exhaust and coolant employing a high-temperature Kalina cycle*, Energy Conversion and Management 198, 111782
- NIKZADFAR, K.; SHAMEKHI, A. H. (2014), *Investigating the relative contribution of operational*

parameters on performance and emissions of a common-rail diesel engine using neural network, *Fuel* 125, pp.116–128

ONETO, L. (2020), *Model Selection and Error Estimation in a Nutshell*, Springer

ONETO, L.; GHIO, A.; RIDELLA, S.; ANGUITA, D. (2015), *Support vector machines and strictly positive definite kernel: The regularisation hyper parameter is more important than the kernel hyperparameters*, *IEEE Int. Joint Conf. on Neural Networks*

ÖZENER, O.; YUKSEK, L.; OZKAN, M. (2013), *Artificial neural network approach to predicting engine-out emissions and performance parameters of a turbo charged diesel engine*, *Thermal Science* 17, pp.153–166

RAKOPOULOS, C.D.; HOUNTALAS, D.T.; TZANOS, E.I.; TAKLIS, G.N. (1994), *A fast algorithm for calculating the composition of diesel combustion products using 11 species chemical equilibrium scheme*, *Advances in Engineering Software* 19, pp.109–119

ROHSENOW, W.M.; HARTNETT, J.P. (1988), *Handbook of heat transfer fundamentals*, McGraw-Hill

ROSASCO, L.; DE VITO, E.; CAPONNETTO, A.; PIANA, M.; VERRI, A. (2004), *Are loss functions all the same?*, *Neural Computation* 16, pp.1063–1076

SAPRA, H.; GODJEVAC, M.; DE VOS, P.; VAN SLUIJS, W.; LINDEN, Y.; VISSER, K. (2020), *Hydrogen-natural gas combustion in a marine lean-burn SI engine: A comparative analysis of Seiliger and double Wiebe function-based zero-dimensional modelling*, *Energy Conversion and Management* 207, 112494

SCHÖLKOPF, B. (2001), *The kernel trick for distances*, *Advances in Neural Information Processing Systems*, pp.301–307

SCHÖLKOPF, B.; HERBRICH, R.; SMOLA, A.J. (2001), *A generalized representer theorem*, *Computational Learning Theory*

SHALEV-SHWARTZ, S.; BEN-DAVID, S. (2014), *Understanding machine learning: From theory to algorithms*, Cambridge University Press

SHAO, L.; MAHAJAN, A.; SCHRECK, T.; LEHMANN, D.J. (2017), *Interactive regression lens for exploring scatter plots*, *Computer Graphics Forum*

SHAWE-TAYLOR, J.; CRISTIANINI, N. (2004), *Kernel methods for pattern analysis*, Cambridge University Press

SYED, J.; BAIG, R. U.; ALGARNI, S.; MURTHY, S.; MASOOD, M.; INAMURRAHMAN, M. (2017), *Artificial Neural Network modeling of a hydrogen dual fueled diesel engine characteristics: An experiment approach*, *Int. J. Hydrogen Energy* 42(21), pp.14750-14774

TIKHONOV, A.N.; ARSENIN, V.Y. (1979), *Methods for the Solution of Ill-Posed Problems*, Nauka

VAPNIK, V.N. (1998), *Statistical learning theory*, Wiley

VOVK, V. (2013), *Kernel ridge regression*, *Empirical Inference*

WAINBERG, M.; ALIPANAHI, B.; FREY, B.J. (2016), *Are random forests truly the best classifiers?*, *J. Machine Learning Research* 17, pp.3837–3841

WATSON, N.; JANOTA, M. (1982), *Turbocharging the internal combustion engine*, Macmillan Int. Higher Education

WILLMOTT, C.J.; MATSUURA, K. (2005), *Advantages of the mean absolute error (MAE) over the root mean square error (RMSE) in assessing average model performance*, *Climate Research* 30, pp.79-82

WOSCHNI, G. (1967), *A universally applicable equation for the instantaneous heat transfer coefficient in the internal combustion engine*, Technical Report SAE Technical paper

YOUNG, D.M. (2003), *Iterative solution of large linear systems*, Dover Publications

Hydrodynamic Optimization of a Small Electric Catamaran Ferry

Sven Albert, NUMECA Ingenieurbüro, Altdorf/Germany, sven.albert@numeca.de

Thomas Hildebrandt, NUMECA Ingenieurbüro, Altdorf/Germany, thomas.hildebrandt@numeca.de

Stefan Harries, FRIENDSHIP SYSTEMS, Potsdam/Germany, harries@friendship-systems.com

Erik Bergmann, FRIENDSHIP SYSTEMS, Potsdam/Germany, bergmann@friendship-systems.com

Massimo Kovacic, Yachtwerft Meyer, Bremen/Germany, massimo.kovacic@yachtwerft-meyer.de

Abstract

The paper presents a design study for an electric catamaran ferry undertaken at the tender stage. Starting from a baseline created to comply with the operational requirements of the future owner, a parametric modeling and hydrodynamic optimization campaign was conducted with the aim of further reducing energy consumption as much as possible, the weight of batteries and the range of a purely electric ferry being of key importance. The ferry being relatively short despite considerable displacement when fully loaded and the clearance of the demi-hulls being small, a free-surface RANS code with free trim and sinkage was employed for the hydrodynamic optimizations. The practical approach of modeling and optimization will be explained and illustrated. The optimization achieved a 40-50% improvement in power requirements.

1. Introduction

The maritime industry steadily gains momentum in introducing new ways of providing boats and ships with clean(er) energy. For more than a century the main source of energy for shipping came first in form of coal and then in form of fuel oils. While this will likely continue for quite some time, with steady improvements in engine efficiency and (transition) technologies such as gas engines made available, more and more projects are worked on that are built on purely electric propulsion. Electric ferries for relatively short distances have turned out to be good candidates for early adaptation. They allow full charging of batteries during the nights when in port and intermediate recharging of batteries when (un)loading, see *Jokinen et al. (2021)*.

The project presented in this paper focuses on the hydrodynamics of a small passenger ferry for transfer between two ports, covering a short distance of a little less than one sea mile. Typically, a ferry of only about 12 m in length-over-all and 21 t of maximum displacement would not necessarily undergo a thorough hydrodynamic optimization campaign, in particular if intended to be run on standard fuel. However, batteries still being expensive and pretty heavy due to lower energy density in comparison to, say, diesel, the effort could be justified. As will be seen the improvements are considerable which may serve to encourage similar studies in the future, see also *Albert et al. (2016)* and *Albert et al. (2020)* for applications of simulation-driven design (SDD) to small craft.

2. Design task

Yachtwerft Meyer, Germany, a specialist for tenders of yachts and cruise ships as well as for special crafts (police and coast guard vessels, rigid inflatable boats etc.) and with strong expertise in composite materials, assumed the leading role as designers while FRIENDSHIP SYSTEMS and NUMECA Ingenieurbüro contributed their expertise of geometric modeling and numerical flow simulation, respectively.

Fig.1 shows the hull of the catamaran ferry, featuring a skeg for a classical propulsion system with shaft, propellers and spade rudders (not shown). The specifications of the ferry as relevant for the hydrodynamic optimizations were taken from the owner's requirements and are summarized in Table I. Various criteria such as stability were not explicitly monitored during the optimizations as they were sufficiently fulfilled for the baseline and not too strongly affected by the form variations considered.

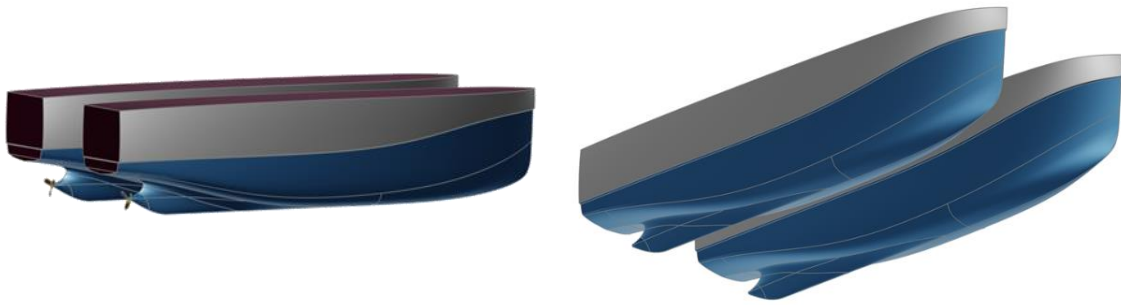


Fig.1: Hull form of electric catamaran ferry (baseline)

Table I: Specification of hydrodynamic design task

Passenger ferry	Catamaran with classical propulsion system
Maximum capacity	60 passengers with luggage
Displacement at max. capacity	21 t
Displacement at min. capacity	14 t
Length	~ 11.5 m
Max. beam over all	4.7 m
Draft	~ 1 m
Design speed	7.0 kn for major leg
Representative lower speed	3.5 kn in port
Distance to cover	~1 nm between ports
Additional criteria	Spray rails should not submerge at max. draft
Battery size	6 × 40 kWh @ 360 V
Battery capacity	Sufficient for 20 runs when fully charged

The aim of the optimization campaign was to reduce energy consumption as much as possible while maintaining maximum passenger capacity. A preliminary study for the two speeds of interest, namely design speed of 7 kn and a representative speed in port of 3.5 kn, showed that more than 80% of battery power would be consumed at the higher of the two speeds when covering the major leg between ports (see also resistance at different speeds given in the result section). Since the operational profile suggested frequent transfers at (close to) maximum and (close to) minimum capacity the resistance at both displacements was taken into account and a multi-objective design task was formulated.

The focus was set on minimizing resistance. This is because the optimization campaign was undertaken during the rather short tender stage as an investment of the bidding party and, furthermore, could be technically justified on the grounds that the skeg geometry was not varied but only adjusted to attach nicely to the bare hull. An unaltering skeg would result in similar wake patterns for all variants investigated. Hence, the propulsive efficiency was assumed to be practically constant. This, naturally, is a simplification. However, if the building order was won further optimizations could be initiated very quickly with additional free variables for both the bare hull and the skeg and for energy consumption as the ultimate objective, using propulsive power instead of resistance.

3. Parametric modeling

Optimizations are typically run to increase the energy efficiency of fluid-dynamically relevant shapes. The process is called simulation-driven design and requires a considerable number of variants to be investigated by means of simulations, notably by Computational Fluid Dynamics codes (CFD). Parametric modeling for the design and optimization of ship hulls, propellers, appendages etc. is now widely accepted and applied in both academia and industry. To balance intelligently a meaningful range of shape variations and a small enough set of free variables to control them, different approaches of parametric modeling have been developed; see *Harries (2020)* for an overview.

In SDD these Computer Aided Design approaches (CAD) are typically subdivided into fully parametric and partially parametric modeling. While fully parametric modeling (FPM) is more powerful with regard to the scope and the precision of achievable modifications, partially parametric modeling (PPM) is easier and faster to set up and handle. The range of available partially parametric modeling approaches is considerable, and they all have advantages and drawbacks, see, for instance, *Harries et al. (2015)*, *Harries and Abt (2019)*. FPM and PPM can be flexibly combined in CAD systems like CAESES.

3.1. Partially parametric modeling

Free-form deformation, cartesian shifts, Lackenby transformation etc. are used when changing a given baseline via parameters. These techniques have one common denominator: Based on an existing baseline, typically modeled interactively and then interpreted as a “dead” geometry, the way of modifying the shape (and not the shape itself) is defined parametrically. The actual modifications are then computed from imposing the modifying entities onto the baseline. While this is very flexible the actual variations are not predefined but rather “just” anticipated.

There are two partially-parametric modeling approaches that follow a slightly different idea: morphing and radial basis functions (RBFs). Here the new shapes are defined upfront by the design team and the partially-parametric modeling approach subsequently brings about a smooth transition between the baseline as a “source” and one or several of the predetermined shape features as “targets.”

Standard morphing builds on a set of topologically identical but geometrically different instances. With just two instances a one-dimensional design space is created, allowing the transition (interpolation) from one instance to the other and even beyond (extrapolation). Using three instances gives a two-dimensional design space and so on. See *Harries et al. (2015)* for details.

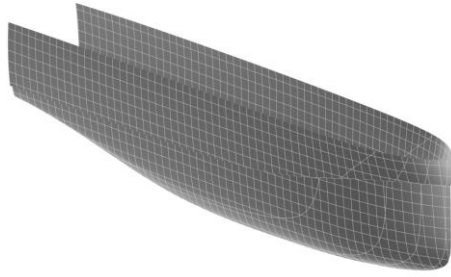
Radial basis functions offer a very intuitive set-up of defining modifications and can be considered a morphing approach in its broader sense. (Note that quite frequently the term morphing is used for most partially parametric modeling approaches.) In CAESES two RBF techniques are available: A discrete approach for interactively changing point data (trimeshes) and a continuous approach for changing mathematically closed geometries represented by B-splines (BReps), *Harries and Abt (2021)*. For the catamaran optimization presented here the continuous approach was chosen since it allows the design team a fine-tuned modification of various regions that are likely to influence the hydrodynamic performance positively. For details of the RBF approach in CAESES, see *Albert et al. (2021)*.

3.2. Application to the catamaran

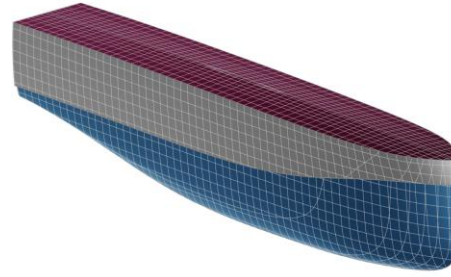
For the catamaran ferry, variation via parametrically changing the targets and using a constant transition factor was employed, using points and curves that were parametrically defined as targets, giving rise to eight free variables from RBFs and two additional free variables from standard transformations, namely a scaling of the catamaran’s demi-hull in transverse direction and a change of the clearance between the two demi-hulls. Based on the bare demi-hull designed by the yard, the optimization campaign comprised setting up sources and targets for variation, preparing the geometry for hydrodynamic analysis and undertaking the actual optimization runs. The workflow is summarized in Table II. Fig.2 illustrates some of the steps.

As can be seen from Fig.2 (E) and (F), here only points and curves were used for defining the sources and targets. The entities are chosen according to their expected impact on calm-water hydrodynamics, namely changing the design waterline, the stem contour, including the introduction of an asymmetry in the forebody, the center plane curve and the characteristic of the transom. In this sense the resulting scope of shape variations is rather intuitive and easy to set up.

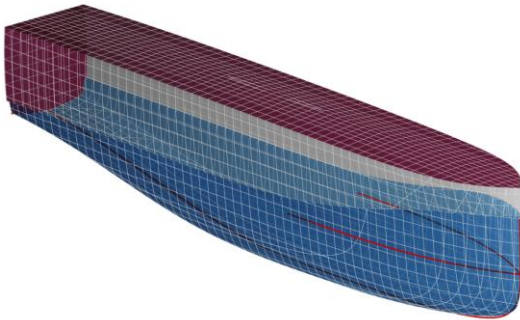
A partially parametric model with a total of 10 free variables was defined as illustrated in Fig.3 and summarized in Table III.



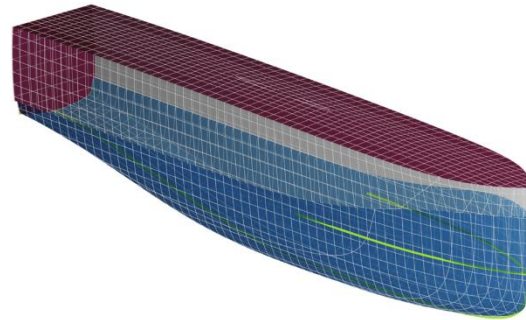
(A) Bare symmetric demi-hull as provided by yard (see Table II step 1)



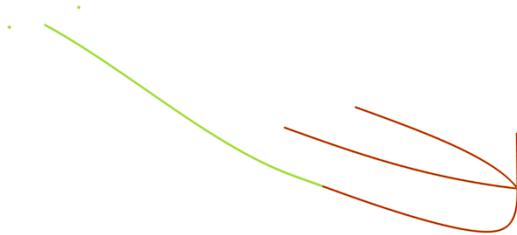
(B) Additions of deck and transom for closing geometry (preparation stage, see Table II step 2)



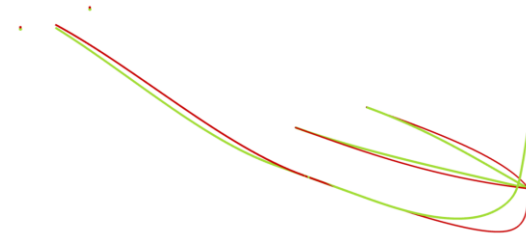
(C) Define source(s), here shown in red, for the design waterline of the baseline (see Table II step 3)



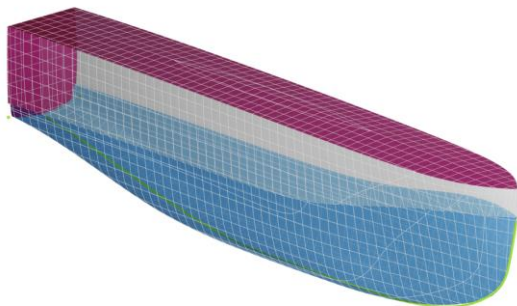
(D) Define target(s), here shown in green, for the modification as anticipated to be beneficial (see Table II step 3)



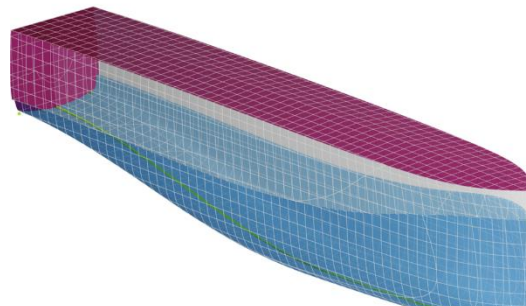
(E) Sources and targets match (causing no changes to the geometry)



(F) Sources and targets differ (giving rise to variation of geometry, see Table II step 4)



(G) Resulting variant for all free variables set to their minimum values (see Table II step 4)



(H) Resulting variant for all free variables set to their maximum values (note the asymmetry of the demi-hull)

Fig.2: Stages of preparing and setting up partially parametric modeling with RBF

Table II: Workflow

Step	Description
1	Import baseline into CAESES® (e.g. STEP, iges)
2	Prepare baseline for variation (e.g. add transom and deck)
3	Define sources and targets to compute corresponding RBFs, introducing free variables
4	Apply changes according to free variables and generate variant of demi-hull without skeg
5	Attach (fully-parametric) skeg to bare demi-hull
6	Merge new variant with flow domain
7	Export flow domain with new variant for FINE™/Marine (here as multi-body stl-file)
8	Set up FINE™/Marine for investigation
9	Run design-of-experiment with FINE™/Design3D
10	Build surrogate model for further optimizations
11	Run optimizations with FINE™/Design3D, adding CFD simulations for better predictions
12	Discuss results with all parties involved and repeat parts of the process

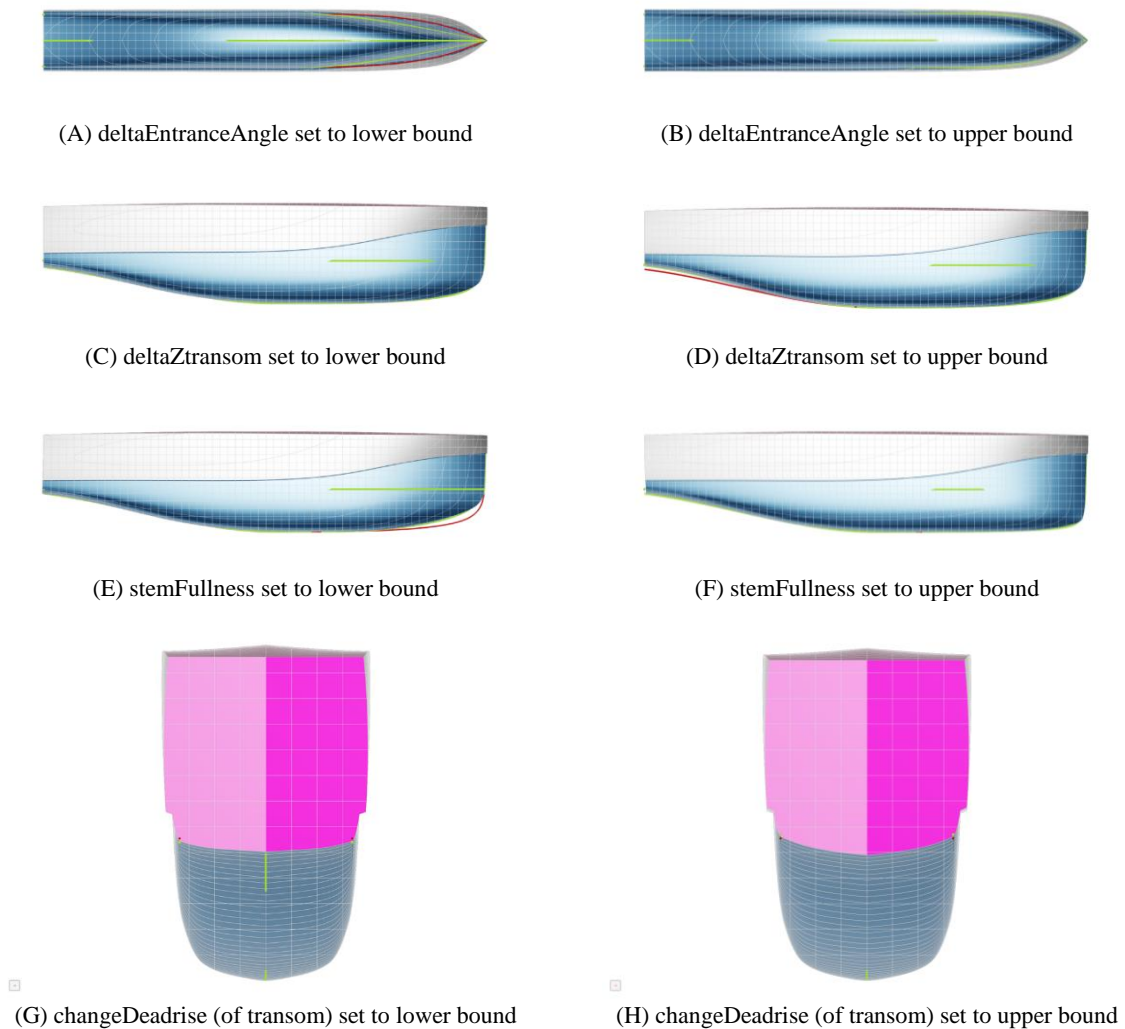
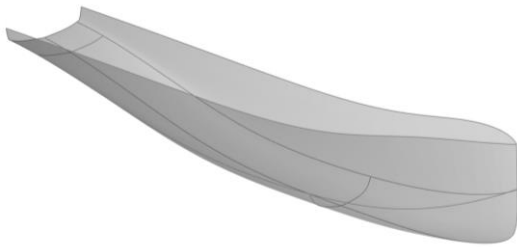


Fig.3: Selected variants by changing one free variable at a time

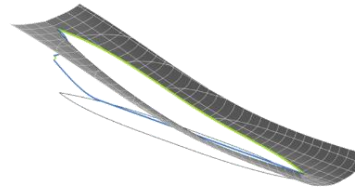
Table III: Parameters used as free variables

Step	Primary region of influence	Name	Description	See also
1	CPC	deltaAngleCPCtransom	Modify the angle of the center plane curve at the transom (aft perpendicular)	Figure 5 (F)
2		deltaParallelMid	Increase or decrease the length of the parallel mid-body	Figure 5 (F)
3		deltaZtransom	Control the submergence of the transom	Figure 6 (C) and (D)
4		stemAngle	Change from a vertical to a tilted stem	Figure 5 (F)
5		stemFullness	Increase or decrease fullness of stem	Figure 6 (E) and (F)
6	DWL	asymmetricBow	Introduce asymmetry to the forebody	Figure 5 (H)
7		deltaEntranceAngle	Increase or decrease the entrance angle of the DWL at the forward perpendicular	Figure 6 (A) and (B)
8	General	changeClearance	Widen or narrow the clearance between the demi-hulls	
9		scaleY	Scale demi-hull in transverse direction	Figure 8 (A) and (B)
10	Transom	changeDeadrise	Push up or pull down transom close to sharpest rounding	Figure 6 (G) and (H)

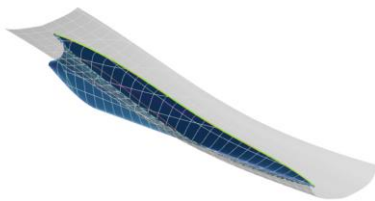
Once a new variant of the bare hull is available it is brought together with a skeg as shown in Fig.4. Since during the optimization campaign the bare hull also varies in beam, center plane curve and transom, it does not suffice to simply attach one given skeg. Instead, a number of defining curves are modeled from which to derive the skeg, see Fig.4 (B), giving rise to a smooth transition between the bare hull and the skeg itself.



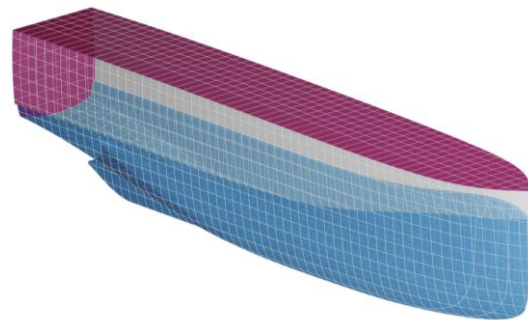
(A) Parts of the bare hull after transformation via RBF



(B) Definition of the skeg via boundary curves



(C) Skeg defined as a Gordon surface



(D) BRep model of entire demi-hull (see Table II step 5)

Fig.4: Stages of adding a skeg to the bare hull

4. RANS simulations on the base design

NUMECA's FINETM/Marine package was used for the viscous CFD calculations, utilizing a volume-of-fluid (VOF) method for free surface capturing, see *Queutey and Visonneau (2007)*. The numerical representation and accuracy of the time-dependent free surface is strongly affected by the spatial discretization in the grid, especially perpendicular to the air-water-interface. FINETM/Marine features an adaptive grid refinement (AGR) technique which can create or remove mesh cells during solver runtime, triggered by various physical phenomena. Here the current location of the free surface acts as the sensor and the mesh is refined until a user-specified threshold in terms of the cell size is achieved.

This procedure is called in certain intervals and ensures an ideal grid at all locations and at all time steps. Such an approach does not require any pre-refined mesh zones where the user would need to anticipate important phenomena in the flow field beforehand, e.g. wave patterns and regions of breaking waves. During an optimization with variable geometry and for two different displacements, which on their own strongly affect the location of the free surface, an AGR thus reduces the necessary CPU time for each variant investigated. Furthermore, an integrated body motion solver couples the hydrodynamic loads on the structures of interest with their inertia, see *Leroyer and Visonneau (2005)*, which is an important factor especially for smaller craft like the catamaran ferry.

The typical starting point for any optimization campaign is a detailed analysis of the baseline, the set-up of a smooth workflow and the investigation of possible numerical sensitivities like boundary conditions and grid resolution. The aim of the project was a reduction of total resistance for the wetted hull, including the lower parts of the freeboard. The superstructure was not taken into account. This is a valid approach since especially for low operating speeds air drag is rather small and even in rough weather the variation of the hull should have only negligible effect on the flow about the superstructure. The cat was supposed to run straight ahead in calm seas, solving for sinkage and trim for the two displacement conditions.

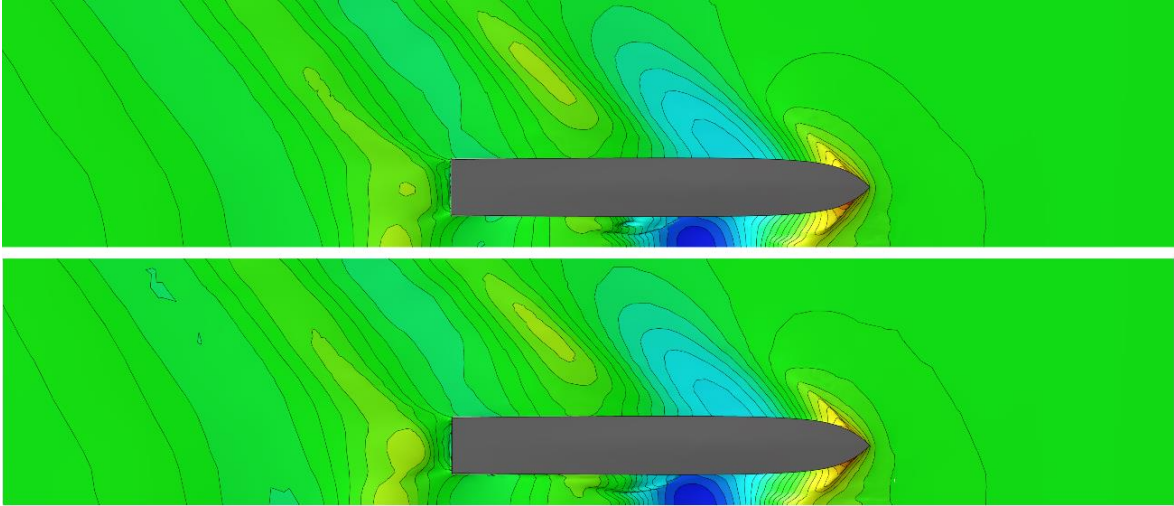
The flow was readily simulated at full-scale, taking advantage of running at both the correct Froude and Reynolds numbers without any need for model-ship extrapolations. Such a resistance simulation can be handled fully automatically using the C-Wizard in FINE™/Marine, which provides meshing templates for various densities as well as the full solver set-up. In conjunction with the stable yet flexible STL file export from CAESES® this ensures a smooth workflow, yielding preliminary results after just two hours of exchanging the baseline geometry. For the set-up of a suitable flow domain and the exchange of data between CAESES® and FINE™/Marine via STL files see *Albert et al. (2016)* for details. Importantly, within CAESES the topology of the flow domain along with the colors and name tags assigned to various parts of the domain (e.g. inner hull, outer hull, spray rail, deck, transom etc.) stay unaltered during any variation. Hence, when exporting them in a multi-body STL file FINE/Marine can readily handle any new variant without manual interaction.

As a next step a grid resolution study and further sensitivity tests were undertaken. The results for the free surface elevation at 7 kn and 21 t are given in Fig.5 (A) for both a rather fine and a coarser mesh. The wave patterns are very similar, especially for the extrema at the bow and in the tunnel between the demi-hulls which have a major impact on the overall resistance. The total resistance computed with the two meshes differ only by about 10 N. This is insignificant for a total resistance of 4372 N that the baseline displayed, see also Fig.6. Apart from being much smaller than the anticipated improvements, see also Fig.11, it can also be assumed that similar deviations would occur for all variants. Naturally, no changes of the set-up take place during an individual optimization run. As a sidenote, all resistance values given in this work were averaged over the last 30% of simulation time to smoothen out possible local flow unsteadiness.

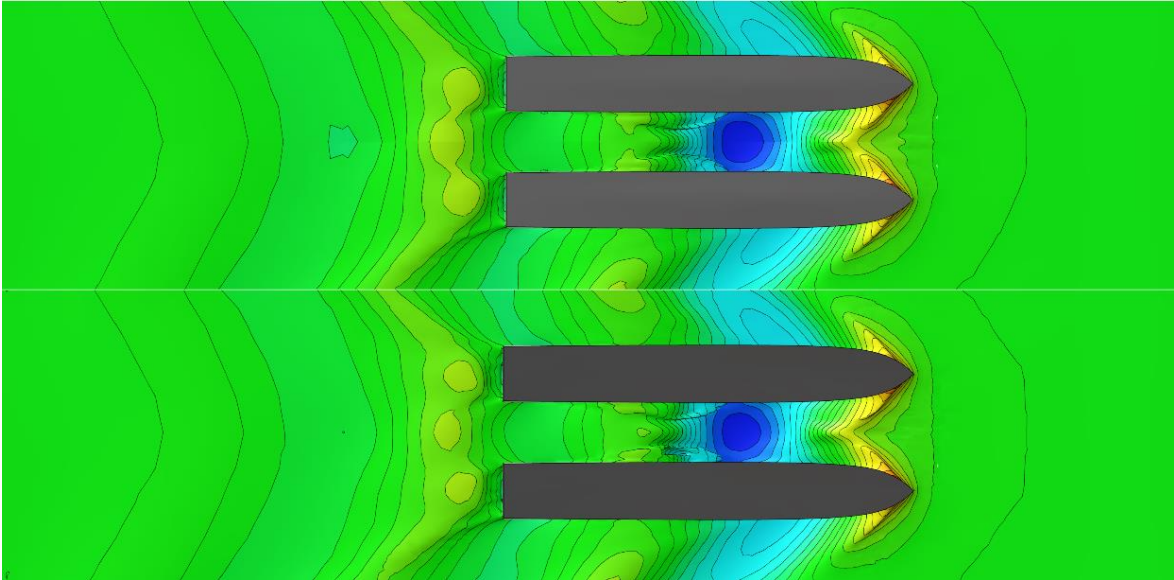
Furthermore, for a catamaran the flow between the demi-hulls can be of high importance due to the interactions of the waves and the stability and steadiness of the flow, particularly for closely positioned demi-hulls at higher Froude numbers. Hence, the baseline was analyzed both with a mirror plane boundary condition and as a full model with the two demi-hulls in place. This was done to evaluate the validity of utilizing mid-ship symmetry – which of course is favored due to being twice as fast. Fig.5 (B) depicts the free surface for both set-ups, using the coarse mesh: The mirror plane is nicely visible since the flow is not perfectly continuous while the full model features a minor asymmetry. Nevertheless, the two wave patterns match very well, the difference in total resistance being 2 N and, hence, negligible.

Consequently, it was decided that a mirror plane simulation on the coarser mesh with 500 000 cells would be sufficient to capture all of the important flow patterns and to get reliable resistance values. This can be considered a “competitive” numerical set-up that should allow for many design variations in a short timeframe, even on local workstations, fairly balancing speed and accuracy.

The total resistance values computed for the baseline are shown in Fig.6. At 7 kn the resistance is more than ten times the one at 3.5 kn, for both loading conditions. And there is an almost 50% resistance increase from the empty ferry with just the crew on board to the ferry fully-loaded with passengers. From the operating profile it is estimated that for around 50% of the time the cat would sail at maximum speed of 7 kn, independent of the loading condition. Hence, higher speed at both drafts clearly dominate the overall power consumption so that they were selected as the relevant operating points for which to optimize. It should be kept in mind that no information at 3.5 kn would be known to the optimizer and that the energy consumption when maneuvering in port or when accelerating to top speed are also left out of the investigation. However, when looking at the prominent resistance values at design speed these simplifications should still yield reasonable results, providing designs with decreased battery consumption, in particular when recalling that the campaign is run at the tender stage.



(A) Influence of mesh density on free surface elevation
 (top: fine mesh with 1.1 million cells, bottom: coarse mesh, 500 000 cells)



(B) Effect of utilizing a symmetry plane
 (top: half model simulation, using a mirror plane, bottom: full model with both demi-hulls)

Fig.5: Initial investigation of mesh density and symmetry plane

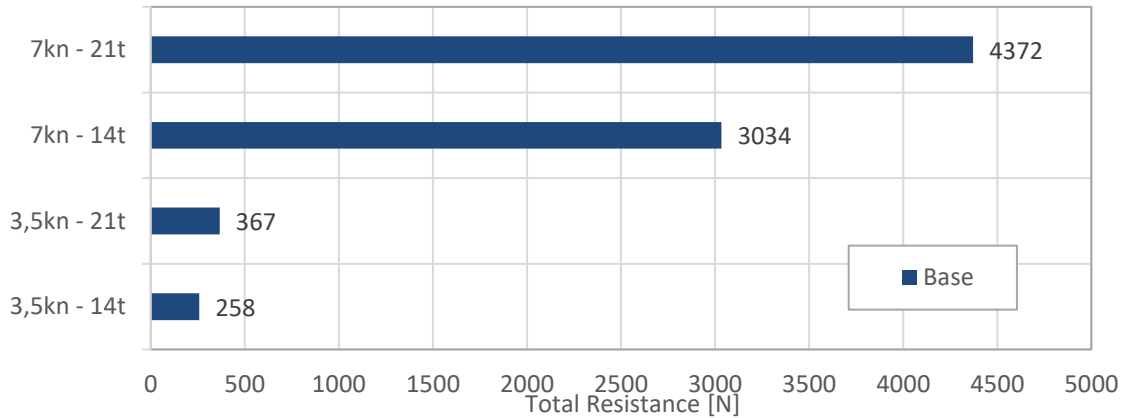


Fig.6: Total resistance for the baseline (Base), using the CFD set-up for the optimization

5. Optimization campaign

5.1. Overview

Next step was the assembly of the optimization chain as illustrated in Fig.7 (A). The optimization tool employed was NUMECA FINE™/Design3D, which controls all the sub-processes like geometry variation and export, meshing, solver runs and data collection in the post-processor. A Python API ensures a flexible and easy to use access to the various tools and exchange of data.

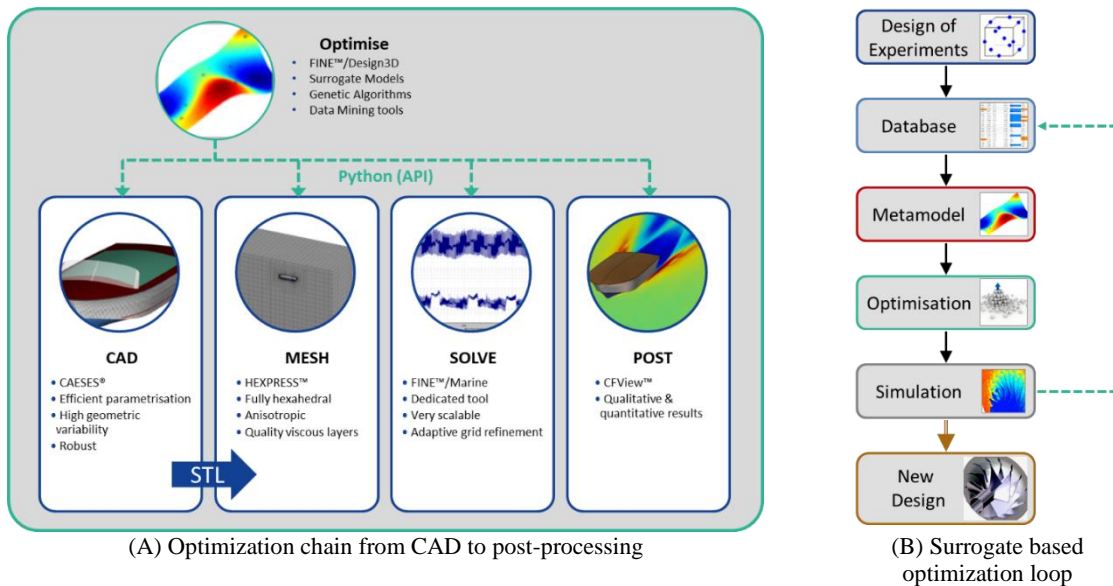


Fig.7: Optimization chain and loop

The optimization loop itself is based on a surrogate model. The approach is shown in Fig.7 (B). It starts with the generation of a database which stems from a sampling of the design space via a Design-of-Experiment (DoE). It aims at a maximum scattering of the samples within the bounds of the free variables with as few designs as possible. Here, 10 free variables were used which span a 10-dimensional design space, Table III.

From this discrete set of data points, bringing together geometry and performance, a surrogate model is built which offers a continuous description that is cheap and fast to evaluate. An evolutionary algorithm then calls this surrogate model thousands of times to generate new candidates in the design loop. The algorithm mimics evolutionary processes with selection of strong traits in a design with respect to the performance and to the constraints over several generations. Weak samples tend to become extinguished while methods like mutation help to keep a large diversity from one population to the next. In the end

such an optimizer yields a high probability of finding optimum solutions, even globally, especially in comparison to local strategies such as a gradient method. Since the actual search is performed on the surrogate model the number of variants can be very high without using any tangible computer resources. When a new and promising candidate is identified it is evaluated by means of (substantially more expensive) CFD simulations, using the optimization chain. The results are subsequently appended to enrich the database and to provide an even better surrogate model. The process is then re-started until convergence.

5.2. Design-of-Experiment

Prior to starting the DoE to create the actual database a few checks for plausibility of parameter ranges and stability of the meshing and workflow templates were made. Naturally, the bounds of the free variables constitute a crucial input to any optimization: It is desirable to have sufficient geometric variability while as few variants as possible should be unusable. The latter can appear quite easily if the chosen parametrization is not well-suited for the design task or if extreme parameter combinations lead to designs that any engineer would readily reject. Moreover, any failure in the optimization chain should be handled correctly by the optimizer. Machine issues or plain technical issues like licensing must be identified so that the optimizer does not neglect any region in the design space which could be of interest. In addition, physical phenomena like excessive drag or strong unsteadiness in resistance values should also be monitored. As mentioned above the time series for total resistance for each variant was evaluated for the last 30% of simulation time, delivering both a mean value as objective and a standard deviation for quality checks.

Results of the DoE, i.e., the database run, are displayed in Fig.8, giving the mean total resistance values for both operating points. The baseline is shown in the center, indicated via a large blue cross, while the points give the performance of the 20 DoE-samples. There is a strong correlation between the two different drafts, although outliers do exist. The overall scattering of the resistance is quite large, and there is only little clustering of the designs, which indicate a nice sampling even with as low as 21 variants in total. As can be seen there are variants that perform far worse but also quite a bit better. An impressive resistance reduction by 25% and 39%, respectively, is (happily) found for the best sample.

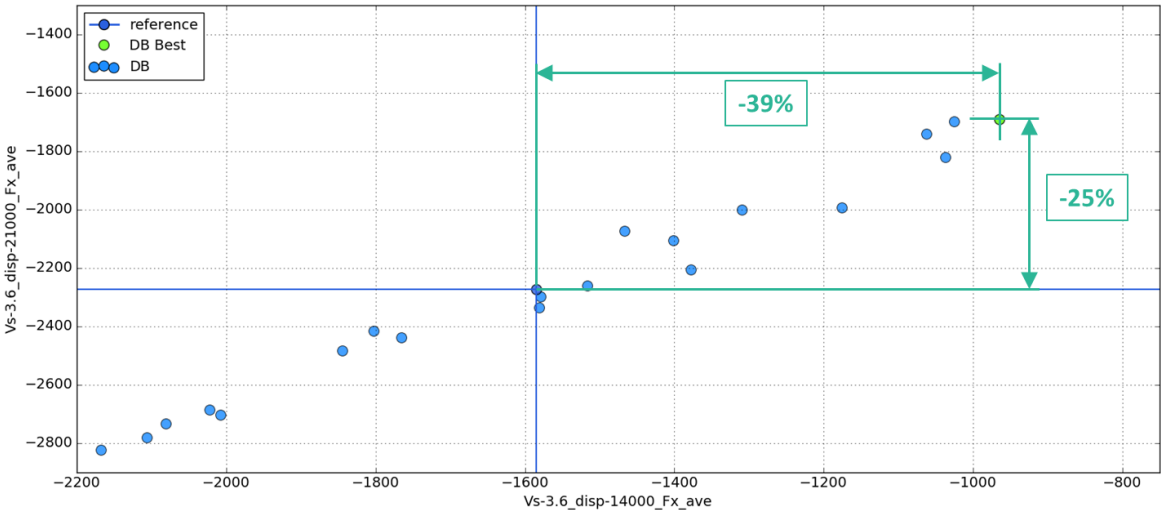


Fig.8: Total resistance values for the database samples for 7 kn at 14 t and 21 t

A surrogate-based optimization relies heavily on the quality of the prediction. If a surrogate model does not predict new and unknown variants with a certain accuracy or even fails to capture trends correctly there is no chance for any optimizer to find good solutions, at least within a reasonable timeframe. One way to quantify the accuracy is the so-called leave-one-out analysis, which calculates the correlation and, hence, the surrogate quality of a given set of data without the need for an additional set of evaluation samples. Such an analysis is depicted in Fig.9. It gives the total resistance values for 7 kn at

14 t from both the flow solver (accurate) and the surrogate (prediction). The samples line up quite nicely, i.e., they are near to the ideal linear correlation, and the R value 0.982 is close to one.

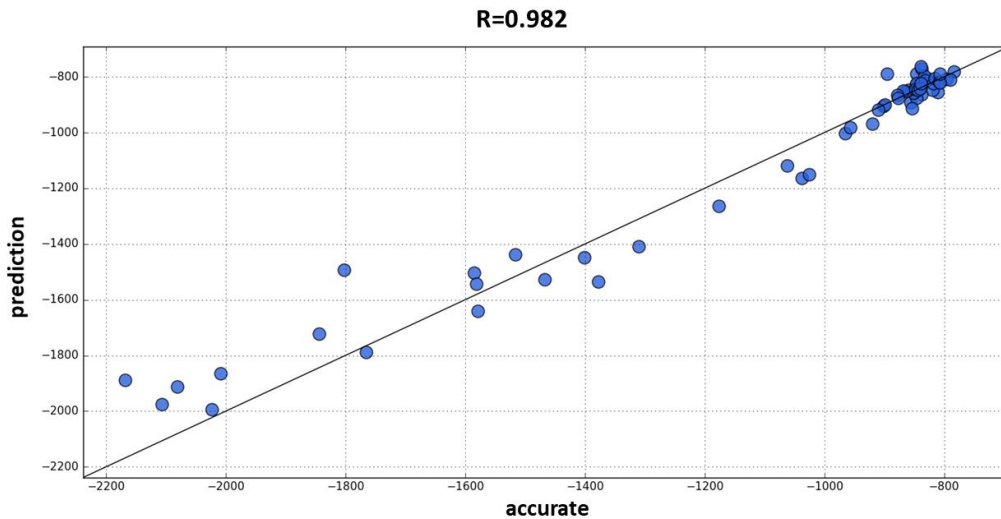


Fig.9: Correlation between surrogate model prediction and CFD values for 7 kn at 14 t

5.3. Multi-objective optimization

As said the resistance values for design speed at both drafts were chosen as the optimization objectives. After a more detailed check of the database it was not deemed necessary to use any constraints or further objectives here. A possible candidate for an inequality constraint could have been the trim angle which should not reach excessive values in order to maintain passenger comfort. But all variants in the DoE were well-behaved and the focus could be put on resistance. Thus, the final optimization turned out to be unconstrained and multi-objective. A strength-based Pareto formulation was employed, *Zitzler et al. (2001)*, which tends to deliver a selection of good designs which still show diversity, i.e., they do not cluster in one region of the design space. This is true especially for very complex problems with many parameters, constraints and objectives. Towards the end of such an optimization a clear Pareto frontier should form, which collects the variants that cannot be further improved in terms of one objective without impairing any other objective. It is then up to the design team to select the best solution from these non-dominated variants by identifying the best trade-off between competing objectives.

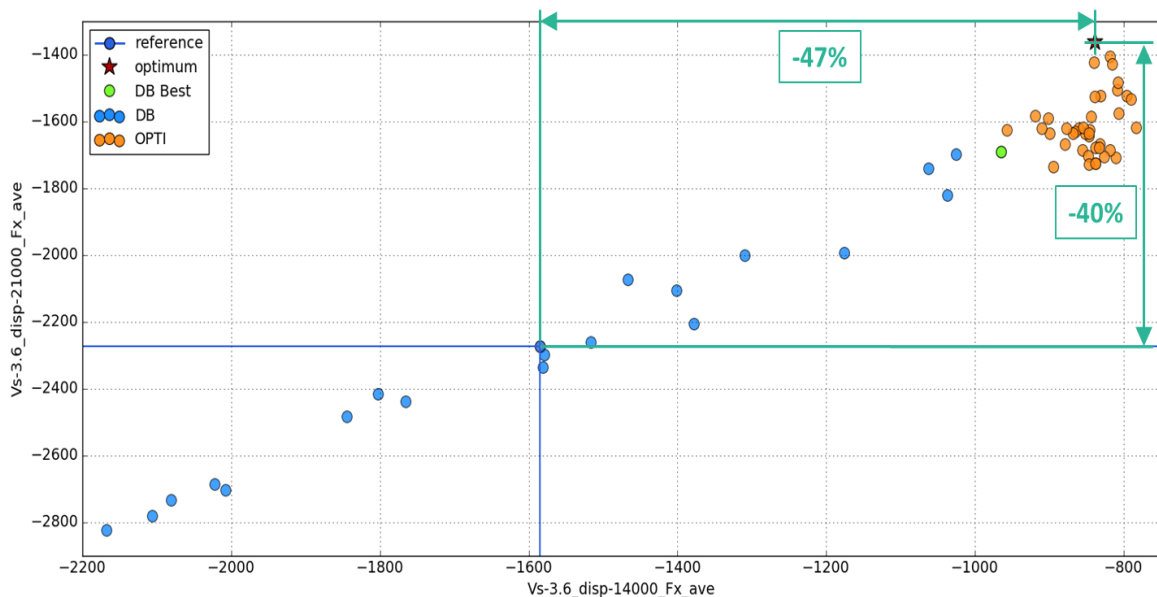


Fig.10: Total resistance values for the optimizer samples for 7 kn at 14 t and 21 t

Results from the optimizer run are given in Fig.10. The best variant from the DoE is given in green. It can be regarded as the new reference point to beat. All promising optimizer variants – double-checked with CFD – are given as orange dots. Interestingly, none of these new designs performs worse than the reference point with regard to resistance at 14 t. This indicates again the validity of the surrogate model which was utilized to produce the improved variants. Due to the short timeframe of the project – and the need to freeze the lines – it was decided to stop the process at this point. The Pareto set, here the designs in the upper right region of Fig.10, is made up of only a handful of variants which suggests that there might be even more room for improvement. Still, another large reduction in total resistance could be achieved. Altogether, the new design reduces power consumption by 40% at fully loaded conditions and by 47% at reduced draft when compared to the baseline.

5.4. Quality checks

To validate results and gains in the optimization, a final set of CFD runs was performed. Both hulls were used (no mirror plane), and the mesh density was increased to five million cells. The AGR thresholds were adjusted so that around 200 000 cells were created additionally just for accurate wave capturing. Furthermore, the mesh was refined to apply a low Reynolds wall model for turbulence. An additional displacement of 17.5 t was also studied to understand the influence on an intermediate draft.

Results for these simulations for both the baseline and the optimized hull are summarized in Fig.11. The trends are not only fully kept but the absolute gains are (by chance) even slightly higher on this refined CFD set-up. Also, at 17.5 t the performance is substantially improved, too, as was anticipated. At the low speeds no improvements are found and there is even a slight increase of total resistance at 21 t. It should be kept in mind that these operating points were deliberately left out of the optimization, primarily for reasons of speeding up the process, so that these results do not come as a surprise. As can be appreciated from the comparison between the baseline and the optimized hull the energy-efficiency of the cat has been improved considerably.

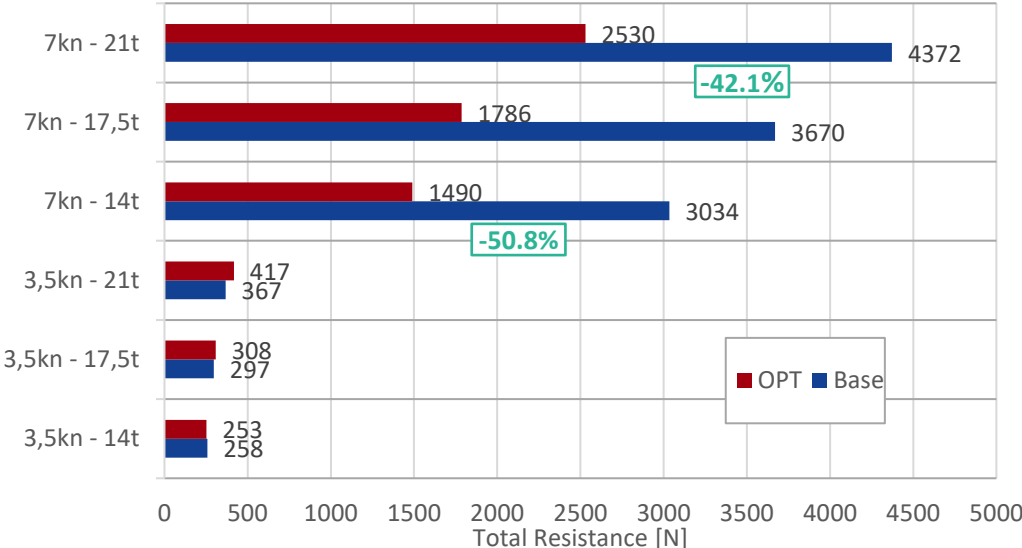


Fig.11: Comparison of design performance of the baseline (Base) and the optimized hull (OPT)

6. Selected results

6.1. Comparison of designs

Fig.12 shows the wave patterns for baseline design and optimized design. An important difference is the decrease in the bow wave system and a less pronounced trough in the tunnel. The stern wave system on the other hand seems quite a bit stronger for the optimized hull.

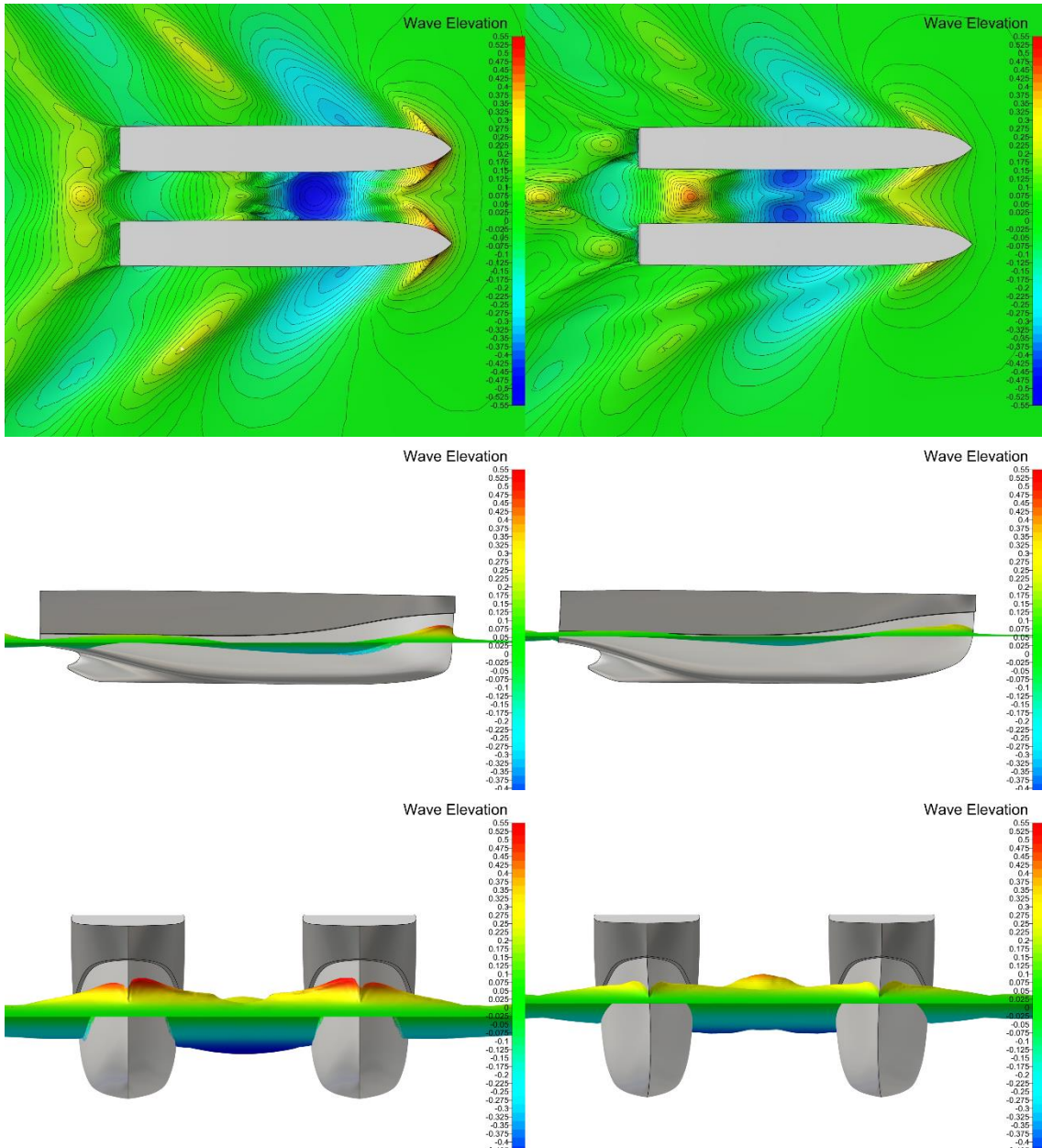


Fig.12: Comparison of wave patterns; baseline (left), optimized (right)

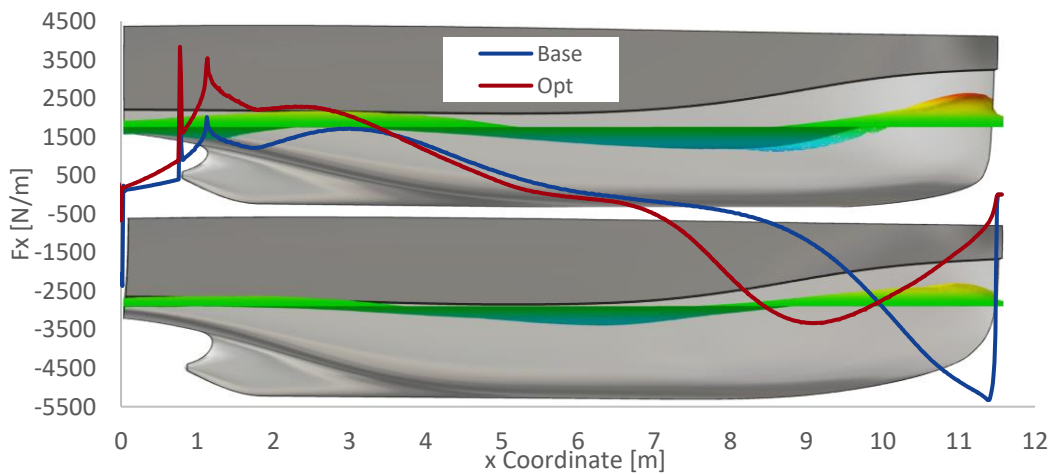


Fig.13: Wave profile and sectional forces along the hull: stern at 0, bow at 11.5 m (upper part: baseline (Base); lower part: optimized hull (Opt))

Nevertheless, the resulting waves far from the hull are reduced for the optimized hull, having a positive effect on total resistance. Moreover, the influence of the slight asymmetry of the bow on the flow can be seen, too. In an unsteady evaluation also an unstable flow pattern can be observed between the demi-hulls of the baseline. This is does not show at all for the optimized hull.

A more detailed insight into the force distributions along the hulls is depicted in Fig.13, giving sectional forces along with the wave profile. The stern is located at $x = 0$ m and the bow at 11.5 m. The smoother bow wave in the optimized hull can be seen clearly. The bow drag is shifted downstream and, in general, the sectional forces are lower for the forebody of the optimized hull. Major gains are observed in the aftbody, however, pushing the hull and thereby reducing the total resistance.

6.2. Resources spent

The total resources spent can be taken from Table IV. The entire project was carried out within a very tight timeframe. Besides showing tangible potential gains already at the tender stage, it also showcases what can be achieved when coupling expertise and modern engineering software.

Table IV: Resources spent

Partner	Description	Resources
Yachtwerft Meyer	Design of the baseline	2 to 3 days
FRIENDSHIP SYSTEMS	Set up and fine-tune RBF	1 day
FRIENDSHIP SYSTEMS	Develop parametric skeg model	1 day
NUMECA Ingenieurbüro	Check CFD and ensure quality	1 day
NUMECA Ingenieurbüro	Streamline process	1 day
NUMECA Ingenieurbüro	Number crunch CFD and run optimization	3 nights
All	Meet and discuss project and results	Several 1-h virtual meetings

7. Conclusions

The paper presented a project for the parametric modeling and hydrodynamic optimization of a small electric catamaran ferry at the tender stage. The parametric modeling was based on RBFs which enable a rather intuitive set-up for shape variations. The hydrodynamic optimization campaign was built on a high-fidelity free-surface RANS solver with free sinkage and trim. The project illustrates what can be achieved by suitably combining expert knowledge from different fields quickly and without any overhead, using the experience from a yard (here Yachtwerft Meyer), the know-how from a software developer with specialization in variable geometry (here FRIENDSHIP SYSTEMS) and the expertise from a software provider with focus on high-end simulations (here NUMECA Ingenieurbüro). Tangible improvements for the design could be found within just a few days of actual work, a few nights of number crunching and a handful of virtual meetings. It is hoped this serves to encourage to undertake simulation-driven design also for smaller craft at a wider scope.

References

- ALBERT, S.; HARRIES, S.; HILDEBRANDT, T.; REYER, M. (2016), *Hydrodynamic Optimization of a Power Boat in the Cloud*, HIPER Conf., Cortona
- ALBERT, S.; CORRÊA, RPATH.; HILDEBRANDT, T., HARRIES, S. (2020), *An Electrified RIVA Powerboat – Optimised*, 12th Symp. on High-Performance Marine Vehicles (HIPER 2020), Cortona
- ALBERT, S.; HILDEBRANDT, T.; HARRIES, S.; BERGMANN, E.; KOVACIC, M. (2021), *Parametric Modeling and Hydrodynamic Optimization of an Electric Catamaran Ferry based on*

Radial Basis Functions for an Intuitive Set-up, 20th COMPIT Conf., Mülheim, pp.58-78

HARRIES, S. (2020), *Practical Shape Optimization Using CFD: State-Of-The-Art in Industry and Selected Trends*, COMPIT Conf., Pontignano

HARRIES, S.; ABT, C. (2021), *Integration of Tools for Application Case Studies, A Holistic Approach to Ship Design – Vol. 2: Optimisation of Ship Design and Operation for Life Cycle*, Springer

HARRIES, S.; ABT, C. (2019), *CAESES – The HOLISHIP Platform for Process Integration and Design Optimization, A Holistic Approach to Ship Design – Vol. 1: Optimisation of Ship Design and Operation for Life Cycle*, Springer

HARRIES, S.; ABT, C.; BRENNER, M. (2015), *Upfront CAD – Parametric modelling techniques for shape optimization*, Int. Conf. Evolutionary and Deterministic Methods for Design, Optimization and Control with Applications to Industrial and Societal Problems (EUROGEN), Glasgow

JOKINEN, M.; BROGLIA, R.; GATCHELL, S.; AUBERT, A.; GUNAWAN, R.; SCHELLENBERGER, G.; HARRIES, S.; VON ZADOW, H. (2021), *Double ended Ferry, A Holistic Approach to Ship Design – Vol. 2: Optimisation of Ship Design and Operation for Life Cycle*, Springer

QUEUTEY, P.; VISONNEAU, M. (2007), *An interface capturing method for free-surface hydrodynamic flows*, Computers & Fluids, 36/9, pp.1481-1510

LEROYER, A.; VISONNEAU, M. (2005), *Numerical methods for RANSE simulations of a self-propelled fish-like body*, J. Fluid & Structures, 20/3, pp.975-991

ZITZLER E.; LAUMANN, M.; THIELE, L. (2001), *Spea2: Improving the Strength pareto Evolutionary Algorithm*, Int. Conf. Evolutionary and Deterministic Methods for Design, Optimization and Control with Applications to Industrial and Societal Problems (EUROGEN), Athens

Optimization of the Aerodynamic Design of a Solar Houseboat Catamaran

Jörg Albrecht, Solarship, Berlin/Germany, albrecht@solarship.de

Abstract

This paper presents an innovative solar-powered houseboat design and the CFD analyses made for the design. The investigation focused on the front and aft side profiles, designing form and arrangement for improved flow, mainly to benefit the maneuverability of the vessel.

1. Motivation

The boat design, Fig.1, together with statics, CFD (Computational Fluid Dynamics) analysis and CE certification were carried out by the designer Dipl.-Ing. Jörg Albrecht. The "optical columns" in the bow area of the houseboat were a particular challenge with regard to the field of vision, statics and aerodynamics.



Fig.1: Solar-powered houseboat design

In general, houseboats are often susceptible to wind and are therefore mostly used in inland waterways, where wind loads do not occur to the same extent as on open water areas at sea. In inland areas, the wind is often slowed by structures or vegetation or other obstacles, so that wind loads can be assumed to be moderate. However, since houseboats have a relatively large wind-attack surface area and are usually lightly built, gusts and sustained high winds may pose real problems for the skipper.

In particular, most houseboats feature very "angular" designs, where the superstructure offers flow separation edges which generate strong, uncontrolled vortices and turbulence. These may induce strong oscillatory motions forcing the skipper to make continuously corrective maneuvers.

2. Considerations for the behavior of houseboats in cross winds

Flow separation problems as addressed here for aerodynamics occur often for underwater hull area in ship hydrodynamics. Although such flow separation problems are well known and widespread, there is hardly any research regarding the wind behavior of houseboats. Our client "Hausbootgeist",

<https://www.hausbootgeist.de/en/>, therefore agreed to have a CFD investigation performed. The CFD model was to be based on our design and intended to investigate the required practical suitability.

Experience (e.g. catamaran builder Burkhard Bader, <http://www.burkhard-bader.de/>, in personal communication) shows that rounded leading edges on the superstructure improve the aerodynamics, since the rounding shifts the center of attack of the wind forces to the rear and the boat can thus turn better into the wind, Fig.2.

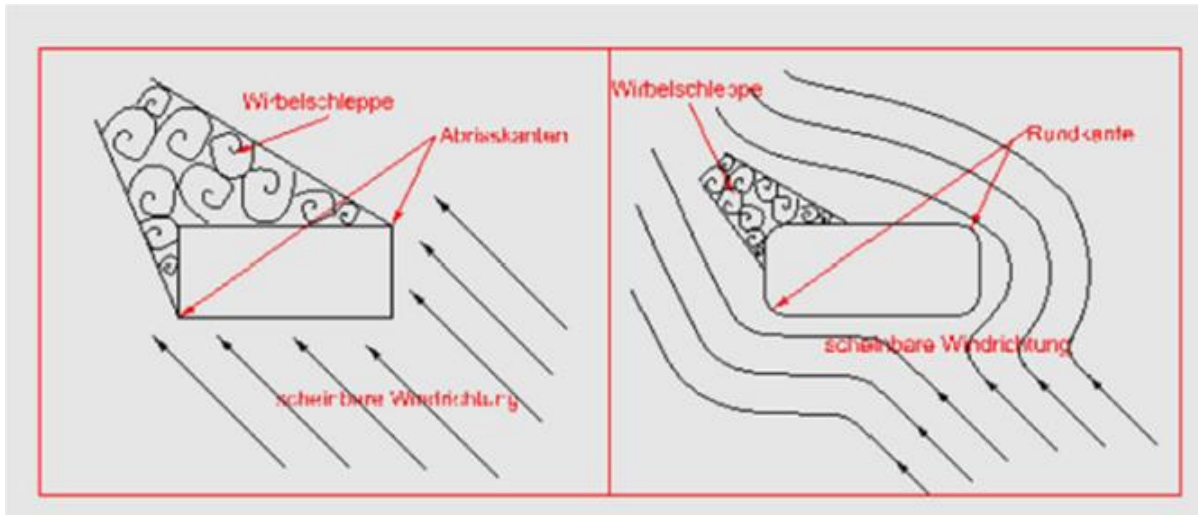


Fig.2: Vortex formation (qualitatively) for superstructure with sharp corners (left) and rounded corners (right). Wirbelschleife = vortex wake; Abrisskanten = flow separation edges; scheinbare Windrichtung = apparent wind direction

The houseboat should "turn into the wind" in cross winds. This is achieved when the lateral center of gravity of the superstructure lies behind the lateral center of gravity of the underwater hull (principle of the wind vane).

Since in most houseboat constructions, as in the current case, the forward deck in the bow area is designed as an open "veranda" and the house superstructure is in the aft area, the lateral center of aerodynamics is already shifted aft. However, for aesthetic design reasons, two optically "wide" supports were planned for the optical design layout of the side, Fig.1. It made sense to use these as aerodynamic "optimization tools" at the same time. These optical features were also part of the stern area design; however, the aft deck is significantly smaller than the foredeck. Here, too, the supports were to serve as "optimization tools" for the aerodynamic flow.

The upstream guide surfaces in the bow area are primarily intended to guide the wind from the front around the structure such that the resistance of the superstructure is reduced and/or maneuverability is improved. The streamlines should also be smoothed in the aft deck area.

To test the effects of the support profiles, several CFD simulations with different profile arrangements were tested. For reasons of time, the first such virtual wind tunnel tests were carried out with the target speed of 13.5 km/h together with the hulls.

3. Implementation and consideration for numerical model

The streamlines are in general a product of the pressure fields with their differing pressure potentials. For example, if the flow is accelerated by profiles, the resulting low-pressure region will result in a pulling streamlines in. Contrarily, flow deceleration will result in high pressure pushing streamlines away.

In the present case, there are two possible arrangement options for the profiles, resulting in different locations of the low-pressure areas in the flow:

1. In the first case, the low-pressure field can be directed outwards, away from the central longitudinal line, i.e. in the lateral outer area of the boat.
2. In the second case, the low-pressure field can be oriented inwards towards the central longitudinal line, so that there the streamlines are "sucked in".

It turns out that the rounding of edges works according to the same principle. When an edge is rounded, it prevents the flow from separating enabling the flow around the edge itself. In addition, by flowing around a rounded edge, as with the convex side of a wing, a negative pressure is generated by the acceleration of the flow, which in turn "sucks in" further streamlines and thus guides the flow elegantly around the corner.

4. Flow simulations

In the reference simulations, the houseboat was analyzed without wind profiles as a reference. The CFD code was Simerics of the Orca3D Marine CFD package. A suggestion for improvement could already be made after this first analysis. The design was then successively modified and improved:

- Modification #1, Fig.3
In the first design, the front profiles were intended to suck in the streamlines and accelerate them out to the side between the profiles and the front wall. The resulting effects were not known until then. The rear profiles, on the other hand, with the negative pressure areas on the outside, were intended to prolong the flow on the side wall, quasi extending the superstructure aerodynamically to the transom stern.

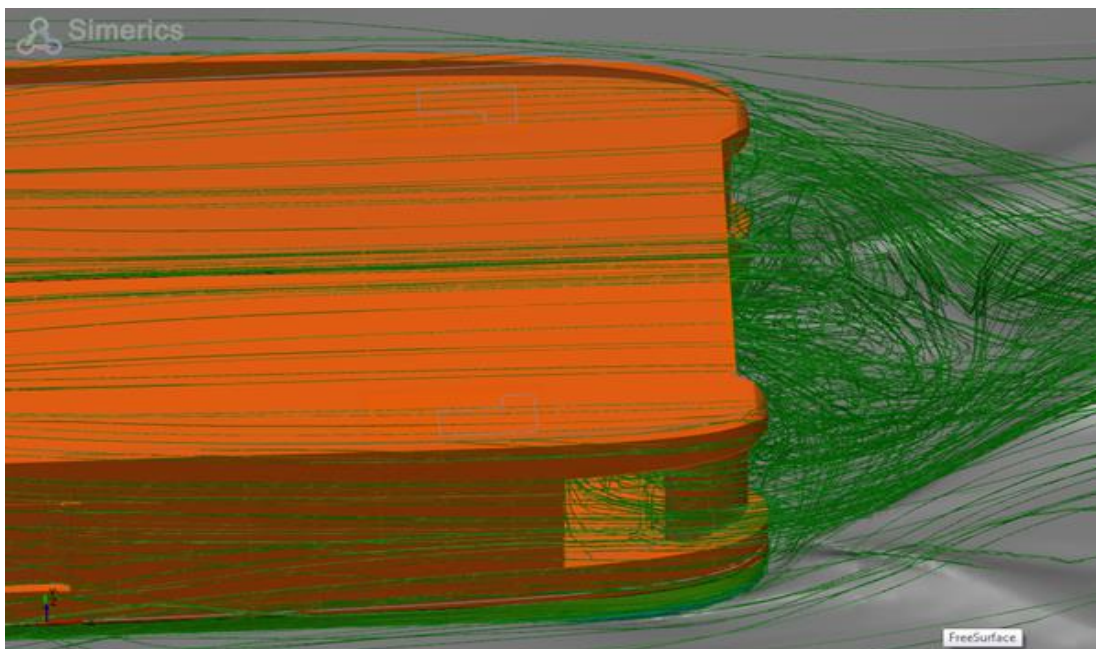


Fig.3: CFD results for modification #1

- Modification #2, Fig.4
The next investigation was to simulate the first design when the boat moves in reverse direction. The general effect from modification #1 is reversed here. The flow profiles also work "backwards".

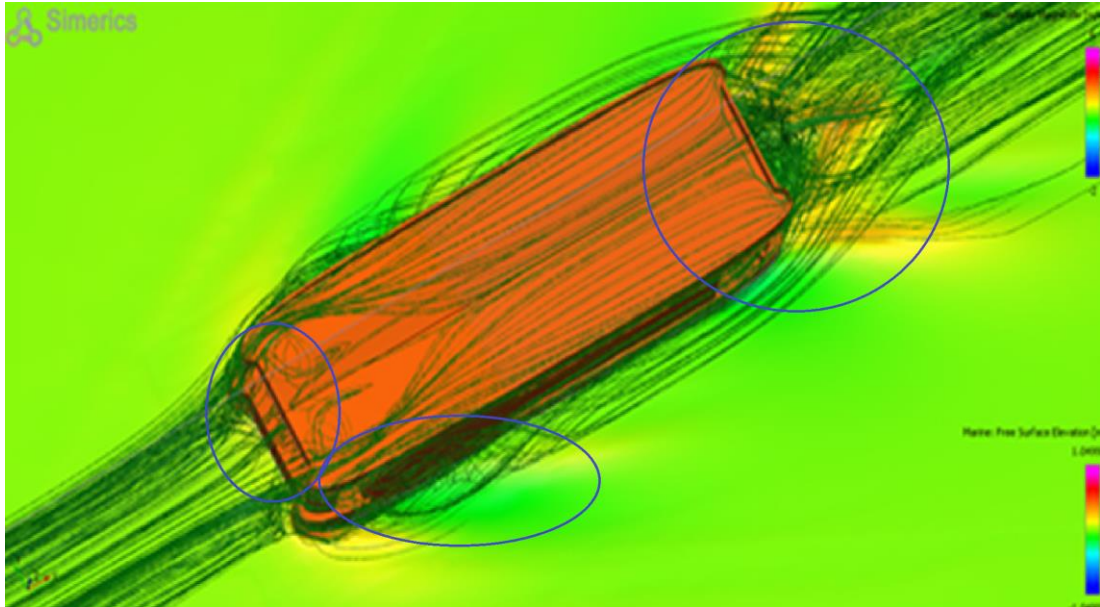


Fig.4: CFD results for modification #2

- Modification #3, Fig.5
This simulation was carried out with a considerable change in design aiming at a significant improvement. The profiles were turned. The overpressure sides of the profiles now pushed the streamlines outwards away from the longitudinal center and the suction side on the outside simultaneously sucked the streamlines outwards as well.

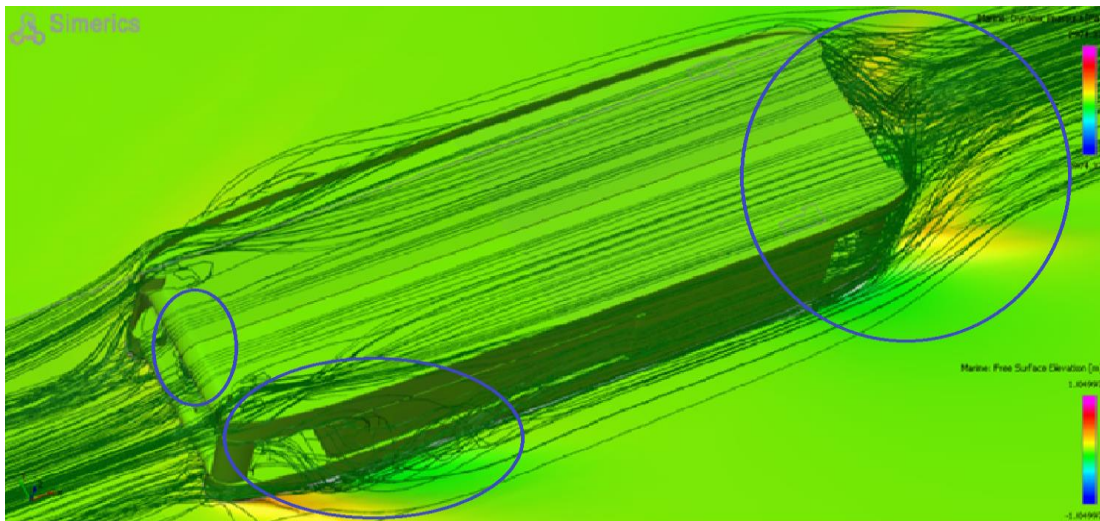


Fig.4: CFD results for modification #3

- Modification #4, Fig.5
In this simulation, the design of the previous simulation was changed, mainly in the stern area and slightly in the bow area.
- Modification #5, Fig.6
Here, the influence of the roof stairs on the flow behavior of the entire houseboat system was examined. Furthermore, the influence of the draft on the current in the catamaran tunnel between the swimmers was investigated.

- Modification #6, Fig.7
 Here, the effect of oblique wind directions on the houseboat was investigated. The inclined flow was carried out at two different angles (45° , 18.4°) and a round geometrical front corner. Improvements with a round corner of the front wall and different speeds were checked. It was found that the round corners with a radius of 450 mm in the front wall prevent the so-called “vortex cheeks” in the bow area and that the flow is largely back on the side wall on the side facing away from the wind (leeward side). The edge of the stern back wall was left with a sharp edge in order to aerodynamically lengthen the aft structure by enforcing flow separation. With increasing wind speed, the streamlines showed ever finer and delimited structures. The wind moments around the vertical axis could be reduced significantly by the rounded front corner.

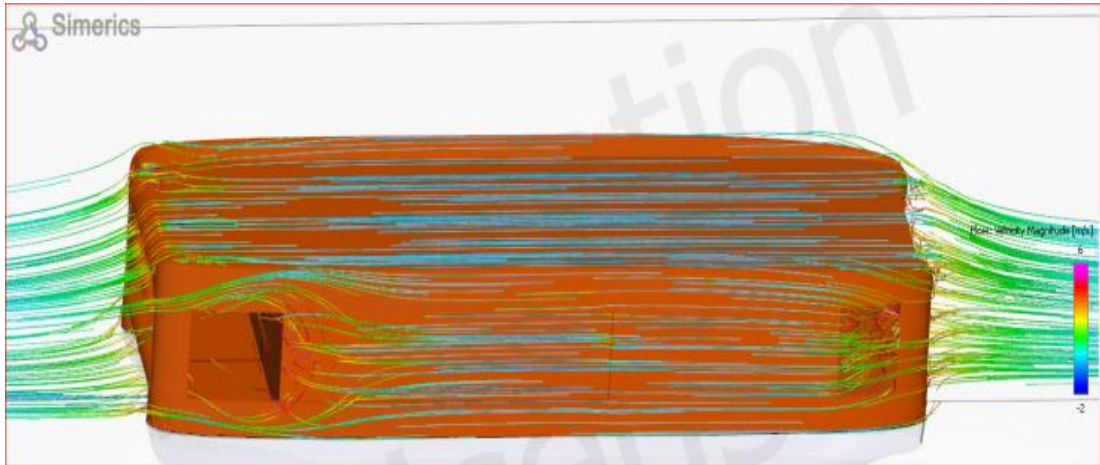


Fig.5: CFD results for modification #4

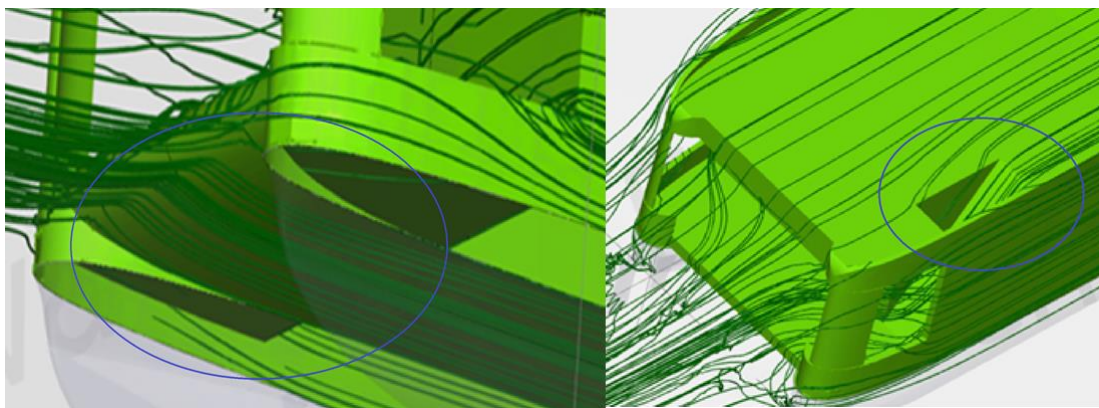


Fig.6: CFD results for modification #5

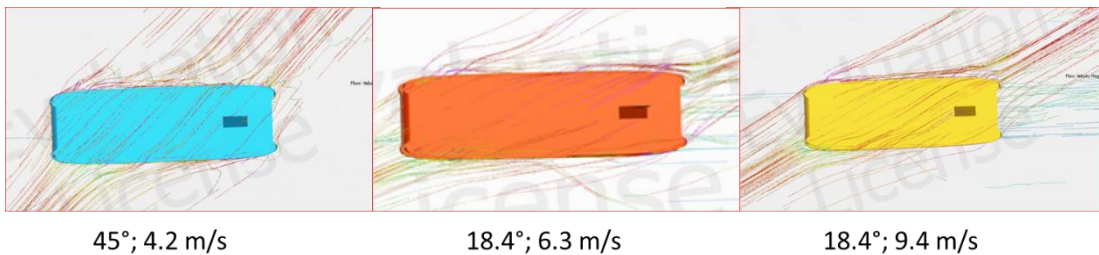


Fig.7: CFD results for modification #6

5. Conclusion

In the quest to decarbonize shipping, every percent of energy savings counts. The current design may be applied in essence also to large-scale cargo shipping. Windshield profiles as shown in Fig.8 could reduce wind resistance on e.g. container ships and improve maneuverability, acting in similar fashion addressing similar problems with wind and sharp edges.

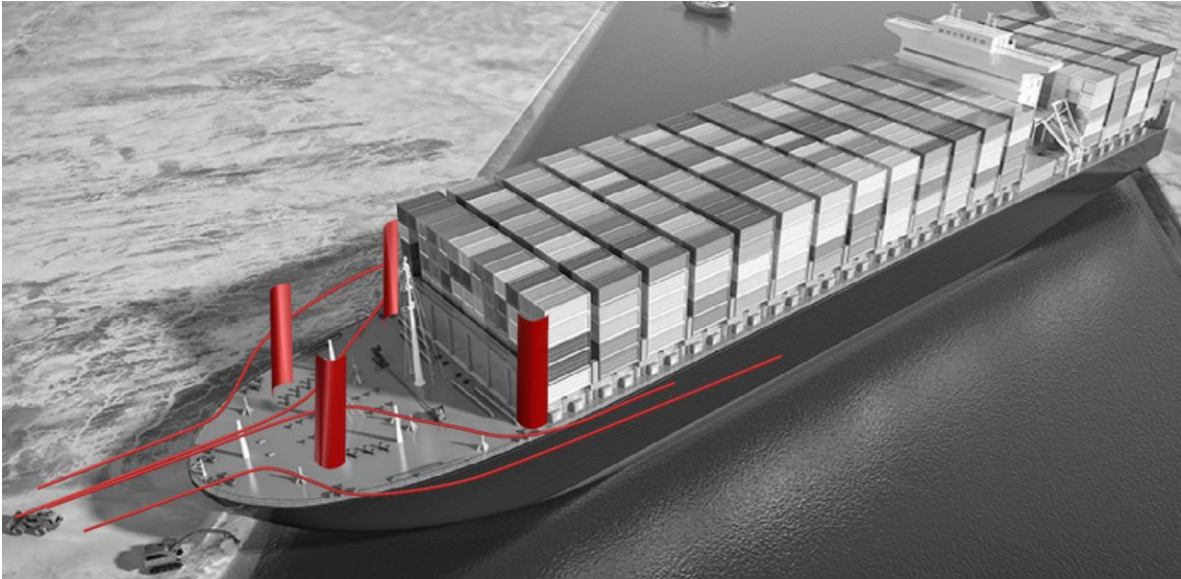


Fig.8: Windshield profiles on containership forecastle

Road to Digitalization, Not so Simple

Matteo Barsotti, IB, Genoa/Italy, m.barsotti@ib-marine.com

Abstract

Today the word digitalization fill most of the shipping news and almost everyone in shipping claim that they are now digitalized. But are they really digitalized? Or they are just collecting data from one flowmeter that maybe is not calibrated? The road to digitalization is not so simple and have to start from the knowledge and fully understanding of the subject and the effort (also economical) that will involve. The starting point of the process is always assessing the need of the customer and then give him the best reply that could be also “No we can’t help you if you are not keen to do some investment and changes” The strongest point is to achieve the goal expected but explaining very well the path. The paper is about the principles of a digitalization path, giving also some examples from real life cases.

1. Introduction

When you try to sell a performance monitoring solution one of the biggest challenges is to convince the customer on the investment to be done but it depends mostly on the goal that he wants to achieve. We can use an example, a direct request by a customer “I want to solve the Cappuccino effect problem”. Of course, it is indeed a very serious, costly, and annoying problem that affect many owners or charterer. The “Cappuccino effect” is when air is inflated during the bunkering operation, and this increase the volume of the tank and then the receiver of the bunker may understand after some time of the shortage of bunker. In these years, there were many measures that were implemented by companies to avoid or better reduce this kind of problem, but it is still a problem for some area and some vessel. This is, as said, very bad and costly not only for the bunker shortage itself but also to claim the bunker trader and then all the legal path that these things must follow. The first step, as for every request, is to assess the fleet in term of type of vessel, the type of equipment and most of all, the measuring equipment. This is because, depending on the results of the initial investigation we will have several replies. What can be the solution to this annoying problem? We can evaluate three main monitoring approaches:

- 1) Install a bunker mass flowmeter: this a real solution to the problem because the mass flowmeter will provide the mass of the fuel bunkered. So, if air is there, this does not affect the mass measurement.
- 2) Monitor through massic flowmeter the consumption of the consumers on board through an automatic data collection: this enable the user to be sure about the consumption and then discover how much is the shortage of bunker. This method of course must take into consideration the accuracy of the flowmeters but most importantly the accuracy of the bunker sounding.
- 3) Monitor through volumetric flowmeter the consumption of the consumers on board through an automatic data collection: this method has a reduced reliability due to the less accuracy of the instrument, but in any case, it is something if we also combine the dataset with Fuel Temperature and density in order to retrieve the mass. This again must take into consideration the accuracy of the flowmeters but most importantly the accuracy of the bunker sounding.

These three methods could solve or at least reduce the bunker shortage due to the Cappuccino Effect. As you can see it is not present any manual noon reporting as it should be clear that a reporting system based on the 24 hours reporting is not reliable to have a sufficient degree of accuracy to limit the Cappuccino Effect. So, when the investigation result in an old fleet with only volumetric flowmeter not on every vessel and not on every equipment able to measure only the flow in pulse and furthermore the clear message is “we cannot spend money” then the reply is to be “no we can’t help you”. It is of course not easy to say no to a customer when you are a vendor, but I think it is always important to be transparent with customer because unfortunately if you cannot measure you cannot understand. This is just an example to say that there is the need to invest time and sometime money to get money back.

2. What is needed?

What really means to digitalize a ship or a fleet? Just connect all the equipment to a PC and then send to shore? Well actually no, this is only the first step but then once you are in office with all the data from your fleet is when the game start. Because you will be able to really enable deep analysis and alerting in the view of the performance optimization.

Before moving into details, it is better to describe, how a digitalization system works, Fig.1.

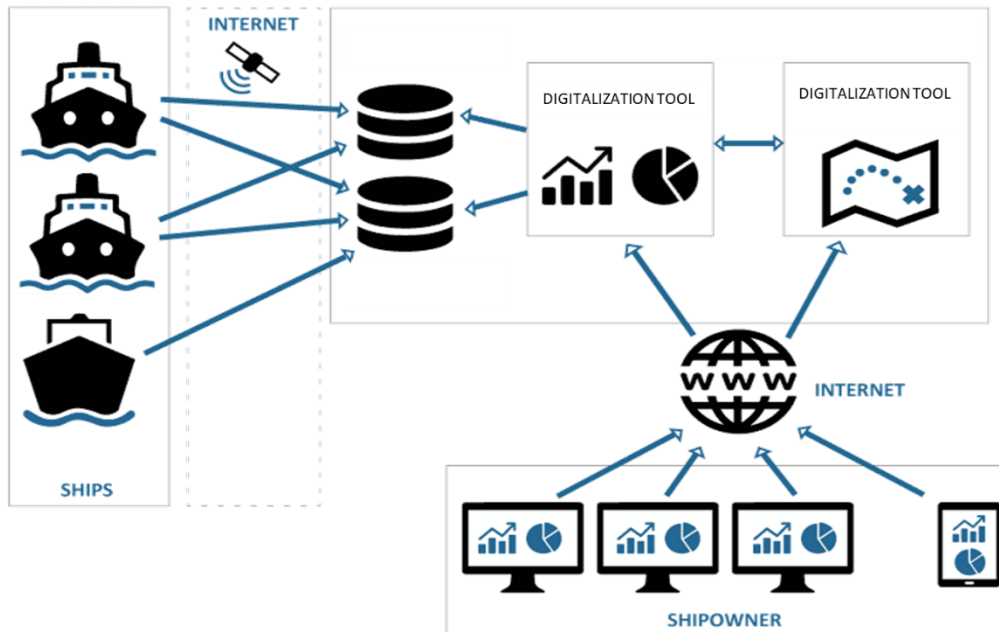


Fig.1: Digitalization scheme

To make it very, very simple, there is a Data Collector on board each ship able to collect all the required data and then are sent to shore to a dedicated Datacenter or Cloud where the Customer will have access to the digitalization tools.

As said, it is not just to connect and store amount of data, but it is a process of acquiring, analysing, and validating all the various output and send them to shore. For this, task it is essential the valuable help of the crew because, at today, is where all the equipment is and then crew is also aware of any problem, any malfunction and most importantly knows the maintenance scheme of each equipment. The maintenance of an equipment is something vital especially for the equipment that needs calibration otherwise you could collect very bad numbers.

Focusing on the equipment involved in the path, which is the minimum set of information needed for starting the digitalization?

Example vessel with Conventional Propulsion 1 ME + 4 DGs + 2 Boilers

Navigation systems:

- Position through GPS
- Speed Through Water
- Speed Over Ground
- Course Over Ground
- Heading True
- Wind Speed and Angle

Automation Systems:

- Shaft power [kW]
- Main engine RPM
- Main engine fuel consumption [Kg/h]
- Draft aft [m]
- Draft fore [m]
- Trim
- List
- DG1 power [kW]
- DG2 power [kW]
- DG3 power [kW]
- DG4 power [kW]
- DGs fuel consumption [Kg/h]
- Boiler 1 fuel consumption [Kg/h]
- Boiler 2 fuel consumption [Kg/h]

Of course, this is a standard solution with all the equipment integrated in the Automation and Navigation and this rarely happens, especially when we are approaching a customer with existing fleets.

Receiving such data means that the system would be able to optimize route, speed, consumption, hull and propeller degradation, power generation, steam generation and trim optimization. So, if the system that will collect the data and provide to shore is not receiving one of these signals this means that the path to digitalization is becoming not very worthy for the customer because one of the potential saving coming from optimizations is not included and they are almost all connected.

If the customer's goal is monitoring the hull and propeller degradation, then it is not possible to provide if we have not at least:

- Position through GPS
- Speed Through Water
- Speed Over Ground
- Course Over Ground
- Heading True
- Wind Speed and Angle
- Shaft power [kW]
- Main engine RPM
- Main engine fuel consumption [Kg/h]
- Draft aft [m]
- Draft fore [m]
- Trim
- List

So, please, beware of vendors that claim successfully saving without these data automatically collected and validated. The Shaft Power and the Consumption in general are measures that requires some specific equipment: Torquemeter and Flowmeters respectively and saying that you can have the same result in terms of optimization if you measure Power with formulas provided by ME makers and consumption using manual sounding, it is a real lie. In any case, the more data we collect the better, but only if we can use such data otherwise, we will fill our database of unused and not useful data.

3. The path to digitalization

The question now is which is the correct path to digitalization? The answer is not simple as some may propose, but it is a challenge for a Ship Owner or Ship manager.

The starting point, as said, is the goal to be achieved and basis that, the second step is to assess the current fleet that the customer wants to digitalize. Statistically we could have this situation: on a company with 50 ships, average 7 year.

- 40% are already ready to be digitalized, then small cost for the customer
- 30% are almost ready to be digitalized, then only flowmeters have to be connected to the system, average cost for the customer
- 20% are not ready to be digitalized the flowmeter and Torquemeter have to be installed, the cost will boost
- 10% are very difficult to digitalize due to outdated Navigation/Automation system and the cost is not worthy.

Then the investigation will move on each vessel, to map all the equipment to be connected and then all the vendors that have to be contacted. In many cases, in a fleet of same type of vessel, we have common provider for navigation system and automation system, but it could also happen to have a long list of vendors involved for navigation, automation, flow meters, torque meters, power meter etc. It is clear that this is not an easy task, but it is possible to do it, it is a matter of investment and efforts. Maybe the customer will digitalize only a part of the fleet excluding the oldest vessel, but in any case, it is important to understand that the process will require quite efforts in coordinating all the vendors and parties involved. This is the biggest challenge and then from a provider of this solution point of view we could help in asking the correct question and then to achieve the goals faster. After collecting all the answers from the vendors there is another challenge: find the best place to install the data collector. This is a job done usually in three, the vessel, the office/superintendent, and the provider but if the vessel is under construction, then the third party is the yard and, in any case, if it is a first installation will require a lot of communication and email before to reach the agreement on the designated location. Following that. there is the cabling purchasing, delivery, and installation. It seems easy but is not, because the task is to estimate the path of each cable, to find the correct requirement for each output and then to purchase and delivery on board that in some case can be very difficult. The installation then require scheme, drawings and sometimes Electrical Engineer skill plus a dedicated person from office that follows strictly all this steps. After this task there will be the installation of the hardware and the services related that enable the system to collect the data. As many of you know, arranging a service onboard can be a real headache especially if you want to coordinate more than one vendor and the vessel is moving around the world. The best solution is going in Drydock or in the Yard, but it depends on the fleet and the customer itself. Usually, we also go onboard during a port stay, during Cargo operation or, if we are lucky, during a stop for repair at berth. After that the data are sent to shore, verified, and validated and then it is time to play with all the recorded data and really start to digitalize your fleet.

Just to summarize all the steps:

- 1) Set the customer goal
- 2) Assessment of the fleet
- 3) On the designated vessels, map all the equipment to be connected
- 4) Contact all the vendors and arrange the services
- 5) Find best location for equipment
- 6) Cable purchase, delivery and installation
- 7) Hardware installation and services on board
- 8) Verify the connection on shore
- 9) Start configuration and use of Optimization and Alerting tools
- 10) Fleet is digitalized

4. Property of the data and Standard

As mentioned before, the path cannot be smooth, major or minor issue may come during each step of the process but what really create the bottle neck is the setting of the output from automation systems.

Many times, it is also because some automation vendors are also digitalization vendors and then may want to propose their solution, but this is part of the game. But most of the times the problem arises on the property of the data collected, because some vendors claim the property of the data they collect and then they request a lot of configurations (and money) to enable the output and open their channel. This is, of course, not the fault of the automation vendors but the problem is that there is not a high-level decision on the property of the data but only some interpretations and there is not a standard communication protocol for the output but a real jungle of output's languages custom NMEA, Modbus, OPC and analogue. This lack of Standardization has only the effect to slow-down all the process and then limit the goal to be achieved.

5. Conclusions

The road to digitalization is not so simple but it is possible to digitalize your fleet and then achieve the goal that you have set, it is just a matter of choosing the right partner. This paper is not, of course, to scare the customer that want to digitalize its fleet but just to make all aware about what it cost in terms of money and effort to run this path to digitalization. It is then clear that the path is easy or easier if you choose the right partner otherwise the risk is that at the end, the customer will spend a lot of money and then he will not have much in his hands. As said in the beginning, there is the need to invest time and money to get money back.

This is the same for everything. Do you want to continue to use HFO after 1st Jan 2020 that is cheaper? Then buy a scrubber. Do you want to save 3% of fuel consumption? Then install a new propeller. It is always a matter of ROI that must be effective and profitable. Despite all the promises of some vendors, some performance monitoring system have a good ROI, but of course it depends on the goal to be achieved, because also the profit will be calculated according to the specific goal. When we heard that a company, with a new tool, has saved this year 3% of fuel, it means nothing because in this number we could have hundreds of factors that could affect the fuel consumption (even the fact that a vessel is not anymore in service); in other words, in order to evaluate a real saving is better to provide evidence, based on real numbers and not just a title on the news.

EU Project CHEK – Ultrasonic Antifouling and other Measures to Meet the CII Challenge

Jan Kelling, HASYTEC, Schönkirchen/Germany, j.kelling@hasytec.com

Abstract

This paper describes our planned contributions to the EU project CHEK and first insights from the project. The project's larger context is decarbonization of shipping through innovative technologies, where ultrasonic antifouling technology is the specific contribution of HASYTEC to increase energy efficiency in operation and bring down the Carbon Intensity Indicator (CII). The application cases in CHEK are a cruise vessel and a bulk carrier. The CHEK project is expected to bring valuable reference installations of large numbers of ultrasonic transducers on large-scale cargo ships, adding to wider acceptance of ultrasonic antifouling technology.

1. Introduction

IMO, www.imo.org, has the ambition to halve GHG emissions by 2050 and to completely decarbonize shipping “as soon as possible” within this century. The initial IMO Greenhouse Gas strategy will be revised in 2023, including these goals. IMO is following a two-tier approach to implement decarbonization measures, focusing first on short-term energy efficiency improving measures, before embarking on more comprehensive medium-term and long-term measures that will include alternative low-carbon/no-carbon fuels, *Bertram (2021)*.

Current measures addressing GHG emissions include three mandatory requirements:

- The Energy Efficiency Design Index (EEDI) for newbuildings mandating successive improvement in design performance of 30% compared to the average of ships built 1999-2009.
- The Ship Energy Efficiency Management Plan (SEEMP) for all ships above 400 GT in operation, making a continuous energy efficiency improvement management plan mandatory, although not stating explicit requirements to content, scope and implementation.
- The Fuel Oil Consumption Data Collection System (DCS) mandating annual reporting of CO₂ emissions for all ships above 5000 GT.

At MEPC 76, in 2021, three additional measures were adopted, affecting all existing cargo and cruise ships after 2023:

- The Energy Efficiency Design Index for Existing Ships (EEXI), essentially making requirement equivalent to EEDI Phase 2 or 3 mandatory to all existing ships.
- A mandatory Carbon Intensity Indicator (CII) and rating scheme for all cargo and cruise ships above 5000 GT. Poor CII ratings will lead to mandatory requirements for corrective action plans to improve the CII. The criteria for CII ratings will get progressively stricter by 1% per year for 2020-2022, followed by 2% per year for 2023-2026.
- SEEMP requirements were made stricter (Enhanced SEEMP) to include mandatory content, such as an implementation plan on how to achieve the CII targets.

These new requirements for existing ships will increase the focus on energy efficiency measures both in design/retrofit and operation. For the operational measures, improved hull management is widely seen as one of the most important measures, with potential gains in the order of magnitude of 10%.

2. Project CHEK

2.1. Overview

The R&D project CHEK (deCarbonising sHipping by Enabling Key technology symbiosis on real vessel concept designs) has as a goal to reduce CO₂ emissions in global shipping. The focus is on the combined application of advanced key technologies in shipbuilding. The CHEK project is supported by the European Union with a total of 10 million Euro from the Horizon 2020 funding program, <https://ec.europa.eu/programmes/horizon2020/en/home>. The Horizon 2020 program is the biggest EU research & innovation program ever, with nearly € 80 billion of funding over 7 years. Its aim is combining European research and innovation to achieve excellent science, industrial leadership and tackling societal challenges.

2.2. Project goals

The CHEK project proposes to reach zero-emission shipping by disrupting the way ships are designed and operated today. The project will develop and demonstrate two bespoke vessel designs – a wind energy optimised Kamsarmax bulk carrier and a hydrogen powered cruise ship, Fig.1 – equipped with an interdisciplinary combination of innovative technologies working in symbiosis to reduce greenhouse gas emissions by 99%, achieve at least 50% energy savings and reduce black carbon emissions by over 95%. The innovative energy-saving technologies include the use of wind energy, batteries, heat recovery, hydrogen as a fuel, air lubrication and ultrasound anti-fouling.

Rather than “stacking” novel technologies onto existing vessel designs, the consortium is proposing to develop a unique Future-Proof Vessel (FPV) Design Platform to ensure maximised symbiosis between the novel technologies proposed and taking into consideration the vessels’ real operational profiles (rather than just sea-trial performance). The FPV Platform will also serve as a basis for replicating the CHEK approach towards other vessel types such as tankers, container ships, general cargo ships and ferries. These jointly cover over 93% of the global shipping tonnage and are responsible for 85% of global GHG emissions from shipping.

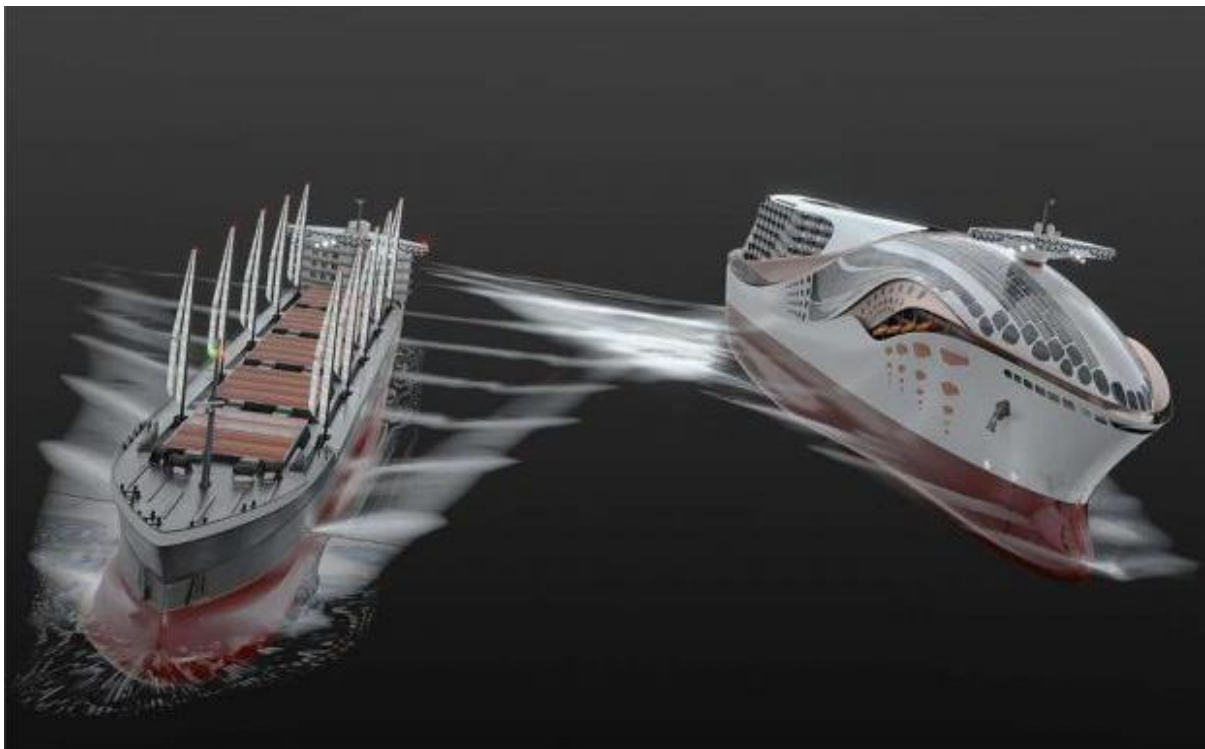


Fig.1: Application cases: Bulk carrier and cruise ship, source: Wärtsilä

In order to achieve real-world impact and the decarbonisation of the global shipping fleet, the consortium will undertake an analysis of framework conditions influencing long-distance shipping today (including infrastructure availability) and propose solutions to ensure the proposed vessel designs can and will be deployed in reality. A Foresight Exercise will simulate the deployment of the CHEK innovations on the global shipping fleet with the aim of reaching the IMO's goal of halving shipping emissions by 2050 and contributing to turning Europe into the first carbon-neutral continent by 2050 (as stipulated by the European Green Deal).

2.3. Project consortium

The CHEK project partners are:

- University of Vaasa (UV), <http://www.uvasa.fi/>, is a business-oriented, multidisciplinary and international university.
- Wärtsilä, www.wartsila.com, is a provider of ship machinery, propulsion and manoeuvring solutions, supplying engines and generating sets, reduction gears, propulsion equipment, control systems, and sealing solutions for all types of vessels and offshore applications.
- Cargill Ocean Transportation, <https://www.cargill.com/transportation/cargill-ocean-transportation>, is a freight-trading business that provides bulk shipping services to customers across the globe.
- MSC Cruises, www.msccruises.com, is a global cruise line, which is part of the Cruises Division of MSC Group, the privately held Swiss-based shipping and logistics conglomerate.
- Lloyd's Register EMEA (LR), www.lr.org, is part of the Lloyd's Register Group, a global independent risk management and safety assurance organisation that works to enhance safety and improve the performance of assets and systems at sea, on land and in the air.
- World Maritime University (WMU), www.wmu.se, was established in 1983 by the International Maritime Organization (IMO).
- Silverstream Technologies, <https://www.silverstream-tech.com/>, was established in 2010 and the company specialises in Air Lubrication Technology, *Silberschmidt et al. (2016)*, which is designed to reduce the frictional impact between the flat bottom of the ship hull and water.
- HASYTEC Electronics GmbH, <https://www.hasytec.de/>, is market leader in ultrasound based antifouling technology, *Kelling (2017,2020)*.
- Deltamarin, <https://deltamarin.com/>, is a ship engineering and design company.
- Climeon AB, <https://climeon.com/>, has well proven technology to convert waste heat to clean power.
- BAR Technologies, <https://www.bartechnologies.uk/>, have used its in-house tool ShipSEAT to design and optimise their own patented and trademarked wind propulsion system called WindWings, <https://www.bartechnologies.uk/project/windwings/>.

2.4. Application cases and applied technology

The project aims to combine a variety of innovative technologies to achieve its goals, Fig.2:

- New energy technologies
 - Fixed wing sails
 - Fuel-cell ready hydrogen engine
- Operational technologies and practices
 - Automated vessel routing/sailing
 - Cruise vessel itinerary optimisation
- Propulsion/Power supply technologies
 - Fuel-flexible gas engine incl. over-the-air software updates
 - Scalable power plant
 - Hybrid energy management
 - Waste heat recovery

- Waste-to-power
- Drag reduction technologies
 - Gate rudder
 - Air lubrication
 - Ultrasound antifouling
 - Ship hull optimization

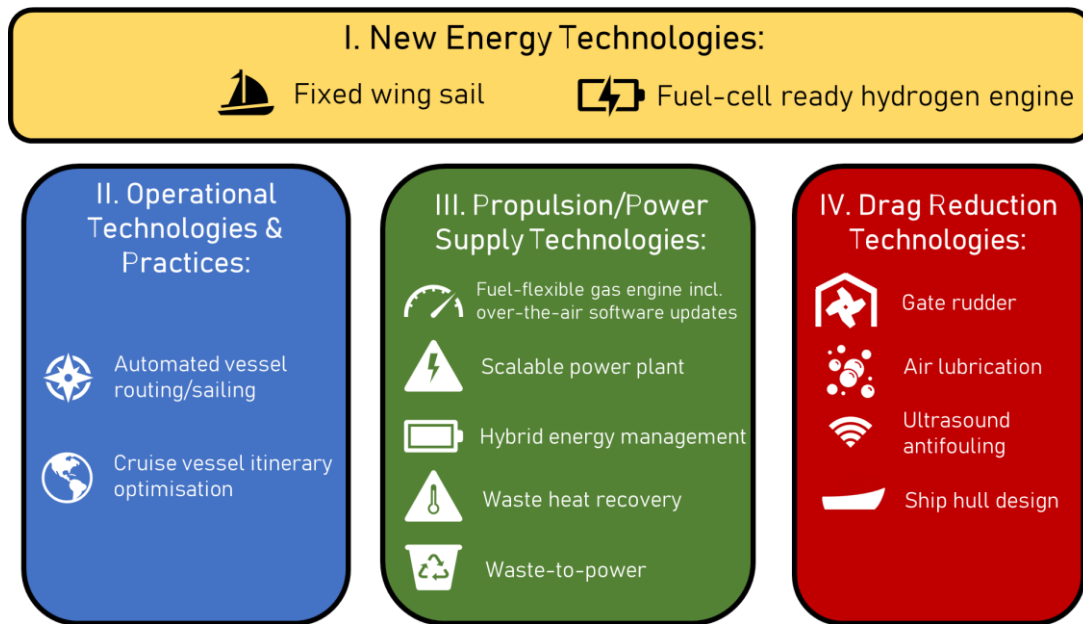


Fig.2: Technological synergy for emission savings

The effectiveness and saving potential of the various options depend on various factors, including ship types and associated typical operational patterns. Within CHEK, two very different ship types are considered, namely a bulk carrier and a cruise vessel. Fig.3 gives the selected measures for the bulk carrier, and Fig.4 for the cruise vessel.

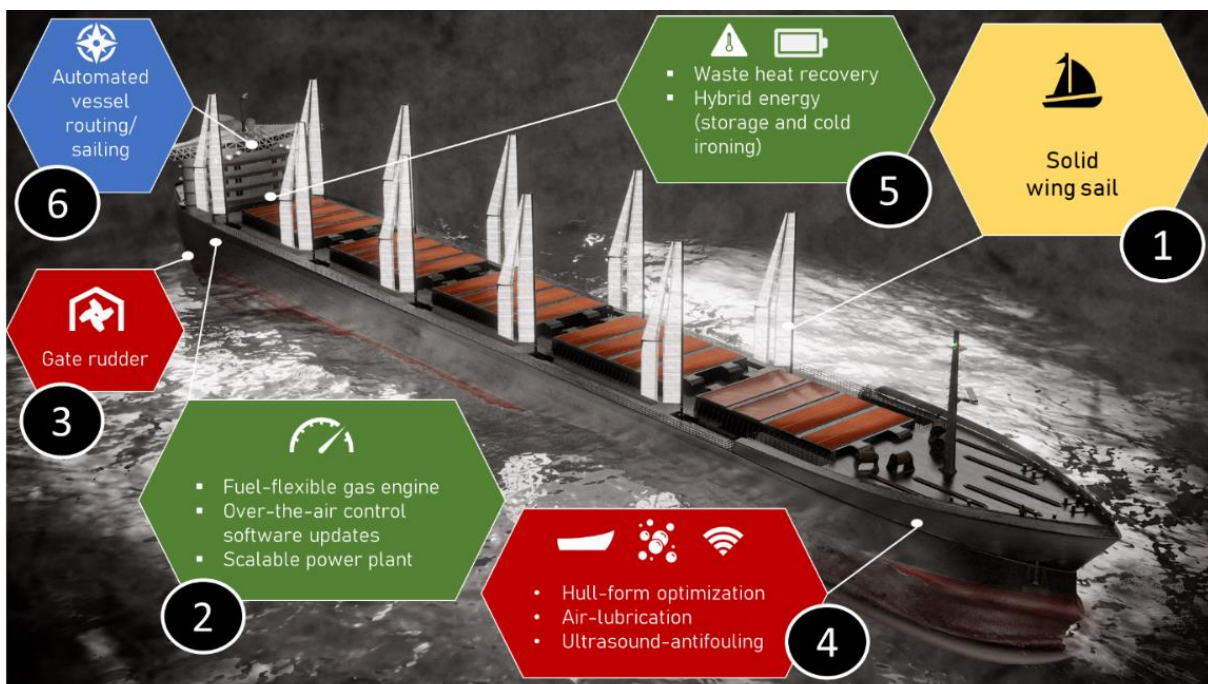


Fig.3: Emission saving technologies envisioned for bulk carrier

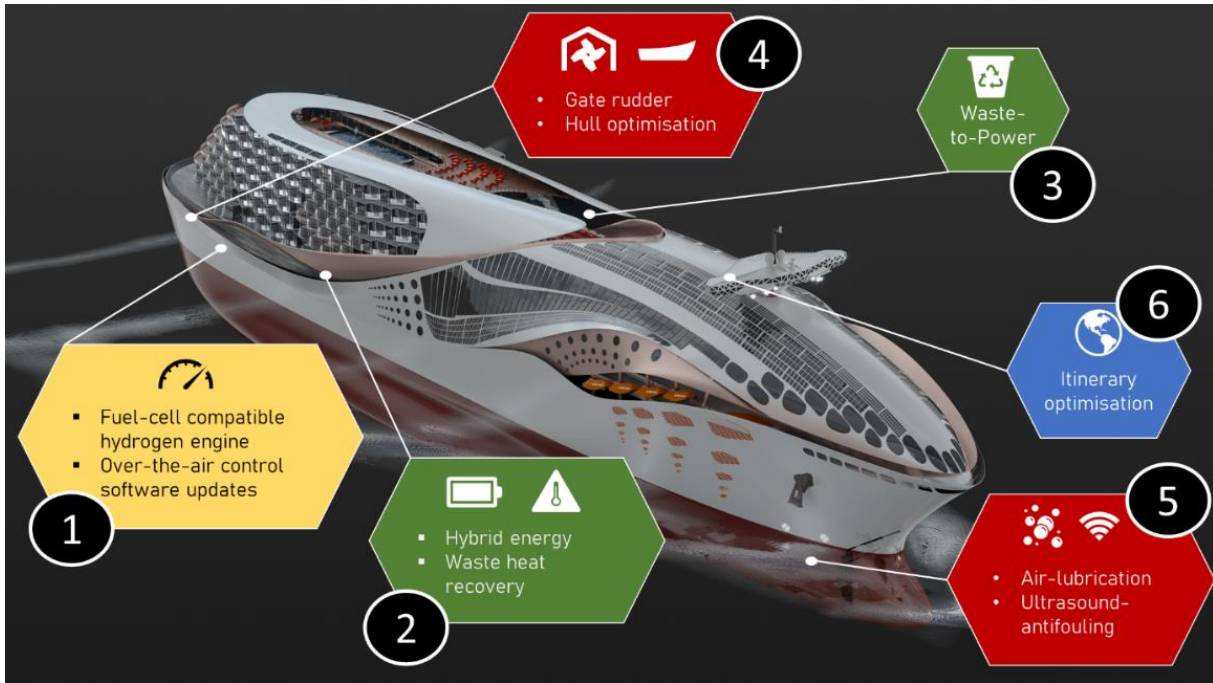


Fig.4: Emission saving technologies envisioned for cruise vessel

Figs.5 and 6 compares the expected CO₂ emissions to a baseline design, where the bars are normalized to 100% for the baseline design, for bulk carrier and cruise vessel, respectively. The selected measures lead to an expected decrease in CO₂ emissions of 40% for the bulk carrier and 50% for the cruise vessel.

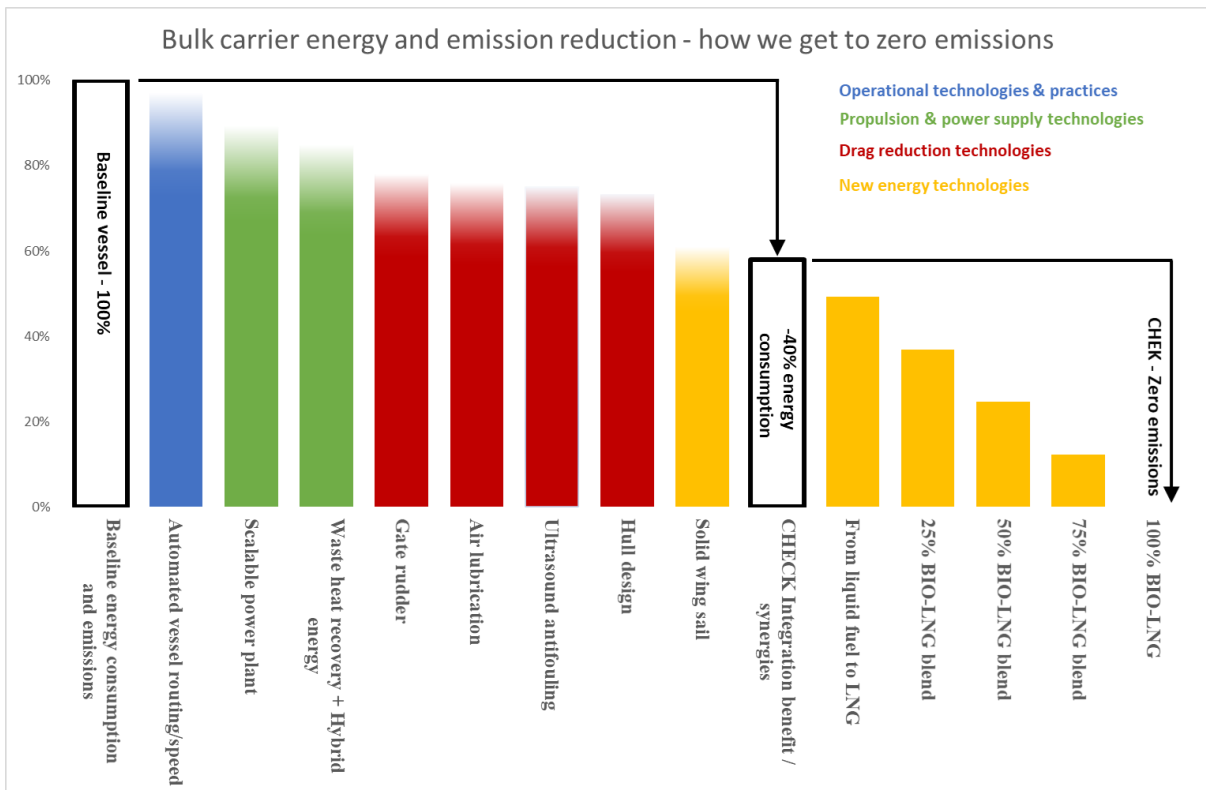


Fig.5: Expected emissions compared to baseline design for bulk carrier

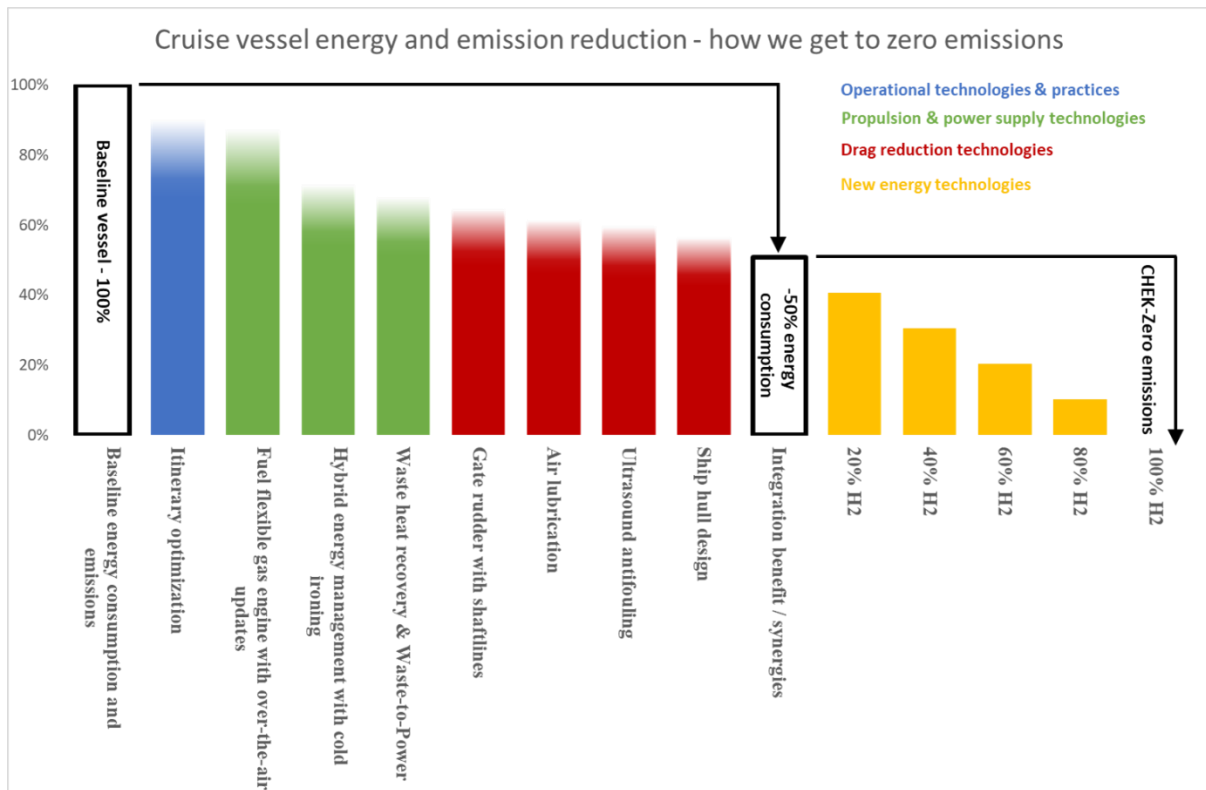


Fig.6: Expected emissions compared to baseline design for cruise vessel

3. Ultrasonic technology contribution within CHEK

In relation to the AFS convention, *IMO (2001)*, the EU Regulation No. 528/2012 details restrictions on the marketing and use of biocide containing products. As an example, almost no copper-based active substances will get permission to be used in the future. This leaves essentially two options:

- taking the risk of using less effective antifouling systems which leads to higher costs for maintenance and repair as well as to higher fuel expenses
- looking for alternatives to replace the traditionally used antifouling systems

Ultrasonic systems are such an alternative and are increasingly adopted by various segments of shipping. Ideally, such ultrasonic systems inhibit the chain of fouling development at the beginning, namely the biofilm.

3.1. Biofilm

Biofilms are formed when bacteria adhere to a solid surface, Fig.7, and enclose themselves in a sticky polysaccharide. Once this polysaccharide is formed, the bacteria can no longer leave the surface, and when new bacteria are produced, they stay within the polysaccharide layer. This layer (the “biofilm”) is highly protective for the organisms within it. In fact, many bacteria may not survive in the environment outside of biofilms. Biofilms are ubiquitous in the environment. They form on our teeth, inside our bodies, in our streams and oceans, on natural surfaces continually wetted by dripping water. They also are formed on ship hulls and inside piping in ships.

In general, while a few fungi can form their own biofilms and a few inhabit bacterial biofilms, the so-called “moulds” generally do not grow in or even on the surface of biofilms. This is because there is generally too much water. Most fungi will not grow under water, and biofilms are almost always under water. Biofilms will not go away on their own, and considerable effort is required to eliminate them.

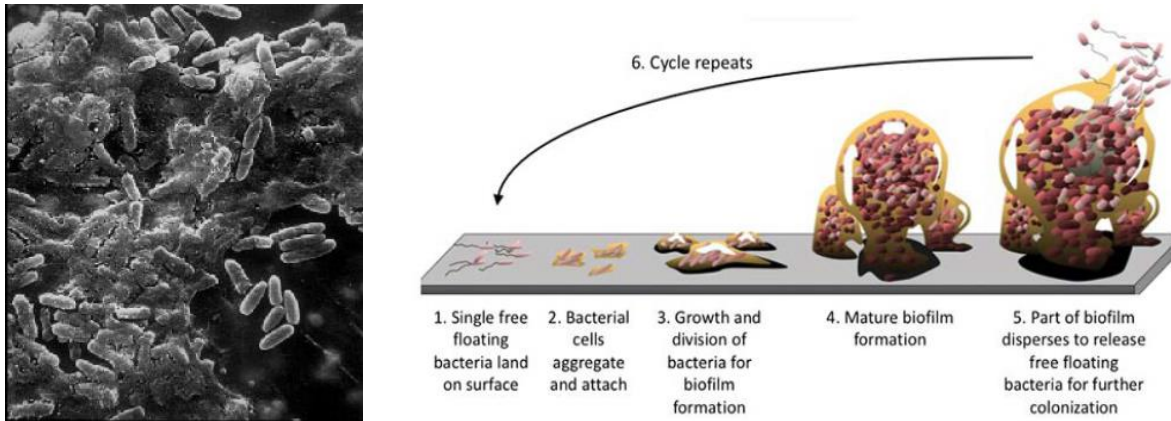


Fig.7: Biofilm under microscope (left) and biofilm growth cycle (right)

Biofilms can be scrubbed away or disrupted, e.g. by very hot water, steam, or concentrated oxidizing agents. However, they will return quickly unless the water source is removed. Hence, there are always biofilms present where water is always present.

3.2. Ultrasonic antifouling technology

Older ultrasound methods followed the idea of getting rid of hard growth which had already attached. Using hard cavitation, this might work in certain situations but may also damage the vessel's steel or coating itself. Consequently, this approach was not accepted by the market. Low-powered ultrasound (avoiding cavitation) destroys the cell structures in biofilm, thus the prerequisite for higher stages of fouling, such as barnacles, shells, and algae. Unlike some coating solutions, ultrasonic antifouling solutions are also 100% effective at zero speed, e.g. in longer stays in port or at mooring. Ultrasonic antifouling solutions have enjoyed exponentially growing market acceptance in shipping over the last 5 years. For details, see e.g. *Kelling (2017)*, *Kelling and Mayorga (2020)*.



Fig.8: Tugboat without (top) and with (bottom) ultrasonic antifouling protection

Fig.8. shows the effectiveness for a smaller workboat, *Kelling (2017)*. Within the CHEK project, the effectiveness of large-scale installations for hull and internal equipment of large commercial ships shall be demonstrated.

4. Outlook

The CHEK project started in June 2021 and has a planned duration of 36 months. During this time, concept designs will be developed, and performance monitoring will validate expected energy savings of installed devices. Project progress and insight gained, with particular focus on the ultrasonic antifouling technology, will be disseminated in suitable conferences like this one.

Acknowledgements

The CHEK project has received funding from the European Union's Horizon 2020 research and innovation program under grant agreement No 955286.

References

BERTRAM, V. (2021), *Fuel Options for Decarbonizing Shipping*, 13th Symp. High-Performance Marine Vehicles (HIPER), Tullamore, pp.12-20

IMO (2001), *International Convention on the Control of Harmful Anti-Fouling Systems on Ships*, Int. Mar. Org., London

KELLING, J.; MAYORGA, X. (2020), *Dynamic Biofouling Protection*, 5th HullPIC Conf., Hamburg, pp.184-187, http://data.hullpic.info/HullPIC2020_Hamburg.pdf

KELLING, J.; (2017), *Ultrasonic Technology for Biocide-Free Antifouling*, 11th Symp. High-Performance Marine Vehicles (HIPER), Zevenwacht, pp.70-76, http://data.hiper-conf.info/Hiper2017_Zevenwacht.pdf

SILBERSCHMIDT, N.; TASKER, D.; PAPPAS, T.; JOHANNESSON, J. (2016), *Silverstream® System – Air Lubrication Performance Verification and Design Development*, 10th Symp. High-Performance Marine Vehicles (HIPER), Cortona, pp.236-246, http://data.hiper-conf.info/Hiper2016_Cortona.pdf

Cruise Ships and COVID-19 Emergency – How Smart Technologies Can Improve the Health Safety of Travel Onboard

Giuseppe Carmosino, Politecnico di Milano, Milan/Italy, giuseppe.carmosino@polimi.it

Francesca Balena, Politecnico di Milano, Milan/Italy, francesca.balena@polimi.it

Silvia Piardi, Politecnico di Milano, Milan/Italy, silvia.piardi@polimi.it

Andrea Ratti, Politecnico di Milano, Milan/Italy, andrea.ratti@polimi.it

Abstract

This paper presents the state-of-the-art of health management design practices on cruise ships, through the method of case study analysis. The Covid-19 pandemic has had a strong impact globally in people's daily lives and in all economic fields. As for the cruise sector, the pandemic has forced companies to reshape organizations and strategies and to rethink the spaces on cruise ships. With the help of smart technologies, design can play an important role in creating safer places. The results show how smart technologies can improve the health safety of travel on board and indicate further areas for development.

1. Introduction

The Covid-19 emergency has strongly marked people's daily lives and all economic fields. Looking at the cruise sector, the annual report released by the Cruise Lines International Association, *CLIA (2020)* has estimated in 2020 large economic losses between mid-March and September 2020: \$77 billion in global economic activity, 518,000 jobs and \$23 billion in wages. Meanwhile, the cruise industry has stepped up health measures and protocols in place to prepare for a gradual resumption of operations in the coming months. In particular, cruise lines have provided strict and science-backed measures for embarkation and on-board activities: a complete testing of passengers and crew, mask requirements and physical distancing, health communications and evaluations, and a coordination with destinations for the shore excursions. Disinfection has played an important role in the safety and well-being of healthcare workers and society. The main disinfection strategies have included chemical treatment to remove any gross contaminants, thermal, chemical or irradiation treatment to remove any remaining microscopic material. However, the disinfection action must be supported by the use personal protective equipment (PPE) by workers and customers and social distance measures, in order to be really effective, *Armani et al. (2020)*. Furthermore, some entertainment companies for cruise ships (e.g. RWS Entertainment Group) have developed, under the guidance of public safety experts (e.g. CrowdRx), specific guidelines for both performers and the audience, in order to restart live entertainment activities in safety, some of which are reported here: online reservation system for the management of capacity in queue lines and seating areas, turnover and time among performances, sanitation treatments, air filtration systems or setting shows outdoors, subdivision of rehearsal spaces into individual zones, reduction of interaction between performers and guests, and keeping performers at a safe distance while showing the illusion of touch, *Seatrade Cruise Talks (2020)*. Lights and digital technologies can provide an additional contribution toward safety through interactive and ephemeral solutions, *Piardi et al. (2012)*. As an artwork for a social reflection in covid time, in 2020 the Korean artist Yiyun Kang showed an interactive projection mapping installation, 'Proxemics: drawing social bubbles', in which visitors were engaged in a real-time interaction with video-projections by drawing their own social bubbles. The artist intent was to make the visitors think about the relationship among user, others and the space around him, and to interrogate about the spatial dynamics in pandemic time, *Kang (2021)*. So, lights and digital technologies can intervene creating temporary and adaptive operations toward spaces, without modifying any element, and at the same time artistic and pleasant operations toward users.

In 2020 travel analysts predicted a phenomenon of 'revenge travel' in the tourist sector, including the cruise one, when tourism would have restarted after the countries shutdown for the covid emergency. This phenomenon would be driven on one hand by people feeling more comfortable with traveling,

due to a lower risk of infection when traveling, on the other hand by a desire of people to get away after a long period of travel restrictions. In addition, experts have predicted an increase in travel motivation toward relax and escape, and a traveller's behaviour toward flexibility and last-minute planning, *Shadel (2020)*. Though a resumption of cruise operations since mid-2020, not all cruise lines have restarted so far. As reported by The Association of Mediterranean Cruise Ports, *MedCruise (2021)*, here some cruise lines which have already restarted: Royal Caribbean Cruises since December 2020, MSC Cruises since January 2021, AIDA Cruises since March 2021, Costa Cruises since May 2021, Carnival Cruise Line, Celebrity Cruises, Crystal Cruises, Norwegian Cruise Line and Princess Cruises since July 2021, Disney Cruise Line only for UK residents, *MedCruise (2021)*.

Destinations will keep controlling COVID-19 negative tests or proof of vaccination, so cruise companies and travel agents are reflecting on traveling in the post-pandemic era. Private islands, exclusive destinations and revenue source for some companies, *Klein (2006)*, may become more popular in future, since they present a controlled environment during shore excursions. Other companies may prefer small and expedition ships, which provide shore excursions in more remote places, *CLIA (2020)*, *Coulter (2021)*.

Sustainability, health and safety represent the primary challenging management issues for cruise sector for the future of cruise travel, *Papathanassis (2017)*.

1.1. Theoretical framework

The cruise industry has recently recognized the importance of understanding how passengers feel the risk and that planning a strategy for a post-covid time becomes essential for a successful restart in cruise industry and in the tourism sector in general. The perception of the risk is proved to affect the travel decision-making and the destination choice of tourists, but unfortunately there is little scientific research about the risk perceptions in cruise holidays, *Holland et al. (2021)*. In relation to cruise travel, the perception of risk concerns especially infections outbreaks, sexually transmissible infections, motion sickness, cruise accidents, terrorism, piracy and crime. However, risk may be perceived differently according to the age, national culture, gender, personality traits, motivation to travel and past travel experience of each passenger, so it's important to target the intentions and preferences of each group of customers and to develop risk management plans onboard. In addition, an emerging category is the technological risk, which is often neglected and needs to be investigated in further research, *Le and Acordia (2018)*.

Regarding customer targeting, companies have recognized the value of customization, identifying the different needs of their customers and subsequently offering customized goods and services, or through additional components such as customized packaging, marketing materials, placement, terms and conditions, product names and stated use, *Pine II and Gilmore (1997)*. Smart technologies, through the acquisition of Big Data, may offer personalized services to each different kind of tourist, in order to enhance the travel experience, *Buhalis and Amaranggana (2015)*. However, the cruise sector still lacks on a critical analysis of the impact of smart technologies on cruise customers. The smart technologies onboard the new cruises may risk increasing inequalities in the definitions of gender, race, class and aging. As warned by several scholars, the design of a digital experience for a generic audience could result in some negative effects, like a frustration for some age groups during the use, *Dini et al. (2007)*, *Spallazzo (2012)*, an homogenization of cross-cultural diversity and specificity, *Barendregt (2012)*, a disadvantage for groups which for socio-economic status or ethnicity may use digital activities less intensively than their counterparts, and a gender stereotyping in the digital contents and activities, *Robinson et al. (2015)*. In this sense this research aims at stimulating cruise industry to consider the customers not as an 'ideal' or 'normal user' to configure, but as a user with specific features to preserve. In addition, the big amount of personal data collected by devices and sensors may represent a critical factor for customers in terms of privacy, safety, security and freedom, so that a correct management of personal data becomes a delicate and critical task when digital technologies are used. The definition of design principles may guide the development of smart technologies (and environments) toward more responsible solutions, some of which could be:

transparency (e.g. clearer information of the use and management of personal data), privacy (e.g. possibility by users of keeping some information private), hierarchy (e.g. communication proportionated to the severity and the source of the reference), value (e.g. a level of insight added to the data analysis), meaning (e.g. giving awareness to users about the mnemonic aspect of active sharing a public content) and presence (e.g. evaluation of the level of 'physical presence' related to users and provision of awareness about the digital-self), *Varisco et al. (2017)*.

In recent time interior spaces have disentangled from rigid categories of time and function, showing more flexible and fluid forms, which provide a functional and typological hybridization of spaces. So new spatialities have emerged, based on new behaviour models and sharing principles. In the tourism context, due to the increase of time travelling a year and to the transformation of mobility as a lifestyle, spaces have become flexible to adapt to different activities. In particular, the main motivations for travel have become equally work as well as leisure, generating so new phenomena of 'bleisure tourism', *Scullica and Elgani (2020)*. Furthermore, mobile technology has created a separation between the act of performing something and the place of performing, so that professional freelancers can work everywhere they can access to technology and any space can become potentially an office, *Scullica and Elgani (2019)*. In regard to the bleisure tourism, in 2021 the company MSC Cruises has launched a travel offer, called Smartworking@Sea, which allow passengers to perform smart working in specific spaces onboard, without losing the leisure and entertainment of a cruise travel, *Leggieri (2021), MSC Cruise Lines (2021)*.

With the emerging experience economy, companies have started to offer experiences, not only goods and services. Experiences are memorable events that a company stages, in a theatrical way, to engage him in an intrinsically personal way. Experience is not about entertaining customers, but engaging them, so that companies see their employees as performing on stage and drive them to act in a way that can engage their customers. In this sense companies have encompassed theatre as a model for performance in staging experiences and so spaces can be set in six areas, as in a theatre: backstage, stage, auditorium, proscenium, entrance, and exit. Stage, proscenium and auditorium represent the focal areas of the experience; backstage areas, not visible by customers, can be designed only for functionality; the entrance and the exit are helpful for the introduction and the reinforcement of the experience, *Pine II and Gilmore (1999)*. Traditional spatial strategies for defining the relationship among environment, coverings and users are no longer sufficient to describe new spatialities as a result of the theatricalisation of spaces as new stages of experience and their hybridisation with new smart technologies, so they need more categories of analyses for a clearer understanding of the development of interior spaces.

2. Methodology

The traditional spatial strategy for the distribution of furniture and coverings in space, such as either on base surface (i.e. floor) or on overhead surface (i.e. ceiling, vault) or on vertical surface (i.e. wall, column) or above the furniture surface (i.e. table, chair, cabinet), *Higgins (2015)*, is integrated by the new categories of spatial layout gained by the theatre model and by the new dimensions of immersivity and portability offered by new technologies. Based on an adaption of the six areas of the theatre model, the spatial strategy for layout includes the entrance/exit (e.g. reception, lobby, cashier's desk), the auditorium (e.g. dining, shopping, seats), the proscenium/stage (e.g. bar, kitchen, screen, stage) and the backstage (e.g. store, toilets). Based on an adaption of the taxonomy of virtual reality systems, *Muhanna (2015)*, technologies may be classified in no immersive (no digital interface), little immersive (e.g. hand-based, monitor-based), partially immersive (e.g. wall projectors, immersa-desk) and fully immersive (e.g. vehicle simulation, cave, binocular head based). In addition, based on an adaption of the technological embodiment continuum, *Flavián et al. (2019)*, technologies can be also classified in touchless or contactless stationary external device, stationary external device with need of touch, portable external device and wearable device. The technological development differentiates the contribution of technology towards health depending on that being low, medium/high or smart. In this sense, the technology continuum developed by the *Texas Assistive Technology Network (2002)* best explains the degree of complexity of electronic component assembly.

Cruise travel is a complex and all-inclusive tourism product which includes a central service and many peripheral heterogeneous services. The central service is onboard and involves travel, accommodation, catering and entertainment. The peripheral services are partly onboard, as the ship facilities (i.e. internet, lounge, laundry, sundeck, gift shop, library) and the additional services (i.e. boutiques, casino, photography, spa), and partly onshore, as itinerary and destinations planning, travel arrangements and transfers, ports and terminal embarkation and disembarkation, excursions, *Penco (2013)*. As a further response to the pandemic by cruise industry, a public document with recommendations on public health has been elaborated by experts in public health, infectious disease, biosecurity, epidemiology, hospitality, and maritime operations. This document supplies a list of recommendation, which are considered as the most effective, scientifically sound ways to make the cruise experience healthier and safer. These recommendations can be summarized in health-related services offered by cruise ships during travel: testing, screening & exposure reduction, sanitation & ventilation, response, contingency planning & execution, destination & excursion planning, mitigating risks for crew members/passengers, *Healthy Sail Panel (2021)*.

The research methodology is based on a qualitative analysis of case studies and aims to answer the following research question: how can smart technologies improve the health safety in spaces on board during the cruise travel?

2.1. Case studies

Case studies have been collected in a theoretical sampling (Eisenhardt, 1989) based on a cluster including cases coming from cruise vessels with smart features and related to cruise risks limited to infections outbreaks, *Le and Acordia (2018)*. The sampling involves fifteen case studies from Cruise Industry and five from university courses on cruise design (BSc course in interior design at School of Design, Politecnico di Milano - AY 2019-20, AY 2020-21), which were collected from January 2020 to January 2021.

Table I: Case Studies Cluster

Cruise related risks				
Infections Outbreaks	Sexually Transmissible Infections	Motion Sickness	Cruise Accidents	Terrorism, Piracy and Crime
Source: Le & Acordia, 2018.				

Table II: Case Studies Collection

	Context	Case study	N.	Unit of analysis	Year	
	Company	Cruise Ship		Environment affected by technology		
INDUSTRY			01	Space equipped with Infrared Body Thermometer	2020	
			02	Space equipped with Contactless Sanitizer Dispenser	2020	
			03	Space equipped with intelligent sanitation UV-C light system (e.g. MRD light system)	2020	
			04	Space equipped with air filtration system (e.g. HEPA filters)	2020	
			05	Space equipped with HVAC system with ionization solution (e.g. Siemens NPBI)	2020	
			06	Space equipped with smart mobile temperature check (e.g. eCruise Health Check)	2020	
			07	Space equipped with smart health screening and temperature monitoring wristband (e.g. Zeeko zCare)	2020	
		Carnival Cruise Lines	Spirit	08	Space equipped with Panedia Cruiseabout VR headset	2016
		Celebrity	Edge	09	Space equipped with Access Tour app for smart mobile devices	2018
		MSC	Meraviglia	10	Space equipped with MSC for Me Wristband	2017
				11	Space equipped with Zoe Personal Assistant (e.g. smart speaker)	2017
		Princess cruises	Caribbean Princess	12	Space equipped with Ocean Medallion	2018
		Royal Caribbean Line	Oasis of the seas	13	Digital wayfinder	2009
		Royal Caribbean Line	Quantum of the Seas	14	Bionic bar	2014
				15	Space equipped with Expedition TW070	2014
ACADEMY	MSC Cruises (fictional projects 2-3-4-5)	Meraviglia (Connect to Greenline)	16	Pilates zone with reservation through smartphone app	2020	
		Meraviglia (SenSea)	17	Smart capsules	2020	
		Meraviglia (Digital Stadium)	18	Indoors with smart floor	2019	
		Meraviglia (Connect to Greenline)	19	Feel the cities	2020	
		Meraviglia (Odissea 2.0)	20	Thalassa	2020	

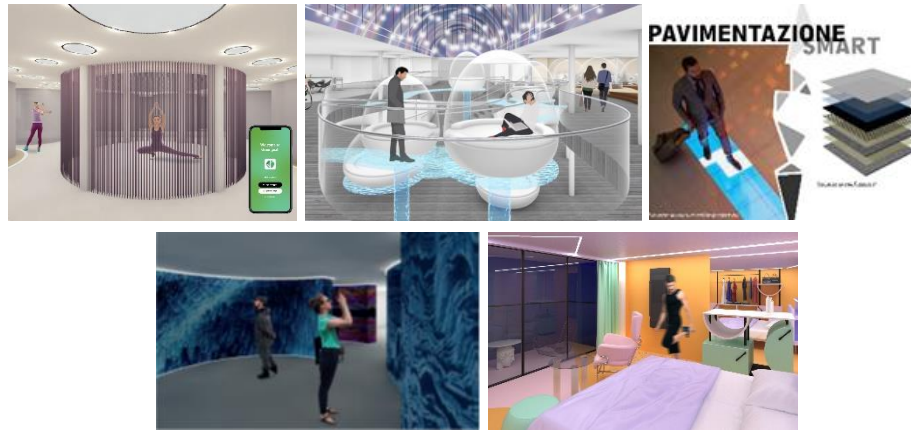


Fig.1: Selection of case studies from university activities: (a) Pilates zone, (b) Smart capsules, (c) Indoors with smart floor, (d) Feel the cities, (e) Thalassa.

Table III: Parameters for the case studies analysis

Technologies	Technological development						
	Low		Middle - High			Smart	
	Source: Adapted from Texas Assistive Technology Network, 2002.						
	Technological embodiment continuum						
	Touchless or contactless stationary external device		Stationary external device with need of touch		Portable external device		Wearable device
	Source: Adapted from Flavián et al., 2019.						
Spaces	Taxonomy of virtual reality systems						
	No immersive (no digital interface)		Little immersive (e.g. hand-based, monitor-based)		Partially immersive (e.g. wall projectors, immersa-desk)		Fully immersive (e.g. vehicle simulation, cave, binocular head based)
	Source: Adapted from Muhanna, 2015.						
	Spatial strategy for distribution						
	Base surface (i.e. floor)		Overhead surface (i.e. ceiling, vault)		Vertical surface (i.e. wall, column)		Above the furniture surface (i.e. table, chair, cabinet)
Services	Source: Adapted from Higgins, 2015						
	Spatial strategy for layout						
	Entrance / Exit (e.g. reception, lobby, cashier's desk)		Auditorium (e.g. dining, shopping, seats)		Proscenium / Stage (e.g. bar, kitchen, screen, stage)		Backstage (e.g. store, toilets)
	Source: Pine II & Gilmore, 1999						
Services	Cruise related services						
	Itinerary and destinations	Travel arrangements and transfers	Ports and terminals	Central service: travel, accommodation, catering, entertainment.	Additional services: boutiques, casino, photography, spa.	Ship facilities: internet, lounge, laundry, sundeck, gift shop, library.	Excursions
	Source: Penco, 2013.						
	Health related services						
Testing, screening & exposure reduction		Sanitation and ventilation		Response, contingency planning, & execution	Destination & excursion planning	Mitigating risks for crew members/passengers	
Source: Healthy Sail Panel, 2020.							

This paper reports the data collection and the analysis of case studies included in the theoretical sampling. However, this research is planned to have further steps: the validation of cases through the use of multiple sources of evidence (i.e. literature, archival documents, interviews and observations), the construction of a chain of evidence (i.e. research questions > data collection > data analysis > discussion > conclusions) and a review draft of case study report by key informants (i.e. cruise companies, design offices for cruise companies), Yin (2003).

The data collection has included low technologies for testing, screening and exposure reduction and health sanitation and ventilation of spaces onboard, represented by the infrared body thermometer, which provides a contactless temperature measurement, HoMedics (2020), and the contactless sanitizer dispenser, which dispenses sanitizer gel without touching it, unlike manual sanitizer bottles or foot-operated dispensers, Oakter (2020).

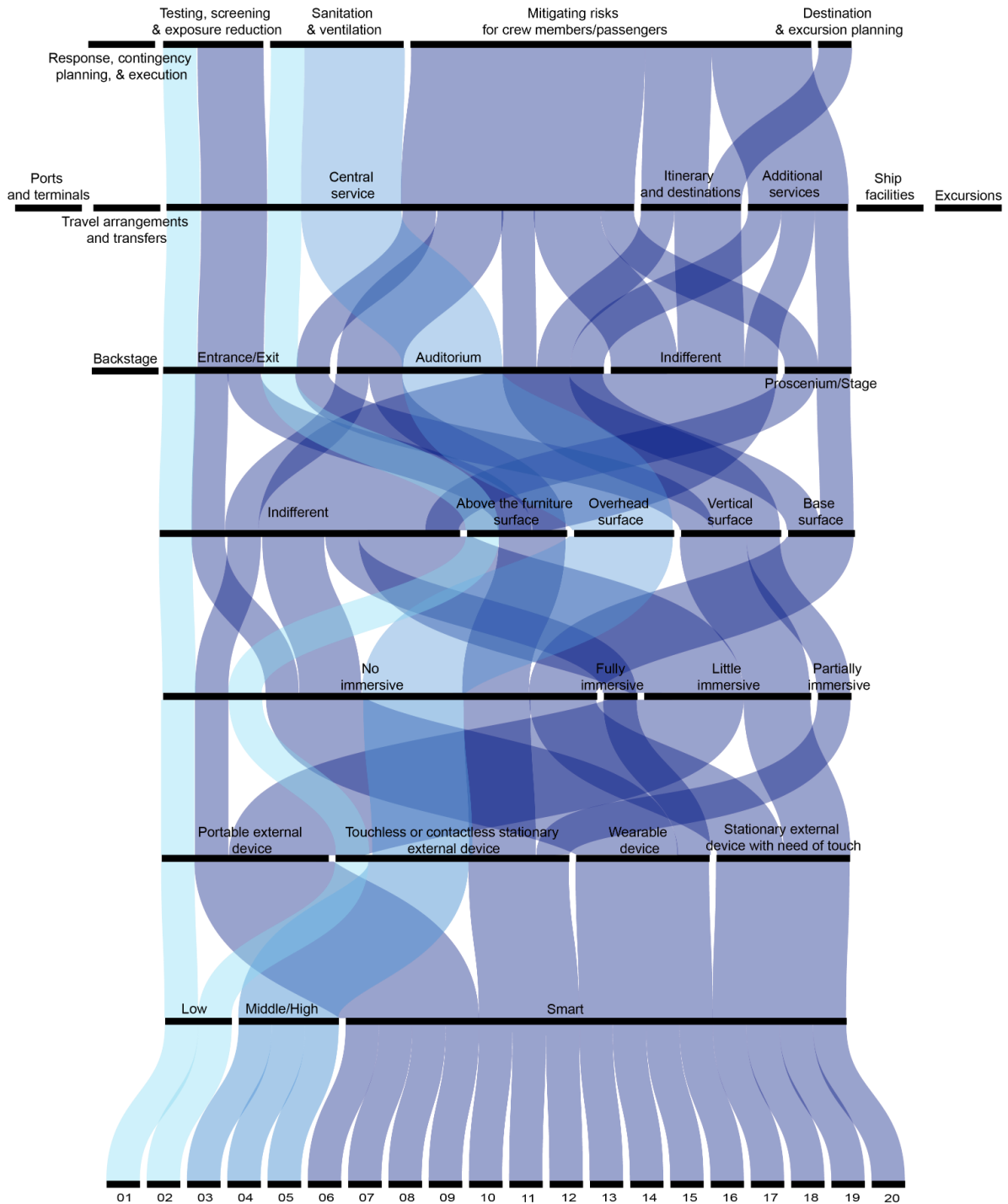


Fig.2: Diagram of case studies analysed for the relationship smartness and health safety

The data collection has included middle/high technologies for health sanitation and ventilation of spaces onboard, represented by the intelligent sanitation UV-C light system (e.g. MRD light system), which sanitize surfaces by shining light or UV directly onto the object, *MRD Lighting (2020)*, the high-efficient air filtration system (e.g. HEPA filters), which can help reduce air contaminants, including particles containing viruses, *Cartledge (2020)* and the HVAC system with ionization solution (e.g. Siemens NPBI), which can achieve constant treatment of both airborne and surface pathogens in ways that filtration alone cannot, *Giles (2020)*.

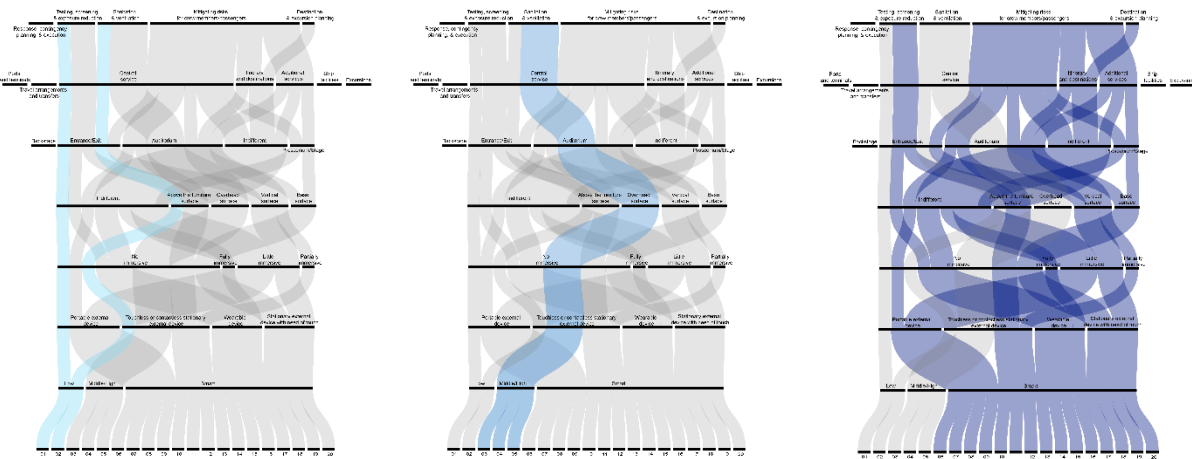


Fig.3: Diagrams of case studies analysed for the relationship smartness and health safety, according to low, middle-high and smart tech cluster.

Moreover, it has included smart technologies for healthier spaces onboard, which are represented by the smart mobile temperature check (e.g. eCruise Health Check), which is a tablet with a facial recognition system and a no-touch thermometer that acquire and transfer passenger's temperature data to the cruise medical system during check-in, *eCruise (2020)*, and the smart health screening and temperature monitoring wristband (e.g. Zeeko zCare), which monitors temperature and captures health parameters of customers continually, <https://gozeeko.com/zcare>. Other case studies are expressed by further smart technologies which can improve health in spaces onboard by mitigating risks for crew members and passengers, and by supporting customers in destination and excursion planning. These technologies involve Panedia Cruiseabout VR headset, which allows customers to look at immersive videos of spaces, so offering them a virtual onboard tour, *Lennon (2016)*, the Access Tour app for smart mobile devices, which offer to passengers an augmented reality tour of the cruise ship with *binaural* audio and soundscaping, *Cruise Industry News (2018)*, the MSC for Me Wristband, which through NFC technology permit the passenger's identity and position recognition and a dedicated check of safety systems on board, *MSC Cruise Lines (2020)*, the Zoe Personal Assistant, which is a smart speaker with a multilanguage AI system able to supply information about on board services, guidance and suggestions or to help in booking a service, *Mathisen (2019)*, the Ocean Medallion, which is a small disk made of two sensors and a battery capable to contactless operations, as cabin door opening, payment, order of food and drinks, location recognition and other services, *McDonald (2019)*, the digital wayfinder, which is often located in the elevator lobbies of most ships and offers guests information about what ship events, ship travel and restaurant information, *Hochberg (2015)*, the bionic bar, that provides a robot bartender, to which passengers can order mixed drinks by using tablets, *Silverstein (2020)*, and the Expedition TW070, which is an app for smart mobile devices, able to offer AR gaming experience in spaces onboard, *Twangster (2020)*. Cases from university show possible scenarios for design of cruise spaces onboard, so stimulating cruise companies toward further solutions and helping research in analysing fields not yet much explored. Academic cases include a pilates zone accessible with reservation through smartphone app (project MSC Meraviglia - Connect to Greenline, 2021), smart capsules which offer private smart experience of entertainment to passengers (project MSC Meraviglia – SenSea, 2021), indoors with smart floor, which can detect the position and movement of customers for safety, consumer tracking and data collection purposes (project MSC Meraviglia – Digital Stadium, 2020), a space with video-projections on walls, which offer an immersive virtual tour of cruise destinations (project MSC Meraviglia - Connect to Greenline, 2021), a cabin equipped with a touch screen display and a patented digital weight system with sensors (e.g. Tonal) for a smart fitness experience (project MSC Meraviglia – Thalassa, 2021).

3. Findings and discussion

Case studies show a variety of solutions for health management onboard. The cases' collection

demonstrates that the cruise sector is experimenting many smart technologies, offering different health related services. Case studies with low technologies display an almost coherent behaviour through the several parameters of analysis, focusing on testing, screening & exposure reduction and sanitation & ventilation service, all related to central service, located in entrance/exit area and with no property of immersion. Case studies with middle-high technologies show a coherent behaviour through the several parameters of analysis, focusing on the sanitation and ventilation service, locating in the auditorium area of spaces and overhead surfaces, and with technologies offering no immersive experiences and touchless or contactless interaction. Cases with smart technologies show a more varied behaviour through the several parameters of analysis, revealing a diffuse use in the various areas of layout of spaces, different configurations on the surfaces in the space, different level of immersion and different technological embodiment for customers. In particular, portable and wearable technologies often cannot be categorized in spatial strategy parameters, since they are capable to be carried or moved. However, these technologies are linked to space due to their capacity of communicating to the surrounding environment through sensors and IoT applications. Blank gaps in the clusters indicate that there are other potential areas to explore, either through independent research or by drawing from other disciplines. In addition, academic design projects confirm the effectiveness of smart technologies in improving the health safety of travel on board and their versatile attitude to respond to multiple tasks.

4. Conclusions

The covid-19 pandemic has exposed many weak aspects of cruise industry and has generated a great debate on environmental and health issues in the sector. Despite the travel restrictions and economic losses, the pandemic has created a great opportunity for cruise companies to rethink their corporate culture, their business models and their human resources management, and to adopt new risk management strategies and concrete sustainable development actions, *Belda Font (2021)*. In this context, technology has played an important role, transforming cruise spaces and guest services onboard toward smarter versions. Since the resumption of cruise travels, touchless and contactless technologies have supported many operations from embarkation to safety operations and on-demand services, including new applications onboard, as the biometric facial recognition, contactless health screening and new types of security scanners. Even the shore excursions have been changed by the introduction of digital technologies which can enhance the experience by providing further information, *Bond (2021)*. The new technologies are revolutionizing the live entertainment sector by including the use of virtual and augmented reality, which potentially reduce the risk of infection, and the offer of immersive experiences, which can engage passengers into all five senses, *Payne (2021)*. Furthermore, smart technologies support a spread use of touchless and contactless operations in different areas and services on cruise ships, so mitigating the risk of infection too.

The evolution of technologies implies opportunities and, at the same time, the appearance of critical factors, such as the management of personal data and the development of a responsible technological innovation. So, cruise industry innovation should not be merely technology-driven but lead by a responsible attitude. A responsible innovation must be (ethically) acceptable, so respecting the right for privacy and data protection, sustainable, so contributing to the sustainable development of the sector according to economic, social, and environmental dimensions, and socially desirable, so enhancing the quality of life and the equality among men and women. In this context, the use of technology assessment and technology foresight can be very helpful for cruise companies in building a real responsible innovation, *Von Schomberg (2013)*.

References

- ARMANI, A.M.; HURT, D.E.; HWANG, D.; MCCARTHY, M.C.; SCHOLTZ, A. (2020), *Low-tech solutions for the COVID-19 supply chain crisis*, *Nature Reviews Materials* 5(6), pp.403-406
- BARENDREGT, B. (2012), *Diverse Digital Worlds*, *Digital Anthropology*, Routledge

- BELDA FONT, C. (2021), *Will the pandemic provide an opportunity for positive change in the cruise industry?* Equal Times, <https://www.equaltimes.org/will-the-pandemic-provide-an>
- BOND, M. (2021), *Technology driving the agenda*, Seatrade Cruise Review, June, <https://www.seatrade-cruise.com/seatrade-cruise-review/seatrade-cruise-review-june-2021-issue>
- BUHALIS, D.; AMARANGGANA, A. (2015), *Smart Tourism Destinations: Enhancing Tourism Experience Through Personalisation of Services*, Information and Communication Technologies in Tourism 2015, pp. 377-389
- CARTLEDGE, G. (2020), *Can technology answer the current COVID-19 challenge?*, Seatrade Cruise Review, September, <https://www.seatrade-cruise.com/resources/seatrade-cruise-review-september-2020-issue>
- CLIA (2020). *2021 State Of The Cruise Industry Outlook*, https://cruising.org/-/media/research-updates/research/2021-state-of-the-cruise-industry_optimized.pdf
- COULTER (2021), *The Future of Cruises and the Cruise Industry, 2022 and Beyond*, Cruise Critic, <https://www.cruise critic.co.uk/articles.cfm?ID=5908>
- CRUISE INDUSTRY NEWS (2018), *Celebrity Rolls Out Edge Access Tour App*, <https://www.cruiseindustrynews.com/cruise-news/19975-celebrity-rolls-out-edge-access-tour-app.html>
- CRUISE INDUSTRY NEWS (2020), *Easy Health Screening, No-Touch Thermometer Readings from eCruise*, <https://www.cruiseindustrynews.com/cruise-news/22656-easy-health-screening-no-touch-thermometer-readings-from-ecruise.html>
- DINI, R.; PATERNÒ, F.; SANTORO, C. (2007), *An environment to support multi-user interaction and cooperation for improving museum visits through games*, Mobile HCI
- eCRUISE, S. (2020). *Right On Time: ECruise's Integrated Health Systems*, Cruise Industry News: Return to Service, September, <https://www.cruiseindustrynews.com/cruise-news/23475-cruise-industry-news-launches-return-to-service-publication.html>
- EISENHARDT, K.M. (1989), *Building Theories from Case Study Research*, The Academy of Management Review 14(4), pp.532-550
- FLAVIÁN, C.; IBÁÑEZ-SÁNCHEZ, S.; ORÚS, C. (2019), *The impact of virtual, augmented and mixed reality technologies on the customer experience*, J. Business Research 100, pp.547-560
- GILES, R. (2020), *Reducing the spread of airborne and surface pathogens for Cruise Ships*, Cruise Industry News: Return to Service, September, <https://www.cruiseindustrynews.com/cruise-news/23475-cruise-industry-news-launches-return-to-service-publication.html>
- HEALTHY SAIL PANEL (2020), *Recommendations from the Healthy Sail Panel*, <https://nclhltdcorp.gcs-web.com/static-files/5492d5db-6745-4b21-b952-49d3639f6e79>
- HIGGINS, I. (2015), *Spatial Strategies for Interior Design*, Hachette UK
- HOCHBERG, M. (2015), *Spotted: Expanded functionality Wayfinders on Anthem of the Seas*, <http://www.royalcaribbeanblog.com/2015/10/28/spotted-expanded-functionality-wayfinders-anthem-of-the-seas>
- HOLLAND, J.; MAZZAROL, T.; SOUTAR, G.; TAPSALL, S.; ELLIOTT, W. (2021). *Cruising through a pandemic: The impact of COVID-19 on intentions to cruise*, Transportation Research

Interdisciplinary Perspectives

HOMEDICS (2020), *HoMedics Non-Contact Infrared Body Thermometer*, Costco Wholesale, <https://www.costco.com/homedics-non-contact-infrared-body-thermometer-.product.100688062.html>

KANG, Y. (2021), *Proxemics: Drawing Social Bubble*, <https://www.yiyunkang.com/proxemics>

KLEIN, R.A. (2006), *Turning water into money: The economics of the cruise industry*, *Cruise Ship Tourism*, pp.261-269

LE, T.; ARCODIA, C. (2018), *Risk perceptions on cruise ships among young people: Concepts, approaches and directions*, *Int. J. Hospitality Management* 69, pp.102-112

LEGGIERI, A. (2021), *Fair working, la nuova frontiera del lavoro sperimentata da Paeda & Associati*. Forbes, <https://forbes.it/2021/02/17/fair-working-nuova-frontiera-paeda-associati/>

LENNON, M. (2016), *Step onboard your cruise ship before you step onboard*, *Cruise Advice*, <http://www.cruiseadvice.com.au/2016/02/step-onboard-cruise-ship-step-onboard/>

MATHISEN, M. (2019), *MSC Unveils Zoe Virtual Personal Assistant*, <https://www.cruiseindustrynews.com/cruise-news/20319-msc-unveils-zoe-virtual-personal-assistant.html>

McDONALD, D. (2019), *Ocean Medallion by Princess Cruises: Guide and Review*, *Cruisewith*, <https://cruisewith.co.uk/cruise-advice/ocean-medallion-by-princess-cruises/>

MEDCRUISE (2021), *MedCruise data: Cruise Operations restart & Cruise ships lay-up*, *MedCruise*, <https://www.medcruise.com/medcruisedata>

MRD LIGHTING (2020), *Intelligent Germicidal Solutions*, *MRD Lighting*, <https://www.mrdlighting.com/intelligent-germicidal-solutions>

MSC CRUISE LINES (2020), *Travel agents handbook*, https://www.mscbook.com/pages/sdl/img/B2B_TA_25012_02_MSC_FOR_ME_PHASE_2_BOOKLET-UK.pdf

MSC CRUISE LINES (2021), *Smartworking in crociera*, <https://www.msccrociere.it/offerte-crociera/smartworking-in-crociera>

MUHANNA, M. (2015), *Virtual reality and the CAVE: Taxonomy, interaction challenges and research directions*, *J. King Saud University, Computer and Information Sciences* 27, pp.344-361

OAKTER (2020), *Contactless Sanitizer Dispensers: Features to Look For & How to Buy*, *Oakter*, <https://oakter.com/blog/contactless-sanitizer-dispensers/>

PAPATHANASSIS, A. (2017), *Cruise tourism management: State of the art*, *Tourism Review* 72(1), pp.104-119

PAYNE, H. (2021), *Entertainment is evolving. Holly Payne explores the future of on board performances*, *Seatrade Cruise Review*, <https://www.seatrade-cruise.com/publications/seatrade-cruise-review-april-2021-issue>

PENCO, L. (2013), *Il business crocieristico: Imprese, strategie e territorio*, F. Angeli

PIARDI, S.; PASINA, I.; TIEGHI, S. (2012), *Reflections on the sidelines of a shipwreck*, 17th Int. Conf. Ships and Shipping Research

PINE II, B.J.; GILMORE, J.H. (1997), *The four faces of mass customization*, Harvard Business Review, pp.91-101

PINE II, B. J.; GILMORE, J. H. (1999), *The Experience Economy*, Harvard Business Press

PRINCESS CRUISES (2018). *Princess Cruises: Princess MedallionClass®*, <https://www.princess.com/ships-and-experience/ocean-medallion/>

ROBINSON, L.; COTTEN, S.R.; ONO, H.; QUAN-HAASE, A.; MESCH, G.; CHEN, W.; SCHULZ, J.; HALE, T.M.; STERN, M.J. (2015), *Digital inequalities and why they matter*, Information, Communication & Society 18(5), pp.569-582

SCULLICA, F.; ELGANI, E. (2019), *Living, Working and Travelling: New Processes of Hybridization for the Spaces of Hospitality and Work*, FrancoAngeli

SCULLICA, F.; ELGANI, E. (2020), *Time. Hybrid Spaces for Users-Bodies between Work and Hospitality*, Mind and Places, A Multidisciplinary Approach to the Design of Contemporary City. (Vol. 4), Springer

SEATRADE CRUISE TALKS (2020), *Been There, Done That: Live Entertainment in a Pandemic*, <https://youtu.be/N8q8SBHHdxM>

SHADEL, J.D. (2020), 'Revenge travel' is the phenomenon that could bring back tourism with a bang, Washington Post, <https://www.washingtonpost.com/travel/2020/07/29/revenge-travel-is-phenomenon-that-could-bring-back-tourism-with-bang/>

SILVERSTEIN, E. (2020), *Robot Bartender at the Bionic Bar on Royal Caribbean Cruises (Plus Menu)*, <https://www.cruisecritic.co.uk/articles.cfm?ID=2454>

SPALLAZZO, D. (2012), *Mobile technologies and cultural heritage: Towards a design approach*, LAP Lambert Academic Publishing

TEXAS ASSISTIVE TECHNOLOGY NETWORK (2002), *Taking a Closer Look at Assistive Technology Devices*, Considering assistive technology in the development of the IEP: A training module in the Assistive Technology, https://assistedtechnology.weebly.com/uploads/3/4/1/9/3419723/assistive_technology_devices.pdf

TWANGSTER (2020), *Spotted: Augmented reality game on Anthem of the Seas*, Royal Caribbean, <http://www.royalcaribbeanblog.com/2020/01/13/spotted-augmented-reality-game-anthem-of-the-seas>

VARISCO, L.; PILLAN, M.; BERTOLO, M. (2017), *Personal digital trails: Toward a convenient design of products and services employing digital data*, 4D Designing Development Developing Design

VON SCHOMBERG, R. (2013), *A Vision of Responsible Research and Innovation*, Responsible Innovation, John Wiley & Sons, pp.51-74

YIN, R.K. (2003), *Case Study Research: Design and Methods*, SAGE Publications

Ship Design: Gameplay Matters!

Alan Guégan, Sirehna, Bouguenais/France, alan.guegan@sirehna.com

Quentin Rathier, Sirehna, Bouguenais/France, quentin.rathier@sirehna.com

Léa Lincker, Sirehna, Bouguenais/France, lea.lincker@sirehna.com

Charles-Edouard Cady, Sirehna, Bouguenais/France, charles-edouard.cady@sirehna.com

Abstract

*Designing a ship consists in achieving a delicate balance between many entangled, conflicting constraints. The inherent complexity of the design process cannot be reduced, but we believe that software tooling can ease the task of the naval architect - making complexity easier to address, if not simpler. To this aim, we have taken inspiration in the Lean Startup principles and developed an early-stage ship design tool called ShipBuilder. Our original intuition was that a lightweight, easy-to-use ship sketching tool could speed up the early stages of the design process significantly, as compared with existing practice. In this talk, we show how our vision was confirmed with hypotheses, MVPs, user feedback, pivots, all terms that can be found in Eric Ries' 2011 bestseller *The Lean Startup*. The result is a ship sketching tool with professional naval architecture features, that requires limited onboarding effort and offers a carefully crafted "gameplay" to ship designers.*

1. Introduction: facilitating early-stage ship design

Operational capability, as defined by the ship owner, is the prime driver of a ship's design. The role of a ship designer is to ensure that the vessel is able to deliver the operational capability while satisfying a number of other criteria such as cost, feasibility, seaworthiness or safety. Evans synthesized the ship design process by introducing the design spiral, *Evans (1959)*. The various criteria are evaluated one after the other in a convergent process that spirals inwards from early-stage concept studies to detailed design stages.

In practice, it is not uncommon to consider several alternatives during the early-stage design phase, Fig.1. A complete loop is run for each alternative, even if a single design will be worked in more detail eventually. All the criteria making up every ship alternative are evaluated, at least roughly, in order to choose the best of all explored concepts.

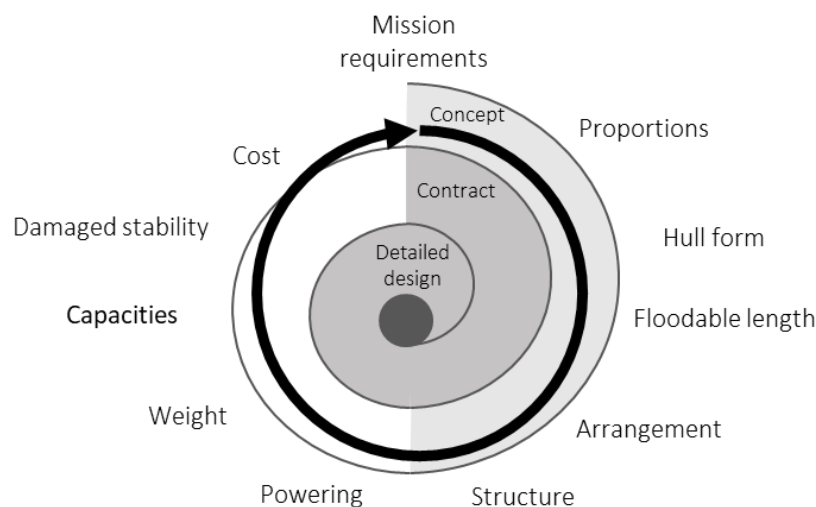


Fig.1: The design spiral, *Evans (1959)*. The thick arrow represents one early-stage iteration, where all the criteria characterizing the ship are evaluated (albeit not in great detail) to elaborate the best possible concept.

In a competitive context, it is vital for a shipbuilder to propose the best concept in the shortest possible time. Ship design tools that have been developed for detailed design phases have been optimized for other purposes – essentially, they focus more on delivering accurate evaluations and detailed models rather than on building coarse models very quickly.

When we set out to develop an early stage design tool, we had the intuition that a tool dedicated to ship sketching would allow ship designers to model the basic features of a ship very quickly and easily, and to evaluate concept ships in a very short time, although in a coarse level of detail.

We considered 3 options for designing the tool:

- Option 1: start from an existing CAD tool, specialized in ship design or not, and implement an “early-stage design” plugin. The plugin would restrict the broad range of features natively available to provide a reduced, easily manageable set of features. The advantage is that model formats, geometric operations, model management features are readily available. However, the single fact that a full CAD environment has to be installed beforehand means it will be harder to access which is why we decided to drop this option.
- Option 2: specify the expected features of an easy-to-use ship sketching tool, then implement, test and deploy the tool. This “waterfall” approach has the advantage that the development scope is defined beforehand; the work can be scheduled a priori, and the project can be managed with a standard cost/quality/delay project management approach. However, at the very beginning of the project in 2016, we felt uneasy specifying features a priori, let alone prioritizing them. To which level of detail shall the models be implemented? Shall users be allowed to edit hull shapes? In which ways? This led us to consider agile development as a third option.
- Option 3: develop features incrementally and leverage user feedback to guide and prioritize the work continuously. In our case, the advantages are many: work can start immediately, on the most basic features; user value is generated incrementally from day 1, with the most valuable features being developed first; the risk to develop useless features is limited, since every feature is developed to, at least, be used right away. We chose to apply option 3 – agile development.

The next two sections provide some background on the method and illustrate a few of the steps we have taken on our journey to a functional early-stage ship design application. Opting for agile methods had an unexpected benefit: spending time with our users and building the application together shifted our focus from implementing features to developing an experience. Looking back, much of our effort was guided by gameplay. We discuss this collateral benefit of the method in the last section.

2. Applying the lean startup principles

2.1. The Lean Startup

In 2011, Eric Ries published what has become a bestseller titled “The Lean Startup”, *Ries (2011)*. Inspired by years of experience in digital startups, the book describes a method to develop creative businesses in a context of extreme uncertainty.

Acknowledging the difficulty of setting up a robust business plan in an unknown – emerging – business environment, Ries claims that the main goal of a startup is to generate knowledge about its environment rather than execute a predefined business plan. The Lean Startup can be read as a handbook for those aiming at creating disruptive businesses and products, with a number of concepts that can be readily applied to a wide variety of domains.

The core of the process is synthesized in Fig.2. The basic principle is to build the product incrementally, and use every release to gather user feedback. User feedback is then used to steer the development of the business (and of the product). The process is applied with a focus on formalized assumptions; Minimal Viable Products (MVP); unbiased (and whenever possible, quantified user feedback).

Assumptions are used at each iteration to formalize the learning into a hypothesis that is specific enough to be built and tested. MVPs designate the increment of the product that can be built in the minimal amount of time, to test the assumption with product users. The focus on execution speed at product-grade quality is the major criterion at this stage. Unbiased user feedback is gathered in a number of ways that depend on the product and business. A/B testing is one such way to obtain objective feedback from the community: two different MVPs are implemented and rolled out to random users to measure the traction of each option.

The canonical concept of pivot states that, when an assumption has been proven wrong, the team shall consider substantial changes in its understanding of the business. When it is pivoting, a startup shall consider substantial changes in the product, the assumptions, and maybe the measure of user feedback.

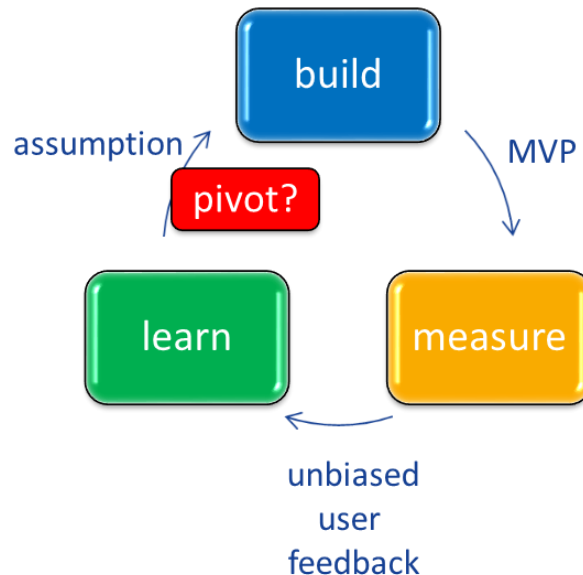


Fig.2: Sketch of the Lean Startup process

2.1.1. The early-stage ship design project

At the very beginning of the project, we set up a small team that comprised a design engineer, a software developer and occasional contributors. The vision of the team was that:

A ship designer with a lightweight sketching app could run early-stage design loops extremely fast, increasing her chances to hit the best possible design.

The development of the tool started in 2018 with the collaborative research project HOLISHIP and it received later funding by Naval Group and Naviris. The version of the tool implemented in the context of HOLISHIP was described, for instance, in LE NENA (2021); the application has undergone a complete makeover, as described in section 3.4, since the project ended by the end of 2020. The development of this new version is still ongoing.

The community of stakeholders and users evolved during the project. It included HOLISHIP partners at the beginning of the project, and now consists mostly of naval architects from Naval Group and Naviris.

The “measure” stage of the Lean Startup process, Fig.2, is regularly amended with interviews and applications of ShipBuilder to existing ships. Users are asked to show and describe how they use the tool (“I designed the ship from the keel up”, “I use the side and top views more than the front view”, “I found it difficult to work with 0.1m cells in z”,...). The two main ways to improve user experience

emerge at this stage, namely the need for additional features (e.g., be able to evaluate a center of buoyancy) and ease-of-use (e.g., fix a confusing layout).

The “learn” stage is when team work is the most intense. Every two or three weeks, users and developers meet to elaborate a workplan for the next iteration. The goal is to formalize the learning by explicitly prioritizing features from the backlog and trying to strike the best balance between:

- usability (friction removed),
- capability (additional features),
- implementation time (short term),
- technical debt (sustainability of the development).

The first two bullet points are about user value; the last two are about implementation costs.

The “build” stage is when the workplan is implemented. The development team implements features as described in the “learn” stage, so that the added value for users can be measured within two or three weeks.

All this process is supported by an extensive use of continuous integration. Every feature starts as an entry in the issue tracker of Gitlab; we use Milestones to prioritize issues; every implementation starts in a feature branch connected to the original issue, and ends with a merge in the master branch. Developments are thoroughly tested and proofread and deployment is automated, to guarantee the quality of the application.

Section 3 describes the main stages the application went through. The assumptions, the application and the feedback from users are described at each step.

3. The steps to a fully-fledged early-stage design tool

3.1. MVP1, a silhouette sketcher

The very first assumption was directly inspired from the vision that we wanted to develop a lightweight application for designing ships. We had some experience with web technologies and knew that a web page would be a good candidate for a simple, versatile design application. The team had general, however limited, insights about ship design: our prime goal was to involve users in the development of the application.

As far as we knew at this stage, the visual aspect of the ship was a cornerstone of the work of naval architects. We had not built a community of users yet, and we were beginners in geometric modelling. In order to start learning geometric modelling and have a starting point for conversations with ship designers, we took the following assumption as a starting point:

Assumption 1
Our lightweight ship design tool shall
offer a visual, editable display of a ship.

The first version we showed to a ship designer is displayed in Fig.3; let us call it MVP1 (for “Minimal Viable Product number 1”). The application is a web page with a large display area where the silhouette of a ship is displayed. Users can add decks to serve as a guide for placing “elements” – compartments or large equipment.

It was one of the first times we implemented an application with a visual display where objects could be dynamically modified. We put as little effort as we thought necessary in the user interface, but we made sure the assumption was verified. The decks are dynamically displayed and updated when users

change the parameters (number of decks, steerage), and the “elements” can be resized either by typing their parameters in text boxes or manually (drag & drop).

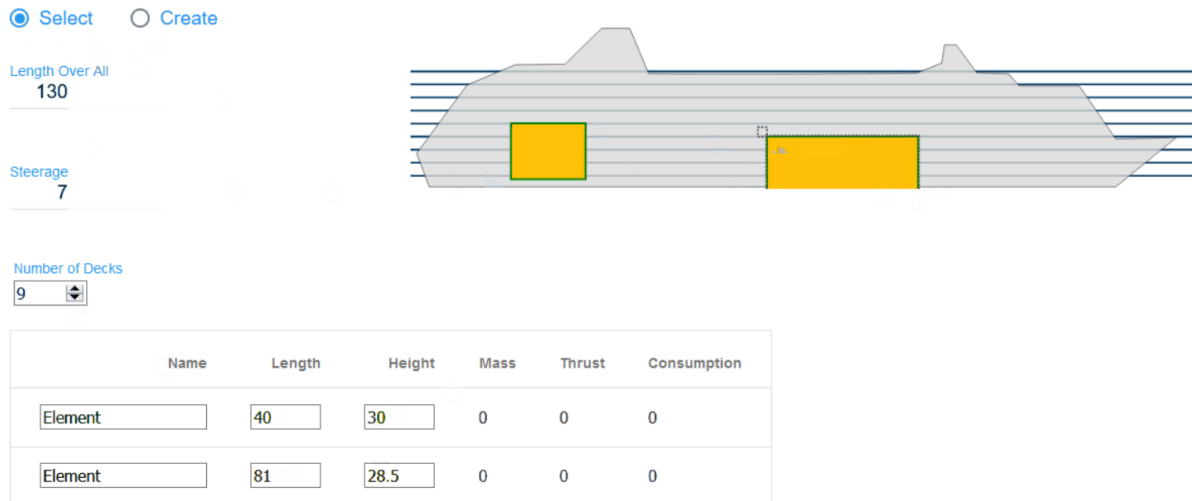


Fig.3: MVP1: the first version allows users to edit the general arrangement of the ship in 2D

We showed the application to a handful of ship designers. The feedback was negative: ships are 3D in nature, and the software was riddled with bugs and far off the quality standards of marketplace applications in terms of look and feel. Properly speaking, this first version was not a minimal viable product and the negative feedbacks were a clear call to improve the quality of our future releases – which we did.

Yet, we had achieved our first goal which was to *start conversations* with users. We had indications on what to implement next (3D modelling); this was our first learning. Also, a seed for the “build” environment had been sown: we had a first repository and a first continuous pipeline set for this project. We had set up a fragile yet complete build-measure-learn loop.

3.2. MVP2, a construction game

The feedback from MVP1 prompted us to go 3D. After we had found a few javascript libraries that supported 3D graphics, we decided to test a new assumption:

Assumption 2
Our lightweight ship design tool
shall support 3D models.

The second version of the tool is represented in Figure 4. Essentially, this version has the same features as the first one, with a large display area, parameters displayed in text boxes, and objects that could be edited by typing or from the graphical display area.

The main difference is that the user handles 3D objects. The objects are parallelepipeds – the simplest 3D objects that could be implemented to test assumption 2. For instance, the aviation hangar on the aft deck of the ship in Figure 4 is represented by a pink block. The general spirit of the application is that of a “construction game” where the ship is modelled as an aggregate of parallelepipeds.

The general aspect of the application has been improved a lot. Parameters have been grouped in thematic “workshops”, while in the first version, for instance, the number of decks appeared on the same page as the size of blocks. Each workshop has a specific tab with parameters related to one aspect

of the model; the size, center of gravity, density,... of each block are grouped in a single tab displayed in Fig.4.

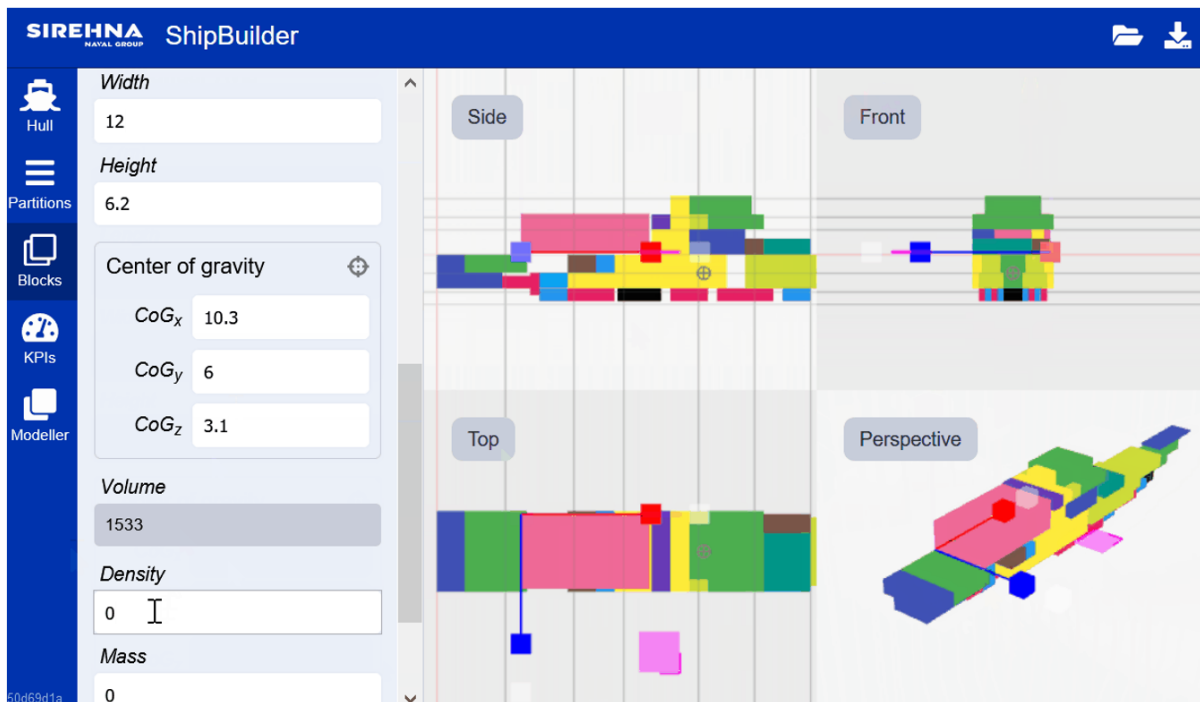


Fig.4: MVP2: the ship is modelled by an aggregation of parallelepipeds

The application that we now called ShipBuilder received better feedback from potential users. One of the partners in the HOLISHIP project called it “a space reservation tool”. We had also built a special relationship with one naval architect, who had developed an early stage ship design tool himself – on totally different grounds, though. He had found our approach interesting, but was still bothered by the absence of a hull below the ship. This led us to formulate the third major assumption.

3.3. MVP3, a construction game with a hull

It took a while before we decided to explore the third assumption, because we anticipated a lot of error-prone, mathematically challenging geometric calculations. Nevertheless, the feedback from our users was unequivocal about the absolute necessity for ships to be equipped with hulls, the size and shape of which should be adjusted to the mission and size of the vessel.

Assumption 3
Our lightweight ship design tool shall
support 3D models with adjustable hulls.

We set out to develop a simplified hull modeller, to be able to apply homotheties to a parametric representation of a hull. After several iterations with the users, the modeller had grown to include basic library management features, and transforms ranging from the well-documented prismatic coefficient adjustment with the *Lackenby (1950)* method to adjusting the LCB, the repartition of the volume between the aft and fore sections of the vessel, or the filling coefficient at the master cross section, Fig.5.

User feedback about the hull modeller was good. Once the base hull had been imported, the transforms were very easy to implement. However, the hull and the parallelepipeds representing the compartments were completely disconnected at the time. Unless the user took care of placing the blocks strictly inside the hull, the corners of the blocks would protrude from the hull, inducing a bias in the calculation of, e.g. the volume of the capacities.

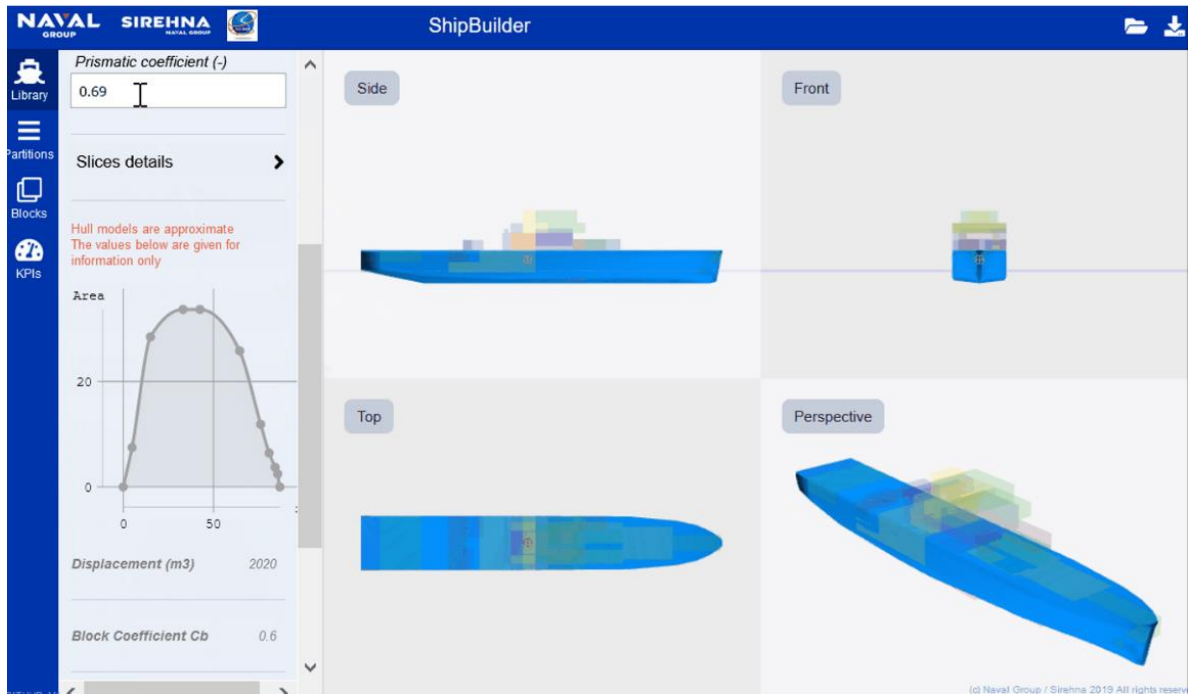


Fig.5: MVP3: ShipBuilder implements basic hull modeller and hull library management features. Users can import a hull of their choice and, e.g., adjust the prismatic coefficient. The area curve, the displacement and other parameters of the hull are updated in real time.

The users made it clear that they wanted to evaluate the volume of compartments and capacities within a few percents already in early-stage design. Protruding cubes did not provide a faithful representation of the compartments within the hull.

3.4. MVP4, trading bricks for cells

We used the feedback from our users to formulate the third assumption:

Assumption 4
Our lightweight ship design tool shall
intersect protruding blocks with the hull.

3.4.1 Pivoting

Once we had learnt how to handle, on the one hand, parallelepipeds, and on the other hand, an arbitrary 3D hull, it was not a huge challenge to intersect the former with the latter. Yet, the “construction game” paradigm had shown several limits, among which:

- The necessity to manage overlaps and voids between blocks, to make sure that the hull was filled 100% - not a percent more, not a percent less,
- The necessity to introduce a library of components (as a minimum: shapes) if we were to handle more complex shapes,
- The need to implement magnetism to align the blocks with the decks of the ship,
- The need for parametric deformation rules and parameters, in order to move the blocks consistently when a deck or a bulkhead is moved.

We knew that these features would take us a long time to implement, with an (uncertain) result that would in all cases be very similar to existing marketplace CAD software. We also knew that parametric CAD models take some time to build and maintain, which is inconsistent with our overall vision of a lightweight sketching app [to] run early-stage design loops extremely fast.

Since the beginning of the project, we had learned that the internal structure of many ships could be adequately represented with an orthogonal structure (horizontal decks, vertical bulkheads), but that the ship herself had smooth general shapes that were not directly connected to the internal structure, except for the main deck, the keel, the transom section. The orthogonal structure of the ship defines a number of cells, and, essentially, each compartment takes up one or more of these cells.

Instead of adding a new feature – intersecting the blocks with the hull – we decided to apply substantial changes to the way we modelled ships. We imagined splitting the entire space with cubic cells, then model the ship’s general arrangement by assigning cells to compartments, not bringing in independent parallelepipeds. This was a big change in the product (the application) but also required our users to change the way they modelled ships. By contrast with previous features, the change could not be incremental, and it was felt by the team as a pivoting moment in the design of ShipBuilder.

The advantages of this new approach are many:

- Overlaps and voids are prevented by construction,
- Compartments are sets of cells, and complex (even non-contiguous) shapes are obtained easily, by assigning a complex (not contiguous, maybe) pattern of cells to a single compartment,
- Blocks are aligned horizontally and vertically by construction (no magnetism needed),
- When the user changes the spacing between two lines of the grid, e.g. between two decks, the blocks above move in a coordinated, straightforward fashion, following the cells defined by the grid.

The main advantage of this new way to model ships is the ease with which decks, bulkheads, compartments can be modelled. The experience is close to that of popular construction videogames accessible to school kids.

3.4.2 MVP4

Recalling assumption 4 – that blocks shall be intersected by the hull – we complemented the new 3D modelling of the general arrangement with a feature that literally trimmed the cells that intersect the hull and kept only the inner part of the cell for all subsequent volume, mass and center of gravity calculations.

The modelling principles are displayed in Fig.6. Users assign cells to “areas” by clicking and dragging the cells in a 2D view of the ship, and the application aggregates and intersects the cells with the hull to generate elaborate 3D objects that can be displayed and used for calculations.

The feedback of our users was extremely positive. The modelling interface is easy to use, the 3D views can be generated in a few clicks, and a number of indicators can be calculated such as weights, volumes, surfaces, hydrostatics, ...

4. Discussion on agile methods, users and the gameplay

4.1 Agile methods

The experience we have had with agile methods shows that involving users during the development process is an absolute must. By involving users from day one, you create a shared experience and a shared ownership that bring value on the long term. Early users are happy to hear about and test the latest evolutions of the application, and they are pleased to provide insightful, valuable feedback on any occasion. Committed users can also be ambassadors and propagate the word-of-mouth about your tool.

Another advantage of involving users at every iteration in the development process is that features are developed incrementally: user value is accumulated in a continuous fashion, both with additional

features and removed friction (see section 2.1.1). Rather than rolling out a tool designed up-front with no user feedback, user value and user experience improve incrementally on every iteration.

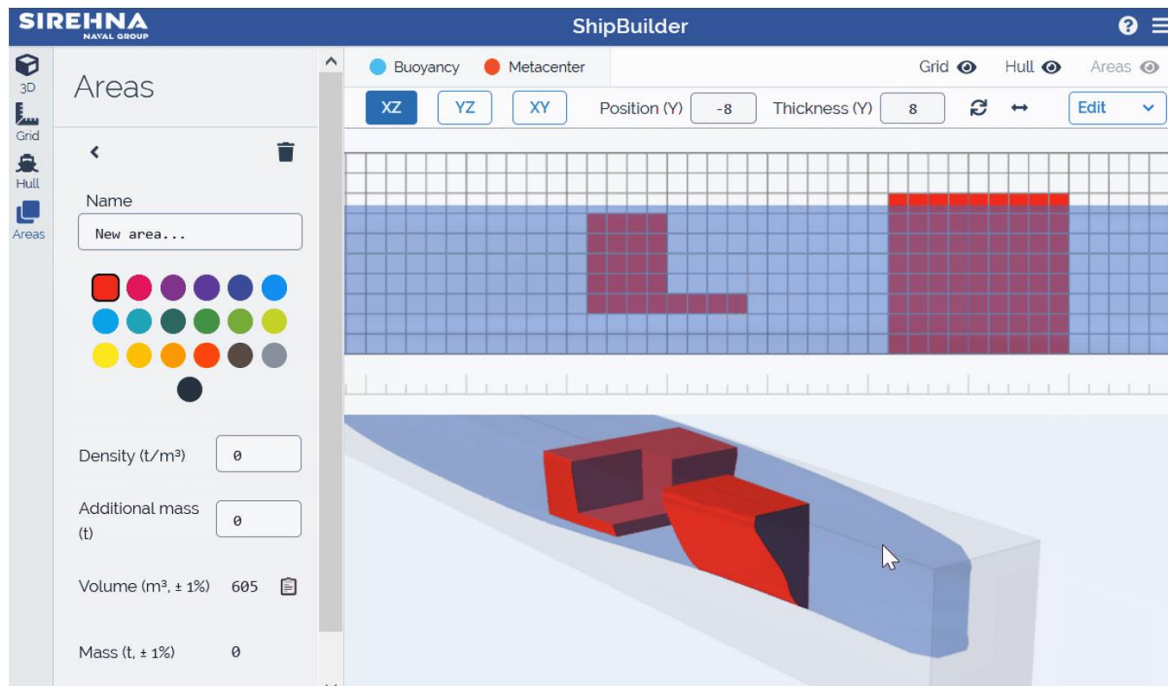


Fig.6: MVP4: cells from a predefined grid are assigned to the red “area” in the 2D top section of the display area. The cells assigned to the area are aggregated, intersected by the hull (blue), then displayed in 3D in the bottom part of the display area.

4.2 Gameplay

Gameplay is a generic term for qualifying the pattern of interactions between a player and a video game, and it plays a crucial role in user experience. The choices we made - consciously or unconsciously - improved the gameplay in four ways:

- Satisfaction: the ship designer receives immediate feedback on every design decision she made,
- Efficiency: MVP4 has dramatically improved design efficiency, by removing a number of hurdles in the modelling process,
- Immersion: the application speaks the language of naval architects, and key indicators go hand in hand with appealing views of the ship,
- Emotion: visualizing the ship’s internal structure intersected by the hull gives an undeniable feeling of achievement.

We have not had many opportunities to explore the social aspects often associated with a good gameplay. However, we hope that the versatility of our application will allow teams to update and evaluate ship models in the course of technical conversations and benefit collaborative work substantially.

4.3 Hand in hand with users

The interactivity that we eventually came up with is reminiscent of some video games, where entire worlds can be built with cubes. The result is a world made of voxels that has two major advantages: the building process is accessible to all (school kids soon become masters at creating cities and castles) and extremely flexible.

This modelling paradigm emerged after the design team had observed naval architects using the first

versions of the tool: the users had requested to be able to place blocks inside the ship, but the first action they took on a new model was to define an orthogonal structural grid with decks and bulkheads. The users had the perception that their job was like a construction game – which it is, when it comes to inserting an engine inside a propulsion room – but they had not perceived that, in the earliest design stages, designing the general arrangement could be seen as assigning functions to pre-existing cells delimited by decks and bulkheads.

The traditional paradigm is that users need to learn how to use software applications. Our ambition was to minimize the efforts of the users and to adapt the software to the user. The team applied agile methods to learn what users needed (not what they wanted). The result is a ship sketching application with an easy-to-use modelling interface, appealing views and reliable naval architecture calculations designed to unleash creativity.

Acknowledgements

HOLISHIP received funding from the European Union’s Horizon 2020 research and innovation programme under grant agreement No [689074])

References

EVANS, J.H. (1959), *Basic Design Concepts*, J. American Society of Naval Eng. 71/4, pp.671-678

LACKENBY, H. (1950), *On the systematic geometrical variation of ship forms*. Transactions of RINA, 92, pp.289-316.

RIES, E. (2011), *The lean startup: How today's entrepreneurs use continuous innovation to create radically successful businesses*, Crown Business

LE NENA, R.; CALVIGNAC, J.; GUEGAN, A. (2021), *Design of a Multi-Purpose Ocean Vessel, A Holistic Approach to Ship Design Vol. 2: Application Case Studies*. Springer

A Standardized Sensor Naming Method to Support Digital Twins and Enabling New Data Driven Applications in the Maritime Industry

Steinar Låg, DNV, Oslo/Norway, steinar.laag@dnv.com
Vidar Vindøy, DNV, Oslo/Norway, vidar.vindoy@dnv.com
Kristian Ramsrud, DNV, Oslo/Norway, kristian.ramsrud@dnv.com

Abstract

In the absence of standards, ship owners, shipyards and vendors have had to settle for proprietary methods to tag sensors associated with ship equipment and systems. This has made it difficult to get structured overviews of the data and been a barrier to fleet-wide analysis and development of new applications. This paper presents a standardized sensor naming scheme, developed by DNV, utilizing the Vessel Information Structures (VIS) - an information model maintained since 2005 to support classification services. The paper presents the developed sensor naming scheme, its role in the ISO 19848 standard and a new web-based sensor naming tool supporting users.

1. Introduction

Sensor data from ships is playing an increasingly important role in ship operations. Many different on-board systems are generating data for automation and decision-support, primarily for dedicated on-board use but to an increasing extent also sent to shore utilizing capable and affordable connectivity options. Over the last years, all maritime players have made significant investments in digitalization, however pilots projects have shown that there are still barriers against sharing and efficient use of such sensor data in new applications, Låg and With (2017).

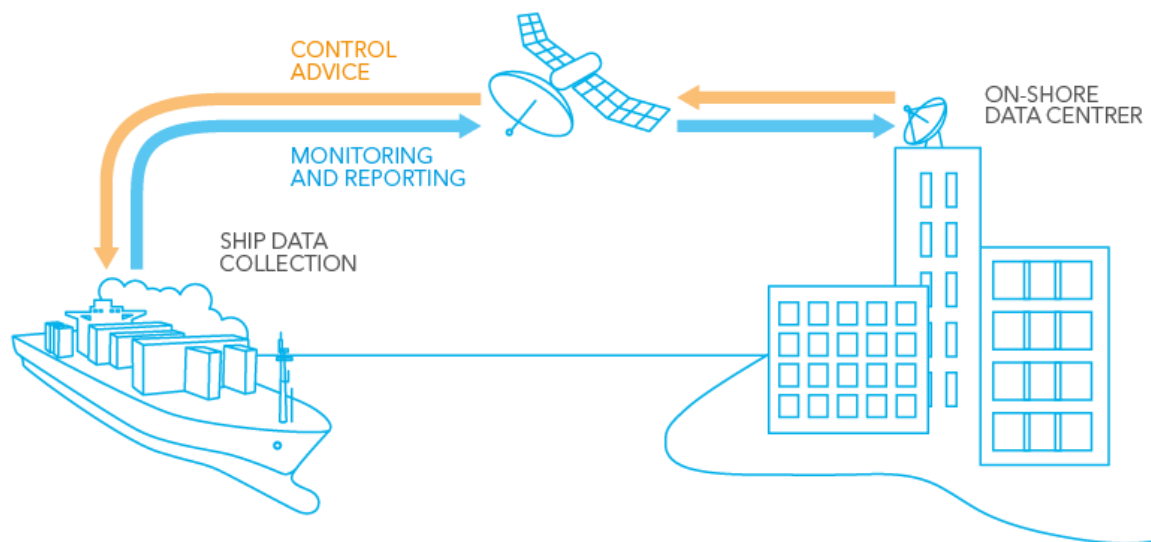


Fig.1: Ship sensor data is used on board and sent to shore

To keep track of metadata and to structure the storage and processing of sensor data, there is a need for a unique identification of sensors as well as the components and systems subject to monitoring by sensors. As no standard naming method has been available, legacy implementations have been based on different proprietary, vendor-defined naming schemes, that have been difficult to interpret. Lack of standards have therefor hampered interoperability, sharing and reuse of data.

In addition to providing uniqueness for referencing, a good naming scheme should also provide additional information and context relevant for the ship, sensor and the monitored component or function. VIS, a rich and mature information model, used in DNV's classification services since 2005, has been found highly suitable for this purpose. This paper describes the new standard sensor naming

method “dnv-v2” defined and maintained by DNV utilizing VIS to help creating a common language for exchange of sensor data in the maritime industry.

2. ISO 19847 and 19848 – standardizing ship sensor data

In the autumn 2018, ISO published two new standards for storage and exchange of ship sensor data:

- ISO 19847 “Ships and marine technologies – Shipboard data servers to share field data on the sea”, *ISO (2018a)*; and
- ISO 19848 “Ships and marine technologies – Standard data for shipboard machinery and equipment”, *ISO (2018b)*

ISO 19847 is a standard for a shipboard data server, defining requirements for functionality, performance, and data handling.

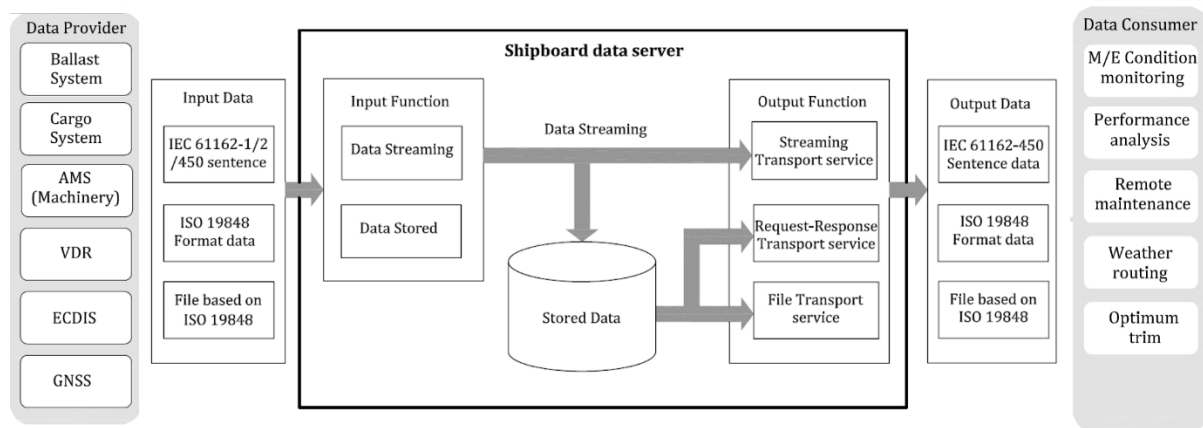


Fig.2: ISO 19847 – Shipboard data server Input/Output model, *ISO (2018a)*, Ch 5.1 Fig 1-4

The contents include:

- Minimum requirements for functionality and interfaces
- Reliability and performance requirements e.g. availability and logging speed.
- Systematics for configuration and meta data
- Data structures & formats (ISO 19848)
- Environmental requirements tailored for maritime e.g. temperatures and vibration levels
- Cyber protection e.g. schemes for authorised access.
- Test requirements, providing the basis for 3rd party verification.

By specifying standard input and output protocols and providing a “neutral ground” for storage between data providers and data consumers, the standard enables interoperability and lowers the integration barrier for new applications.

ISO 19848 is more of a data standard, standardizing data concepts and data structures, that the ISO 19847 data server must use. The standard defines:

- Time Series data, in the form of Tabular data or Event data.
- Sensor meta data (Data Channel Property)
- Systematics for sensor naming (Data channel ID)

The Time Series data is the payload data, i.e. the actual readings or measurements from the different sensors. The Tabular Data structure is suitable for uniform high-frequency sampling of multiple channels of physical measurements such as temperature and pressure, while the Event data structure is suitable for low-frequency asynchronous data sources such as event- and alarm logs.

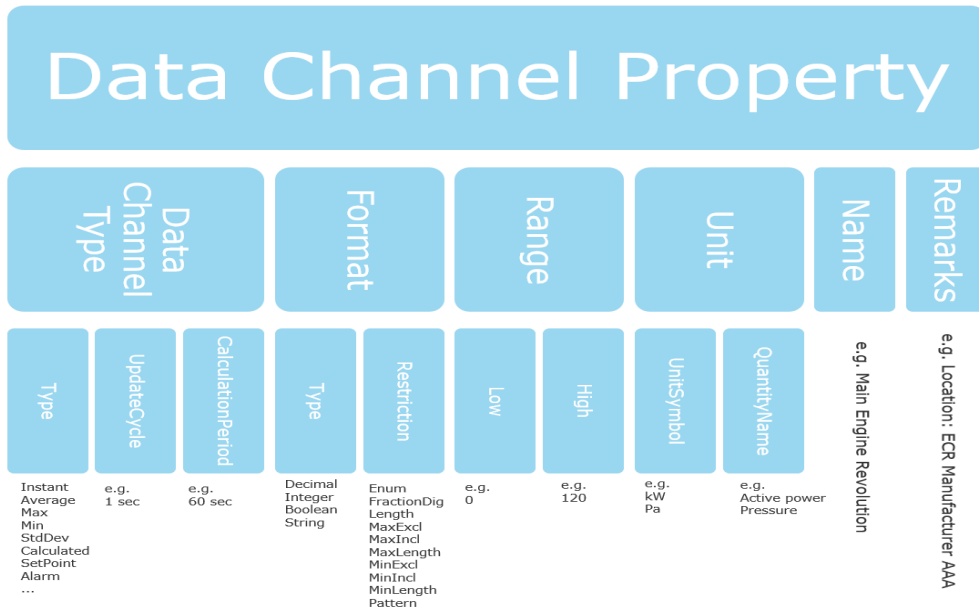


Fig.3: ISO 19848 Data Channel Property - standardized sensor meta data

ISO 19848 also defines a standard data structure for Data channel properties, which essentially is meta data for the sensor, e.g. unit of measure, validity range and format. Such meta data is essential for correct interpretation and use of the data but is often insufficient or absent. The various data structures have been defined in XML, but implementation options in CSV and JSON are included in the standard.

Although 19848 is mandatory for a 19847 shipboard data server, it is also highly relevant for data providers and data consumers on board as well as shore-based data platforms to be able to ingest the ISO-19848 data.

Finally, ISO 19848 defines standard methods for constructing “universal IDs” – a unique reference to a sensor on board a vessel. The universal ID is a URI (Uniform Resource Identifier) and could be a unique URL (Uniform Resource Locator – i.e. a hyperlink) representing that particular sensor signal. The structure is flexible in that it allows different “naming rules” with associated code books to be defined by different “naming Entities”.

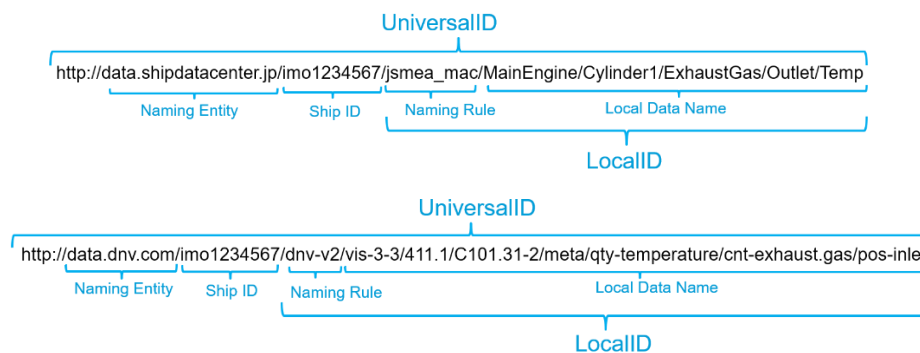


Fig.4: ISO 19848 Standardized sensor name using the “jsmea-mac” and “dnv-v2” naming rules

In the initial version of ISO 19848, two naming rules were introduced, one from JSMEA (Japan Ship Machinery and Equipment Association) and one from DNV. DNV’s naming rule, called “dnvgl-vis” in the initial revision and “dnv-v2” in an ongoing revision of the standard, is based on the VIS (Vessel Information Structures) information model.

VIS is further explained in the next chapter, and we will return to a detailed description of the “dnv-v2” naming rule in chapter 4.

3. VIS master information system

3.1. General

The VIS provides the master information used as basis for the classification processes in DNV. An important part of the VIS is the Generic product model (Gmod), a functionally oriented model describing the vessel. The Gmod and its use in the classification processes is described in *Vindøyt (2008)*.

The Gmod provides:

- a functional breakdown of the vessel
- a library of product types that may be installed on the vessel, and a functional breakdown of these
- unique codes and names for all items
- allowable assignments between functions and product types

Based on the Gmod, unique vessel product models (Pmods) may be set up by a partly automatic and partly manual process.

3.2. Gmod scope

The Gmod is intended to cover

- All types of vessels subject to classification by DNV
- All vessel lifecycle phases
- All product types with a classification scope installed on board classed vessels
- All regulatory regimes relevant for classification
- All engineering disciplines

3.3. Gmod principles

The Gmod is based on 7 principles:

- a) The functional breakdown of the vessel is set up as a hierarchy, with 14 level 1 vessel functions, currently totally 2883 functions. The coding of the vessel functions is based on the inherent hierarchy of the decimal system. All vessel function names are globally unique.
- b) A library of product types is provided, currently comprising 773 items. The product types are grouped according to their associated engineering discipline. The codes of the product types start with the discipline code followed by a number. All product type names are globally unique.
- c) Product types may be given a functional breakdown based on the same principles as used for the vessel. Currently, 2727 product functions are defined. The codes of the product functions start with the code of the product type, followed by a hierarchical number based on the decimal system. Product function names are unique in the context of the product type.
- d) Allowable assignments between functions and product types are set up. This applies to vessel functions and to product functions.
- e) In some cases, more than one product type may be assigned to a function. This is covered by the concept Product selection, a set of product types from which the wanted product type may be selected.
- f) In some cases, selectable branches are set up in the function hierarchies. This is covered by the concept Function selection.

- g) Some functions are commonly set up in multiples, e.g. a vessel will normally have more than one fuel oil pump. Such functions are set up to be individualised, and the function code is appended by an i.

3.4. Normal assignment and naming

See principle 3.3 d). The allowed assignment between a function and a product type is denoted a 'normal assignment'.

Example 1:

Function	Normal assignment to product type	Common name
621.21 Fuel oil conducting	S90 Piping	Fuel oil piping

This implies that S90 is the only product type that is allowed to be assigned to function 621.21, on any vessel.

The Gmod provides a 'common name' for the combination 621.21/S90: 'Fuel oil piping'. Common names are set up for all allowed combinations of functions and product types. They provide physically oriented names aligned with common terminology in the maritime industry.

Common names are defined at all levels of the Gmod.

Example 2:

Function	Normal assignment to product type	Common name
411.1 Propulsion driver	C101 Reciprocating internal combustion engine	Propulsion engine
C101.41 Reciprocating linear piston motion to rotation conversion	C465 Crankshaft	Crankshaft

For the full path 411.1/C101.41/C465, the common name will be 'Propulsion engine/Crankshaft'

The common name here consists of the two parts

411.1/C101 Propulsion engine

...41/C465 Crankshaft

3.4. Pmod creation

- The Pmod creation is initiated by applying a filter to the Gmod. The filter is based on high-level vessel characteristics, *Vindøy and Dalhaug (2016)*. The filter will remove functions that are irrelevant for the vessel type.
- Remaining non-existing functions are removed manually
- Product selections and function selections are resolved
- Individualisation is performed, by setting the cardinality of the function and by providing a unique identifier for each individual function.

The effort required to make a Pmod is on average 20 hours, when performed by trained personnel.

3.6. VIS versioning

The VIS including the Gmod is systematically revised to

- Follow development in scope and content of maritime regulations
- Correct errors
- Improve user-friendliness

Normally, a main VIS release is published twice a year. The main releases are identified by a release number, currently 3-4. Minor updates are performed at need and are identified with a letter appended to the release identifier, e.g. 3-4b.

In connection with a VIS release, information about the changes to be implemented will be made available. In some cases, the associated vessel information will have to be converted to be aligned with the latest version of the VIS. DNV converts all Pmods upon each main VIS release.

3.7 Gmod and Pmod use

Pmods have been created for all vessels in DNV class since 2005, i.e. about 25000, corresponding to around 25 - 30% of the world's fleet. This is probably one of the largest sets of digital twins available anywhere.

The Pmods have been the basis for DNV's classification services since the introduction in 2005. Based on user experience, the Gmod and therefore also the Pmods have been revised two times per year since the introduction. This implies that the Gmod now has been subject to 16 years of extensive use, comments and revisions, and is today a well proven reference.

The Gmod is used for many purposes, for a full description, *Vindøyy (2008)*. Each time the Gmod is taken into use for a new purpose, some modifications or additions will normally be required.

Following the publication of ISO 19848 in 2018, where the Gmod is a reference, it has now been made available also for external users. New references as quantities, and modifications and additions to the Gmod supporting the use for sensor annotation was published in VIS 3-4, June 2021.

4. DNV's sensor naming standard

4.1. General

The main purpose of sensor name (tag) is to have a unique reference (identifier) that can be used in sensor-related data such as the measurements, configuration, meta data, analysis or results from processing the data. The advantage of having a standardized naming scheme is to have reference that can be interpreted accurately and automatically across a fleet of vessels and from different manufacturers. A standardized approach makes exchange of sensor data between different systems and companies easier and less error prone.

The rules for constructing the standard sensor name string will typically require inclusion of elements providing additional information or context about the sensor, for example location, measured quantity, and the monitored equipment on board the vessel. Although this kind of meta data is typically stored separately and in more detail in dedicated data structures (ISO 19848: Data Channel List) having some key attributes directly available from the sensor name is increasing transparency and convenience for human interpretability. It also helps getting a structured overview when the number of data point gets high e.g. into the thousands, which is not uncommon for a modern ship.

As described in Chapter 2, ISO 19848 defines LocalID as a unique and standard identification of each sensor or data channel onboard a given ship. The "dnv-v2" naming rule defines how such a LocalID can be generated using Reference libraries and associated codebooks. The reason for using the version suffix "v2" is to distinguish it from the first version of the naming rule "dnvgl-vis" presented in the initial publication of ISO 19848 in 2018.

The reference library used in the "dnv-v2" naming rule is "vis", i.e. the Vessel Information Structures, DNV's information model used for ship classification (Chapter 3).

4.2. Selection of PrimaryItem and SecondaryItem

In the “dnv-v2” naming rule, the basis for the sensor name is to select one (or two) suitable item(s) or node in the Gmod tree of VIS, the first one, <PrimaryItem>, is mandatory and the second one, <SecondaryItem>, is optional.

<PrimaryItem> is a reference to the node in the Gmod hierarchy describing the function or product on board the ship that the data channel is assigned to or associated with. <PrimaryItem> is represented by an <ItemPath>. Normally, this would be the function or product on which measurements are performed, i.e. the monitored item.

	Function/product	Category
VE	VE	asset type
400a	400a	asset function group
410	410	asset function composition
411	411	asset function group
411i	411i	asset function composition
411.1	411.1	asset function leaf
CS1	CS1	product selection
C101	C101	product type
C101.4	C101.4	product function composition
C101.41	C101.41	product function leaf
C465	C465	product type

Fig.5: Crankshaft in the VIS Gmod hierarchy

For example, if a sensor is monitoring some quantity of the crankshaft in a propulsion engine, then the crankshaft is selected as <PrimaryItem> and the naming rule requires the path reference “411.1/C101.41/C465” to be included in the Local ID (sensor name). The “dnv-v2” naming rule also offers a verbose option which will retrieve the Common Names for the relevant functions in VIS codes. In case of selecting the verbose option “411.1/C101.41/C465/~propulsion.engine/~crankshaft” will be included in the Local ID string. Note that “verbose” is just an optional extension to improve readability for humans. It is not part of the unique Local ID and shall be ignored by URI parsers.

In some cases, the data channel is not adequately described by the <PrimaryItem>. Therefore, it is possible to add an optional second reference to another node in the Gmod hierarchy, <SecondaryItem>, describing another function or product on board the ship, which also is associated with data channel.

Example: Consider a sensor measuring cooling water temperature at cylinder 5 in the propulsion engine. The monitored item is the cooling system of the propulsion engine, since the sensor is measuring temperature of the cooling water. The cooling system is represented in <LocalId> as /411.1/C101.63/S206. In this case it is appropriate to use <SecondaryItem> to specify that cylinder 5 (/411.1/C101.3i-5) is the location of the measurement. The <LocalId> would then contain the following string: /411.1/C101.63/S206/sec/411.1/C101.3i-5. The key word “/sec” is used to separate the PrimaryItem and SecondaryItem in the VIS Item path string.

If the verbose option is used, the following string is appended:

“/~propulsion.engine/~cooling.system/~for.propulsion.engine/~cylinder.and.piston.unit.5.”

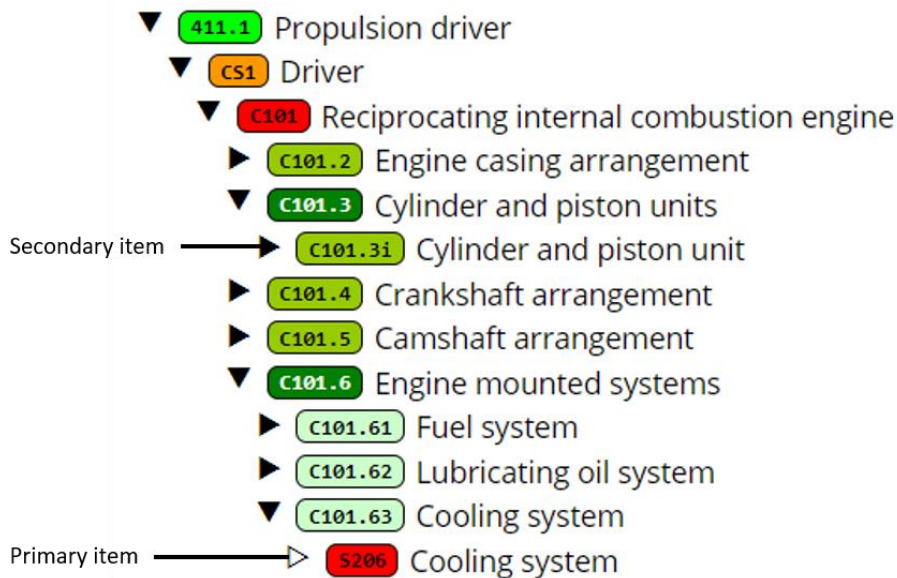


Fig.6: Selection of PrimaryItem and SecondaryItem in the VIS Gmod hierarchy

4.3. Selection of meta tags

The selection of PrimaryItem and optionally SecondaryItem, is not sufficient to create a unique sensor name, as the VIS Gmod only describes functions and products on board, but nothing about the sensor itself. One may also have multiple sensors associated with the same function or product i.e. the same item in Gmod hierarchy. To be able to distinguish between such sensors, the dnv-v2 naming rule defines eight meta tags serving as sensor descriptors providing the means for creating unique LocalID. The metadata tags are optional but at least one shall be used. A metadata tag consists of a name and value. The allowed tag names and their meaning are listed below:

- “qty” (quantity): describes the physical quantity associated with the data channel. Quantity is used in a broad sense which includes any kind of measurement relevant for ships and their operation. The provided codebook is a superset of the quantities in ISO 80000 with additional quantities relevant for the maritime context. Examples: pressure, temperature, heading, speed.over.ground.
- “cnt” (content): describes a substance of which a property is measured. The tag “cnt” is an abbreviation for “contents” as it typically is a substance (e.g. liquid or gas) that is contained within the relevant VIS item such as a tank or piping system. Examples: exhaust.gas, fuel.oil, sea.water.
- “calc” (calculation): describes different calculations that may be applied to a measurement, e.g. time-based aggregation or averaging across several signals. This tag may be omitted for data channels which contain instantaneous (i.e. not aggregated) measurement values. Examples: mean, maximum, sum, first.
- “state”: describes data channels which contain binary or categorical data rather than measurements of physical quantities. Examples: opened, closed, running, not.running, on.off, failed.
- “cmd” (command): describes data channels containing commands, for example an instruction to a system to enter a specific state. A command is often a consequence of a state, e.g. a system may be commanded to stop due to a measurement exceeding a certain threshold. Examples: start, stop, shut.down, slow.down.
- “type”: describes type of data source. This tag shall be omitted if the source of data is a sensor signal. Examples: set.point, manual.input, control.output
- “pos” (position): describes a relative position of the sensor on the function/product where it is installed (as opposed to <Location> which describes position of the function/product itself on board the vessel). This tag is useful to differentiate between multiple sensors on the same

function/product. In addition to the values in the provided codebook, digits are also considered standard values (i.e. they may be used with the hyphen-syntax as in /pos-2). Examples: inlet, outlet, upper, lower, 2.

- “detail”: a free text used to provide additional important information about the sensor which is not conveyed by the other elements of Local ID, or to assure uniqueness of the Local ID. Examples: xyz567, at15degrees.

To facilitate consistency and automatic validation DNV provides codebooks with standard values for all tags (except the “detail” tag, which has a free text value) at data.dnv.com/naming-rules. However, for flexibility and to cover all possible use cases, there is also a need for custom tag values. Therefore two syntaxes are supported; for standard values the tag name and tag value separated by a hyphen ("-") and for custom values the tag name and tag value separated by a tilde ("~"). The first (standard) syntax signals that the value should be validated against a codebook. The second (custom) syntax signals that the tag value is custom and should not be validated. Example: “/cnt-marine.gas.oil” and /cnt~orange.juice.

4.4. Compiling the full sensor name

The selection of PrimaryItem and optionally a SecondaryItem produces a “VIS Item path”. The determination of one more meta tags describing the sensors produces a “Tag Elements” string. These strings are combined to form the Local ID.

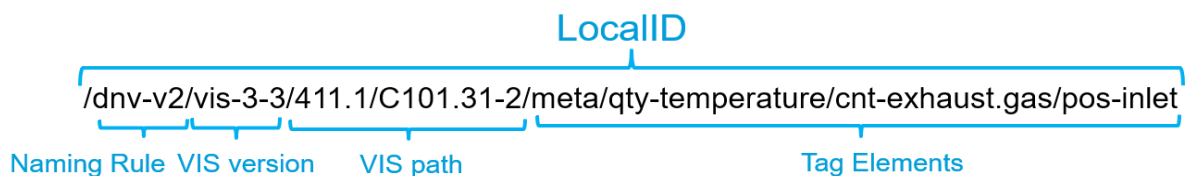


Fig.7: A fully compiled LocalID according to the dnv-v2 naming rule

The key word “/meta” is introduced to separate the “VIS Item path” and the “Tag Elements” string, to enable parsers to decompose the combined string. Some examples are provided below.

Table I: LocalId examples

Example 1	Pressure sensor in the propulsion engine fuel oil pump
VIS Item path	/621.22i/S110.1/S101/sec/411.1/C101
<TagElement>s	/meta/qty-pressure/cnt-fuel.oil
LocalID	/dnv-v2/vis-3-3/621.22i/S110.1/S101/sec/411.1/C101/meta/qty-pressure/cnt-fuel.oil
Example 2	Temperature of exhaust gas at the inlet of the propulsion engine’s second turbocharger
VIS Item path	411.1/C101.65/S210/sec/411.1/ C101.663i-2/C663
<TagElement>s	/meta/qty-temperature/cnt-exhaust.gas/pos-inlet
LocalID	/dnv-v2/vis-3-3/411.1/C101.65/S210/sec/411.1/C101.663-2/C663/meta/qty-temperature/cnt-exhaust.gas/pos-inlet
Example 3	Running indicator (binary value) for the third generator set (auxiliary generator)
VIS Item path	511.1i-3/C101
<TagElement>s	/meta/state-running
LocalID	/dnv-v2/vis-3-3/511.1i-3/C101/meta/state-running

4.5. Management and operations

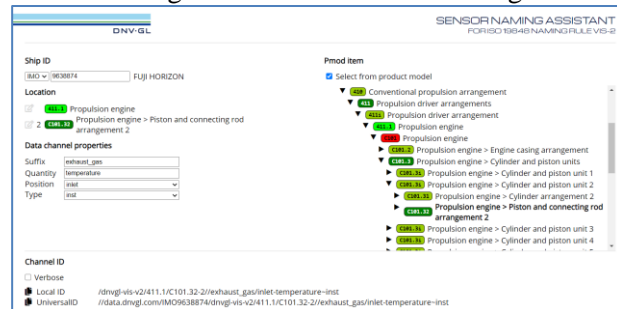
Both the Naming rule and the Reference libraries can be updated over time and are therefore associated with versions. The current version of Naming rule is “v2” and the current version of the VIS (Reference library) is 3-4a. These and future versions of Naming rules and Reference libraries will be defined and maintained at <https://data.dnv.com/dnv-vis/>. At the same site DNV will provide the meta tag codebooks, user guidance documentation as well as a Sensor naming assistant, a web-based tool intended to aid implementers, see Chapter 5.

In addition, the informative Annex C of ISO 19848 also provides explanatory information and examples to assist implementers.

5. Support utilities

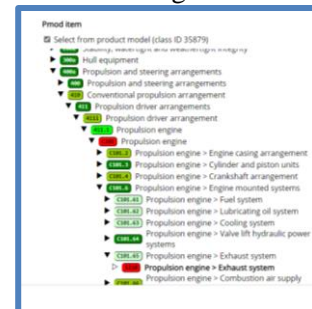
Defining a sensor naming standard alone will not alone change the industry. To make standard useful, we need to acknowledge practical challenges with using the standard. For that reason, DNV offers a variety of support utilities that mitigates a significant amount of conversion problems from existing legacy sensor tags to a standardized tag:

Understanding the standard: Sensor naming assistant



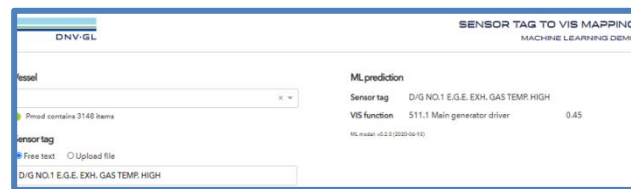
Interactive web tool enabling exploration and experiments with generation of VIS based sensor names

Understanding VIS: VIS navigator



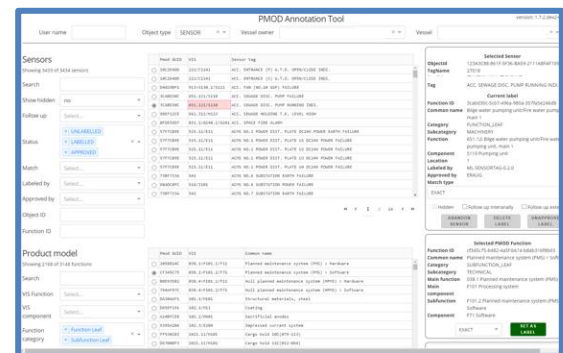
Search and explore the VIS structure

Reduce sensor naming complexity: Machine Learning assisted contextualisation



From the existing sensor names, the tool suggests an ISO19848-C compliant name. This is enabled by machine learning algorithms trained on a large set of sensors where the correct Annex C names are verified.

Handle large number of sensors – reducing conversion effort



ML can automatically bulk-suggest an unlimited number of sensor names using the ML based tools. DNV provides this as part of a tools and support processes for verifying correct names and improving the sensor name accuracy

Manufacturers deliver products and like to have a standard set of sensor names repeatedly used for every manufactured product. This conflicts with the requirements in the standard to include vessel specific information. The VIS structure enables manufacturers to create what we call “VIS-ready” names, enabled by the VIS hierarchical structure. Manufacturers will then populate the sensor name with known information about the product, and leaves ship installation details to actors assembling the component to a vessel.

Manufacturer

Reusable sensor names

Sensor name	Main bearing 01 temp PV	C101 – Engine
VIS-ready name	/dnv-v2/vis3-4a/C101.44i-1/C261/meta/qty-temperature	C261 – Main bearing

Installed on the ship

Vessel specific info added

VIS-ready name	/dnv-v2/vis3-4a/ IMOno/411.1 /C101.44i-1/C261/meta/qty-temperature	411.1 Propulsion engine
----------------	---------------------------------------------------------------------------	-------------------------

Fig.4: Manufacturers can create reusable, VIS-ready sensor names

References

ISO (2018a), *ISO 19847 Ships and marine technologies – Shipboard data servers to share field data on the sea*, Int. Standard. Org., Geneva

ISO (2018b), *ISO 19848 Ships and marine technologies – Standard data for shipboard machinery and equipment*, Int. Standard. Org., Geneva

LÅG, S.; WITH, S.B. (2017), *Standardization as an enabler of digitalization in the maritime industry*, DNV GL Group Technology & Research Position Paper 08/2017

VINDØY, V. (2008), *A Functionally Oriented Vessel Data Model Used as Basis for Classification*, COMPIT 2008, pp.60-69

VINDØY, V.; DALHAUG, K. (2016), *High level vessel characterization*, COMPIT Conf., Lecce

Creating Sustainable Marine Structures Through the Adoption of Composites

Jonathan Evans, STRUCTeam Ltd, Cowes/UK, jonathan.evans@structeam-ltd.com
Nico Voorzee, STRUCTeam Ltd, Amsterdam/Netherlands, nico.voorzee@structeam-ltd.com

Abstract

The application of composite technologies continues to grow across all segments of the marine industry. In comparison to traditional materials, composites offer a progressive and sustainable approach to manufacturing through weight reduction in the vessel's structure, resulting in better fuel efficiency and lower emissions. This paper addresses the embodied CO₂ value of the vessel from cradle to gate. The sustainability benefits of applying composites to marine structures compared to metallic vessels are highlighted alongside a selection of case studies demonstrating sustainable practices. The main barriers for entry are explored alongside the importance of regulatory requirements to support the adoption of composites in design engineering.

1. Introduction

The use of composites is constantly being adopted in new industries, with benefits including weight saving, corrosion resistance, electrical resistance (for Glass Fibre Reinforced Polymers (GFRP)) and ultra-low magnetic signature which helps to reduce noise in incoming data for communications systems whilst protecting the equipment from environmental effects. The effect of reducing weight on the vessel structure is one of the key benefits to reduce the quantity of materials used and also to reduce the fuel consumption during the service life of the vessel.

In the current crisis of global warming and recent warning from the IPCC (Intergovernmental Panel on Climate Change), the effects on the environment of building from product is becoming one of the key factors that drive decisions on materials and operational sustainability of products. The effect of reducing weight, along with using a lower energy intensive process to produce the material, shows a lower embodied CO₂e, leading to lower amount of greenhouse gases being released into the environment.

To illustrate the decision on material, manufacturing and operational efficiency choice, an example has been taken of a typical 16m patrol vessel with the following material options:

- Aluminium
- Glass fibre (GF) (E-glass) PVC Core Infused
- Carbon Fibre (CF) (Standard Modulus) PVC Core Infused
- Carbon Fibre (CF) (Standard Modulus) PVC Core Prepreg

Table I: Vessel material options and structural weights

	Aluminium (Baseline)	Glass Fibre PVC / Infusion	Carbon Fibre PVC / Infusion	Carbon Fibre PVC / Prepreg
Vessel structure weight	5,500 kg	4,481 kg	3,654 kg	3,077 kg

2. Equivalent CO₂ (CO₂e) – “Cradle to (factory) gate”

CO₂e is the value of measuring the carbon footprint of all greenhouse gases released into the atmosphere through the processing of raw materials, intermediate processes and final manufacturing process to create a product. The scope of the CO₂e value in this case study is limited from cradle to factory gate, taking into account emissions during production only.

Each material, including its constituents, intermediate and final manufacture processes, has a value of CO_{2e}, which can be multiplied by the mass of the material, giving a total CO_{2e} value for the product when released from the factory.

2.1. Effect of raw material choice on embodied CO_{2e}

For raw materials production, materials which require a high amount of energy to convert from a mixture of constituent materials, to their usable form, typically embody a higher amount of CO_{2e} (i.e. conversion from polyacrylonitrile (PAN) precursor to carbon fibres or conversion from alumina and bauxite to aluminium). The temperature is approximately 3x higher for carbon fibre production than aluminium. Natural materials, such as balsa wood, which is typically used as a core material in the deck and superstructure of vessels, have a negative CO_{2e}, which is a step towards becoming carbon-neutral. This is because through the tree's life, it will absorb CO₂ and emit O₂, requiring very little energy to be grown and harvested.

2.2. Effect of intermediate processing on embodied CO₂

Intermediate processes to convert the fibres to usable fabrics, such as stitching, weaving and application of resin film to the glass or carbon fibres only requires 10-15% of the energy compared to the production of the raw material. Therefore, the intermediate process contributes to similar percentage of CO_{2e}. This is mostly due to the processes being performed on weaving/stitching machines at ambient temperature. It is typical that only 30% of the energy is used for these processing machines, with the remainder being wasted through heating and lighting of the factory space.

2.3. Effect of manufacturing process on embodied CO₂

Manufacturing processes again mostly take place at ambient temperatures, where elevated temperatures are used for curing the product at 50-100C for a short period at the end of the composite manufacturing process. Factory inefficiencies such as heating and lighting play a significant role in the energy usage, however these are accounted for in the appropriate CO_{2e} values in the product.

2.4. Total embodied CO₂ in vessel (Cradle to gate)

The CO_{2e} for the example vessels is outlined in Fig.1, accounted for from cradle to gate. Fig.2 outlines a comparison on structural weight, material cost and CO_{2e}.

Aluminium, assumed to be 100% virgin metal, has the highest CO_{2e} of the options, mainly due to the weight difference of the final product (as shown in Fig.2).

The E-glass fibre vessel, the "cost effective" option, has a weight saving of 20% over the aluminium vessel, but the lowest CO_{2e} of the options due to the relatively low CO_{2e} value of E-glass fibre, having only 10% of carbon fibre. In this vessel, the resin CO_{2e} is the most significant contributor to the overall CO_{2e} content.

The carbon fibre vessels (both infused and pre-preg) contains significant CO_{2e} due to the large contribution of CO_{2e} from the raw material, however due to the 35-45% weight saving compared to aluminium, still contains less CO_{2e} than the aluminium vessel.

In order to gain potential further savings, it has been highlighted earlier that most of the CO_{2e} generated during part production is through energy used to heat and light factories. The CO_{2e} released into the atmosphere for these overhead costs is dependent on the location of the factory, with some countries, like the U.K. releasing approximately 40% less CO_{2e} per kW than Germany.

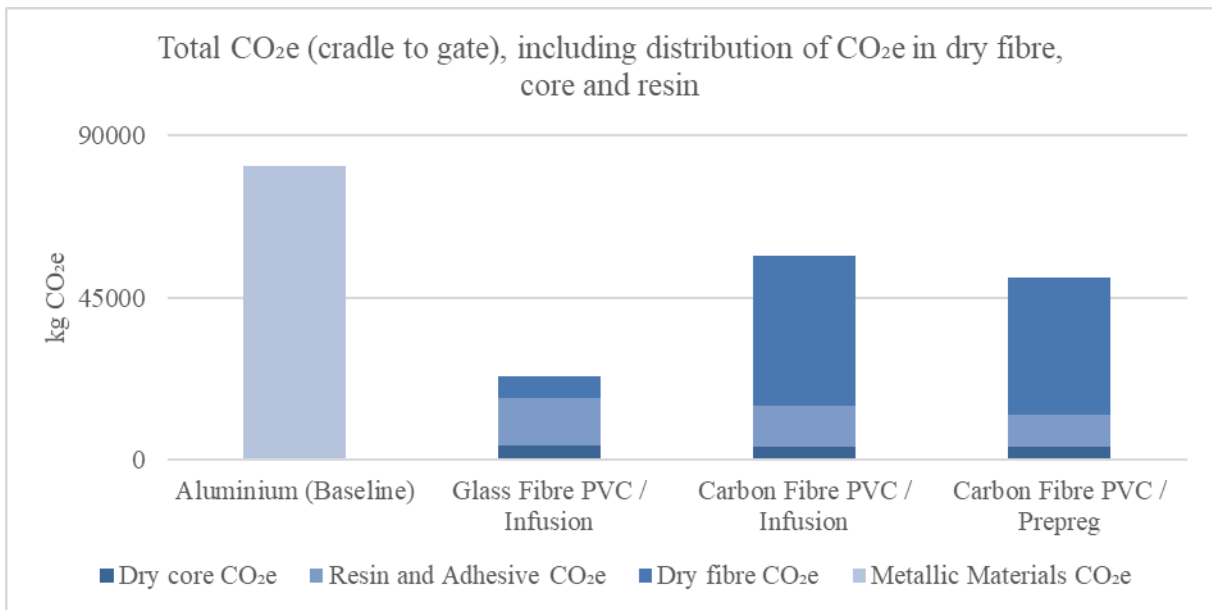


Fig.1: CO₂e values from cradle to gate, including material type breakdown

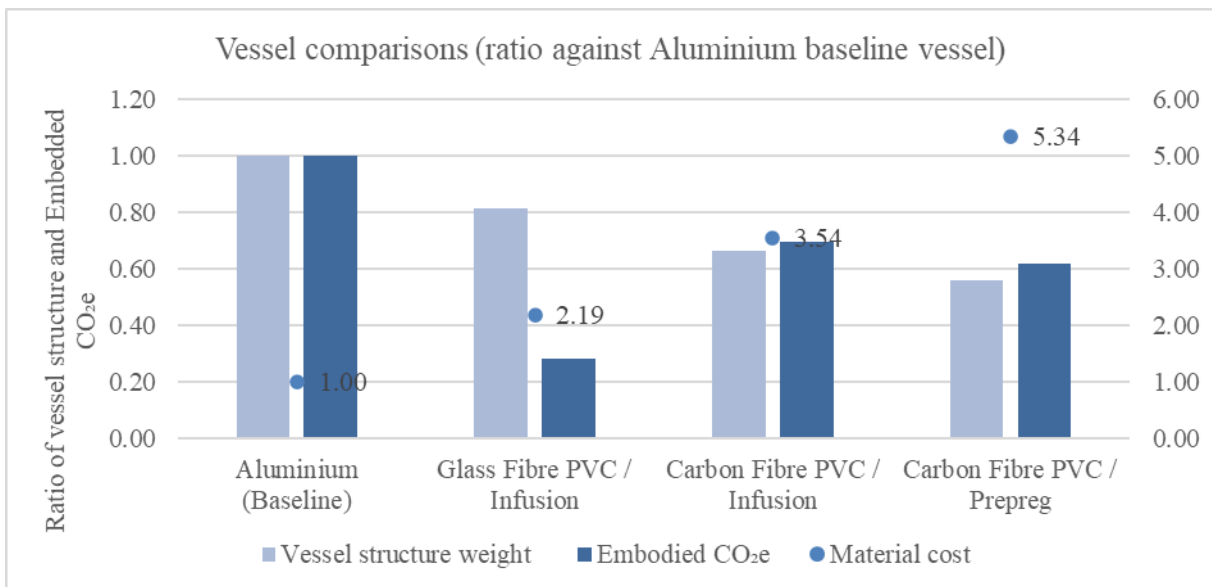


Fig.2: Vessel comparisons for weight, CO₂e and cost, compared to Aluminium baseline

2.5. Operational CO₂e savings

The other key factor in a vessel’s emissions of CO₂ is during the operational life of the vessel. In order to understand and quantify the potential CO₂ savings from creating a lighter structure, the diesel usage has been estimated using the assumption that the vessel’s residuary resistance is roughly proportional in the displacement operational range. It is assumed for this vessel that the majority of fuel consumption for a typical workboat will be operating as a displacement vessel.

Fig.3 outlines the CO₂e savings from fuel consumption only, assuming a vessel has 50% utilisation over a service period of 30 years.

The carbon fibre vessels indicates that a reduction in weight can save up to 9% of CO₂e over a 30-year period compared to an aluminium vessel, which is equivalent to 300 tonnes of CO₂e for this example vessel.

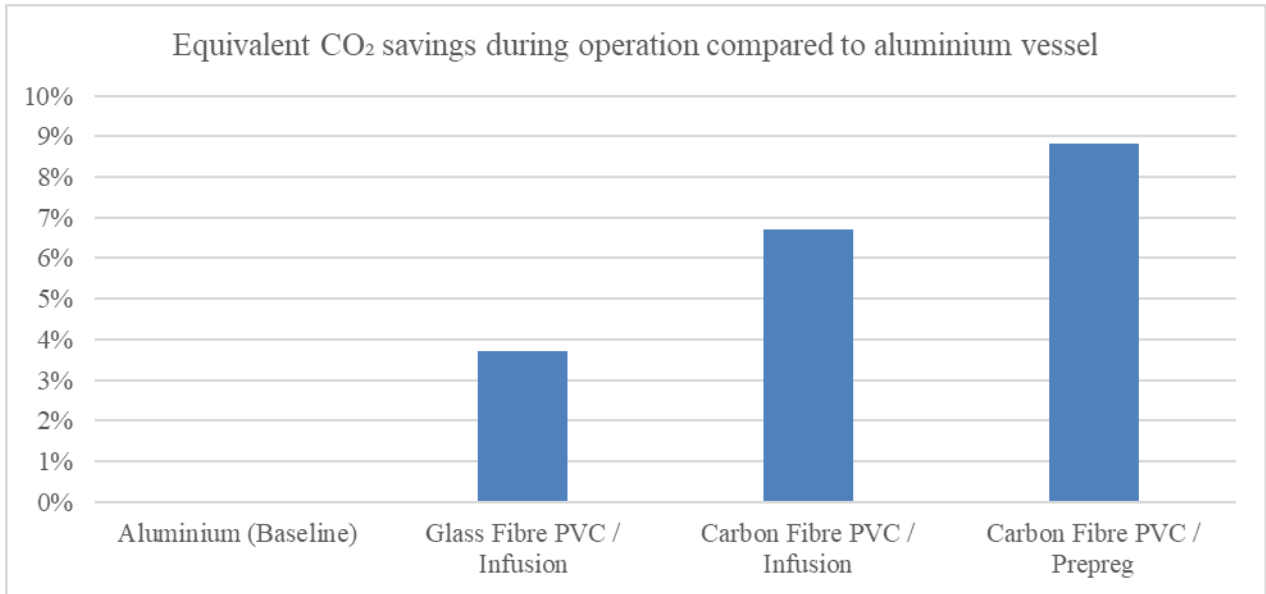


Fig.3: Equivalent operational CO₂e emissions from diesel

2.6. Overall CO₂e savings

When the volume of CO₂e is compared between “cradle to gate” and operational volume, the embodied CO₂e from materials and manufacture is only 0.65–1.6% of the total greenhouse gas emissions, indicating that the materials selection is a small portion of potential savings, however composites can be utilised for their weight reduction advantages to reduce the operational emissions, along with their other corrosion and fatigue resistant properties.

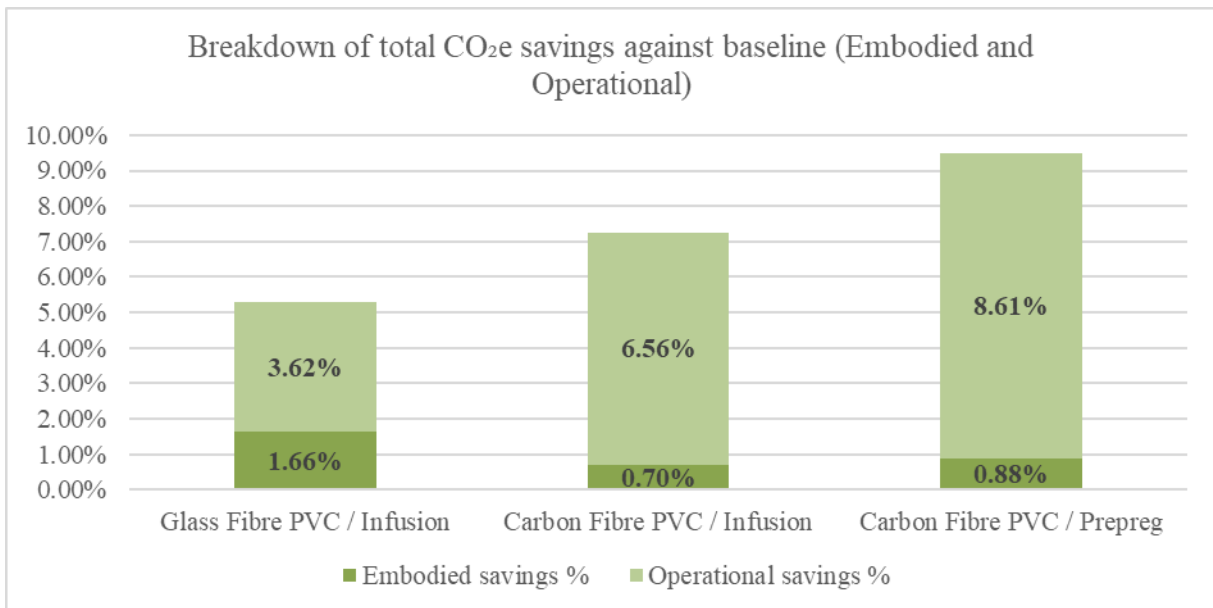


Fig.4: Breakdown of total CO₂e savings compared to baseline Aluminium vessel

Fig.4 outlines the breakdown of potential emissions savings compared to the aluminium vessel. All options have cumulatively small overall CO₂e reductions from 5.3% to 9.3% improvements. Which is far from the net-zero goal from the IPCC in 2040.

Although the reduction of CO₂e from composite vessels could easily be overcome by the use of recycled aluminium, the weight savings, and therefore operational emissions would not feel any benefit from this option.

3. Challenges of adopting composites

There are many perceived barriers to entry to adopt composite materials, many of which are related to the relative youth of the composites industry, which can take some time to develop without strong commercial or regulatory backing. Although composites have been adopted in the smaller leisure and racing marine market, the larger commercial and more regulated corner of the marine sector has historically been slow to recognise the benefits of composite materials. There are a few key barriers which delay the current adoption of composites:

- Design and analysis
- Regulations and certification
- Repair and maintenance

3.2. Design and analysis

Unlike metallic materials, which have the same properties in all directions, composites are orthotropic, giving three times the number of properties. Whilst this is one of the key benefits of composites, where fibres can be orientated to follow the load path, reducing wasted materials, this can increase the level of complexity of design. Thankfully, there are increasingly more software packages being developed as a “plug in” to the normal Finite Element workflow to ease the broadening of engineer’s expertise to design using the benefits of composite materials.

3.3. Regulations and certification

Aside from the future regulations relating to sustainability, the main barrier into the larger commercial marine sector is fire performance. Composites used in the majority of products do not have sufficient resistance to temperatures above 90-100C, and will start to deform and burn above these temperatures. Fire resistant resins can be used in order to reduce the smoke and toxicity of the burning composite, enabling composites to be adopted into areas which aren’t relied on for escape routes, where safe “failure” of the composite can occur in the event of a fire. Following the IMO’s release of “Guidelines for use of Fibre Reinforced Plastic (FRP) within Ship Structures” in 2017, many ship builders are looking into incorporating composites into strategic areas of ships, where the weight reduction, increased stiffness and low magnetic signature are some of the key benefits for adoption of composites, leading to increased stability, fuel savings and reduction of power requirements for hatches as a few examples.

3.4. Repair and maintenance

Another key barrier for composites, which is linked to a strong previous development of metallic-skilled workforce, is the repairability of vessels whilst in operation. Many ships are currently repaired whilst at sea using welding both above and below the waterline on an ad-hoc basis. As composite resins require a controlled humidity in order to cure and achieve the desired mechanical properties, the majority of situations where a repair could be made with metals, composites require a controlled environment and therefore would be preferable whilst docked. For a vessel operator, similar to the current industry, vessels can be provided with a service contract, where repairs from damages and scheduled inspections, refits etc. are provided along with the vessel.

4. Product end of life

4.1. Recycling and re-use of composite materials

Due to a ban of landfill from 2030, through the EC DIRECTIVE 2008/98, released in 2008, with the ultimate goal of preventing waste, the wind industry has been taking steps to implement recycling solutions for all wind turbine blades.

There are currently three main options which are being implemented in the industry: Mechanical recycling, development of 100% recyclable blades using thermoplastic materials and development of chemical recycling of epoxy-based wind blades.

Mechanical recycling is the shortest-term solution, where the composite material is shredded, and the recyclates being re-used as a concrete additive. Although this is a quick, simple solution using well known methods, this solution is not a fully satisfactory option in the long term.

The second, medium term option, being implemented in the ZEBRA project by LM wind power, aims to have a 100% recyclable blade through the adoption of thermoplastic resins, which can be recycled using depolymerisation and dissolution. Thermoplastics also benefit from reduced CO_{2e} content in comparison with current epoxy and polyester resins which are used in the large majority of composite products.

The third option, which is longer term, is the chemical recycling of epoxy-based composites. Currently polyester based composites can be chemically recycled, with a high percentage of the recyclates having the option to be re-used. Historically the majority of cost-effective composite leisure vessels were manufactured using polyester which opens an avenue for them to be recycled, however the use of epoxy resins has increased in the marine sector which provides more challenges to recycle cost effectively.

The wind industry possesses two large advantages to enable development; the industry is dominated by a handful of large blade manufacturers, which can collaborate easily, and a high capital in order to fund the recycling technologies. The marine industry on the other hand, is segmented with a large number of smaller manufacturers, making collaboration very difficult.

As the materials used in wind blades and most composite vessels is similar, the technologies developed by the wind market can be utilised by the marine segment, giving opportunities for the marine sector to have sustainable options at end-of-life. However, this needs to be facilitated by a global body, such as DNV, in order to benefit the whole sector.

What is clear is that the development of these technologies will require a close cooperation between among others, chemists, material scientists, designers and process engineers to innovate economically sustainable recycling solutions as demonstrated by all the examples.

5. Conclusion

Composite materials, although being high in CO_{2e} by unit weight, typically result in a lighter structural weight which yields savings in both CO_{2e} and CO₂ emissions when considered for the vessel's service life. Although initial material costs are higher than their aluminium counterparts, the investment is returned within the first 10% of operational period, however this is rarely considered as the builder is typically not the operator of the vessel and is driven by building cost effectively.

The barriers of entry for composite products are driven by three main factors; design and analysis, where understanding of composite materials is being adopted in the majority of teaching institutes, and the integration into engineering packages already used for metallics, regulations and certification, where fire safety is dominating the reluctance to incorporate composite materials into the commercial sector and repair and maintenance, where the composite materials require more control during repair operations to ensure sufficient mechanical properties.

Recycling of composites has been forced by EU directives, where the ban of landfill from 2030 has been implemented, leading to change and development of recycling methods by cost effective and environmentally sustainable means. The marine industry, due to its segmented nature, cannot be the leader for development of recycling technologies, and must adopt learnings from other industries such as the wind industry.

6. Summary

- Key drivers for projects are set to change from cost dominated decision to sustainability goals/requirements.
- Composites can be used as a method for reducing CO2 emissions by reduction of vessel weight.
- “Net zero” emissions target by 2040 from IPCC has to be met by use of renewable based energy production to offset the use of structural materials, but impact can be reduced by reducing weight.
- Onboarding of composites can be supported through collaboration to reach common goal of sustainability.
- Current recycling technology developments can be transferred from wind sector. Facilitator required for knowledge transfer.

Acknowledgements

STRUCTeam engineers have 120 years of accumulated experience in the design of cost-effective composite structures.

References

EUCIA (2020), *Eco Impact Generator for Composites*, <https://ecocalculator.eucia.eu/>

J. SELLIER, J.; CALMON, M.; LIPOCZI, G. (2015), ‘*Cost Effective Composite Solutions for Highly Loaded Marine and Offshore Structures*’, LIMAS Conf.

Advanced CFD-based Design Approach for High-Performance Sailing Catamarans

Sven Albert, NUMECA Ingenieurbüro, Altdorf/Germany sven.albert@numeca.de

Rodrigo Corrêa, NUMECA Ingenieurbüro, Altdorf/Germany rodrigo.correa@numeca.de

Thomas Hildebrandt, NUMECA Ingenieurbüro, Altdorf/, Germany thomas.hildebrandt@numeca.de

Anton Du Toit, Du Toit Yacht Design, Cape Town/South Africa, anton@dyd.co.za

Samantha Krenski, Du Toit Yacht Design, Cape Town/South Africa, sam@dyd.co.za

Abstract

This paper aims to examine the performance effect of combining both daggerboards and vestigial keels as underbody appendages on an existing sailing catamaran design which previously had either only keels or only daggerboards. The impact of the underbodies on sailing and rudder performance is explored in detail in a range of wind conditions, making use of a velocity-prediction-program (VPP) in a RANSE-CFD code. Several variations to the appendages design and position are investigated to find a trade-off between the protective benefits of a keel and the superior performance of a daggerboard.

1. Introduction

In this paper, the Balance 526 Sailing Catamaran is investigated, Fig.1, a design by Du Toit Yacht Design in Cape Town, South Africa. It is a 16 m vessel (LOA) with 8.28 m beam (overall), aiming to deliver both comfort and speed. On the comfort side, 3 double cabins can accommodate 6 people, and a significant amount of payload is possible. The high-quality interior design is practical while at the same time luxurious. On the performance side, the catamaran can reach over 20kn, without being hard pressed. This is due to the lightweight construction of e.g. composites and closed cell foam, as well as some well laid-out aerodynamic and hydrodynamic design.



Fig.1: The Balance 526 Sailing Catamaran

The sailing boat can be supplied with either daggerboards as stabilising appendages or vestigial keels. Daggerboards can achieve a slightly higher boat speed, especially when sailing upwind. Furthermore, they are retractable, making landing and transporting much easier. The keels on the other side provide safety against grounding and damage to the rudder. Since no boat built was equipped with both types of appendages, this will also be investigated in this work.

For sailing boats several options exist to evaluate the performance, ideally using a velocity prediction program (VPP). These come in many different forms and aim to output the boat speed depending on e.g. the sails configuration, true wind angles (TWA) and true wind speeds (TWS). A VPP hence needs to evaluate all the forces acting on the craft and indicate the equilibrium position. In this work we use NUMECA's RANS CFD code FINE™/Marine in conjunction with a dedicated software extension, developed by Finot Conq in France.

2. Some basics on sailing boats

Sailing boats are known since thousands of years, during which the boat and sail types evolved largely, especially the latter now exist in various shapes and forms. Most modern (smaller) sailing yachts do use a main sail and a foresail, though. Sailing in general is a highly dynamic and complex process, with the two main players being aerodynamic forces and hydrodynamic forces, Fig.2A. Simply put, the wetted parts of the boat (hull, appendages) are subject to drag forces and side forces, plus the buoyancy. On the aerodynamic side, sails create the two main forces lift and drag, plus moments due to their resultant force acting high above the vessel's centre of gravity. These forces and moments are strongly coupled to the vessel motions. Main factors in this system are the apparent wind angle and speed, which are formed by the TWA and TWS and the boat's speed and direction. The lift and drag forces generated by the sails depend strongly on the local angle of attack, and they impact the useful propulsive force. This leads to some significant differences in sailing operation, depending on the TWA, Fig.2B. In the full upwind area (red), no propulsive force is generated; depending on the boat, this angle is around 30°. As the TWA increases, so does the lift on the sails and hence the possible boat speed, and on higher TWA (>90°) the drag also plays an increasing part in moving the vessel, until at 180° drag is the dominant driver.

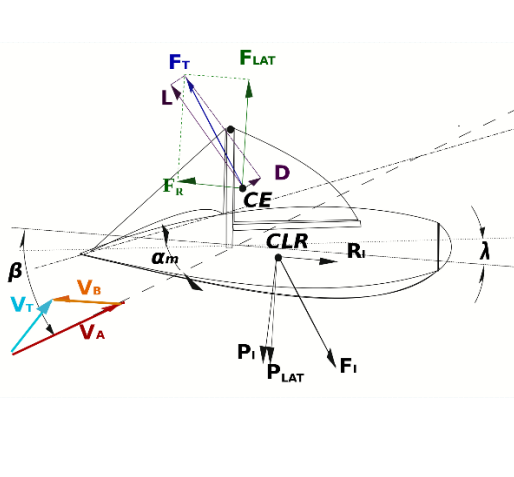


Fig.2A: Forces on sailing boats, source: wikipedia

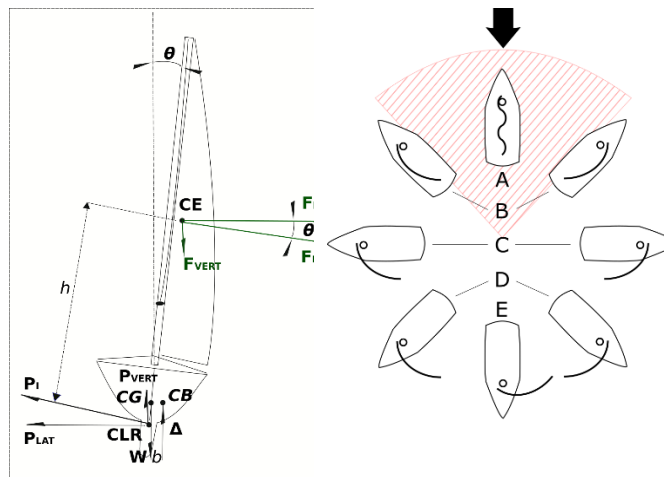
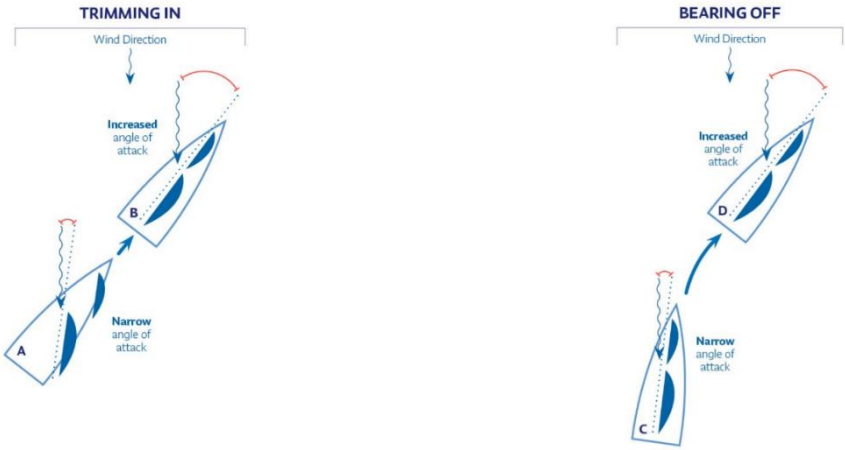


Fig.2B: Operating conditions depending on TWA, source: wikipedia

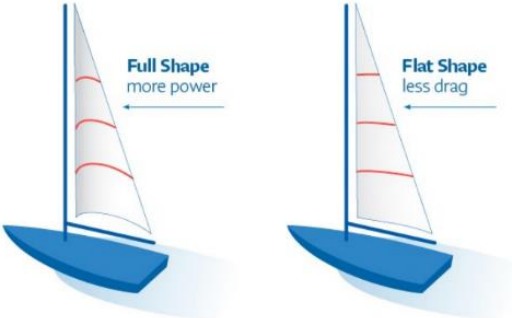
The angle of attack on the sails is a key factor. There are various ways to modify it on the boat, Fig.3. Trimming in is a change of the sail position relative to the boat, while keeping course, while bearing off is basically the reverse: the course is changed and the sails untouched, Figs.3A and B. As with all lift producing surfaces the camber (line) heavily affects the lift achieved, as well as the maximum lift possible before stall and of course, also drag. By loosening or flattening the sail camber can be varied, Fig.3C. Furthermore, an atmospheric boundary layer exists, also on the water, Fig.3D. This means that

with lower altitude wind speed decreases, and this affects both TWS and apparent wind angle along the mast. Hence sails often can have their twist modified, that is a change of sail angle along its height, Fig.3E.

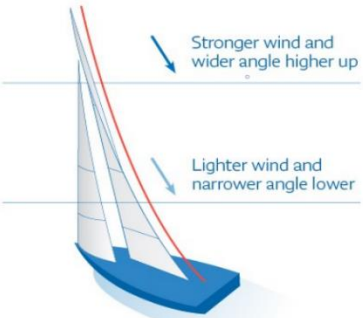


A: Trimming in to increase power

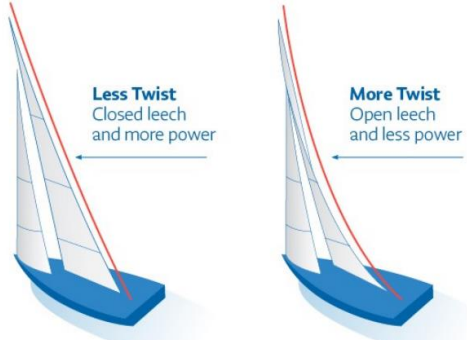
B: Bearing off to increase power



C: Sail camber and its effect



D: Wind gradient



E: Sail twist and its effect on sail power

Fig.3: An overview on how to modify the sail power (source: northsails.com)

All these measures change lift and drag along the sails and can hence affect the boats equilibrium position (heel, trim, sinkage) and its speed and leeway. In this work the concept of sail power is used: It is more or less directly related to the maximum lift to drag ratio on the sail, and will serve as a main parameter in the CFD-VPP, combining flatness and twist of the sails. Interested readers are referred to the Offshore Racing Congress (ORC) website.

3. Our velocity prediction program

A full-featured 3D CAD model is the entry point for this work. Theoretically, all such geometrical features can be meshed and taken into account in the CFD simulations. However, as will be explained

later, superstructure parts like mast, boom and stays can be handled in the VPP library, as well as the sails. In terms of the sails' arrangement, two configurations are given, Fig.4: main sail plus genoa and main sail plus spinnaker. The latter is used for downwind course and provides large propulsive forces via drag. All of the simulations shown are using a main sail and jib configuration, where a jib is basically a smaller genoa sail that does not overlap the main sail. The boat is run in full scale using our free surface code FINE™/Marine. Displacement is fixed at 12.5 t.



Fig.4: CAT CAD geometry and two sail configurations: main and genoa (mid) and main and spinnaker (right)

Fig.5 depicts a typical VPP on the left side: it consists of a matrix of CFD runs, with fixed boat angles (trim, heel), and fixed displacements. A full matrix can make hundreds of simulations necessary. This discrete data set is then approximated via a surrogate model, to find all configurations in between and hence also the ideal operating conditions. When the surrogate model is trained all combinations of TWA and TWS can be evaluated, which is a big plus. However, this is only valid when the geometry considered does not change.

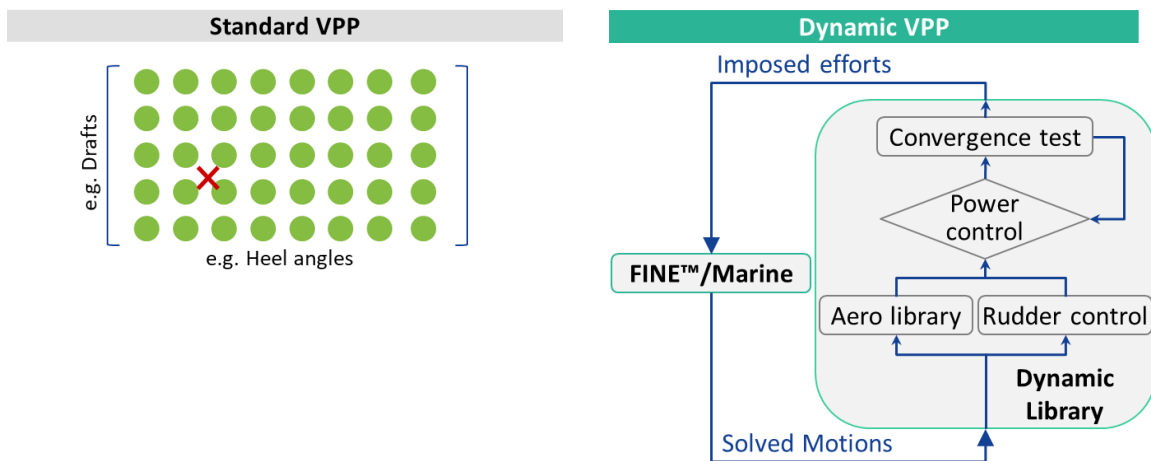


Fig.5: Comparison of a standard VPP to our dynamic approach

Fig.5 (right) shows the dynamic VPP: it consists of the flow solver and a dedicated dynamic library that contains all the VPP relevant data and control loops. The flow solver feeds the current body orientation into the library, which in turn calculates apparent wind angles and speeds. These are used in the aerodynamic part and for the sail polars to calculate sail forces and application points. A rudder controller rotates the rudder to balance the moments in gyration. A control loop for the sail power including a

convergence check ensures that the user defined bounds for e.g. allowable heel angle are kept, and also depowers the sails if necessary. Output of the library are the summed aero forces and moments, which are applied in the flow solver and the new boat motion is solved for. This cycle is repeated in physical simulation time at each time step until convergence is achieved, meaning the equilibrium point (hydrodynamic and aerodynamic forces and moments) is found.

This VPP needs one simulation only per TWA and TWS (input parameters) while optimising the sail power to find the best possible boat speed. It is furthermore a five degree-of-freedom (DoF) simulation that allows high accuracy and an overall very realistic boat behaviour.

The library has been developed in partnership with Finot Conq and is originally intended for very fast racing yachts like those used in the Vendée Globe. The one fixed DoF is the gyration, which is handled by the rudder controller. A limiter is implemented that invalidates the current VPP iteration if the rudder stalls due to too high angle of attack. The rudder itself must not be meshed; it is represented via a lifting line, which is fed a table of c_L and c_D coefficients over angles of attack.

All the hydrodynamic forces on the sailing boat are solved with the RANS CFD code, while a modified Offshore Racing Congress (ORC) model handles the aero forces. This includes the sail forces but also extra features like the mast or the superstructure. Finally, the atmospheric boundary layer is also fully implemented; no need to create a fine and adapted CFD mesh here.

4. Case preparation

The link between any CAD software and a CFD system is always a critical one: even when using the same geometry filter like IGES or STEP different software often handles geometry differently. In this case only a few surfaces are missing after import into OMNIS™, and these are approximated efficiently using OMNIS™/ Auto-Seal, Fig.6. It is based on an octree algorithm and required the user only to input points defining the inside and the outside of the open geometry. The rest is fully automatic and only takes a bit of CPU resources. In the present case, some very tricky closing surfaces are created (windows to roof) in a couple of minutes, allowing a seamless progress towards the meshing.

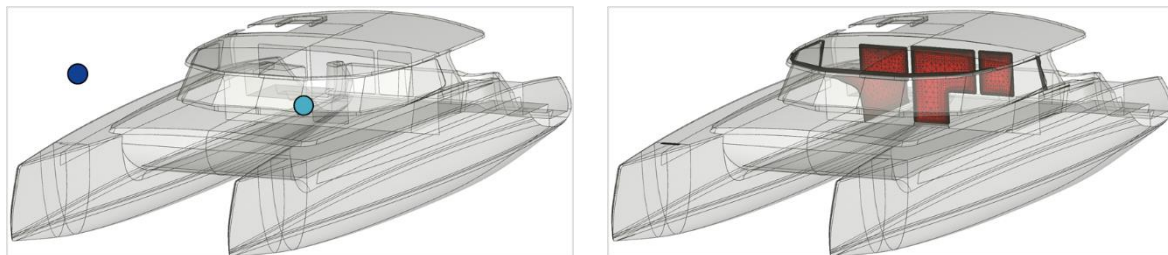


Fig.6: Preparation of the geometry via OMNIS™/AutoSeal: automatic creation of closing surfaces

Meshing tool is OMNIS™/HEXPRESS which creates unstructured hexa-dominant or fully hexahedral (this work) numerical grids. Smart algorithms like curvature detection or edge- and surface-proximities allow for a fast creation of high quality meshes. The focus in this work lay fully on the wetted geometry, around 800k cells are used for this, without the viscous layers. Tunnel and superstructure were deliberately kept coarse, increasing the cell count by only 300k. A high Reynolds-type viscous layer is inserted on the wetted parts, adding another 400k cells, hence totalling to 1.5M. Fig.7 gives an impression of the meshes for two appendage configurations.

To feed the VPP library with the rudder polars for the lifting line an intermediate CFD step is necessary. It is a quite simple mono fluid simulation that contains only the rotate-able rudder, Fig.8. The top patch is a Euler wall, the rest of the domain boundaries are either velocity or pressure conditions. A low Reynolds approach is used here, and the rudder angle of attack is modelled via a rudder rotation in a sliding interface.

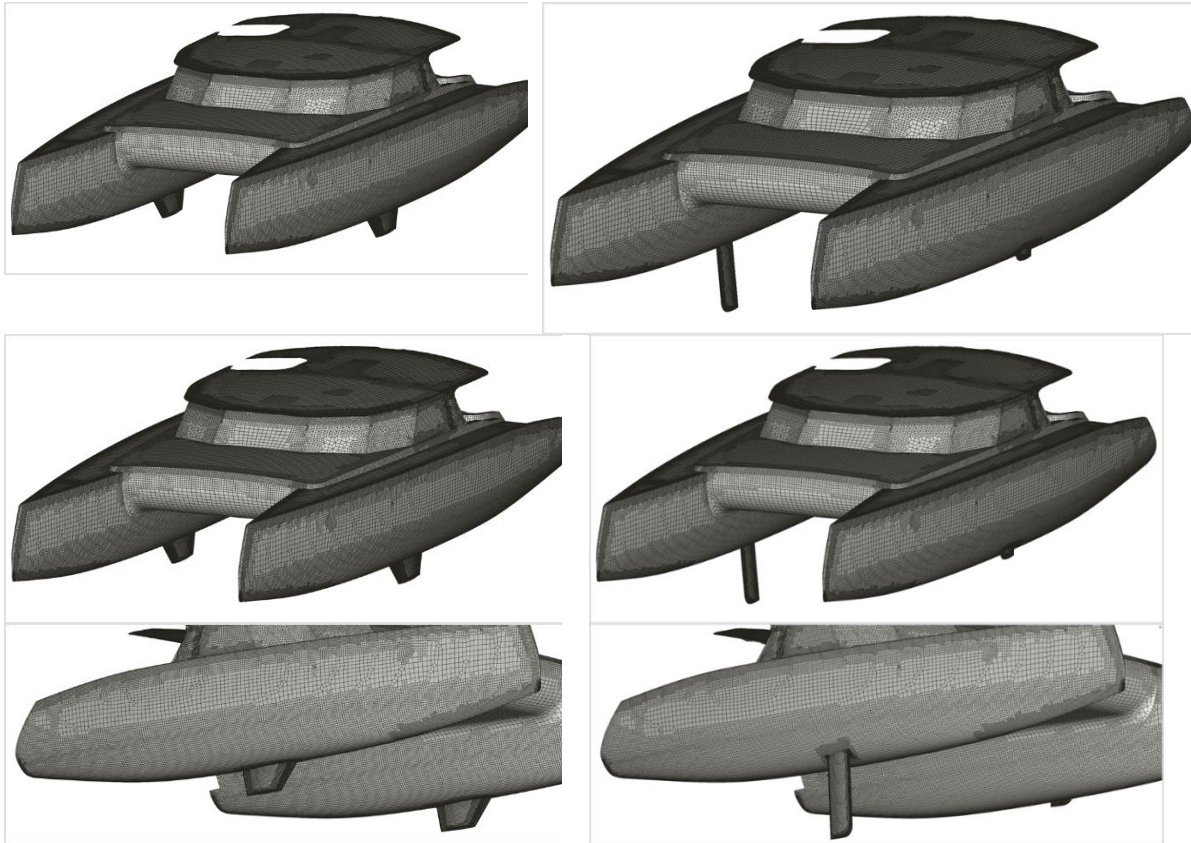


Fig.7: High-Re meshes for two appendage configurations

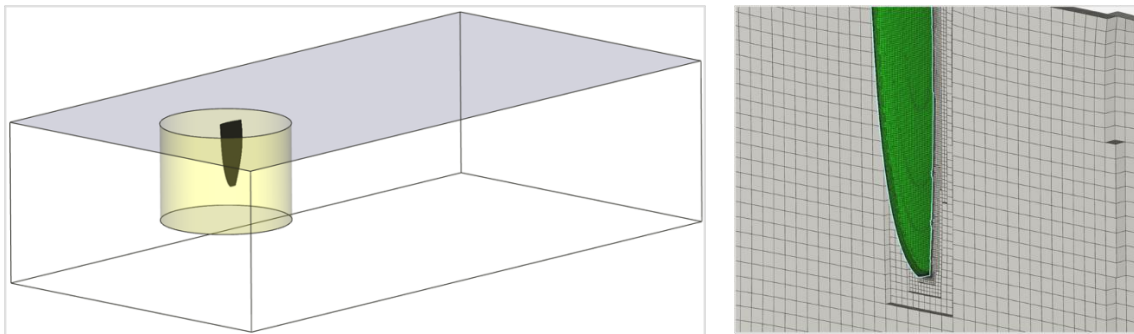


Fig.8: Domain and mesh for the calculation of rudder polars

The resulting polars are given in Fig.9, showing the lift coefficient over the drag coefficient. Polars for three inlet velocities and hence Reynolds numbers are calculated, these are used accordingly later on in the VPP simulations.

A final input into the VPP is the sails data. This consists of the sail polars, and the layout or sections of the sails considered. Polars (lift and drag over apparent wind) were not available from the sails' maker, and there was no time left to calculate them by ourselves in CFD. However, the VPP library contains a default set of polars, coming from an IMOCA 60 racing yacht. These are using high-fidelity sails, and hence the results of the VPP simulations must surely be seen as an overly positive result in terms of boat speed. Since these polars contain internal knowledge from Finot Conq, they cannot be shown. Lastly, the sectional data is defined according to Fig.10, and has to be provided for all sails as a simple .txt file (as all inputs are).

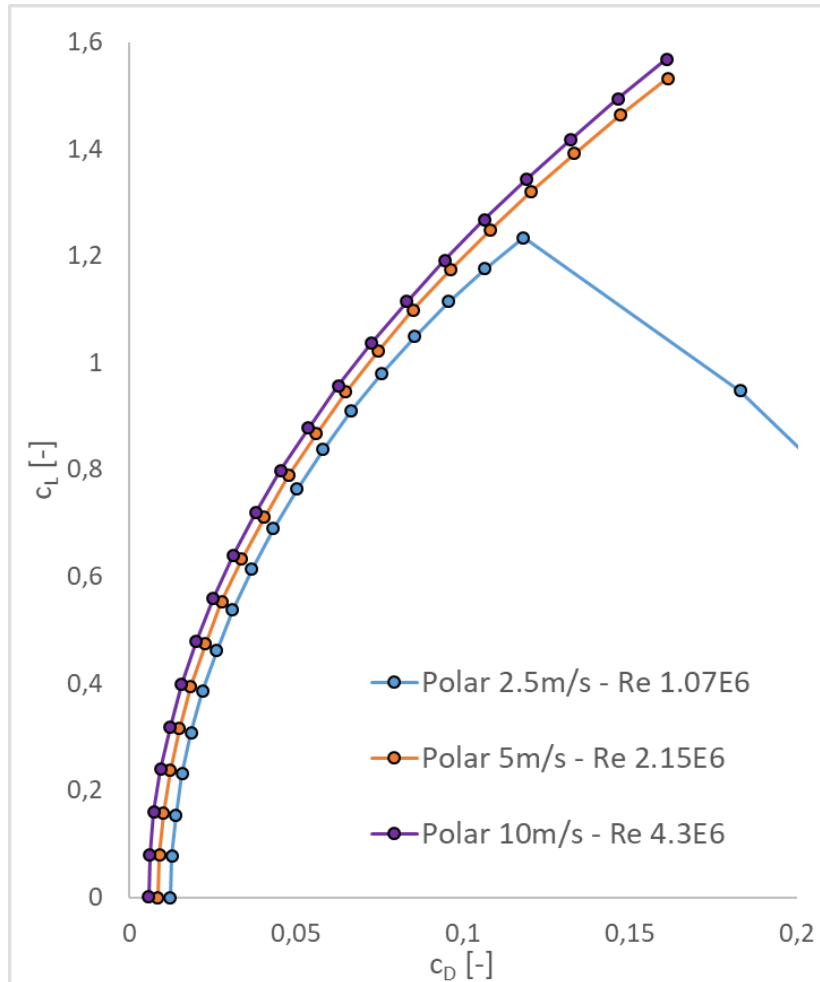


Fig.9: Calculated rudder polars for three Reynolds numbers

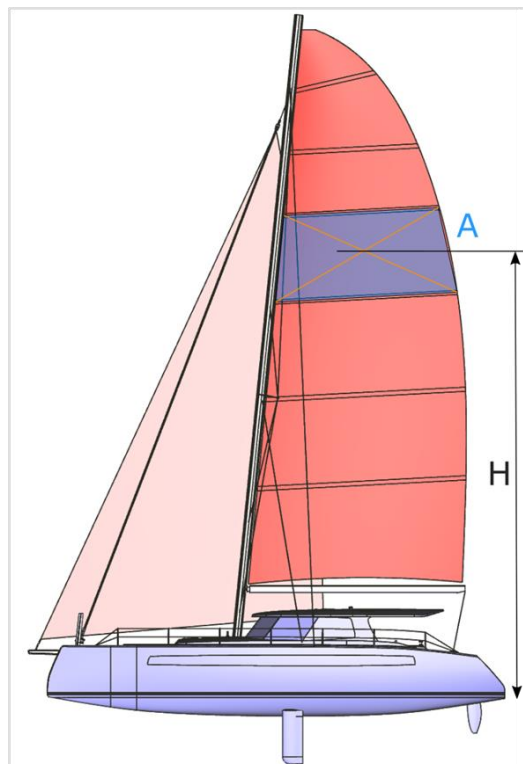


Fig.10: Sail section input into the VPP

5. Results

The results of a typical VPP simulation are shown in Fig.11. It depicts the boat speed as well as heel and trim angles over the physical time, and several phases are observed. The boat is initialised with a user defined speed at time step zero, after which the VPP is fully active and the five DoF are solved. In a first VPP iteration the sails are operating at 100% power, and the simulation is run until convergence of forces, moments and motions. At convergence the equilibrium point is found, that is the boat speed and orientation at 100% sail power (~90 s in Fig.11). In the same simulation a second VPP iteration is started, reducing the sail power (by default to 61%). This leads to a loss of boat speed and also a reduction of trim and heel, and the simulation is again run until convergence (~130 s). To find a new and probably more suitable sail power setting a parabolic relation is assumed between the two boat speeds and power values, and the new sail power value is calculated as the parabola's apex. This sail power is then used in the third VPP iteration and run until convergence. Fig.11 shows that this iteration already gives a higher boat speed than at 100% sail power (~160 s), and the VPP can be continued to optimise the sail power even further. Typically, four to five iterations suffice.

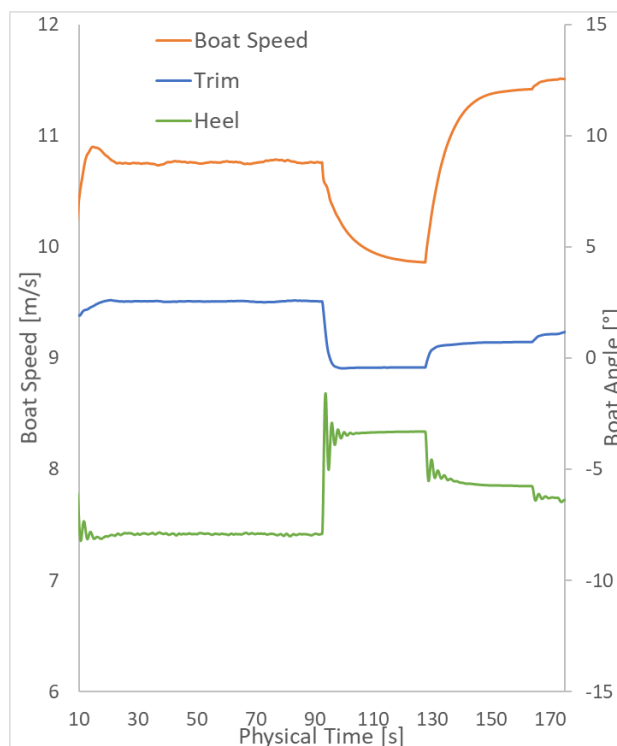


Fig.11: Typical output of the VPP: boat speed and angles with varying sail power

There are now two main questions: why is the boat faster and how to interpret the sail power? When reducing the sail power and hence forces on the sails, of course a negative impact on boat speed is observed. The boat's motions are affected too, however, and a reduction of heel can increase the effective sail area facing the wind and also impact the hull's resistance. The latter is even more depending on the boat trim, and the reduced sail's work will de-trim the hull from bow down upwards, largely reducing hydrodynamic resistance. In the end it is a typical optimisation problem, with the best trade-off to be found. The sail power is a combination of several parameters, and one cannot retrieve the actual sail settings to be used for a given operating point. Instead, the efforts from the sails, which are an output of the VPP as well, need to be correlated with aero matrices provided by the sails' maker.

Sailing boat performance is normally plotted in a polar diagram as shown in Fig.12. The radial coordinate gives the boat speed, while in circumferential direction the TWA is plotted. Zero degree is on the top side and again fully facing the wind. The catamaran is run at various operating points, covering TWA from 30° to 180° and TWS from 12 to 24 kn. In this sail configuration (main sail and jib) highest boat speed is reaching almost 22 kn at 90° TWA and 24 kn TWS.

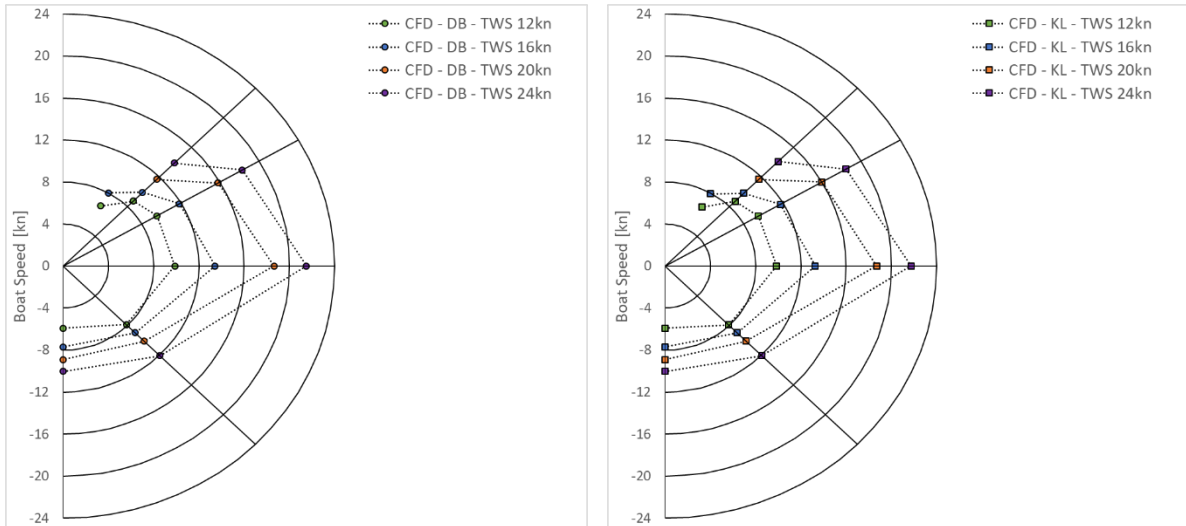


Fig.12: Final VPP results: boat speed polars for the daggerboard (left) and keel (right) configurations

One objective of this work is the comparison of different appendage types. All configurations investigated (keels, daggerboard, both) are shown in Fig.13. Using the daggerboard on top of a keeled hull is clearly the worst configuration, with the penalties increasing with higher TWS. A surprising result is the performance of the daggerboard though. It was expected to achieve superior speed over the keel, especially in upwind conditions. In these first sets of simulations this could not be clearly observed, there are only slightly higher boat speeds for low TWS (0.1 to 0.2 kn), and the trend reverses at higher TWS. This is currently investigated further and might be shown in a later work. A final remark regarding the low performance of the catamaran downwind: we are running with the jib as a fore sail, and the sail of choice should be a type of spinnaker (drag sail). This is perfectly possible in the VPP presented and will also be part of continued work.

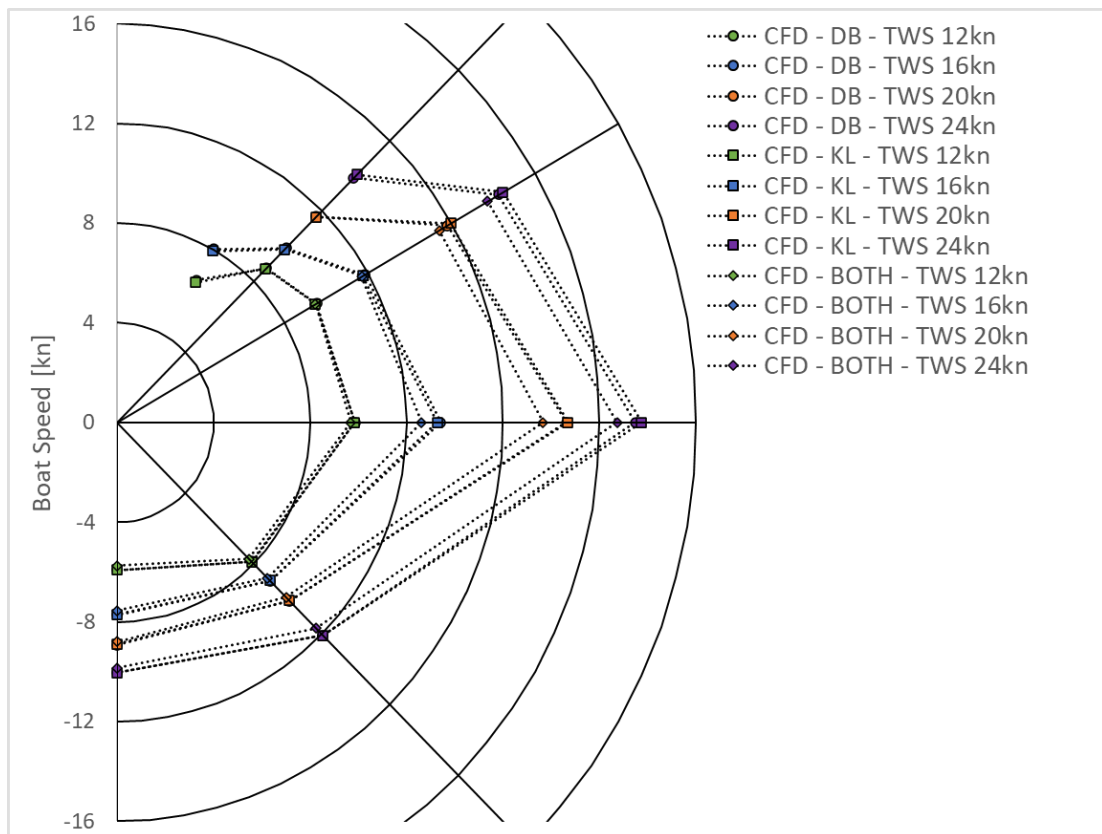


Fig.13: All polars in comparison

Now quite a few operating points are considered, but what about the sail power, the optimisation for boat speed at each operating point? This is given in Fig.14, listing the boat speed in m/s in the grey columns and the ideal sail power according to our VPP in the column next to it. For a lot of operating points 100% sail power just gives the highest speed, no need to de-power the sails for optimised boat orientation. There is a clear trend observable though: as the TWA decreases and as TWS rises the de-powering also increases, and the boat speed can be improved in these regions by up to 15%, compared to 100% sail power. In downwind sailing conditions the catamaran is just a well behaving boat, and it stays in its comfort zone for a large operating range. In Fig.14, four operating points are missing (TWA 30°, TWS 20 and 24 kn): here the limiter on the heel allowed kicked in and the VPP simulations are stopped. The limit is set to 15°, after all this is a pleasure boat (and a catamaran on top) and not a racing yacht. But again, the dynamic VPP would be perfectly suitable to calculate and optimise these points as well. In fact, that is the origin of the VPP presented.

Daggerboard									
		TWS [kn]							
		12		16		20		24	
TWA [°]	30	3,398	91,40%	4,13	77,10%				
	45	4,511	100,0%	5,098	96,00%	6,014	92,60%	7,137	79,10%
	60	4,921	100,0%	6,103	100,0%	8,13	94,70%	9,399	78,90%
	90	5,079	100,0%	6,906	100,0%	9,587	100,0%	11,059	95,10%
	135	4,057	100,0%	4,623	100,0%	5,206	100,0%	6,215	100,00%
	180	3,046	100,0%	3,96	100,0%	4,587	100,0%	5,162	100,00%

Keels									
		TWS [kn]							
		12		16		20		24	
TWA [°]	30	3,332	87,70%	4,086	77,10%				
	45	4,486	100,0%	5,052	100,0%	6	93,10%	7,244	79,60%
	60	4,887	100,0%	6,051	100,0%	8,222	96,00%	9,497	88,00%
	90	5,065	100,0%	6,826	100,0%	9,618	100,0%	11,189	95,60%
	135	4,072	100,0%	4,617	100,0%	5,194	100,0%	6,208	100,00%
	180	3,041	100,0%	3,966	100,0%	4,575	100,0%	5,16	100,00%

Both									
		TWS [kn]							
		12		16		20		24	
TWA [°]	60	4,887	100,0%	6,027	100,0%	7,936	100,0%	9,128	91,60%
	90	4,983	100,0%	6,497	100,0%	9,085	100,0%	10,671	100,00%
	135	3,98	100,0%	4,535	100,0%	5,095	100,0%	6	100,00%
	180	2,95	100,0%	3,88	100,0%	4,521	100,0%	5,066	100,00%

Fig.14: Computed sail power depending on TWA and TWS

Since we are doing CFD here, we obviously are obliged to present some nice and colourful pictures. Presenting all the data would leave the scope, but as a teaser Fig.15 is given, showing the version with keels at 24 kn TWS and 90° TWA, the sails are slightly depowered in this final state. Due to the leeway motion of the boat a large bow wave builds up on the port side of the port hull, and an overall nice wave pattern is achieved. The side and front views give an indication of the heel and trim, and one can imagine that the fun really starts here on the real boat!

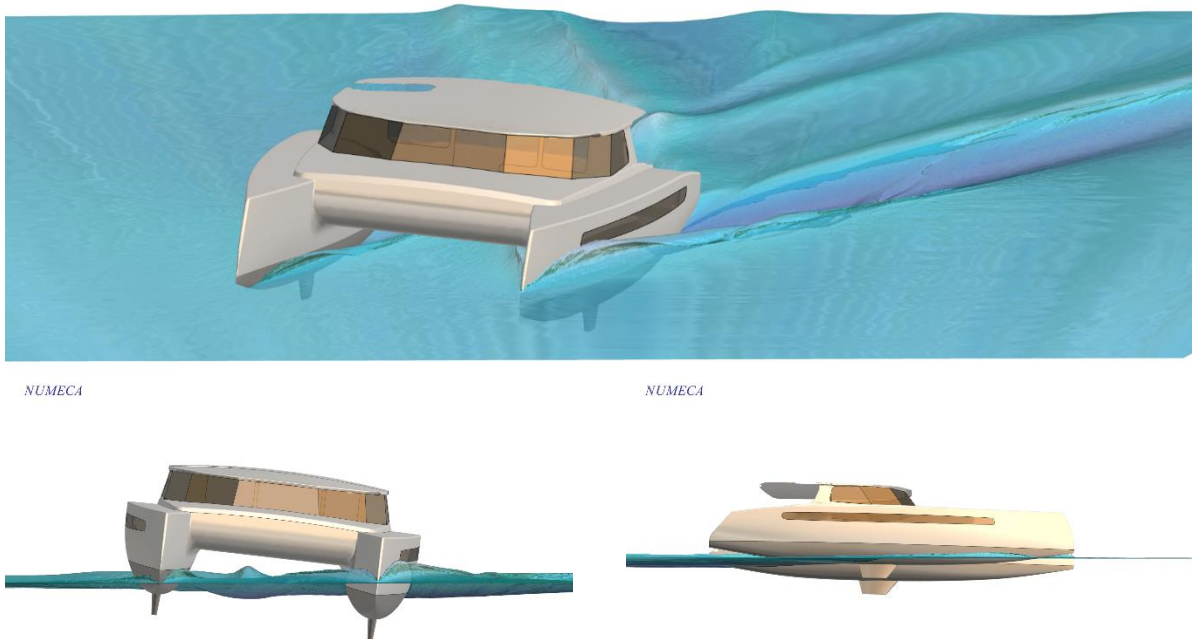


Fig.15: Boat operation at 24kn TWS and 90° TWA, Sail Power 95.6%

6. Conclusions

A CFD-based velocity prediction program for all types of sailing boats has been shown. It is very dynamic, calculating equilibrium points for a given set of true wind speed and angle in only one simulation. On top of that a de-powering scheme for the sails is implemented as well, optimising the sail power to find the best trade-off between boat orientation (trim, heel) and extracting the most useful energy out of the wind. This was done on an 16m Sailing Catamaran for which all the necessary inputs were available. The boat was furthermore run with different appendages (keels, daggerboard, both) and the effect on boat speed could be examined. While there is already a large amount of data and operating points present, work continues to evaluate in more detail the effect of the various appendages, and also increase the number of sail types used.

Websites referenced

<http://dutoityachtdesign.co.za/project/balance-526-sailing-catamaran/>

https://en.wikipedia.org/wiki/Forces_on_sails

<https://www.finot-conq.com/>

<https://www.northsails.com/sailing/en/2018/08/upwind-sail-power-by-bill-gladstone>

<http://www.numeca.de>

<https://www.orc.org/index.asp?id=41>

References

LEROYER, A.; VISONNEAU, M. (2005), *Numerical methods for RANSE simulations of a self-propelled fish-like body*, J. Fluid & Structures, 20/3, pp.975-991

MALLOL, B. (2012), *Computation of Free-Surface Viscous Flows around Self-propelled Ships with the Help of Sliding Grids*, Conf. Computer and IT Appl. Maritime Ind. (COMPIT), Liege

QUEUTEY, P.; VISONNEAU, M. (2007), *An interface capturing method for free-surface hydrodynamic flows*, Computers & Fluids, 36/9, pp.1481-1510

VISONNEAU, M; QUEUTEY, P; DENG, G.B; WACKERS, J; GUILMINEAU, E; LEROYER, A; MALLOL, B. (2012), *Computation of Free-Surface Viscous Flows around Self-propelled Ships with the Help of Sliding Grids*, Conf. Computer and IT Appl. Maritime Ind. (COMPIT), Liege

WACKERS, J.; AIT SAID, K.; DENG, G.B.; MIZINE, I.; QUEUTEY, P.; VISONNEAU, M. (2010a), *Adaptive grid refinement applied to RANS ship flow computation*, 28th ONR Workshop on Naval Hydrodynamics, Pasadena

Challenges in the Application of Ultraviolet Irradiation for Biofouling Control

Emmet Ryan, Newcastle University, r.emmet2@ncl.ac.uk
Serkan Turkmen, Newcastle University, serkan.turkmen@ncl.ac.uk
Simon Benson, Newcastle University, simon.benson@ncl.ac.uk

Abstract

This paper presents insights drawn from an experimental campaign investigating how intermittent Ultraviolet (UV) irradiation can successfully provide antifouling control on submerged surfaces in a marine environment, but also causes several potentially negative impacts on the surface properties. Specifically, the effect of intensity and exposure time has important consequences to antifouling effectiveness but also influences the surface microstructure, which can have subsequent performance impacts on the target hull or component including photodegradation and increased roughness.

1. Introduction

The operational, economic, and environmental consequences of biofouling are a constant problem throughout the marine industry. All submerged surfaces are susceptible to biofouling with detrimental impact such as an increase in hydrodynamic drag, reduction in vessel performance and adverse functioning of submerged or semi-submerged marine engineering systems and sensors. Biofouling is therefore a direct contributor to increased fuel consumption, emissions, maintenance costs, and down time on ships and other ocean-based systems.

Existing antifouling solutions rely on coating applications to inhibit surface fouling organism growth. An effective and potentially more eco-friendly alternative for marine anti-biofouling may be possible through the application of ultraviolet (UV) radiation. For example, an LED panel antifouling approach has been demonstrated successfully on an isolated location on a boat hull over a 21-month period as shown in Fig.1.



Fig.1 - Demonstration of UV-C LED Fouling Prevention, *Jongerijs et al. (2018)*

This example indicates how technology innovations may enable UV biofouling control to be applied to many different surfaces and diverse applications across the maritime industry. Importantly, it has been observed that intermittent UV application can achieve successful antifouling results. This significantly increases the design versatility for this approach to biofouling control.

However, the application of UV irradiation to exposed underwater surfaces, particularly ship hulls, creates additional design, implementation and impact challenges. It is these secondary impacts on the

target surface, and their implications on the environmental and economic performance of the ship, that is the focus of this paper.

The paper first reviews important design factors for implementing UV irradiation systems on a ship or other marine system. An experimental campaign, previously reported by *Ryan et al. (2020)*, is then summarised to demonstrate how intermittent UV can achieve successful antifouling results on submerged surfaces. These experiments investigate several parameters important to intermittent UV including the intensity, positioning and shadowing of the UV source. The study also investigates practical issues for UV application including the manufactured variability of light emitting diodes and photo-degradation of the applied surface.

The results not only demonstrate the potential application but also some limitations of UV irradiation methods for biofouling control. These insights are discussed within the paper. They identify the need for further research investigating the application of UV in combination with polymer coatings compared to its use as a standalone alternative to existing systems. If the application of UV is to be used in synergy with existing materials, further research is essential to determine the required UV dosage necessary to prevent biofouling from highly challenging fouling species, while also avoiding negative consequences such as polymer photo-degradation and surface roughening.

2. Background

Biofouling growth affects design, operation and maintenance across the entire maritime sector and beyond and has the potential to influence all submerged surfaces. In the case of ships, vessel performance can be impacted both externally through growth on the hull, and on internal systems - for example seawater cooling system inlets may become obstructed by growth, heat exchangers may become clogged resulting in reduced efficiency, and microbial influenced corrosion may result from biofilms, *Lewandowski and Beyenal (2009)*.

The need for biofouling control is intrinsically linked to critical environmental impacts from shipping, particularly the airborne impacts from greenhouse gas emissions and the waterborne toxicity impacts of biofouling control system.

The International Maritime Organization (IMO) greenhouse gases strategy aims to reduce overall carbon intensity from international shipping, with a target to reduce CO₂ emissions across the industry by at least 50% by 2050 compared to 2008 level. In addition to the uptake of alternative low-carbon and zero carbon fuels, design and technical innovation, including biofouling control, is considered as an essential contributor to emission reductions.

Existing antifouling solutions rely on toxic chemical coating applications to inhibit surface fouling organism growth. Such chemical coatings have several disadvantages, including harmful contamination of the local marine ecosystem through the leeching of toxins into the surrounding environment. In addition to the direct environmental impact, the use of current chemical applications requires expensive periodic cleaning and recoating of surfaces to maintain antifouling protection. Due to the negative environmental impact, the use of chemical antifouling systems is becoming increasingly regulated.

The development of effective alternatives to chemical coatings is therefore highly desirable from both an environmental and economic perspective.

The application of ultraviolet irradiation on to submerged surfaces is a potential alternative to conventional chemical-based coating systems. UV irradiation methods and technologies are extensively applied and proven in the fields of medical sterilisation and water treatment. These techniques are based on the principle that if UV radiation of sufficient dosage is applied to a target organism the resulting photochemical reaction which occurs damages the cells of the organism. The recent development of robust, low power UV-C Light Emitting Diodes (LED's), available at effective UV-C wavelengths, has made the consideration of this UV irradiation method practicable for marine antifouling applications.

3. UV Irradiation Design Factors

3.1. Mechanism for UV Irradiation of Microorganisms

When ultraviolet radiation/light is absorbed by the cells of microorganisms, damage is caused to the genetic material (such as DNA and RNA) within the cell. This damage renders the organisms incapable of being able to reproduce, thus preventing biofouling growth. This is the principle by which UV is used in water treatment and purification systems and the basis for its proposed use in antifouling applications, *EPA (2011)*.

Light is a form of electromagnetic energy with both particle and wave properties. It is transmitted in packets of energy called photons, *Bolton and Cotton (2011)*. The fundamental unit of optical power is a watt (W) and is defined as a rate of energy of one joule (J) per second.

Optical power is dependent on the number of photons, and significantly the wavelength of the light. The energy per photon increases inversely to the wavelength of the light according to Planck's equation of photon energy *Ryer (1997)*. Therefore, short wave ultraviolet light has much more energy per photon than visible light, *Lenk (2011)*. It is this high energy that causes changes to micro-organisms DNA and makes UV light useful for microorganism inactivation and potentially applicable for marine antifouling applications.

The detailed mechanisms of UV DNA disruption are complex and beyond the remit of this paper, therefore only a concise overview of the process is described. The process of photochemistry occurs when sufficient photon energy is absorbed by a molecule to cause the molecule to become excited, resulting in a chemical reaction. UV light in the 200nm to 300nm spectral band is referred to as the germicidal irradiation or UV-C range, because at these high energy wavelengths, UV light is absorbed by the DNA and RNA of microorganisms at relatively low dose rates. It is this absorption of UV photons by microorganisms that results in a photochemical reaction that changes the structure of their DNA and RNA. In this state microorganisms are termed inactivated i.e. still metabolically alive for a period but no longer able to replicate, *Bolton and Cotton (2011)*.

A fraction of damaged organisms may self-repair through a process called photo-reactivation, whereby microorganisms exposed to visible light during or after UV exposure can survive. This may be significant in the medical and water treatment fields but is not considered to be a challenge for antifouling applications because any reactivated organisms on a surface will be subject to further irradiation and will likely be permanently inactivated, *Kowalski (2009)*.

3.2. UV Dosage and Duration

The fundamental factor that determines if UV light will be successful at preventing biofouling growth on a target surface is the dose applied i.e. the intensity of the light (irradiance) and duration of exposure on the target surface. UV dose is typically expressed in units of mJ/cm² (1 mWs/cm² = 1 mJ/cm²). If the application of UV-C light on a submerged surface is of a sufficiently high dose, then the bacteria and unicellular algae in the initial attachment stages of biofouling are inactivated and cannot multiply. Therefore, the initial biofilm necessary to establish fouling is prevented.

Irradiance from a light source reduces inversely in proportion to the square of the distance to the target surface. Therefore, for UV projected antifouling applications the greater the distance from the source, the lower the effective intensity at the target surface. This inverse square law dictates the maximum distance that a UV light source can be located from a surface in order to adequately prevent fouling. In addition to this, the clarity of the water also impacts on the maximum distance that a UV source can be located from a target surface. Any reduction in UV transmittance (UV-T) of light which is caused by the scattering and absorbance of UV in the water by suspended particles such as organic matter will reduce the effective distance of a projected UV antifouling system. Reduced UV-T may require increased dose rates or a reduction in the distance from the light source to the target surface.

3.3. Microorganism Response

The response and resistance of microorganisms to UV light varies greatly depending on the species. This is significant as there are more than 4000 potential biofouling species in the marine environment. In considering the practicability of a UV based antifouling system it is essential to determine the required UV dose necessary to inactivate all biofouling organisms that may be encountered. UV dose-response is determined by irradiating water samples containing the specific microorganism and measuring the concentration of microorganisms before and after UV exposure. The decay curve of microorganism species is logarithmic with the slope defined by a rate constant specific to that species.

3.4. UV-C Light Emitting Diodes

The use of UV lamps for water disinfection is well proven and dates to the early 20th century, with the first UV water treatment plant commissioned in Marseille in 1910, *Bolton and Cotton (2011)*. However, conventional UV lamps contain toxic mercury. Due to the waste/disposal and associated negative health effects associated with mercury, the manufacture and use of traditional UV lamps is set to be restricted, with new limits set out by the United Nations Environmental Programme Minamata Convention. Furthermore, to permit UV-C wavelengths to be transmitted, conventional lamps must be made using fragile quartz glass.

The recent development of UV-C Light Emitting Diodes (LEDs) provides major advantages over traditional UV-C lamps. UV-C LEDs require less power, are smaller, more robust, are not limited in on/off power cycles and do not contain environmentally harmful mercury which is currently used in UV-C lamps. It is the advancement of UV-C LED technology that makes the utilisation of UV irradiation potentially practicable for marine anti-fouling applications.

LEDs have been available for over fifty years; however, UV-C LEDs with wavelengths applicable to antifouling only became commercially viable and available in the 2000's, *Song et al. (2016)*. LEDs are small, robust and have a much lower level of power consumption compared to relatively large fragile lamps. LEDs have a long operational lifetime and can be powered on/off instantaneously without affecting performance. This compares favourably to lamps which have a long off/on warm period and lower lifetime.

LED power supply sources are less complicated when compared to traditional lamp ballast circuits, *Branas et al. (2013)*. This reduces production costs and increases the reliability for LED power supply circuits. Furthermore, LEDs produce lower levels of heat and the devices can be engineered to efficiently dissipate heat in water therefore mitigating the potential biofouling and increasing UV output, *Lawal et al. (2018)*.

4. Experiments

A series of field tests, previously reported by *Ryan et al. (2020)* and only summarised here, demonstrate the effectiveness of UV-C irradiation of biofouling with low-cost LEDs, focusing on intermittence and positioning of the UV-C source.

4.1. LED Bench Tests

To confirm the UV intensity level from each UV-C LED used during field tests, an EXTECH SDL470 UV-C wavelength meter was used to measure the power density output from each LED used for experiments within this study. Tests were completed on widely available UV-C LED units (LG Innotek LLHMA22-00JB02A Waterproof Modules). These modules were subsequently used for the field tests.

Each LED was measured with the unit in direct contact with the sensor face with maximum intensity value recorded. Each LED was tested under identical conditions using a DC digital bench power supply set to a constant 10 Volts DC, 0.023 Amps supply. The results recorded a wide percentage variation in

the UV intensity output between LED modules. According to the LED module specification data, the typical irradiance measurement for the LED modules should be circa 0.5 mW/cm^2 . However, the measurements recorded range well below the specified value (UV-C = 0.043 mW/cm^2 to 0.138 mW/cm^2). This variation may be due to the 278nm LED emission being at the edge of the UV sensors measurement spectrum i.e. UV-C Sensor (280 – 240 nm), with the frequency bandwidth centre for the UV-C sensor = 254 nm.

4.2. Proof of Concept Field Tests

Initial field tests were completed to establish how projected UV-C irradiation from low-cost LEDs could prevent biofouling growth in a marine environment. To determine this, a LLHMA22-00JB02A Waterproof UV-C LED Module was mounted above a 220mm x 120mm x 5mm Perspex test plate with the UV-C projecting directly onto the plate surface. The LED was supplied with a constant 10 VDC, 23 mA supply via the bench digital control DC Power supply which has supplied from a 220 VAC source. Biofouling growth was periodically inspected visually and compared against an identical control test plate. A crucial aspect of the design of the LED test rig was to define the maximum distance that the UV-C LED could be mounted above the plate to effectively inactivate fouling microorganisms.

A UV intensity threshold of $0.0116 \mu\text{W/mm}^2$ was used for the field test design. The UV intensity emitted from the LED was taken as $0.70 \mu\text{W/mm}^2$ based on the UV LED intensity test results, Table I. Given the potential for a high level of dissolved matter at the test site, a conservative estimate of 50% UV transmittance was assumed. Therefore, at a distance of 20 mm the expected UV intensity on the plate surface was estimated at $0.175 \mu\text{W/mm}^2$. This was a factor of 15 times above the calculated threshold.

Based on the above calculations, test rig 1 incorporated a bracket to mount the UV-C LED at distance of 20 mm above the 220 mm x 110 mm Perspex test plate and included an electrical supply junction box as per Fig.2. As a control test rig 2 was built to the same dimensions and included the same mounting bracket in order to account for any reduced growth that may have resulted from shadowing on the plate surface from the bracket.



Fig.2: Field Test Plate Arrangement

Poolbeg Marina (53.3435° N , 6.2163° W) located in Dublin Port on the lower River Liffey Estuary was identified as the site to carry out field testing. Previous studies at the location noted a diverse marine ecosystem with fast biofouling growth over a short time period recorded on environmental sensors at the site. The rigs were mounted to the marina in a South facing orientation in order to maximise exposure to sun light and encourage growth on the plates, Fig.2. The plates were submerged from 22nd September to 8th November 2018.

The rigs were visually inspected to compare the differences in biofouling growth between the UV-C applied plate and the unprotected control plate throughout the 47-day deployment, Fig.3. Additionally,

the LED power supply was monitored to ensure correct circuit operation and consistent voltage/current levels were supplied to the LED and therefore a steady UV dose was applied to the plate for the duration of the field test.

After 15 days of deployment the control plate showed deposits of early fouling settlement on the plate surface which appeared to be consistent with the early stages of attachment of marine organisms. In contrast, the UV protected plate had no visible deposits in a large area below the LED, with some indication of fouling at the plate periphery.

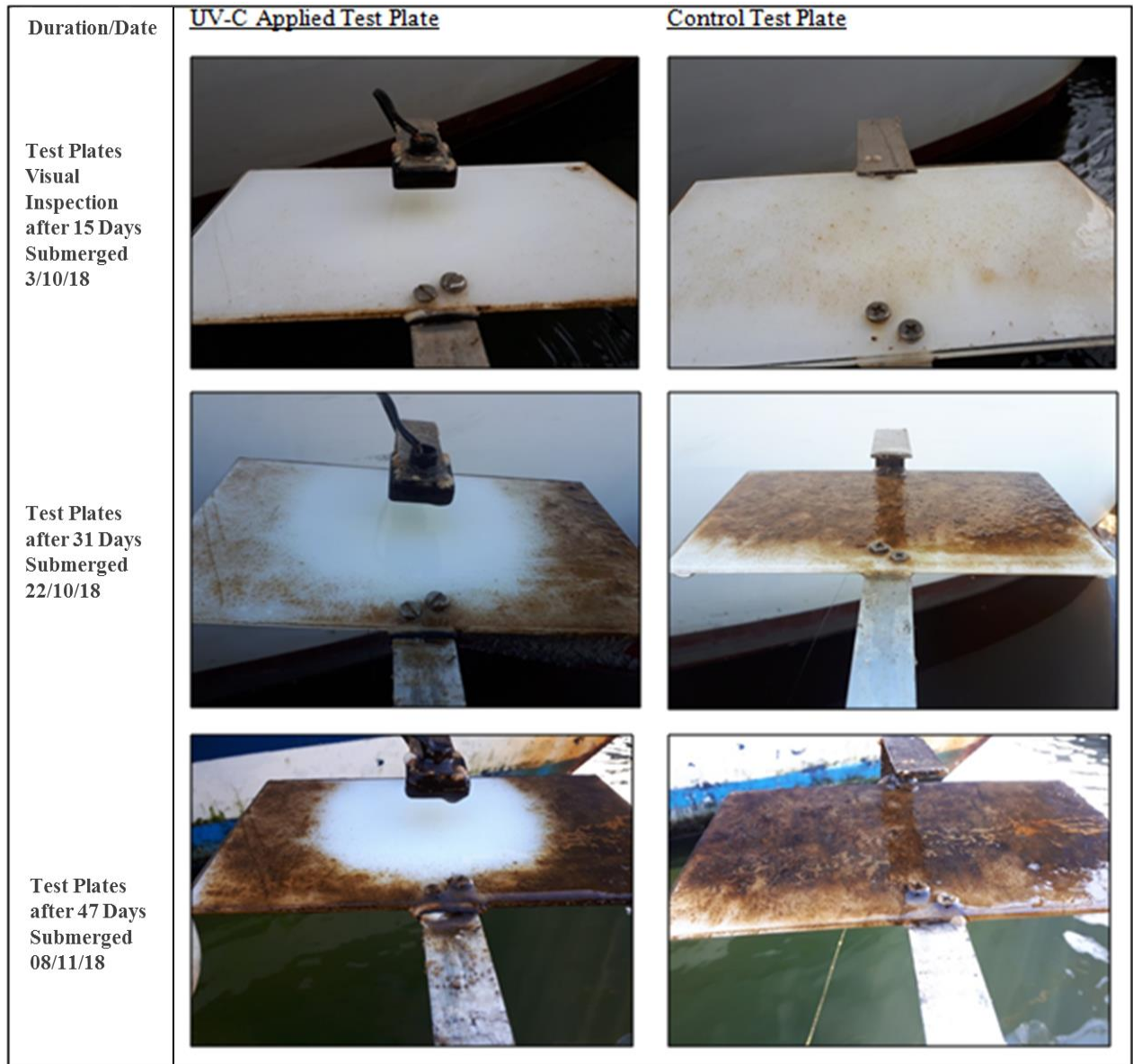


Fig.3: Proof of Concept Field Test Plate Observations

After one month submerged the UV applied plate had a clearly defined area below and extending out from the UV-C LED that remained entirely foul free with fully established growth towards the plate periphery which indicates a distinct area where the UV dose is insufficient to prevent growth. The control plate had 100% coverage and showed evidence of hard fouling species on the plate surface.

At the conclusion of the 47-day field test the UV protected plate had an entirely clean surface area free from fouling of approximately 100mm x 100mm. The area outside the LED coverage area had algae type growth coverage. The control plate on had 100% algae type growth coverage with some small

crustaceans firmly attached. Both test plates had small areas of lost fouling coverage which was likely to have been the result of flowing debris at the marina site coming into contact with the submerged plates and removing biofouling. Significant fouling growth was observed on the rear of LED module and the power supply cable throughout the field test. This was particularly prominent when the plate was submerged and growth was suspended in the water.

Following the cleaning of the UV test plate, an area of visible discoloration of the Perspex directly below the LED was observed, Fig.4. This is considered a direct result of the prolonged application of UV-C to this area and an indication of photo-degradation.

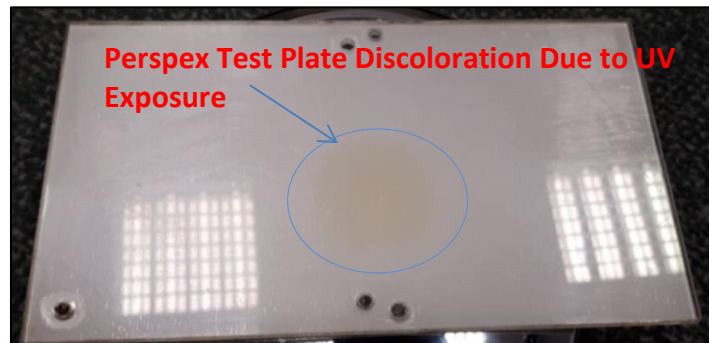


Fig.4: Test Plate Discoloration Due to UV-C Application

4.3. Effect of Exposure Time on Antifouling Performance

In order to examine the impact of reduced UV-C LED exposure time on antifouling performance, the UV-C test rig was fitted with a new LED module. The original DC power supply circuit was modified to include a programmable timer which was programmed with a duty cycle of 5 minutes on 100 minutes off. The low on time duty cycle was selected to ensure that an excessive level of prolonged UV did not have a detrimental effect on the overall number of organisms in the tank.

To encourage biofouling and allow research to continue throughout the winter months, testing was relocated from the field test site to a heated seawater aquarium tank at The National Sea Life Centre in Bray, Co. Wicklow, Ireland. A (900 mm x 300 mm x 220 mm) test tank was setup to accommodate testing, Fig.5. The plates were setup at the bottom of the tank to promote settlement and growth. The seawater used in the test tank was pumped directly from the Irish Sea via a screening inlet filter and was preheated before being added to the tank. An artificial source of sunlight was mounted directly above the tank operating for 12 hours per day. 25% of the tank water was replaced daily with fresh pre-heated seawater. This water renewal routine was carried out to promote growth and to ensure a continuous supply of biofouling organisms.

This aquarium tank test ran from the 18th December 2019 to the 6th February 2019. Fig.5 displays the growth on the two plates throughout the test period. No solid fouling was observed on either test plate, this was possibly due to the Teflon filter on the aquarium main seawater inlet preventing larger organisms from entering the tank. Although the UV-C dosage was reduced from 100% operation for the marina field test to an operational cycle of 5 minutes on, 100 minutes off, a similar foul free area was observed on the LED applied test plate, with only a small increase in growth on the plate. At the test conclusion the UV test plate had a 95 mm x 90 mm foul free area. The control plate had 100% coverage of heavy algae type fouling, Fig.6. There was no visible discoloration or evidence of photo-degradation on the UV-C LED applied Perspex plate following a post-test inspection.

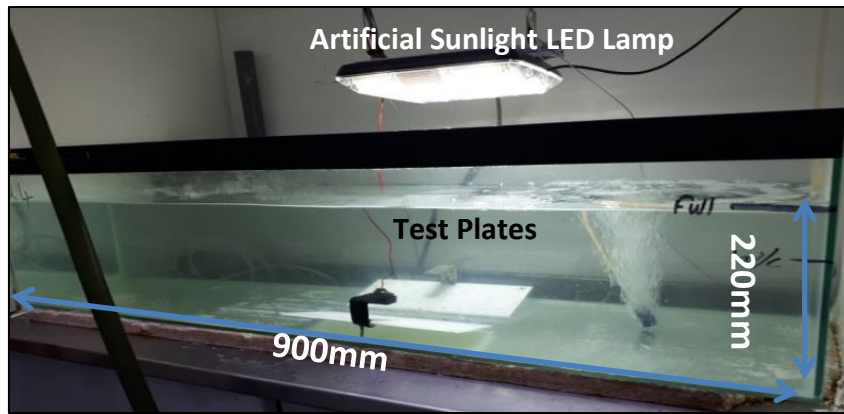


Fig.5: Aquarium Test Tank Setup



Fig.6: Test Plate Growth Record with Reduced Exposure Time

4.4. Assessment of the Effective Antifouling Distance of UV LED

The objective of this experiment was to ascertain the maximum distance that a UV-C LED could effectively maintain growth prevention on a submerged surface. For this test, the UV applied rig was modified with the LED centre mounted at one end of the test plate. The Perspex plates were covered in microscope glass test slides and deployed at the original marina site from 15th March to 10th May 2019.

As with the previous tests, the control plate had 100% plate fouling coverage. The UV-C protected plate indicated a maximum achievable antifouling distance of 70 mm with this arrangement, Fig.7. The foul free plate surface on the protected plate broadly followed the manufacturers specified irradiation beam projection pattern. A finding of potentially greater significance from this test is the visible deposits of heavy biofouling accumulation on the UV applied plate within the protected beam area. This growth occurred in small crevices between the glass test slides. This indicates that significant growth can establish in areas that are subjected to minor shadowing from direct UV application and demonstrates a potential challenge for future UV based antifouling systems in protecting complex 3D surfaces.



Fig.7: Effective Antifouling Distance of UV-C LED

5. Discussion

The field experiments demonstrate that intermittent application of ultraviolet (UV) radiation can achieve successful antifouling results. This research involved an experimental campaign which investigated several principal parameters of constant and intermittent UV applications on submerged test surfaces. Field tests included the variation of applied UV intensity which was undertaken by modifying exposure duration and positioning of the UV irradiation source.

Specifically, the results show:

- It is possible to keep submerged surfaces free of biofouling in the marine environment using a projected UV based antifouling application.
- The intermittent application of UV irradiation can be sufficient to keep surfaces foul free if it is applied at a sufficiently high intensity.
- UV-C intensity measurements indicate that a manufacturing variability exists between LEDs of the same model and specification.
- Minor shadowing from direct UV irradiation exposure can impede antifouling performance.
- Prolonged UV-C LED exposure is likely to result in the photo-degradation of polymer-based materials.

Previous research indicates that prolonged exposure to UV irradiation on polymer-based materials may cause damage. UV radiation is absorbed by many polymers, which results in photo-degradation, bond scission and chemical transformations creating structural changes that can lead to the loss of material characteristics and properties. Polymer degradation can manifest as cracking of flexible components. Significantly, fibre reinforced polymer-based composites are used extensively in the boat building and marine industry; with over 70% of smaller craft i.e. vessels less than 50 m in length constructed from polymer based composite materials. In addition, the majority of current hull and offshore structure antifouling coatings are based on polymers.

Increased surface roughness has been recorded as an early indicator of photo-degradation post UV irradiation exposure. Previous research reported roughness values for foul release antifouling coatings

ranging from 20 μm to 120 μm , with a general rule that for every 10 μm of surface roughness, frictional resistance increases by 1%. Therefore, resultant surface roughness due to prolonged UV-C exposure could impact significantly on hydrodynamic frictional resistance and performance.

Further research is required to ascertain the required UV levels necessary to prevent fouling, while maintaining the dosage below a level that may cause surface damage. There is also a need for further research investigating the application of UV in combination with different polymer coatings compared to a standalone alternative to existing systems. If the application of UV is to be used in synergy with existing materials, further research is essential to determine the required UV dosage necessary to prevent biofouling from highly challenging fouling species, while also avoiding polymer photo-degradation and surface roughening.

6. Conclusions

This paper demonstrates potential application but also some limitations of UV irradiation methods for biofouling control. An experimental campaign has demonstrated the fundamental principle that the delivery of UV-C irradiation onto submerged surfaces can achieve successful antifouling results and prevent the establishment of biofilms. These experiments indicate that surface embedded and targeted/projected UV irradiation of sufficient dosage, can be effective at interrupting the early stages of the biofouling surface settlement process, therefore, prevent biofouling growth before it becomes established.

For UV biofouling control to be further developed, there is a need for an improved scientific understanding of the UV response of target biofouling species and the interaction between UV irradiation and the substrate of submerged surfaces. In particular:

- Determination of the required UV irradiation dosage for effective fouling control against multiple challenging biofouling species is necessary. This is essential to ascertain the required UV intensity, distance from a target surface and intermittency of the UV application.
- The effect of prolonged UV exposure on polymer coated and uncoated surface microstructure which can influence material properties and increase hydrodynamic drag through surface roughening is required. This is necessary to evaluate UV exposure thresholds for such materials.
- The influence of static/dynamic biofouling growth in combination with UV antifouling performance is required.
- Overall foul control performance benefits and potential damage of applying UV irradiation on existing coating systems is necessary.
- Evaluation of effective methods of delivering UV irradiation to target surfaces is required.
- Quantitative evaluation of ship performance and marine system efficiency benefits from the application of UV biofouling control methods.

References

- BOLTON, J.R.; COTTON, C.A. (2011), *The ultraviolet disinfection handbook*, American Water Works Association.
- BRANAS, C.; AZCONDO, F.J.; ALONSO, J.M. (2013), *Solid-state lighting: A system review*, IEEE Industrial Electronics Magazine 7/4, pp. 6-14.

EPA (2011), *Water Treatment Manual: Disinfection*, Co. Wexford, Ireland Environmental Protection Agency

JONGERIUS, M.; PAULUSSEN, E., VISSER, C., (2018), *UVC antifouling solutions*, 19th International Congress on Marine Corrosion and Fouling.

KOWALSKI, W. (2009), *Ultraviolet germicidal irradiation handbook: UVGI for air and surface disinfection*. New York: Springer Heidelberg Dordrecht

LAWAL, O.R.; COSMAN, J.; PAGAN, J. (2018), *UV-C LED Devices and Systems: Current and Future State*, International Ultraviolet Association News, 20/1

LENK, R. (2011), *Practical lighting design with LEDs*, Wiley-IEEE Press.

LEWANDOWSKI, Z.; BEYENAL, H. (2009), *Mechanisms of microbially influenced corrosion*, Marine and industrial biofouling, Springer, pp. 35-64

RYAN, E.; TURKMEN, S.; BENSON, S. (2020), *An Investigation into the application and practical use of (UV) ultraviolet light technology for marine antifouling*, Ocean Engineering, 216, 107690

RYER, A. (1997), *Light measurement handbook*

SONG, K.; MOHSENI, M.; TAGHIPOUR, F.J.W. (2016), *Application of ultraviolet light-emitting diodes (UV-LEDs) for water disinfection: A review*, Water Research 94, pp. 341-349

Passive Air Lubrication: Demonstrating a Research Vessel Coated with a Hull of Air

Stefan Walheim, KIT, Karlsruhe/Germany, stefan.walheim@kit.edu

Thomas Schimmel, KIT, Karlsruhe/Germany, thomas.schimmel@kit.edu

Matthias Barczewski, KIT, Karlsruhe/Germany, matthias.barczewski@kit.edu

Lutz Speichermann-Jägel, KIT, Karlsruhe/Germany, lutz.speichermann-jaegel@kit.edu

Robert Droll, KIT, Karlsruhe/Germany, robert.droll@kit.edu

Susanna Dullenkopf-Beck, KIT, Karlsruhe/Germany, susanna.dullenkopfg-beck@kit.edu

Johannes Oeffner, Fraunhofer CML, Hamburg/Germany, johannes.oeffner@cml.fraunhofer.de

Jonathan Weisheit, Fraunhofer CML, Hamburg/Germany, jonathan.weisheit@cml.fraunhofer.de

Jean-Christophe Minor, Avery Dennison, Soignies/Belgium,

jean-christophe.minor@eu.averydennison.com

Marina Beltri, Aqua Biotech Group, Mosta/Malta CML, mmb@aquabt.com

Abstract

Superhydrophobic air-retaining surfaces represent a bioinspired approach to friction reduction in shipping. A ship, which is coated with permanent layer of air will show a reduction in (i) friction, (ii) biofouling, (iii) corrosion and (iv) noise. AIRCOAT aims to develop a passive air lubrication technology for marine applications, using self-adhesive foils instead of paints and is inspired by the Salvinia effect. This paper introduces the biomimetic concept with emphasis on the recently demonstrated AIR Spring Effect, which provides a 100-fold higher stability of the air layer against pressure fluctuations. A first test under marine conditions was successfully performed by coating more than the half hull of a 12-meter research vessel with AIRCOAT foil.

1. Introduction

Maritime transport emits around 940 million tonnes of CO₂ annually. This is about 2.5% of global greenhouse gas emissions. The European Commission's target is to reduce emissions from shipping by at least 50% by 2050. The H2020-AIRCOAT project is developing a bio-inspired solution, with the aim of reducing friction (viscous drag) by inserting an envelope of air between the ship's skin and the water. Oeffner *et al.* (2020) has already reported on the potential of this approach and on initial investigations.

1.1. The Biomimetic Concept of the Salvinia Effect

The Salvinia effect or Salvinia paradox has its name from the floating fern *Salvinia molesta*, Barthlott *et al.* (2010). The floating leaves of the Salvinia plant are densely covered with hairs (trichomes) to form a permanent air retention under water. These hairs have a fur of nanocrystals made of wax. Their surface thus is superhydrophobic, which keeps water from getting between the hairs, Fig.1.



Fig.1: Biomimetic microstructure (a) and leaf of the Salvinia plant (b) with micro-structured hydrophobic hairs (c)

As early as 2007, five criteria for air storage under water were identified: 1) hydrophobic surface chemistry, 2) nanostructured topography, 3) hierarchical architecture, 4) undercut structural features (overhanging structures) and 5) elasticity of hairs, *Solga et al. (2007)*. All these features are present on the upper surface of *Salvinia* leaves and account for the *Salvinia* effect. The *Salvinia* paradox, on the other hand, is the presence of the hydrophilic tips of the hairs, which are otherwise so hydrophobically endowed *Barthlott et al. (2009)*. The leaf thus "affords" itself hydrophilic areas and is therefore very different from many other superhydrophobic surfaces such as that of the lotus leaf. These water-attractive areas at the tips of the hairs stabilize the air-water interface.

2. Results and discussion

2.1. The Air Spring Effect

The *Salvinia* paradox is based on the fact that the air-holding hairs are superhydrophobic, but have hydrophilic tips at their ends that stabilize the air-water interface. In our recent publication *Gandyra et al. (2020)* we have used experimental and theoretical approaches to investigate the contribution of this pinning effect to the extraordinary stability of *Salvinia*'s air layer against pressure changes.

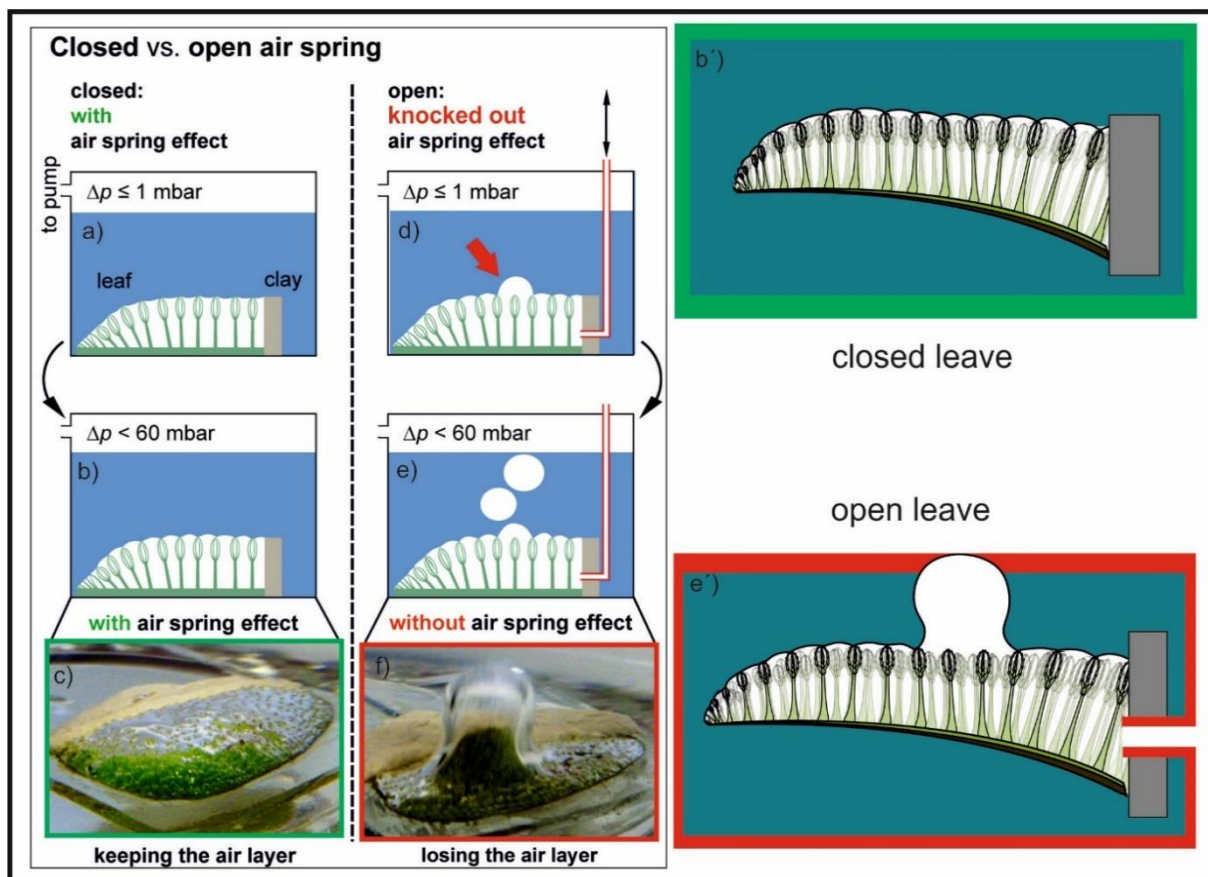


Fig.2: 100-fold increase in air layer stability was demonstrated based on the recently demonstrated AIR Spring Effect. The restoring force of the entrapped thin air layer stabilizes the air-water-interface against pressure fluctuations (a-c). An infinitely thick air layer approximated here by an open leaf forms a bubble at very moderate underpressure of only 60 mbar. (d-f), *Gandyra et al. (2020)*. A thick air layer would be very susceptible to pressure fluctuations, which would lead to air bubbles and thus to air loss in the flow. Therefore, a thin layer of air is much more stable against hydrodynamic effects and pressure fluctuations than a thicker layer of air.

Among other things, the capillary adhesion method was used there to measure the adhesion forces of individual hairs on the water surface to about 20 μN per hair. The leaves maintain a stable air layer up

to a negative pressure of about 65 mbar, which could be observed by confocal microscopy and fluorescence labelling. Combining both results, we obtain a total pinning force that is only ~1 % of the total air holding force. Therefore, the restoring force of the trapped air layer against pressure fluctuations is responsible for the remaining 99 %. The model of trapped air acting as a pneumatic spring ("air spring") was verified in this paper by an experiment in which the air layer is short-circuited, resulting in an immediate loss of air. *Salvinia molesta* thus increases its air layer stability to pressure fluctuations by a factor of 100 by using the enclosed air volume as an elastic spring.

Through these observations and quantitative evaluations on the adhesion force of the trichomes, it can be said, that with the action of the air layer as an elastic spring, a key factor for understanding the air-holding properties of *Salvinia molesta* under fluctuating pressure has been identified and quantitatively understood. These results have been incorporated into the development of the AIRCOAT foil and have led to the current state of development of the film. In general, it can be said, that the thinner an air layer is, the more rigid it is against pressure fluctuations.

2.2. Application of the AIRCOAT Foil

Over several development stages, the AIRCOAT film was finally produced on a larger scale at KIT in a continuous moulding process. After cutting the films and further processing by Avery Dennison, a self-adhesive film was produced which could now be tested for the first time on a vessel in a maritime environment.

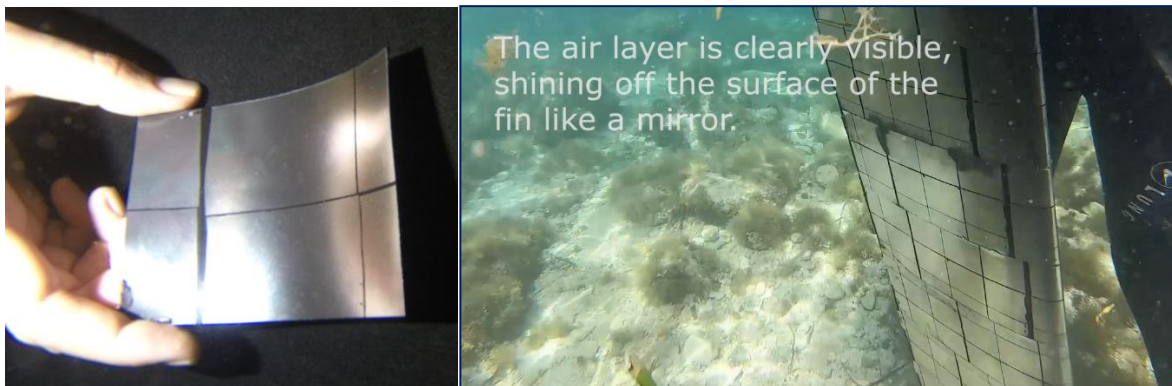


Fig.3: AIRCOAT foil under water in the lab (left). Fin surface coated with air-retaining AIRCOAT foil (right) in maritime environment. The air layer under water reflects the light like a mirror and gives the fin a silvery appearance.

2.2.1 Mounting of the self-adhesive AIRCOAT Foil in the shipyard

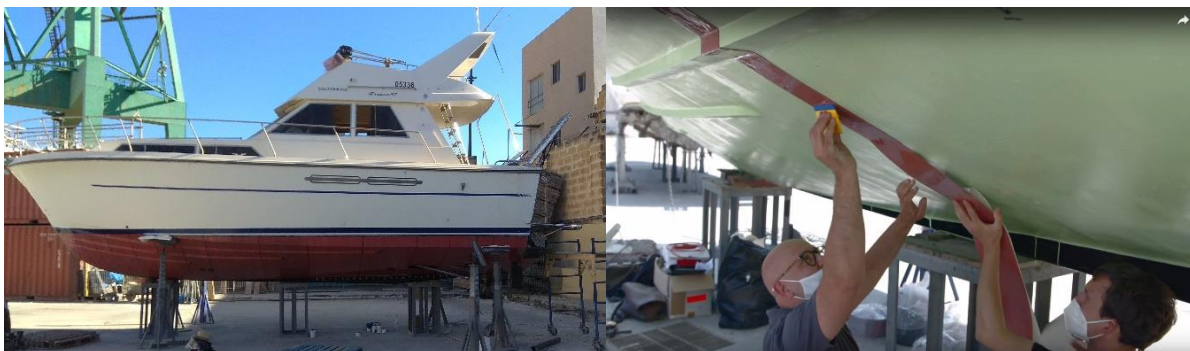


Fig.4: In June 2021 the research vessel 'Gipsy Lee' was coated in Valetta/Malta with AIRCOAT foil. The application of the self-adhesive AIRCOAT foil to the primed hull is seen on the right.

The application of the film on the test vessel took place in Valetta/Malta in June 2021. For this purpose, one side of an approximately 12 m long ship was covered with vertical strips of the film.

2.2.2 Air layer monitoring under water

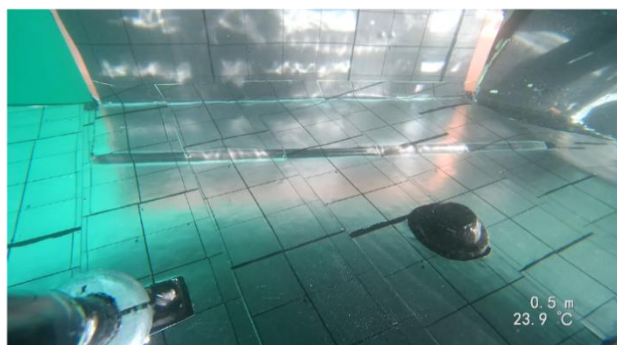


Fig.5: Underwater shots after a first test run. The air layer is clearly visible. The dark stripes are unstructured areas of the film.

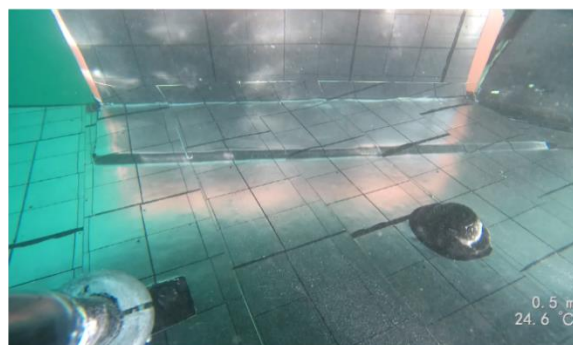
To observe the air layer during the first hours of immersion a monitoring device with fixed angles between light source and camera was built in a frame made from aluminium profiles with custom mounts to fixate torch and camera. The orientation of cameras and torch can be changed as well as the distance between them. This device was installed in a stern location at the transom just above the water line to avoid any damage from waves and current. The camera used was a Paralenz Dive+ camera with a fixed orientation and fixed focal length. It was installed in a distance of about 30 cm and due to the wide field of view almost the complete underwater portion of the portside transom is visible in Fig.6. The air layer is clearly visible as the characteristic silvery shimmer spread all across the image. The image in the upper left presents the initial conditions as the vessel is floating in still water in the harbour just minutes after it was moved from the dry dock into the water. The camera recorded a video over several hours and selected screenshots are displayed in Fig.6. The air layer was present all time. In between air bubbles adhered to the air layer, which were washed away at a later point as the vessel was moving at about 3 knots for approximately 30 minutes. The air layer, however, stayed present.

After two days the air was still present. The monitoring device was removed and pictures were taken from another perspective. Still, the silvery shimmer is present at a large portion of the transom. Air bubbles are attached to the air layer at some parts and other parts lost the air layer as indicated by black spots.

Initial air layer



~30 min air layer



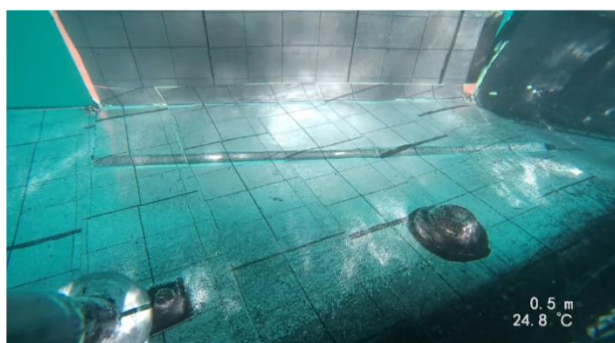
~60 min air layer



~90 min air layer



~120 min air layer



~150 min air layer

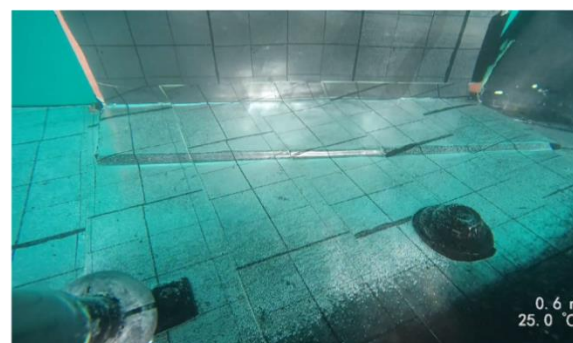


Fig.6: Condition of the RV air layer over time. This photo series shows the nature of the RV air layer under sea water conditions in the Mediterranean Sea over a period of ~150 min. One can see a change in the air layer by the altered intensity of the silvery shimmer, i.e. the air layer is slightly decreasing over time. Note also the temperature increase of 1.1 °C.

3. Conclusions

The effect of the air layer as an elastic spring is a key factor in understanding the air retention properties of the floating fern *Salvinia molesta*. These results have been incorporated into the development of the AIRCOAT foil and have led to the current state of development of the film. In general, the thinner an air layer is, the better it is protected against pressure fluctuations, to which it is always exposed in hydrodynamic applications.

The coating of the ‘Gipsy Lee’ was the first attempt at a large-scale coating of a ship with a superhydrophobic air-holding surface. The production of such large-scale, lithographically defined structures in the form of a self-adhesive film thus represents a milestone for micro- and nano-technological surface functionalisation.

Acknowledgements

The AIRCOAT project has received funding from the European Union's Horizon 2020 research and innovation programme under grant agreement N° 764553.

References

BARTHLOTT, W.; SCHIMMEL, TH.; WIERSCH, S.; KOCH, K.; BREDE, M.; BARCZEWSKI, M.; WAHLHEIM, S.; WEIS, A.; KALTENMAIER, A.; LEDER, A.; BOHN, H.F. (2010), *The Salvinia paradox: superhydrophobic surfaces with hydrophilic pins for air retention under water*, *Advanced Materials* 22(21), pp.2325-2328

GANDYRA, D.; WALHEIM, S.; GORB, S.; DITSCHKE, P., BARTHLOTT, W. SCHIMMEL, T. (2020), *Air Retention under Water by the Floating Fern Salvinia: The Crucial Role of a Trapped Air Layer as a Pneumatic Spring*, *Small*, 2003425

KOCH, K.; BOHN, H.F.; BARTHLOTT, W. (2009), *Hierarchically sculptured plant surfaces and superhydrophobicity*, *Langmuir* 25, 14116

OEFFNER, J.; HAGEMEISTER, N.; BRETSCHEIDER, H.; SCHIMMEL, T.; JAHN, C. (2020), *Reducing Friction with Passive Air Lubrication: Initial Experimental Results and the Numerical Validation Concept of AIRCOAT*, *HIPER Conf.*, Cortona, pp.405-417

OEFFNER, J.; JALKANEN, J.P.; SCHIMMEL, T. (2020), *From nature to green shipping: Assessing the economic and environmental potential of AIRCOAT on low-draught ships*, *Transport Research Arena*, Helsinki

SOLGA, A.; CERMAN, Z.; STRIFFLER, B.F.; SPAETH, M.; BARTHLOTT, W. (2007), *The dream of staying clean: Lotus and biomimetic surfaces*, *Bioinspiration Biomimetics* 2, p.126

Model-Based Assessment of a Fuel Cell Driven Very Large Crude Carrier Concept

Chara Georgopoulou, Lefteris Koukouloupoulos, George Dimopoulos, DNV, Piraeus/Greece,
chara.georgopoulou@dnv.com

Eirik Ovrum, DNV, Hovik/Norway

Lampros Nikolopoulos, Kostas Bougiouris, Euronav Ship Management, Athens/Greece

Abstract

Aiming at decarbonizing shipping activities, the industry investigates energy conversion alternatives that depend less on carbon-based fuels, including fuel cells. Since no real data on large scale fuel cell installations onboard vessels are available, simulation models can support the performance assessment of fuel cell powered ships in comparison to their conventionally driven counterparts. This paper presents an energetic performance assessment of a Very Large Crude Carrier (VLCC) using modelling and simulation techniques. The solid oxide fuel cells (SOFC) replace the conventional internal combustion engine and supply power to the propeller through an electric propulsion train. The fuel cell (FC) stack is supplied with pre-reformed liquefied natural gas (LNG) and its hot exhaust gas passes through a catalytic burner to ensure that no hydrogen traces escape. The exhaust heat is used to produce electric power through a waste heat recovery (WHR) and steam generator system. Electric loads are also covered from the fuel cell stack, whereas steam demands are covered by a dedicated gas boiler. To maintain the pressure of the LNG fuel tank, a reliquefaction system is considered, adding to the electricity consumption of the system. The fuel cell powered system is modelled using our in-house DNV COSSMOS (Complex Ship Systems Modelling and Simulation) platform. The fuel consumption and emissions are calculated per operating mode and speed. Annual operational data on a real VLCC are used, based on analytical information provided by Euronav, an owner and operator of VLCC's. The combination of real ship data and energy system simulations provides a realistic picture of the performance of a fuel cell VLCC. A conventional VLCC machinery fueled by marine gas oil (MGO) is also modelled and compared to the fuel cell case. The results are assessed per mode and the total fuel efficiencies of the two different systems are calculated, over a complete year of operation, with several different operating modes with different propulsion, electric power, heat, and steam demands. On annual terms, the total baseline efficiency is 42%, whereas the fuel cell powered one is 60%.

1. Introduction

Fuel cells are mainly considered an option for decarbonization of the shipping industry due to their capacity to operate at high efficiencies when using hydrogen as fuel. Until hydrogen becomes a standardized marine fuel, LNG can be used as a transitional fuel from conventional carbon-based fuels to a carbon-free economy. Fuel cells have the capacity to operate with variant fuels, including LNG with proper fuel reforming.

Large scale fuel cells have not been demonstrated on ships and there is uncertainty related to their performance. Process modeling and simulation tools offer the advantage to analyse the performance of a technology in the computer in an easy and resource saving manner. The future performance and benefits of the technology can be assessed, verified, and compared to the baseline systems.

This paper presents an energetic performance assessment of a Very Large Crude Carrier (VLCC) powered by solid oxide fuel cells (SOFC), burning pre-reformed liquefied natural gas (LNG). At the SOFC inlet, waste heat recovery is used to produce additional electricity at a steam generator system. To maintain the pressure of the LNG fuel tank, a reliquefaction system is considered, adding to the electricity consumption of the system.

The performance analysis is conducted using simulation models in DNV COSSMOS (Complex Ship

Systems Modelling and Simulation). Two models are developed: a conventional VLCC machinery and an FC powered counterpart. The models can predict fuel consumption and emissions at a range of operating modes and speeds. Apart from the specifications of the systems, key input to the model is a representative annual mission profile of a real VLCC, derived from actual operational data from a real Euronav VLCC. The annual energy consumption of the FC powered vessel is calculated and compared against the baseline case.

Section 2 presents the specifications of the vessel case, including the baseline machinery description and the mission profile. Section 3 presents the developed model of the baseline and fuel cell systems. Section 4 is dedicated to the simulation results at design conditions and on an annual basis. Finally, section 5 summarizes the conclusions of this paper and suggestions for further works.

2. Case specifications

2.1. Baseline

The case study vessel is an A-series VLCC of Euronav that operates worldwide, with typical voyages between Gulf of Mexico to Asia, Brazil to Asia, Arab Gulf to Europe, and others. The vessel machinery system includes one 2-stroke marine Diesel engine of 24 MW MCR (max continuous rating) at 65.7 RPM, three 4-stroke Diesel generator sets of 1530 kW at 900 RPM, a main engine economizer, and an auxiliary boiler. Daily data on the operation of the VLCC were analyzed to produce a representative mission profile as shown in Fig.1. For each mode and speed, the frequency of annual time in that mode, the propulsion power in kW and the electricity demand (kW) were determined.

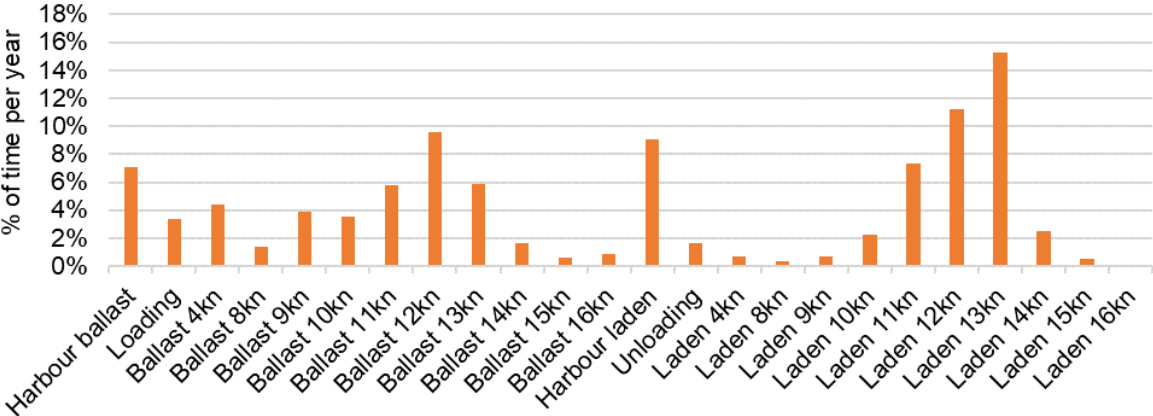


Fig.1: Time per year and operating mode

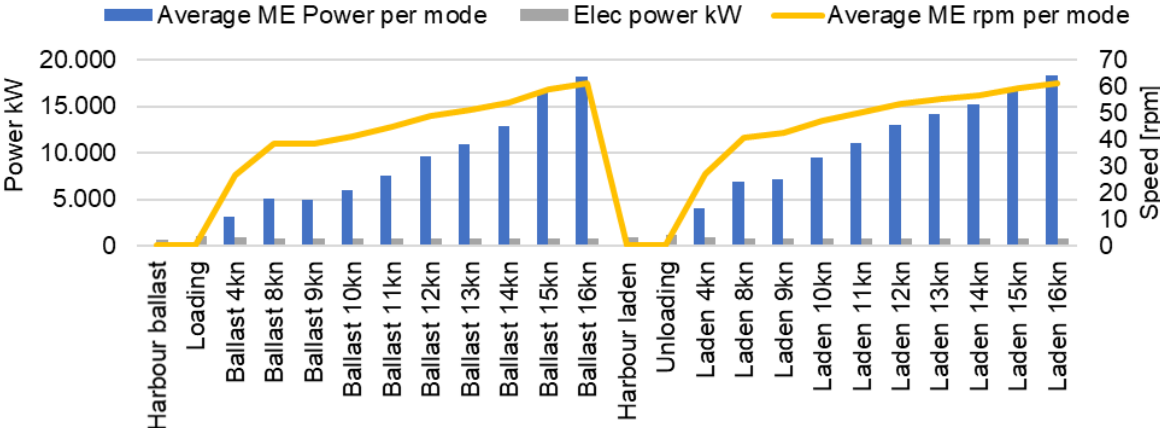


Fig.2: Power and electricity demands

2.2. Fuel-cell powered variant

A solid oxide fuel cell (SOFC) burning pre-reformed liquefied natural gas (LNG) is considered. SOFCs are high temperature fuel cells, that electrochemically produce DC electric current by oxidizing streams of pre-heated fuel and air, at a typical operating temperature of about 800oC. The pre-heaters operate by using the hot fuel cell exhaust. The remaining exhaust heat is utilized in a waste heat recovery WHR component to produce steam. The steam is then led to a steam turbine (ST) for additional power production. This combined cycle system is an expansion of novel marine fuel cell concepts. The purpose of testing its performance for a VLCC is to understand the potential benefits of combined cycle operation over the typical efficiency of fuel cells, which is at the order of 55 to 58%.

From the analysis of actual propulsion power demand data over a period of two years, it has been observed that the demand exceeded a threshold of 14 MW, only for less than 10% of the vessel sailing time, as shown in Fig.2. Consequently, the nominal fuel cell stack size was determined at 15 MW, accounting for 1 MW of parasitic consumptions. Fig.3 shows a comparison of the parasitic loads for both cases. It is notable that the order of magnitude of parasitic loads is similar between the baseline and fuel-cell driven system, despite the inherent technical differences.

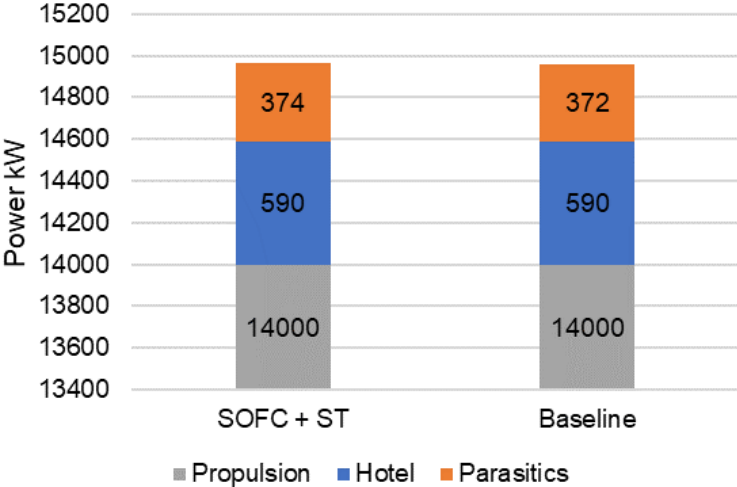


Fig.3: Power demands for the baseline and the SOFC machinery

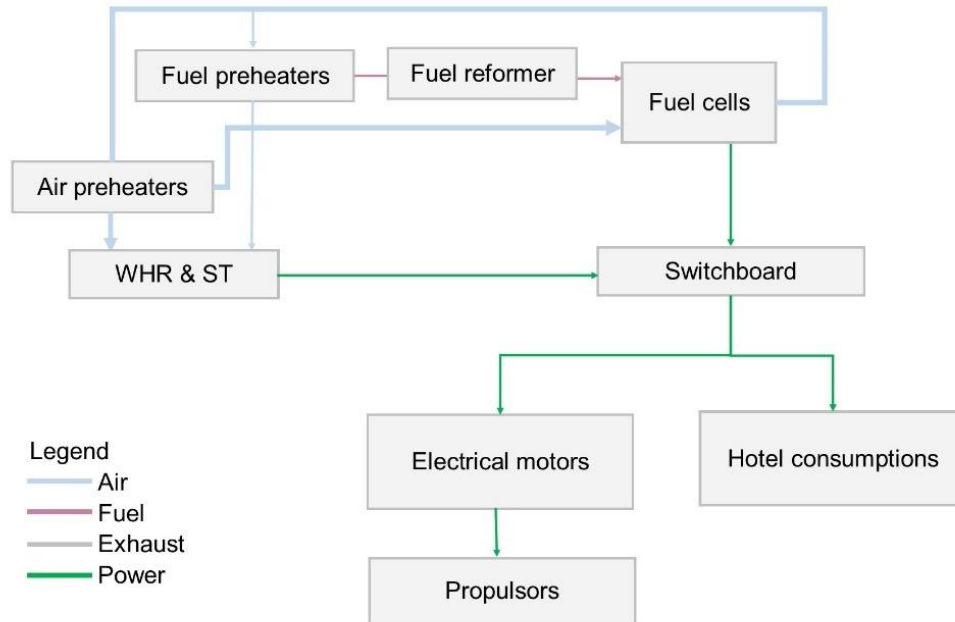


Fig.4: Schematic representation of the analysed SOFC with WHR and ST system

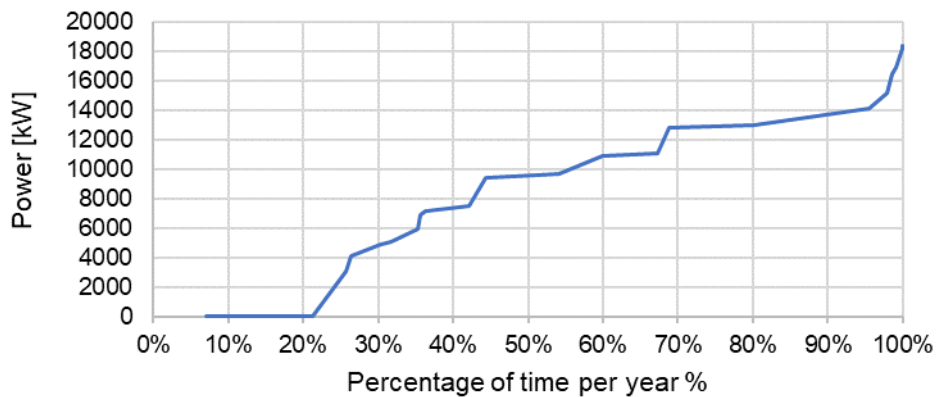


Fig.5: Cumulative curve of percentage per year at increasing propulsion power levels

3. Model development

3.1 Baseline model

A digital twin of the vessel's machinery was built in the DNV COSSMOS modelling framework to quantify performance of the actual ship machinery (Fig.6). The COSSMOS library contains a list of component models of ship machinery systems, which can be connected to form complex ship system models. Each component model comprises a set of mathematical equations that describe the principles of operation of a ship component, at the necessary accuracy level fit-to-purpose for its intended use. For this paper, the engines are modeled using lookup tables of part-load performance with manufacturer data, including algebraic functions for fuel adjustments. The power train components (generators, switchboard, shaft power-take out, and consumers) are modelled with load-dependent performance curves. The auxiliary boiler and heat exchangers (economizers) are lumped first-principles models, implementing mass and energy balances.

3.2 Fuel-cell powered VLCC model

Using the DNV COSSMOS library, an integrated system model of a VLCC powered by two SOFC modules and WHR was built. The component models were: SOFC, reformer, pumps, exhaust gas force draft fan, heat exchangers for air and fuel pre-heating, waste heat recovery section, steam turbine, switchboard and electric power train components up to the propeller, and electricity consumers. The integrated model can capture the part-load performance of the fuel cell, including power production capacity, air and fuel flow properties, system, and exhaust temperature. The model can also evaluate the heat requirements for fuel and air preheating and the waste heat recovery potential, i.e. the steam and power production from the remaining fuel cell exhaust heat. Finally, the integrated model can calculate the fuel consumption at different overall power production thresholds, the overall system efficiency, the steam turbine power production, and the system fresh water demands for steam reforming.

The integrated model is shown in Fig.7. Air enters at atmospheric conditions with support from a force draft fan. The air and fuel streams are pre-heated, using the SOFC exhaust heat, before entering the SOFC. The preheating process is accomplished at two different temperature levels for both streams, to exploit as much as possible the available heat. Heat is also consumed in the reformer, requiring an additional fuel pre-heater before the SOFC. The remaining heat is used to produce steam in the WHR and fresh water for producing the reformat.

The SOFC module is modelled by combining individual component models for the fuel cell, the reformer, the catalytic burner and the air and fuel preheaters, as shown in Fig.7. The fuel cell model was developed based on literature works from *Aguiar et al. (2004)*, *Kandepua et al. (2007)*, *Amati et al. (2009)*, *Salogni and Colonna (2009)*, *Li et al. (2010)*. It was verified against *Aguiar et al. (2004)*, demonstrating a relative error on power prediction of 2.5%. A catalytic burner model was also developed to ensure that no hydrogen flows within the system at the fuel cell exit. The model implements a cathode recycle to maintain the SOFC temperature at high levels, better manage pre-heating streams and save heat for the WHR. The reformer model is the same as the one presented in *Dimopoulos et al. (2013)*.

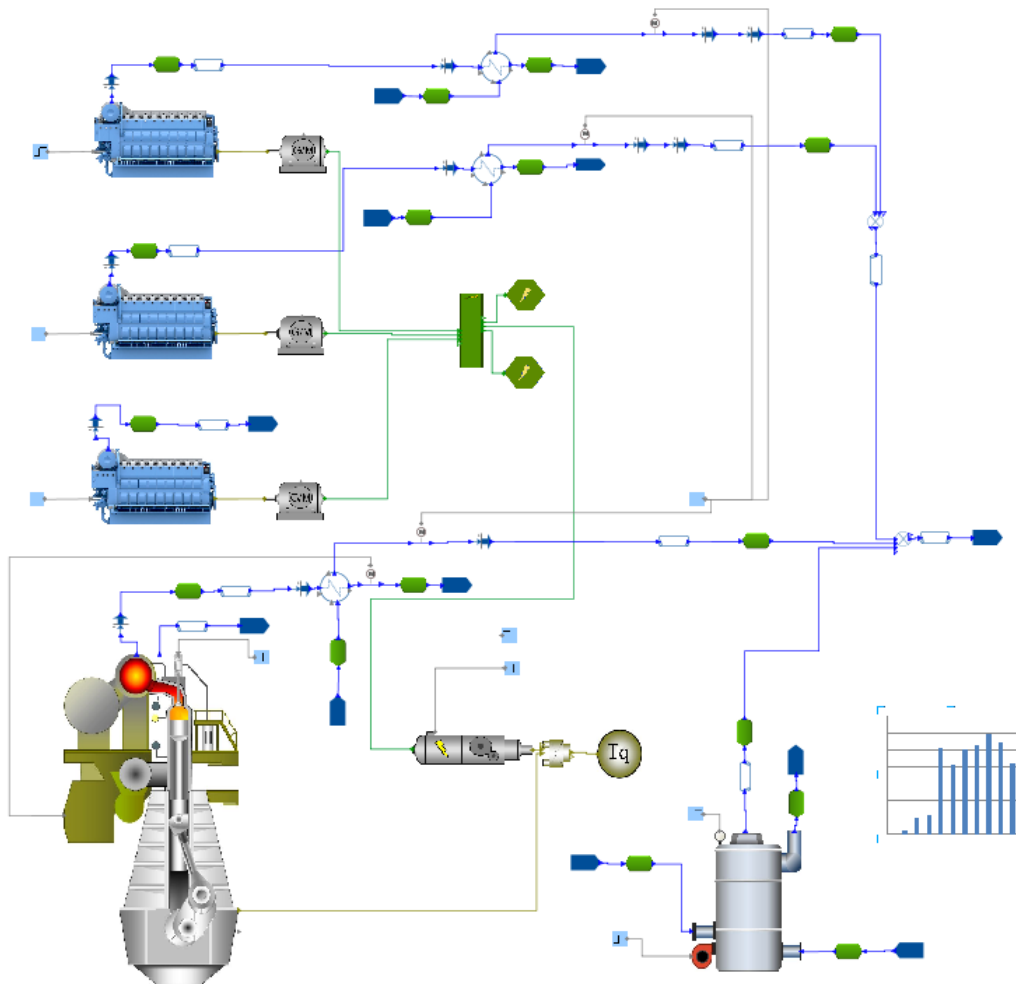


Fig.6: Baseline VLCC machinery system model in DNV COSSMOS

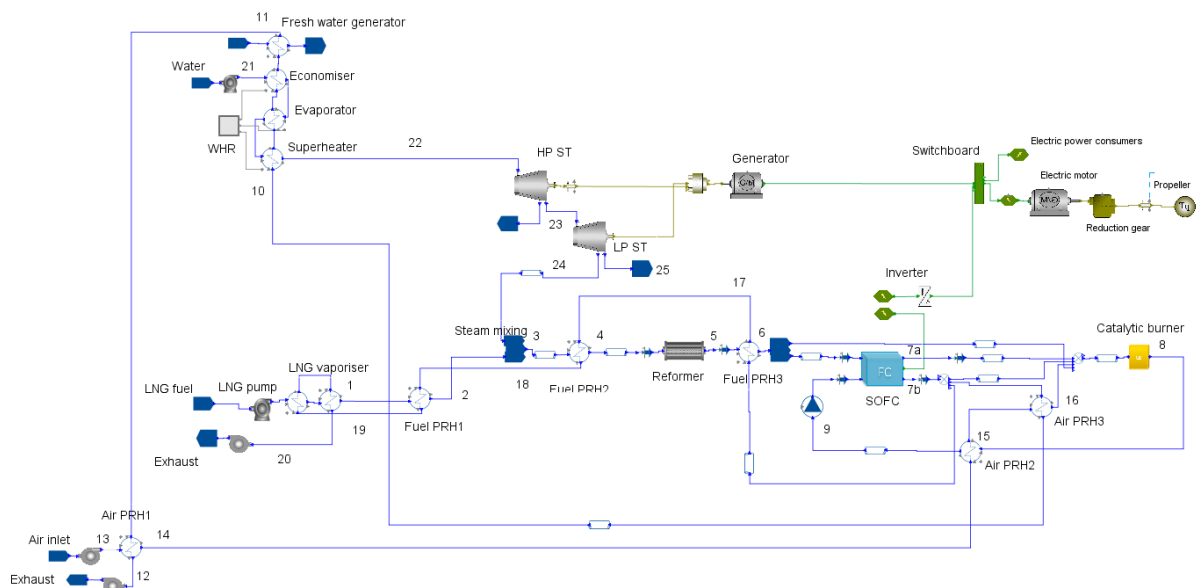


Fig.7: COSSMOS model of fuel-cell powered VLCC with WHR and cathode recycle

4. Simulation results

The model was used to analyse the vessel performance at design conditions against the baseline machinery. Since the baseline system is fueled by MDO, whereas the fuel-cell powered one is driven

by LNG, all fuel units are converted to HFO equivalent, accounting for low heat value differences between the fuels. The overall system performance (including parasitic loads, hoteling demands, etc.) was 44% for the baseline ship and 63% for the fuel-cell driven one. It is noted that this efficiency is at design conditions of the FC system.

The fuel consumption was then calculated at a range of speeds from 8 to 16kn, at stationary points (harbor, loading and unloading), and at maneuvering conditions, as shown in Fig.8. The fuel cell driven variant is consuming significantly less fuel compared to its conventional counterpart.

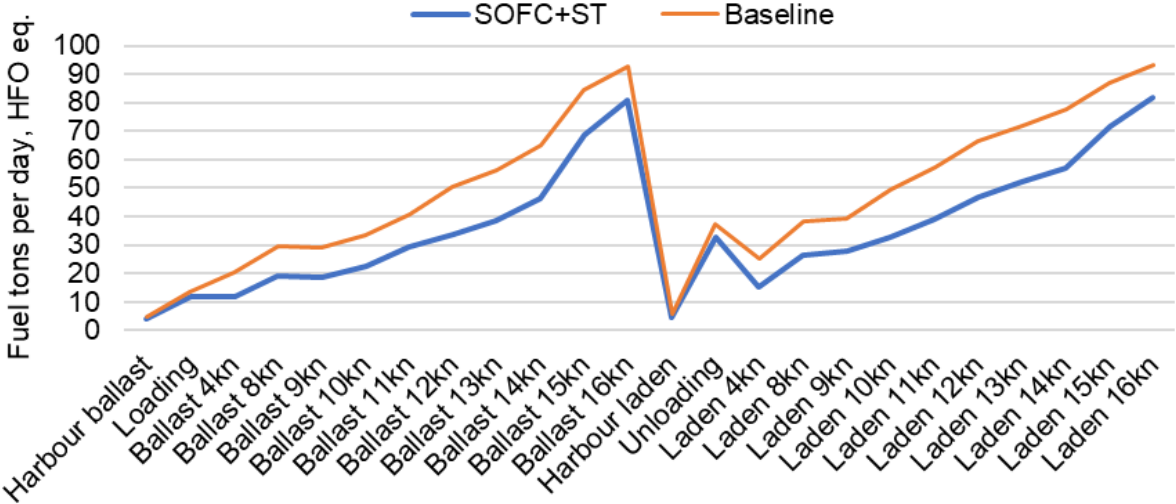


Fig.9: Baseline VLCC machinery system model in DNV COSSMOS

The aggregated annual performance was calculated by integrating the results on annual basis, using the frequency of service at different operating modes per year. The annualized baseline system efficiency was 42%, compared to 60% of the fuel-cell driven one. Fig.9 shows the annualized average fuel consumption for the two machinery cases. It is noted that this efficiency refers to the annual energy consumed divided by the annual energy produced for propulsion and electricity loads.

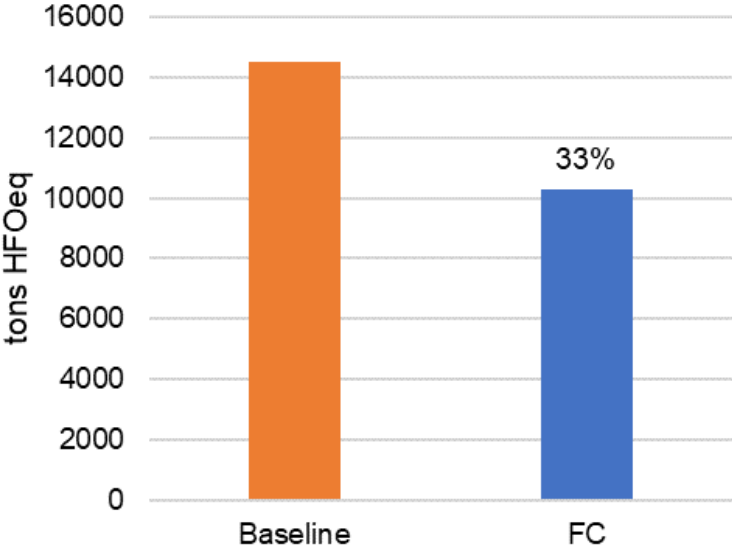


Fig.9: Annual fuel consumption in tons per day HFO eq.

4. Conclusions

The purpose of this paper was to demonstrate how modelling and simulation tools can help estimate the future performance of systems for specific application cases, including novel technologies like fuel cells. Models can flexibly and economically predict the performance of alternative technical configurations using a computer, supporting decision making at preliminary concept design stages.

The paper presented a model-based comparison of a fuel cell driven VLCC against its conventional counterpart. A complex system model was developed in DNV COSSMOS, comprising of SOFC fuel cell stacks, air and fuel pre-treatment, exhaust gas waste heat recovery and steam production, steam turbine generator. The model was used to predict design and annualized vessel performance, accounting for parasitic and hotel loads. The model results were compared against a conventional VLCC machinery system performance.

Alternative configurations could also be tested using the same models presented in this study, including the tuning of the fuel cell model on manufacturer data, the removal of the waste heat recovery unit, the inclusion of advanced organic Rankine cycles, and more.

The results demonstrated a significant improvement in efficiency, both at the design point and for the annual mission profile of the ship. At design conditions, ship overall efficiency was 44% for the baseline ship and above 63% for the fuel-cell driven one. On an annual basis, the fuel cell case achieved 33% less fuel in HFO equivalent terms

References

- AGUIAR, P.; ADJIMAN, C.S.; BRANDON, N.P. (2004), *Anode-supported intermediate temperature direct internal reforming solid oxide fuel cell. I: model-based steady-state performance*, J. Power Sources 138, pp.120-136
- AMATI, V.; SCIUBBA, E.; TORO, C.; ANDREASSI, L. (2009), *Modelling and Simulation of a Hybrid Solid Oxide Fuel Cell Coupled with a Gas Turbine Power Plant*, Int. J. of Thermodynamics 12/3, pp.131-139
- BATTELLE MEMORIAL INSTITUTE (2017), *Manufacturing Cost Analysis of 100- and 250-kW Fuel Cell Systems for Primary Power and Combined Heat and Power Applications*, Prepared for: U.S. Department of Energy, DOE Contract No. DE-EE0005250
- BOSSEL, U.G. (1992), *Final report on SOFC data – Facts & figures. Annex II Modelling and evaluation of advanced SOFC. Programme of R&D on Advanced Fuel Cells*, International Energy Agency, Berne
- DIMOPOULOS, G.G.; STEFANATOS, I.V.; KAKALIS N.M.P. (2013), *Exergy analysis and optimisation of a steam methane pre-reforming system*, Energy 58, pp.17-27
- DIMOPOULOS, G.G.; GEORGOPOULOU, C.A.; STEFANATOS, I.C.; ZYMARIS S.A.; KAKALIS, N.M.P. (2014), *A general-purpose process modelling framework for marine energy systems*, Energy Conversion & Management 86, Pg. 325-339
- KANDEPUA, R.; IMSLAND L.; FOSSA, B.A.; STILLER, C.; THORUD, B.; BOLLAND, O. (2007), *Modeling and control of a SOFC-GT-based autonomous power system*, Energy 32, pp.406-417
- LI, M.; BROUWER, J.; POWERS, J.D. (2010), *A finite volume SOFC model for coal-based integrated gasification fuel cell system analysis*, ASME J. Fuel Cell Science and Technology 7

MARRA, D. (2012), *Development of Solid Oxide Fuel Cell stack models for monitoring, diagnosis and control applications*, PhD Thesis, University of Salerno

OVRUM, E.; DIMOPOULOS, G. (2012), *A validated dynamic model of the first marine molten carbonate fuel cell*, Applied Thermal Engineering 35, pp.15-28

SALOGNI, A.; COLONNA, P. (2009), *Modelling of solid oxide fuel cells for dynamic simulations of integrated systems*, Applied Thermal Engineering 30/5, pp.464

Power Distribution in Ultra-Efficient and Zero-Emission Ships

Mårten Storbacka, WE Tech Solutions, Vaasa/Finland, marten.storbacka@wetech.fi

Abstract

This paper presents the concepts of ultra-efficient power distribution systems for vessels in the merchant fleet. By utilising inverter-based technologies and DC (Direct Current) power distribution to link the consumer with the generated power, we are not only optimising efficiency of the electrical power distribution itself but also optimising both the consumer operation side and the power generation side. Inverter-based technology i.e. power electronics is thanks to its flexibility able to link virtually any type of power source and energy storage system to a distribution network and hence it is also a key technology when building the future of ultra-efficient and zero-emission shipping.

1. Introduction

Electrical power generation and distribution became a necessity in marine vessels since the implementation of electrical machinery onboard ships. Electrical motors driving pumps, fans, winches, compressors, propellers etc. are almost always part of a function specific machinery or system with functionality and capacity tailored according to the need. Hence the size and types of electrical machineries are of a scalable design – very much the same as in land-based industries. However, even though the shipping industry follows land-based industry standards for electrical machines and equipment in general, there is an additional layer of rules and standards for the marine industry i.e. standards set by IMO Conventions, www.imo.org. The IMO Convention for Safety of Life at Sea (SOLAS) specifies the minimum standards for among other things, equipment and in our case electrical equipment, components and solutions. This means that the standards that are followed in international shipping industry often are more rigid when compared to land-based industry standards and naturally this factor is limiting the availability of technology that can be introduced onboard ships. One can say that there is the great upside of SOLAS technical and control provisions that ensure a good enough standard of construction, equipment and operations of ships while the downside is the relatively limited availability of equipment that meet these provisions.

We will briefly discuss the technical evolution of electrical power generation and distribution in ships and which main factors are affecting the pace before we will look at the main drivers that now are accelerating this evolution. Further, we will take a not that in-depth look at today's technologies that are utilised in power distribution systems and get an understanding of the main benefits therein. Today's technologies in this context is related to power electronics and direct current (DC) power distribution. Implementation of such technologies will open up to benefits such as variable speed power generation and limitation of fault currents, and we will contemplate on the impact and what it means for the shipping industry.

In this paper we limit the scope of electrical power distribution utilising direct current (DC) to low voltage (LV) standards. There is a requirement to go high voltage (HV) standards when the total electrical power demand grows in excess of around 20 MW and at HV levels we are discussing a totally different type of power electronics with multiple DC voltage levels and so on.

LV standards of power electronics e.g. variable frequency drive technologies are far more straightforward in comparison and hence remain in the position of most cost-effective technology in this regard for the vast majority of vessels sailing in the merchant fleet.

2. Technical evolution in shipping

Considering the technical evolution in shipping industry it is fairly easy to dismiss the whole industry as being conservative and careful in its nature, at least if one compare with some of the land-based

industries. However, at least the following two important key-notes should be taken into consideration when comparing shipping industry with any other land-based industry, namely safety and remoteness.

2.1. Shipping industry is part of the logistics chain

As per today, about 90 % of logistics on the planet is involving shipping in some form. When products are manufactured in land-based production facilities the selected location is based on certain criteria such as availability of raw materials, labour and energy. The consumer market being worldwide and most often in other locations than the factories, it means that the goods manufactured, and also quite commonly, the raw material for production needs transport i.e. logistics. Shipping being the primary means of global logistics it means that the demand for safety and security is a top tier. Safety of goods to arrive on time at designated destinations as well as safety of the crew of a ship crucial. Disturbances in shipping logistics creates ripples through the fabric of our whole society.

With Safety this crucial it means also that factors that undermines safety and puts an e.g. merchant ship at risk is avoided as far as possible. This unwillingness to jeopardise the logistics chain echoes all the way down to selection of technologies to be implemented onboard.

The other factor is the remoteness. For a deep-sea sailing vessel, it is well understood that functionality of machineries i.e. the technology implemented onboard must remain in operational condition even if part or parts of the machinery malfunctions. This because the vessel is most of the time in a remote location i.e. sailing on the sea, far away from external sources of assistance. The technology onboard which is involved in keeping the vessel sailing, the essential systems, must be maintained and repaired independently by the ship crew.

Already these two keynotes set rigorous demands and requirements on the technology installed onboard a vessel, and of course the same goes for technology used in vessel electrical power generation and distribution.

2.2. The drivers behind technical evolution in shipping

To go straight to the point, economy and environment are arguably the two top-drivers of technical evolution in shipping industry. This goes for the general technical evolution as well as for electrical power generation and distribution. While there are many aspects of technical evolution, we are here focusing on energy efficiency improvements. It can be stated that improving efficiency of shipping operations is always sought for. Ship owners and operators strive to improve the efficiency in operations in order to improve their economy and minimise uncertainties. By improved efficiency in operations a ship owner and its vessel (fleet of vessels) will be more attractive in the eyes of the charterer – entities that purchase shipping services.

Operational expenditure (OPEX) became even more in focus since the financial crisis that erupted in later part of 2008 and ship owners as well as ship designers started to look at means to reduce fuel consumption in addition to optimizing cargo capacity in vessel designs. A new era in ship design came along where fuel consumption got more, and deserved, attention. Nowadays we are talking about the pre-, and post-2008 ship designs.

One of the recognised areas with potentials to improve efficiency was related to electrical power generation and distribution. Fuel prices had sky-rocketed and one of the means to reduce fuel consumption without reducing operations was to increase the efficiency also in this area.

Another driver for efficiency improvements comes from IMO who set forth the Energy Efficiency Design Index (EEDI) in July 2011, www.imo.org, which in few steps stimulates technical innovation in ship design and machineries.

2.3. 140+ years of electrical power generation and distribution in shipping

The commercial electrification of marine vessels started in 1880s, *Chai et al. (2017)*. Since then, many things were going on and evolution had its pace but the mainstream of merchant vessel electrification is based on alternating current (AC) power distribution until this day. We are not going to analyse efficiency improvement steps that have taken place in this 140+ year way of generating and distributing electrical power the traditional way but instead look at why it is feasible to steer towards direct current (DC) power distribution.

As a starting point it is good to clarify that there is no clear-cut border line between AC and DC power distribution – both technology bases are needed and will be utilised also in the future. For instance, AC power is generated by rotating electrical machines that we commonly know as generators. An electrical power generator is converting the rotating energy i.e. torque produced by a prime mover e.g. a reciprocating internal combustion engine (RICE) typically into a three-phase (or more) electrical system. As we are after highest possible efficiency in yet viable power generation technologies, shaft torque will remain an important source of power and hence we are in a foreseeable future continuing to use rotating electrical machines to generate power onboard vessels.

By implementing new improved materials in generators such as Neodymium-Iron-Boron permanent magnets we are reducing the losses in the torque to electrical current conversion. Already for some time now the generators onboard ships have power losses of only two to four percent over a wide power and speed range thanks to permanent magnet technology. We will come back to power generating technologies utilising permanent magnets later in this paper.

With AC power in form three phase currents generated in rotating electrical machines we still need to distribute that to the consumers in an efficient way. By utilising the traditional method of distributing AC current to a consumer e.g. an electrical motor driving a pump, with a fixed frequency of 50 or 60 Hz we are firstly generating that constant frequency in the generator. Then we by means of an electrical power distribution network transfer that fixed frequency electrical power to the electrical motor. Simply by connecting that motor to the generator it will start rotating with a constant speed. That constant shaft speed is defined by how the electrical motor is constructed and it is always the same. The total losses of the simple electrical system described here comes from the losses in the generator, losses in the electrical distribution (wiring, fuses and breakers) and losses in the electrical motor. From an electrical point of view, this is the most efficient way to get that electrical motor to rotate and produce torque to use for driving the impeller of a pump. Any additional components introduced to that electrical circuit will add losses, from an electrical power generation and distribution perspective that is.

2.3.1. System level approach

That small electrical system described here will in most cases not be sufficient for serving the power distribution needs in a vessel. A transformer that transforms the voltage level of electrical power is in most cases also needed and this component adds not only losses but also increases weight and takes up precious space in the machinery of a ship. More important however is to look at the efficiency of the system we have described here. Looking at the system from the consumer end firstly, as it is the consumer that draws energy from the generator (newer the other way around) we had a constant rotating speed electrical motor driving a pump. A pump operating with a constant speed produces a constant pressure head and constant flow while the system that the pump is working in most often needs a means to alter i.e. control the pressure and flow according to the needs of the system the pump is part of. With a constant speed operated pump, the flow rate is controlled by means of a throttling valve, which introduces frictional losses to the system. A means to increase the efficiency of a pump system is to introduce variable speed control of the impeller and this is readily achieved with a variable speed drive (VSD) to control the speed of the electrical motor that drives the pump. A variable speed drive also known as a variable frequency drive (VFD) is a component that adds losses to the electrical system due to the conversion steps that takes place within the AC drive (we call it AC drive as it is connected to an AC power distribution system). However, the conversion loss of an AC drive is dwarfed in comparison

to the system losses in which the pump is working. To further argue the case, with a constant speed operating pump in a liquid cooling system, a three-way valve is introduced to control how much flow goes through a heat exchanger to regulate the temperature and how much is by-passed. That is a great way to regulate temperature but as all closed systems must be capable of the extreme conditions as well, conditions that rarely occurs in normal operations, it means that such systems are most of the time operating in sub-optimal conditions. Simply put, an extensive amount of coolant is unnecessarily pumped around in the system for most of the time, year after year.

2.3.2. Power generation system

Looking at the generator side of the small system we have described here the AC generator is part of that pump system as well. The AC generator delivers the electrical power to drive the electrical motor which in turn drives the pump impeller. The AC generator will experience the load fluctuations of the pump system in the form of increased or decreased demand of electrical current.

In order to handle the load fluctuations of the pump the generator driver, which we call a prime mover, typically a RICE have to react on the increased or decreased demand in torque. We come to realise that the generator and prime mover is a system itself that is interacting with the pump system – we have a system in a system.

Traditionally the AC generator is delivering a constant frequency e.g. 60 Hz, which as described earlier sets the rotating speed of the electrical motor. With a constant frequency demand on the AC generator, it also means that the prime mover will have a constant rotating speed. The AC generator design and construction is in the same way as the electrical motor design setting the rotating speed demand on the prime mover.

2.3.3. RICE as prime mover of the AC generator

In shipping industry the RICE we are discussing here is very much the same machine that typically utilised for driving a propeller shaft in a main propulsion system of a vessel. Main differences appear in size, power, rotational speed, combustion cycle principle and fuel type used. Putting those aside it is in practice the same reciprocating internal combustion engine we are looking at.

In the case where the RICE is driving an AC generator in a traditional generating-set application, a remarkable limitation in efficiency is issued from constant speed operation. The constant speed is as described earlier needed in order to get a constant speed of the electrical motor driving a pump. When we have a constant speed operation on the RICE, we will limit the optimisation of fuel consumption as the variable power output is a function of a fixed speed, Fig.1. The optimal efficiency area of the RICE is limited and with a fixed speed function the load point will stray away from the optimal operation area of the RICE load curve.

Considering that the power generation system described here is a derivative from the land-based industry it means that the drawback of constant speed operation in a vessels electrical power generation did not get much attention until lately. The main reason for this is because constant speed operation is not really a drawback in land based electrical power distribution systems. In land-based systems AC generators are typically connected to a larger electrical power grid which is built to distribute electrical power to the consumers on a much larger scale. The fundamental difference between the two distribution scenarios is land based grids have a great number of generators and consumers interconnected while on a vessel the grid the same is very limited. In land-based grids power demand is balanced between a vast number of consumers, which allows the AC generators and their prime movers to operate in a predefined and constant power mode, with constant speed, generating 50 or 60 Hz. When operating in a constant speed and load at the design point, being it e.g. 95 % of maximum power, the efficiency is the best possible as well, Fig.2, for a principle single line diagram of a land based AC electrical distribution system.

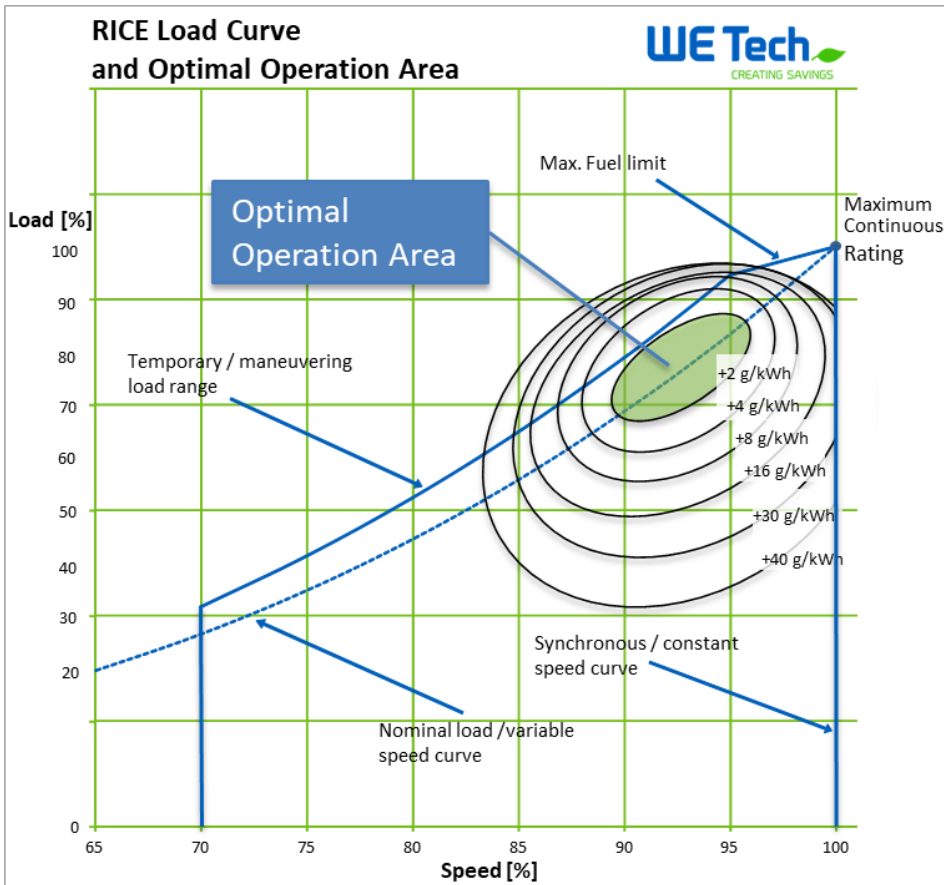


Fig.1: Generic Engine speed/load curve with efficiency areas

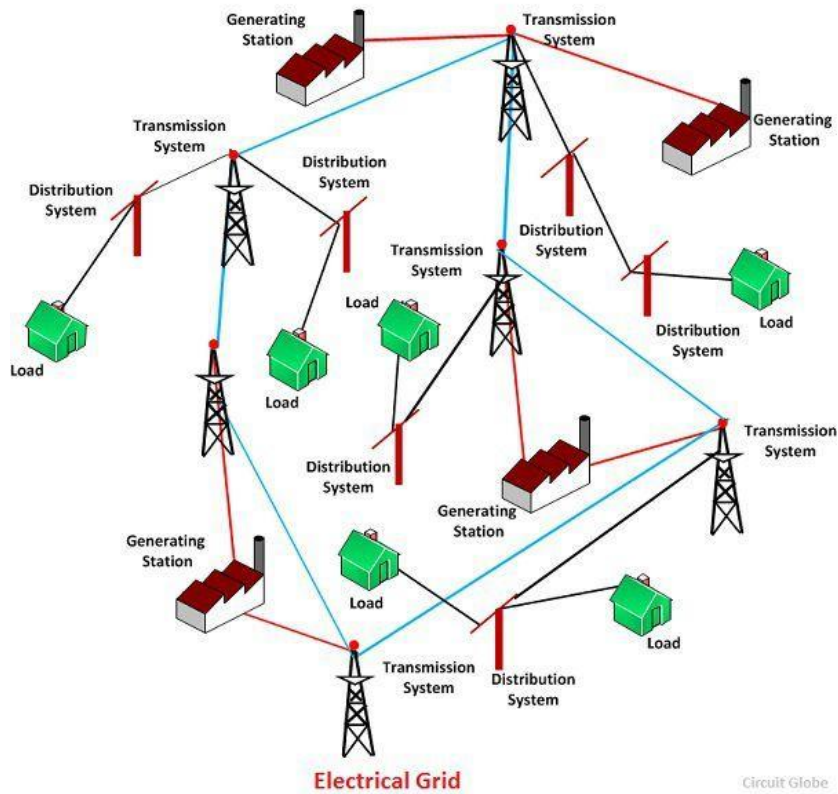


Fig.2: Principle of land-based AC electrical power distribution system

3. Breaking free from the land-based 60 Hz principle

As we have described earlier there is a remarkable incentive to optimise efficiency of the pump system by introducing variable speed operation of the pump. We also realised that there is a strong incentive to utilise variable speed in the power generation as the prime mover, being it a RICE is clearly benefitting from reduced speed when the load is reduced.

With variable speed operations being beneficial in both ends of the system i.e. in power generation end as well as in the consumer end when it is an application considering converting electrical power to torque e.g. pumps, fans, winches, propellers and so on, it became interesting to look at the realm in between. Translated into concrete readily available technology we need variable frequency drive technology in both ends of the system and then it does not make any sense to have a fixed 60 Hz AC system in between. Here a need for a major paradigm shift appears. As limited size electrical power distribution systems onboard vessels have technologies derived from the land based 50/60 Hz world it means that component manufacturers are supplying land-based technologies that fulfils recognised marine standards and gets classification society approvals for use.

3.1. DC-link to the rescue

Taking a look at the AC drive technology that we now implement in both ends of the small pump system described here in order to achieve best possible efficiencies in various load conditions it becomes apparent that some conversion steps can be omitted, Fig.3.

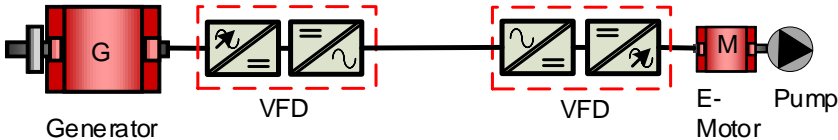


Fig.3: Pump system with VFD in generator and consumer end

As the AC drive or VFD on both sides have a DC-link inherently between its conversion steps from AC to DC and back to AC, we can omit the AC in between. This simplification of the system means less components to install and maintain and reduced losses in the electrical system. Further, with a DC-link distribution between generator and consumer it means that AC system specific items like transformers and harmonics are of no concern. Looking at the components of the DC-link distributed system, ref. Figure 4, we remain in principle with the same VFD technology as in the previous example, only renaming components as inverter unit (INU) from inverting DC back to AC on the motor side while on the generator side we actively rectify AC to DC with a rectifying unit we also name INU. The reason for this is because both sides use same hardware and differs only in their application software. With different application software in the INU added with additional filtering techniques we can design electrical power distribution systems that meets vessel machinery design requirements.

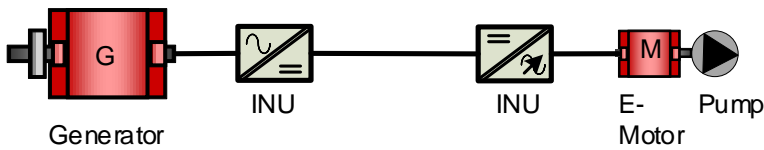


Fig.4: Generator to consumer with DC-link and INUs

3.2. DC and AC distribution network topologies

As we do not have to remain in the land based 50/60 Hz system thinking any longer, we can focus on improving the efficiency in the various systems onboard a ship which are connected to the power distribution network. By implementing different power distribution network topologies and combining both AC power distribution and DC power distribution we are able to optimise the power distribution system to a great extent. As explained earlier we are interested in optimising the systems within the system by utilising variable frequency drives. However not all systems onboard a ship ask for variable speeds to be most efficient and e.g. smaller pump systems might not yet have a variable speed design implemented. Hence in order to not make a power distribution network overly complex we keep part of the network as 50/60 Hz AC distribution sub-networks. Here we talk about DC and AC hybrid network topologies that designers work together with the system suppliers to implement in vessel specific design projects. In figure 5 an example in form of a simplified principle single line diagram is showing a DC-link based topology that have an AC distribution network as well. The example albeit simplified has a topology meeting dynamic positioning redundancy class 2 (DP-2). Electrical consumers which benefit from variable speed operation are connected to the DC-link switchgear with their dedicated INU while consumers with no benefit of variable speed operation can be connected to the AC switchgear. Only main components such as generators, ESS, grid converters and propulsors are shown in Fig.5.

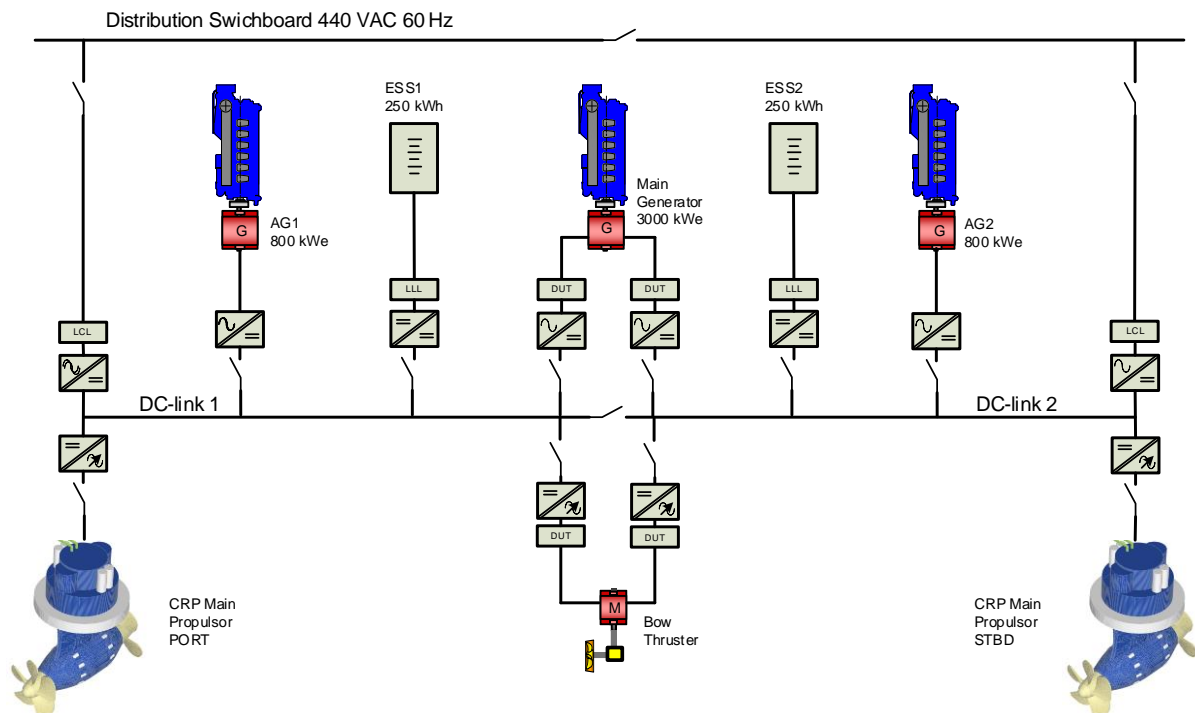


Fig.5: Principle single line diagram of a ship wide Hybrid DC Machinery

3.3. Benefits from DC-link power distribution

As the technologies involved in VFD and DC-link power distribution comes with a cost it is important to balance that fact with the benefits it brings. The benefits with biggest impact to operational expenditure (OPEX) is without doubt the variable speed power generation principle but there are several other factors that contribute to offset the cost of technology i.e. capital expenditure (CAPEX) discussion.

3.3.1. OPEX improvements by implementing a variable speed generating set

As there are many answers to the question about benefits of running a marine generating set (electrical power generator and RICE combined on a common base, working as a unit) in variable speed we usually

$t = 6000 \text{ h/a}$	Shaft generator running hours per annum.
$P = 1000 \text{ kW}$	Average electrical load.
$\text{SFOC}_{\text{design}} = 160 \text{ g/kWh}$	Specific fuel oil consumption of slow speed main engine at vessel design speed.
$\text{SFOC}_{\text{sub-opt}} = 240 \text{ g/kWh}$	Specific fuel oil consumption at sub-optimal load point deviating from RICE load curve due to constant speed operation, Fig.1.

$$\begin{aligned}
 E &= 1000 \text{ kW} * 6000 \frac{\text{h}}{\text{a}} \Rightarrow E = 6000000 \frac{\text{kWh}}{\text{a}} \\
 240 \frac{\text{g}}{\text{kWh}} &\Rightarrow 0.24 \frac{\text{kg}}{\text{kWh}} \Rightarrow 0.24 \frac{\text{kg}}{\text{kWh}} * \frac{6000000 \text{ kWh}}{\text{a}} = 1440 \frac{\text{tonne}}{\text{a}} \\
 240 \frac{\text{g}}{\text{kWh}} - 160 \frac{\text{g}}{\text{kWh}} &= 80 \frac{\text{g}}{\text{kWh}} \Rightarrow 0.080 \frac{\text{kg}}{\text{kWh}} \\
 0.080 \frac{\text{kg}}{\text{kWh}} * 1000 \text{ kW} &= 80 \frac{\text{kg}}{\text{h}} \\
 80 \frac{\text{kg}}{\text{h}} * 6000 \frac{\text{h}}{\text{a}} &= 480 \frac{\text{tonne}}{\text{a}} \\
 \frac{480 \text{ tonne/a}}{1440 \text{ tonne/a}} * 100 \% &= 33 \%
 \end{aligned}$$

As the main engine is stopped when vessel is at berth, and if no shore power is available for taking care of vessel electrical load, a generating set will have to take care of the remaining hours of operation per annum i.e. 2760 h.

$$\begin{aligned}
 E &= 1000 \text{ kW} * 2760 \frac{\text{h}}{\text{a}} \Rightarrow E = 2760000 \frac{\text{kWh}}{\text{a}} \\
 200 \frac{\text{g}}{\text{kWh}} &\Rightarrow 0.20 \frac{\text{kg}}{\text{kWh}} \Rightarrow 0.20 \frac{\text{kg}}{\text{kWh}} * \frac{2760000 \text{ kWh}}{\text{a}} = 552 \frac{\text{tonne}}{\text{a}}
 \end{aligned}$$

As we calculated earlier the direct savings potential from variable speed generating set is around 16.7% while we reach 33 % direct savings in electrical power generation by utilising a shaft generator. Secondary savings potentials are somewhat more arduous to quantify, and operation profiles always plays a big role.

3.3.3. Weight savings from limited fault currents

The conventional method of distributing electrical power onboard a ship is to ensure direct galvanic connection to link the consumer with the generator. As a ship in operation has many consumers in forms of electrical motors etc. and widely varying electrical power demand there are typically also several power generators that potentially are online simultaneously. In electrical engineering we are knowledgeable that electrical current follows certain dynamics, which are defined as rules and laws e.g. Kirchhoff's current law (1st law) which states that the current flowing into a node (or a junction) must be equal to the current flowing out of it, https://isaacphysics.org/concepts/cp_kirchhoffs_laws. We also know that current flows through a path with have the lowest impedance (Z). From these simple facts we understand that in case of an electrical short-circuit to ground anywhere in an electrical distribution system, all of the electrical current i.e. the fault current will flow through the fault location. The fault current is not only generated by the generator(s) but also from the electrical motors connected to the system. This type fault current dynamics are mitigate by fuse links or electrical protection relays that are designed to cut the current path after a certain time delay. As a time delay is present in a short-circuit it means that the electrical power distribution system including switchgear bus-bars, circuit breakers and cabling that links the consumers to the distribution switchgear must be dimensioned to withstand a certain short-circuit current for a defined period of time, <https://ieeexplore.ieee.org/document/8007394>.

By introducing DC-link power distribution and INUs we get control of the dynamic fault current scenario. Power electronics in the INU and AFE units are continuously measuring and switching the electrical currents of the distribution system and we can parameterise the amount of fault currents that are introduced to a potential short-circuit. With this ability to set limitations on fault currents we do not need to dimension the equipment to withstand the dynamic levels as introduced with conventional vessel electrical power distribution systems. This means that switchgear busbars, cabling and circuit breakers can be considerably lighter in comparison. The weight savings in the electrical power distribution system is very valuable in ship design and it also has a considerable impact on CAPEX.

3.3.4. Improved safety and redundancy of the electrical systems

The electrical power distribution network topology is not limited to conventional main switchboard with two to four generating sets plus an emergency switchboard with its emergency generating set when implementing DC-link power distribution. Multiple DC-link busbar systems together with dual to quad stator winding systems of the generators presents redundant power distribution systems with virtually no increase in CAPEX. Only partial black-outs and partial loss of propulsion in failure conditions increase total safety of the ship.

3.3.5. Higher nominal speed of generating sets

With DC-link power distribution where the generating sets are connected directly to an INU there requirement to match RICE nominal speed with either 50 or 60 Hz network frequency. The generating set nominal speed can be increased to a maximum with RICE combustion process optimisation in mind. Conventional limitations are based on pole number of the generator where the pole pairs must be divisible with either 50 or 60 Hz. This means that for a typical 31 cm cylinder bore Dual Fuel RICE the output is 530 kW/cylinder for a 60 Hz compatible generating set as the nominal speed is 720 rpm. For a 50 Hz compatible generating set the nominal speed is 750 rpm and then the same RICE delivers 550 kW/cylinder, *Wärtsilä (2017)*. As example for a twelve-cylinder generating set the difference is already 240 kW in benefit of the 50 Hz compatible 750 rpm version.

3.3.6. Improved electrical efficiency with DC-link and permanent magnet machines

When comparing conventional Diesel Electric propulsion systems with a Hybrid DC Machinery, <http://wetech.fi/solutions/solution-five/>, where DC-link and high efficiency permanent magnet generators and propulsion motors are utilised, the total efficiency is improved in the range of 4.5 % at nominal load point. The efficiency of the conventional Diesel Electric machinery declines substantially in part load conditions. See Fig.6 for topology comparison. The permanent magnet type generators maintain a very high efficiency over a wide speed and load range and outperforms other generator types thanks to almost zero rotor-losses and maintained magnetic flux-density over full speed range. The Hybrid DC Machinery have two conversion steps only, performed by same hardware INUs, between generator and propulsion motor.

3.3.7. Utilising Energy Storage Systems for spinning reserve and peak shaving

The energy efficiency in a Hybrid DC Machinery is further improved by introducing a modest size battery type energy storage system (ESS). Lithium-ion type battery modules are connected in strings that match the DC voltage level in the DC-link. Direct connection is possible but not feasible as that sets limitations on DC voltage level control. That's why an efficient ESS system also incorporates DC-to-DC conversion, again with the same INU hardware running a dedicated application software.

The principles of ESS utilisation in a Hybrid DC Machinery are focusing on three areas, namely peak shaving, spinning reserve and black out prevention. With the peak shaving functionality the generating sets are supported with batteries taking fast load changes (load peaks) and keeping electrical load as seen for generating set constant.

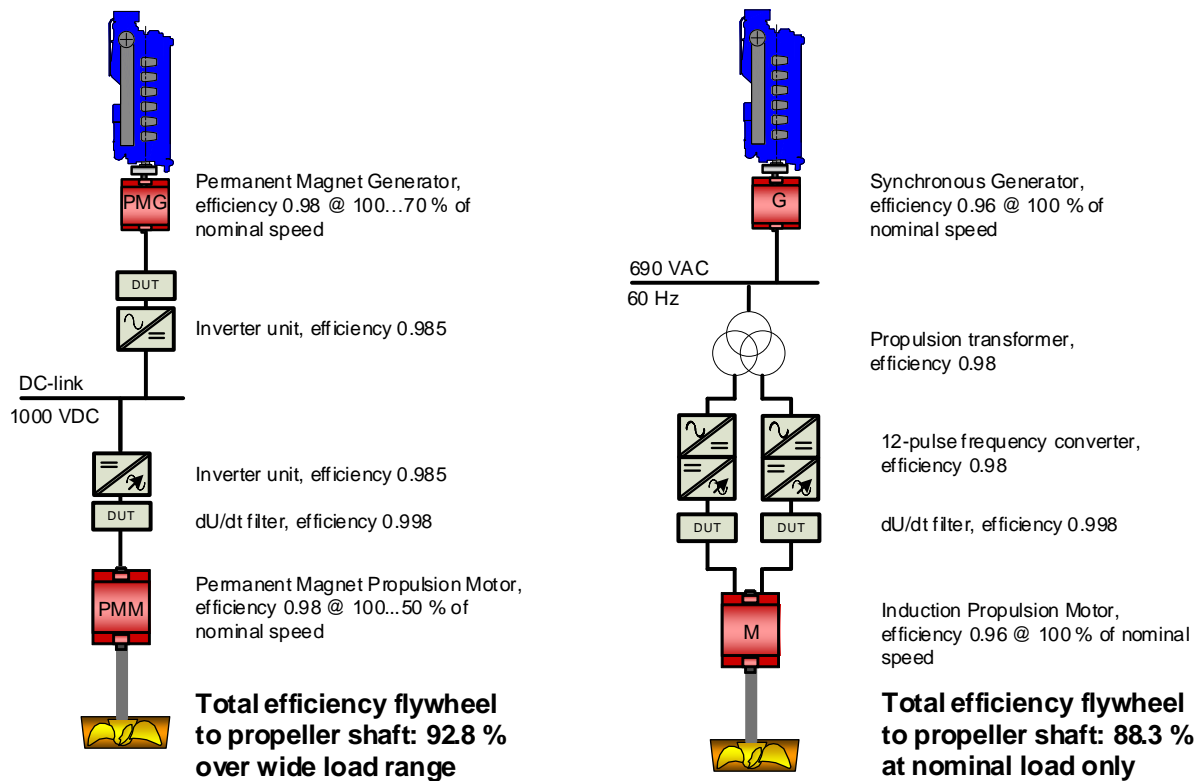


Fig.6: DC-link power distribution and permanent magnet machines efficiency comparison with conventional Diesel Electric propulsion

This ensures an efficient and surge free operation of the Auxiliary Generators while all large consumers are provided a very fast load response and the electrical network is kept stable. Spinning reserve functionality provides an energy reserve for power generation, allowing for operating a single generator at all times i.e. no parallel running of generators resulting in low load conditions on two generating sets, which happen when they are sharing a load. Black-out prevention is improving vessel safety as the ESS is keeping the electrical network alive until a stand-by generating set is started and connected to the network. This function allows single generating set (or shaft generator) operation also during manoeuvring.

The battery sizing in a Hybrid DC Machinery is depending on vessel operation profile. For deep-sea sailing merchant vessels, the functionalities described here is handled by an ESS with energy storage capacity (in kWh) of one third of a generating set power (in kW). As an example, a 1000 kW generating set manages with a single ESS of 330 kWh with a battery technology allowing for 3C/1C discharge/charge capacity. 3C equals three times the nominal charge current.

3.4. Limiting factors of DC-link based distribution networks

DC-link power distribution networks onboard ships have existed already more than ten years but has not yet become mainstream due to several reasons. As these designs and implementations are still in their infancy it also means that necessary technologies to support the designs such as availability of DC current breakers with high power capacities and DC busbar modules are limited. Electrical engineering education has not yet shifted towards this new paradigm to be and component suppliers has not yet shifted their manufacturing capacities towards DC based technologies. The land-based industry that is not that depending on megawatt (MW) class variable frequency drive solutions for improving energy efficiency will remain mainstream and the marine sector that is implementing ultra-efficient DC-link based technologies has not yet scaled up. And as with any new world thinking the change resistance is always present.

4. Future proof DC-link power distribution

As the technology leaps forward and zero emission technologies evolve the electrical power distribution based on DC and AC distribution systems will be there to connect the machinery systems together. The concepts of MW class variable frequency drive technologies which are already in use in shipping industry today is flexible and provides the means to distribute power from virtually any source that already exist or will be invented. Hybrid solutions based on batteries and fuel cells is evolving and pilot projects are under development.

Considering zero emission and carbon neutral fuels for powering vessels the development of the large bore main engines is ongoing and proof of concepts already exists. What is still today on a slower development path is the smaller bore generating set engines. Higher speed generating set engines face more challenges to burn e.g. ammonia (NH₃) and the cost per kilogram of small bore engines burning carbon neutral fuels is not looking promising. Hence the shaft generator that can tap electrical power directly from the propeller shaft of large bore slow speed main engines will become a far more common source of electrical power in merchant shipping.

References

CHAI, M.; B.D. REDDY, S. LINGESHWAREN, S. K. PANDA, D. WU, X. CHENG (2017), *Progressing towards DC electrical systems for marine vessels*, Energy Procedia 143, pp. 27-32, <https://www.sciencedirect.com/science/article/pii/S187661021736407X>

IMO (2021), Energy Efficiency Measures, <https://www.imo.org/en/OurWork/Environment/Pages/Technical-and-Operational-Measures.aspx>

WÄRTSILÄ (2013), *Wärtsilä 20 Product Guide*, p.2, Wärtsilä

WÄRTSILÄ (2017), *Wärtsilä Solutions for Marine and Oil & Gas Markets*, p.62, Wärtsilä

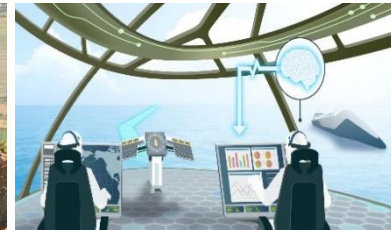
Index by Authors

Albert	106,180	Lincker	151
Albrecht	121	Minor	203
Balena	140	Nikolopoulos	209
Barczewski	203	Oeffner	203
Barsotti	127	Oneto	88
Beltri	203	Ovrum	209
Benson	192	Perez	29
Bergmann	106	Piardi	140
Bertram	12,21,37,45	Plowman	45
Bougiouris	209	Ramsrud	161
Brans	71	Rathier	151
Cady	151	Ratti	140
Carmosino	140	Rinne	71
Coraddu	88	Ryan	192
Corrêa	180	Schimmel	203
Dimopoulos	209	Speichermann	203
Droll	203	Storbacka	218
Dullenkopf	203	Turkmen	192
Du Toit	180	Vindøy	161
Evans	173	Voorzee	173
Gambini	62	Walheim	203
Geertsma	88	Weisheit	203
Georgopoulou	209		
Guegan	151		
Guere	62		
Harries	106		
Hildebrandt	106,180		
Kalikatzarakis	88		
Kana	71		
Kelling	132		
Koukoulopoulos	209		
Kovacic	106		
Krenski	180		
Laag	161		
Limbrunner	7		

14th Symposium on
High-Performance Marine Vehicles – “Technologies for the Ship of the Future”



Cortona / Italy, 29-31 August 2022



Topics: ultra-efficient & zero-emission ships / alternative fuels / 2030 & 2050 target technologies / electric ships
advanced designs / shipyard 4.0 / future materials / future use of oceans / blue economy /
intelligent & connected ships / future antifouling / biomimetic marine technologies

Organiser: Volker Bertram (volker@vb-conferences.com)

Advisory Committee:

Catherine Austin	I-Tech	Robert Dane	Ocius	Kohei Matsuo	NMRI
Carlo Bertorello	Naples University	Stefan Harries	Friendship Systems	Christian Oldendorff	Amplifier
Carsten Bullemer	Maritime Data Systems	Thomas Hildebrandt	Numeca	Prasanta Sahoo	FIT
Emilio Campana	CNR	Jan Kelling	Hasytec	Pierre Sames	DNV
Roy Campe	CMB	Jiulun Liu	Wuhan Univ Technology	Noah Silberschmidt	Silverstream Technologies
Andrea Coraddu	TU Delft			Teus van Beek	Wärtsilä

Venue: The conference will be held at the “Oasi Neumann Hotel” in Cortona/Italy

Format: Papers to the above topics are invited and will be selected by a selection committee.
Proceedings will be electronic pdf version in colour.

Deadlines: anytime Optional “early warning” of interest to submit paper
18.5.2022 First round of abstract selection (1/3 of available slots)
18.6.2022 **Second round of abstract selection (remaining 2/3 of slots)**
1.8.2022 Final papers due (50 € surcharge for late submission)

Fees: 650 € / 350 € regular / PhD student – early registration (by 1.8.2022)
750 € / 400 € regular / PhD student – late registration

Fees are subject to VAT
Fees include proceedings, lunches and coffee breaks, and conference dinner
Fees apply also to authors

Sponsors: Tuttech Innovation, Hasytec – further to be announced

Media Partner: Hansa

Information: volker@vb-conferences.com